Eye Tracking: A Perceptual Interface for Content Based Image Retrieval

Oyewole Oyekoya

Ph.D. Thesis, April 2007

Department of Electronic & Electrical Engineering

Adastral Park Campus

University College London

Supervisor: Prof. Fred Stentiford

This thesis is submitted to the University of London in fulfilment of the requirements of the degree of Doctor of Philosophy. I, Oyewole Oyekoya, confirm that the work presented in this thesis is my own. Where information has been derived from other sources, I confirm that this has been indicated in the thesis.

Acknowledgements

First and foremost, I am very thankful to my supervisor, Fred Stentiford, for his advice, criticism and source of new ideas. He has been significant in shaping my path for future ambitions. I am thankful to Adetokunbo Bamidele, Shijie Zhang, Vishwa Vinay, Dipak Patel and Antonio Gonzalez for their invaluable discussions during the course of this research.

Thanks to all the staff and students from University College London and British Telecommunications Plc based at Adastral Park who took part in the eye tracking experiments.

We are grateful to David Hands and Damien Bayart from the Perception Coding group for the provision of the eye tracker used in the experiments. I'd like to thank Noel Brahma, Rebecca Simpson and John Gilby from SIRA Innovations Ltd for the six weeks placement opportunity, where I was coached on the commercialisation of research. This was helpful in securing a Centre of Scientific Enterprise Ltd (CSEL) scholarship to write a commercial evaluation section in this thesis.

This work was supported by the Engineering and Physical Sciences Research Council, SIRA Innovation Ltd, British Telecommunications Plc and the Imaging Faraday Partnership. This research has been also conducted within the framework of the European Commission funded Network of Excellence 'Multimedia Understanding through Semantics, Computation and Learning' (MUSCLE).

Finally, my special thanks to Margaret for her encouragement, love, patience and support especially through the financial hardship experienced between 2001 and 2005. This thesis is dedicated to her.

Abstract

In this thesis visual search experiments are devised to explore the feasibility of an eye gaze driven search mechanism. The thesis first explores gaze behaviour on images possessing different levels of saliency. Eye behaviour was predominantly attracted by salient locations, but appears to also require frequent reference to non-salient background regions which indicated that information from scan paths might prove useful for image search. The thesis then specifically investigates the benefits of eye tracking as an image retrieval interface in terms of speed relative to selection by mouse, and in terms of the efficiency of eye tracking mechanisms in the task of retrieving target images. Results are analysed using ANOVA and significant findings are discussed. Results show that eye selection was faster than a computer mouse and experience gained during visual tasks carried out using a mouse would benefit users if they were subsequently transferred to an eye tracking system. Results on the image retrieval experiments show that users are able to navigate to a target image within a database confirming the feasibility of an eye gaze driven search mechanism. Additional histogram analysis of the fixations, saccades and pupil diameters in the human eye movement data revealed a new method of extracting intentions from gaze behaviour for image search, of which the user was not aware and promises even quicker search performances. The research has two implications for Content Based Image Retrieval: (i) improvements in query formulation for visual search and (ii) new methods for visual search using attentional weighting. Futhermore it was demonstrated that users are able to find target images at sufficient speeds indicating that pre-attentive activity is playing a role in visual search. A current review of eye tracking technology, current applications, visual perception research, and models of visual attention is discussed. A review of the potential of the technology for commercial exploitation is also presented.

Table of Contents

Table of Figures

Lists of Tables

Chapter 1. Introduction

1.1. Motivation

Images play an increasingly important part in the lives of many people. This has prompted significant growth in research into techniques of automatic indexing and retrieval of images otherwise known as Content Based Image Retrieval (CBIR).

The problem of adequate visual query formulation and refinement [74] is an outstanding problem in CBIR. Indeed lack of high-quality interfaces for query formulation has been a longstanding barrier to effective CBIR [76]. Users find it hard to generate a good query because of initial vague information [75]. The mouse and the keyboard dominate the types of interfaces found in computers today. Eye tracking offers a an adaptive approach for visual tasks that has the potential to capture the user's current needs from eye movements. Humans are capable of making rapid decisions from limited information. The eye movement data arising during these decisions can be examined for indications of visual query formulation. This thesis investigates the gaze behaviour associated with formulating and refining queries under varying image search conditions and time constraints.

The representation of high level concepts is another problem in CBIR and low-level features (such as colour, shape and orientation) do not reflect the user's high-level perception of the image content. Whereas key words form a convenient feature for characterising documents, there is no such obvious attribute present in images. In addition there is no agreement on what might constitute a universal syntax for images that could capture the meaning that we all see in images. Every user can possess a different subjective perception of the world and this can be measured to some extent using an eye tracker. The research reported in this thesis is concerned with exploring information from eye tracking data obtained during the course of visual search that may be used to expedite the search.

1.2. Objectives

This thesis proposes that eye tracking data provides information relevant for query formulation in image retrieval that is not otherwise obtainable through existing conventional interfaces. There are four objectives in this thesis.

Firstly, the relationship between gaze behaviour and a model of visual attention needs to be assessed in order to partly validate the model used in the image retrieval framework and to assess the validity of the gaze data in visual search. This is necessary to determine whether users look at salient regions as determined by the attention model.

Secondly, many computer users use a mouse as an interface device. The additional benefits of using eye movement in a target image identification task need to be identified.

Thirdly, experiments must be designed to explore the image retrieval framework proposed. The experiments should follow a balanced design where all treatment combinations have the same number of observations.

Finally, analysing gaze parameters obtained from the time sequence of the eye tracking data analysis may provide informative measures for a CBIR system and improve image retrieval. Exploring the limits of the speed of operation of the eye gaze interface for image retrieval may indicate a role of pre-attentive vision in visual search.

1.3. Contribution

The literature review provides a comprehensive account of background research in the field. The results in this thesis contribute to existing research on models of attentional guidance. The speed efficiency of eye selection was confirmed in the context of image identification. A novel eye tracking interface was created for image retrieval which enables the extraction of retrieval requirements from eye movement data. Finally it was established for the first time that pre-attentive attention is influenced by top-down guidance during visual search.

The research is supported by experiments whose results were tested for significance and provide a basis for further research in visual attention, visual perception and human computer interaction.

A review of the applications and commercial potential of the technology is also provided.

1.4. Structure

The scope of the work involves investigating issues of human computer interaction, visual attention and perception. The thesis is structured in the following way:

- Chapter 2 provides a detailed review of current applications, state of the art in eye tracking technology and relevant research in visual perception and attention modelling. A commercial review of eye tracking technology is also presented. The outstanding issues and the ensuing thesis statement are discussed and presented in this section.
- Chapter 3 presents the general framework behind the proposed system. An introduction to the technical aspects of the eye-movement equipment employed and its operation. Also presented is a detailed description of the choice of attention model.
- Chapter 4 presents the initial experiment, which explores gaze behaviour on images possessing different levels of saliency.

- Chapter 5 then specifically investigates the benefits of eye tracking as an image retrieval interface in terms of speed relative to selection by mouse, followed by the implementation of the proposed system in terms of the efficiency of eye tracking mechanisms in the task of retrieving target images. Additional analysis of the fixations, saccades and pupil diameters is conducted on the human eye movement data collected from the experiment.
- Chapter 6 describes experiments designed to investigate gaze behaviour on the system using alternative target selection criteria derived from the analysis of gaze behaviour from preceding empirical findings. Also presented are experimental findings under faster selection conditions.
- In chapter 7 a discussion and a review of thesis objectives are presented, outlining the future directions and implications of the research.
- The appendix presents the technical specifications of current commercial eye tracking equipment and additional experimental details (i.e. questionnaires and instructions).

Chapter 2. Review of Literature

2.1. State of the Art

Research activity in eye tracking and visual attention has increased in the last few years due to improvements in performance and reduction in the cost of eye tracking devices as well as better understanding of the human visual system. The eye (Figure 2.1) is a complex sensing device composed of a series of optical elements: two lenses (cornea and eye lens), an aperture (pupil) and a light sensitive transducer in a form of a thin layer of tissue (retina) that transforms electromagnetic energy into neural impulses that are further transmitted to the visual cortex via the optical nerve.

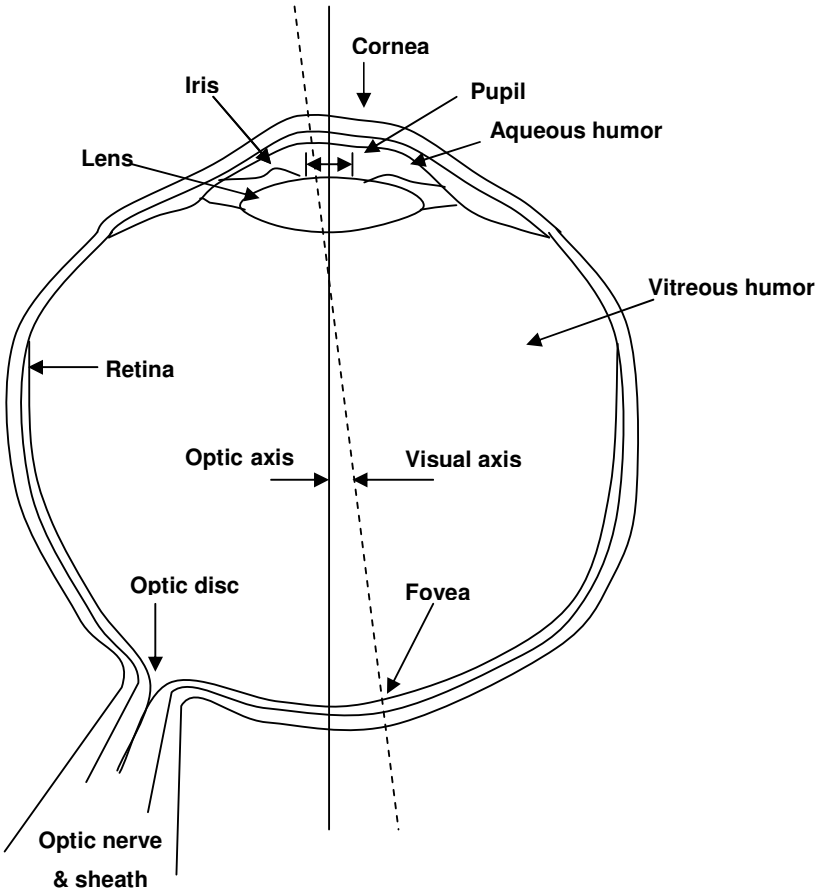

Figure 2.1: The Eye (adapted from [11])

Figure 2.2 illustrates several key characteristics of the eye that makes its gaze direction measurable from a video camera image. Eye pointing is precise because there is a centralized

region in the retina called the fovea where there is increasing image resolution towards its centre.

The retina contains receptors sensitive to light (photoreceptors) containing approximately 127 million cells i.e. 120 million *rods* that can detect relative small amounts of lights and 7 million *cones* that can capture the colours of the human visible light spectrum. The receptor cells are not homogeneously distributed over the retina. There is a region called the fovea (foveola) of high receptor density (mostly *cones*) and therefore high spatial resolution in the centre of the retina. Outside this area with a radius of about one degree of visual angle, the density decreases exponentially with growing eccentricity. This means that we possess very detailed vision in the centre of our visual field and only coarse perception in the peripheral regions. The foveola is a small central region, typically 0.17mm or 0.6^{o} in radius, where the image of the object of people's fixation lies. This physiological phenomenon means that humans have natural and precise control of eye motions. The visual axis is the line from the centre of the foveola through the centre of the corneal sphere, also known as the optical node point of the eye. By definition, the eye's gaze point lies on the visual axis. The eye's optic axis is defined as the axis of symmetry for the eye's optical system. The location of the foveola is generally offset from the eye's optic axis, so the optic axis is distinct from the visual axis. The foveola of the eye is usually located to the temporal side of the eye, causing the visual axis of the eye to point to the nasal side of the optic axis. The angle between the optical and visual axes of the eye, which is about 5^{o} has a standard deviation of about 2^{o} over the human population. The surface of the cornea is approximately spherical. The corneal sphere is smaller than the eyeball and its surface protrudes out of the eyeball sphere by approximately 1.5mm. The typical radius of curvature for the cornea is 7.7 +- 2.0mm.

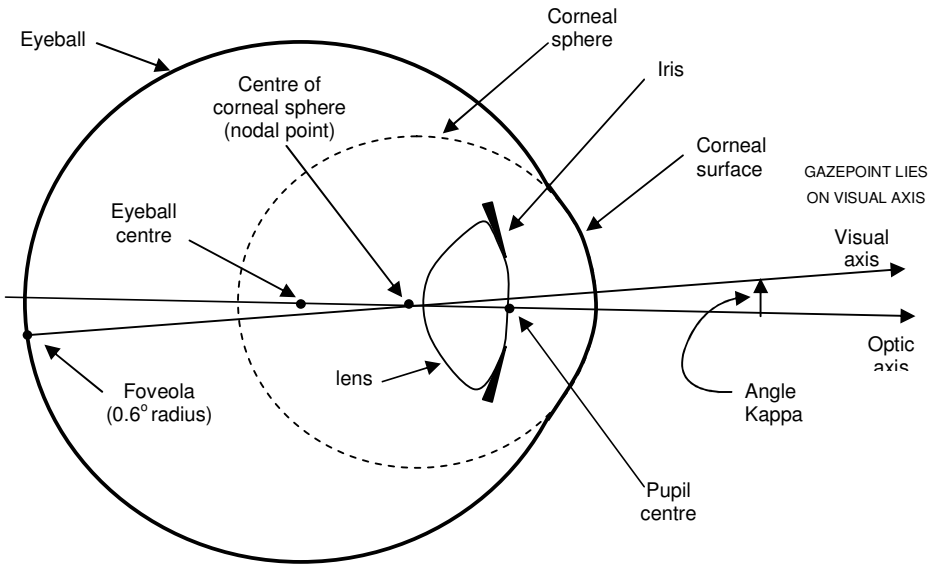

Figure 2.2: Schematic of the Eye (adapted from [37])

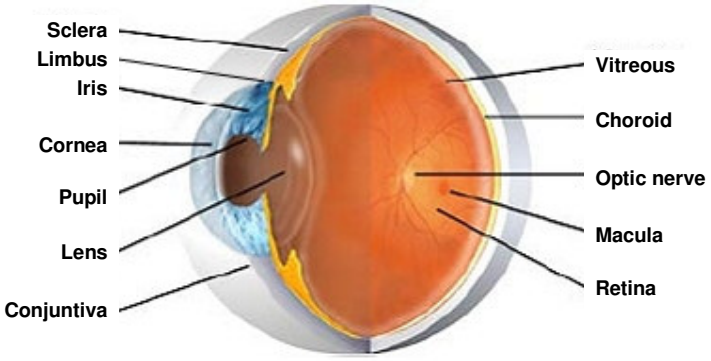

Figure 2.3: Colour Schematic of the Eye (adpated from [19])

Research literature [11][18] identifies the types of eye movements used to reposition the fovea: pursuit, vergence, vestibular, and physiological nystagmus (miniature movements associated with fixations), fixations and saccadic movements. *Eye pursuits* are involuntary movements that follow objects in smooth motion. This is slower than a saccade and acts to keep a moving object foveated. *Vergence* movements are voluntary and used to re-focus the pair of eyes depending on the distance of the target. There is a convergence of both eyes relative to each other when looking at nearby objects and a divergence when looking at distant ones. *Vestibular nystagmus* is a pattern of eye movements compensating for the movement of the head. *Physiological nystagmus* is a high frequency movement that continuously shifts the image on the retina. This involuntary movement occurs during fixations.

Two types of movement need be modeled to gain insight into the overt localization of gaze in an image retrieval task.

- *Fixations* naturally correspond to the desire to maintain one's gaze on an object of interest. Visual perception takes place mainly during fixations, which are motionless phases occurring between saccades on static scenes. Fixations are characterized by miniature high frequency oscillations (drifts and microsaccades), which stops the image from fading away causing the scene becoming blind. Henderson and Hollingworth's review [22] indicated the variability of fixation durations, which range from less than 50ms to more than 1000ms in a skewed distribution with a mode of about 230ms. The length of time that it takes to scan (i.e. saccaded to locations) and determine the relevance of a fixated location (i.e. fixated locations) varies and tends to be dependent on a number of factors. The influence of visual perception is discussed further in the latter part of this chapter.
- *Saccades* are the expression of the desire to voluntarily change the focus of attention. During saccades, the eyes are moved to a different part of the visual scene and occurs in a series of fast, sudden jumps rather than continuously. Planning a saccade usually involves

peripheral processing in order to determine the saccades landing point, in particular in abstract scenarios when only little contextual information is provided. While the saccades initialization can be made voluntary, the actual movement is ballistic, i.e. their trajectory cannot be modified after initialization. During the saccade, no visual information other than a blur can be perceived.

These are the primary requirements of eye movement analysis: the identification of fixations and saccades. It is clear that data from eye tracking systems will inevitably contain series of voluntary and involuntary movements however these movements are fixated on those elements of an object which carry or may carry essential and useful information [84].

2.1.1. Eye Tracking Technology

A number of eye gaze detection methods have been developed over the years. Direct visual observation of the eye gives a general indication of the character of eye movements. In fact Yarbus [84] reports that Javal (1879) used a mirror for this purpose. The experimenter could only observe large movements, and could not notice the rotation of the eye through one degree and corresponding movement of the eyes through 0.2mm. Later, optical instruments (such as lenses, microscope or specially devised instruments) were used to detect small movements.

In the past, several authors also used methods by which the connection between the eye and the recording system was mechanical. The movement of the cornea was transmitted by three known methods: a lever and balance arm, elastic balloon filled with air (eye movement altered pressure) and attachment of a lever or thread to small cups (made of Plaster of Paris or aluminium). Low accuracy and a complicated setup meant that this method was outdated very quickly. Techniques mostly used in the twentieth century involve the use of: electro-oculography (EOG), scleral contact lens/search coil [61], and reflected light (limbus tracking, video-based combined pupil and/or corneal reflection and dual purkinje tracking). Electro-oculography, or EOG, relies on (d.c. signal) recordings of the electric potential differences of the skin surrounding the ocular cavity. The changes may be detected by a pair of electrodes fixed to corresponding points of the skin and then amplified and recorded. The main advantage of this method is the non-requirement of a clear view of the eye resulting in a large dynamic range. Techniques based on corneal bright spot, and still and motion-picture photography were also used in the early part of the 20^{th} century with relatively poor accuracy as reported by Yarbus [84]. Methods employed before the 1970s used invasive methods that required tampering directly with the eyes. Such techniques based on contact lenses offer high accuracy and large dynamic range but require an insertion into the eye! Mirror surfaces on the lens [84] causing reflection of light beams or employment of a search coil embedded in a scleral contact lens coil, which is then measured moving through an electromagnetic field [61], can be used to calculate eye positions.

The availability of image processing hardware and possible applications of gaze tracking system for human computer interaction prompted a revisit to the reflected light techniques due to its non-invasive feature. These recent tracking techniques use mainly infra-red light to illuminate the eye, causing a reflection and/or sharper images of the eye. The sclera is the tough, opaque tissue that serves as the eye's protective outer coat. The iris is the coloured part of the eye. It controls light levels inside the eye similar to the aperture on a camera. The exterior of the iris, i.e. the border between the iris and the sclera is called the limbus. Limbus tracking requires optical detection of the boundary between the normally white sclera and darker iris (Figure 2.3). Occasional coverage of the top and bottom part of the limbus by the eyelids is a limitation. A similar pupil tracking method can also be applied on the smaller and sharper boundary between the pupil and the iris. The shining of infrared light can also lead to several reflections on the boundaries of lens and cornea (called *purkinje* reflections). Four purkinje reflections are created: two from the cornea and two from the lens. The first reflection (also called the *glint*) is measured relative to the location of the pupil centre. This forms the basis of most current commercial eye tracking systems. The DPI (Dual Purkinje Image) eye tracker [8] tracks this first reflection along with the fourth to calculate gaze directions. It requires the head to be restricted and is relatively expensive. The weakness of the fourth reflection requires that surrounding lightning must be heavily controlled. The video based combined pupil and corneal reflection method uses these two ocular features to disambiguate head movement from eye rotation, and as a result does not need to have a fixed head unlike the DPI eye tracker.

Recent advances in imaging sensors, video cameras and image processing systems have made the recent eye tracking systems one of the most promising fields for improving human computer interaction. However, one of the most pressing issues is simplifying the personal calibration procedures. Calibration is normally needed because of individual differences of eyeball size and difficulty in measuring the position of the fovea. The FreeGaze System [72] also referred to as attention extractor reduces the burden of personal calibration. The eye tracker attempts to limit errors arising from calibration and gaze detection by using only two points for individual personal calibration. The position of the observed pupil image is used directly to compute the gaze direction but this may not be in the right place due to refraction in the surface of the cornea. The eyeball model corrects the pupil position for obtaining a more accurate gaze direction. An experiment performed to test the equipment had interesting results:

- Gazing at points on the screen many times often causes burden and fatigue.
- Increase in the number of calibration points does not affect the accuracy of gaze detection.
- Users move their eyes between the gazing and confirmation periods in the calibration session, which causes degradation.
- Freegaze could not detect the Purkinje image of subjects who wore soft contact lenses.

These typical problems highlight some of the challenges for future research. Table 2.1 lists some of the recent commercial eye trackers available on the market [24][25][26][27][28][29][37] and highlights their characteristics. These improvements in eye trackers has led to reductions in price and more importantly a significant increase in sampling rates from 50Hz to 1250Hz. The Dual-purkinje trackers have always had an advantage over video-based PCR eye trackers due to their high sampling rate (up to 4000Hz) and accuracy. However, price and usability issues have made them unlikely candidates for applications in human computer interaction. The advances in imaging sensors and software have led to a significant increase in research into video-based eye tracking methods.

Several models of eye trackers deal with specific eye tracking issues in different ways, with the same goal of maximising accuracy and processing speed. It is stated that an ideal eye tracker must have the following characteristics [66]:

a. Offer an unobstructed field of view with good access to the face and head.
b. Make no contact with the subject.
c. Meet the practical challenge of being capable of artificially stabilising the retinal image if necessary.
d. Possess an accuracy of at least one percent or a few minutes of arc; e.g. not give a 10^{o} reading when truly 9^{o}. Accuracy is limited by the cumulative effects of nonlinearity, distortion, noise, lag and other sources of error.
e. Offer a resolution of 1 minute of arc per second; and thus be capable of detecting the smallest changes in eye position; resolution is limited only by instrumental noise.
f. Offer a wide dynamic range of one minute to 45^{o} (= 3000-fold) for eye position and one minute arc per second to 800^{o} per second (= 50,000-fold) for eye velocity.
g. Offer good temporal dynamics and speed of response (e.g. good gain and small phase shift to 100Hz, or a good step response).
h. Possess a real-time response (to allow physiological manoeuvres).
i. Measure all three degrees of angular rotation and be insensitive to ocular translation.
j. Be easily extended to binocular recording.
k. Be compatible with head and body recordings.
l. Be easy to use on a variety of subjects.

Though desirable, not all these requirements are prerequisites for acceptable eye tracking interfaces. Several methods of improving the accuracy of estimating gaze direction have been proposed. The Eye-R system [67] is designed to be battery operated and is mounted on any pair of glasses. It measures eye motion using infrared technology by monitoring light fluctuations from infrared light and utilizes this as an implicit input channel to a sensor system and computer. As a person walks around, information is exchanged between the Eye-R module and the exhibit with infrared sensor that the user fixates on. This information is transferred to a

server using a computer network. All targets/exhibits are fitted with an infra-red sensor in this networked environment. Some commercial manufacturers of eye trackers [25][28] now have a head-mounted system that has an attached miniature camera that records the scene being viewed by the user. Mulligan [42] uses a low cost approach to track eye movement using compressed video images of the fundus on the back surface of the eyeball. It is capable of high performance when off-line data analysis is acceptable. More accurate results may be obtained when the imagery is analyzed off-line using more complex algorithms implemented in software. A technical challenge for these types of trackers is the real time digitization and storage of the video stream from the cameras. New video compression technology allows streams of video images to be acquired and stored on normal computer system disks; however lossy compression can lead to loss of important information. Bhaskar et al [3] propose a method that uses eye blink detection to locate an eye which is then tracked using an eye tracker. Blinking is necessary for the tracker to work well and the user has to be aware of this.

Researchers are now examining the applicability of eye tracking technology in context and this has increased the potential of the systems in delivering on accuracy and usability. Illumination conditions and physiological differences of the eye have been the main limitations with which current hardware has struggled to cope. More recent hardware advances have encouraged further research into computer vision and image processing techniques for collecting and analysing images of the eye. The resulting data also requires good analysis, usable in individual domains.

Identification and analysis of fixations and saccades in eye tracking data are important in understanding visual behaviour. Salvucci [63] classifies algorithms with respect to five spatial and temporal characteristics. The spatial criteria divide algorithms in terms of their use of velocity, dispersion of fixation points, and areas of interest information. The temporal criteria divide algorithms in terms of their use of duration information and their local adaptivity. It was concluded that velocity-based and dispersion-based algorithms fared well and provided similar performance.

Criteria	Fixation Identification Algorithms				
	Velocity-Threshold	Hidden Markov Model	Dispersion Threshold	Minimum Spanning Tree	Area of Interest
Velocity based	X	X			
Dispersion-based			X	X	
Area-based					X
Duration sensitive			X		X
Locally adaptive		X	X	X	

The five fixation identification algorithms are also described and compared in terms of their accuracy, speed, robustness, ease of implementation, and parameters. The Hidden Markov model uses probabilistic analysis to determine the fixation or saccade state. The Dispersion

Threshold iterates through the eye protocol and groups consecutive points that lie within a given dispersion. It was observed that Hidden Markov Models and the Dispersion Threshold algorithms fared better in terms of their accuracy and robustness. The Minimum Spanning Tree uses a minimized connected set of points and provides robust identification of fixation points, but runs slower due to the two step approach of construction and search of the minimum spanning trees. The Velocity Threshold, which is based on point to point velocity, has the simplest algorithm and is thus fast but not robust. Areas of Interest, which identify fixations within given rectangular target areas, are found to perform poorly on all fronts. These findings are implemented in the Eyetracer system [62], an interactive environment for manipulating, viewing, and analyzing eye-movement protocols. Eyetracer facilitates both 'exploratory analysis' for initial understanding of behaviours and model prototyping and 'confirmatory analysis' for model comparison and refinement. Eyetracer addresses two main problems: fixation/saccade identification and tracing of fixations to its corresponding visual target. It identifies fixation using four algorithms based on velocity threshold, hidden markov model, dispersion threshold and regions of interest. The output of fixation id is a sequence of <x,y,t,d> fixations where x and y is location, t is onset time and d is duration. Three tracing algorithms (fixation, target and point) trade off tracing speed and accuracy. The tracing process is said to be robust to alleviate problems of equipment noise and individual variability which causes off-centre or extraneous fixations. The tracing algorithms have three inputs: an eye movement protocol (eye tracking data), set of target areas defines rectangular regions where fixations for the various possible targets may occur and a cognitive process model expressed as regular grammar. Applications include coding of experiment protocol and building of intelligent gaze based interface.

NASA's Lee Stone [38] focuses on the development and testing of human eye-movement control with particular emphasis on search saccades and the response to motion (smooth pursuit). The specific goal is to incorporate recently acquired empirical knowledge of how eye movements contribute to information gathering and of the relationship between the eye movement behaviour and the associated percept, into computational tools for the design of more effective visual displays and interfaces that are matched to human abilities and limitations. Much of the focus is on proposing a new control strategy for pursuit eye movement modified from an existing model. Stone concludes that current models of pursuit should be modified to include visual input that estimates object motion and not merely retinal image motion as in current models.

Duchowski [12] presents a 3D eye movement analysis algorithm for binocular eye tracking within Virtual Reality. Its signal analysis techniques can be categorised into three: position-variance, velocity-based and Region of Interest-based, again using two of Salvucci's criteria [63]. It uses velocity and acceleration filters for eye movement analysis in three-space. This is

easily adapted to a 2D environment by holding head position and visual angle constant. Gazepoints in the virtual environment are calculated by the 2D to 3D mapping of gaze vectors. The computed gaze direction vector is used for calculating gaze intersection points. The algorithm is then presented showing how issues such as noise and filtering techniques are handled. The algorithm is then evaluated using a virtual environment for aircraft visual inspection training. It was concluded that cognitive feedback, in the form of visualized scan-paths, does not appear to be any more effective than performance feedback (search timing). Also, the number of fixations decreases following training.

Deciphering eye movement data in terms of fixations and saccades can vary from simple averaging to sophisticated markov models. Additionally, identification of pursuit eye movements is needed for video images. Extending the analysis from normal 2D images to a 3D environment is a possibility, thus widening the range of applications for eye tracking technology.

2.1.2. Current Applications

Eye tracking offers a new way of communicating with human thought processes and can be used in both active and passive modes in several applications.

In active 'control mode', eye tracking can be used to direct a computer through the motion of the eyes as in the case of eye-aware communication programs [4][13][21]. Eye tracking equipments are used as interface devices in several diverse applications. The tracking of eye movements has been employed as a pointer and a replacement for a mouse [21] , to vary the screen scrolling speed [46] and to assist disabled users [6]. Schnell and Wu [65] apply eye tracking as an alternative method for the activation of controls and functions in aircraft. Dasher [80] is a method for text entry that relies purely on gaze direction. The user composes text by looking at characters as they stream across the screen from right to left. Dasher presents likely characters in sizes according to the probability of their occurrence in that position. The user is often able to select rapidly whole words or phrases as their size increases on the screen. In comparison with on-screen keyboards, it is not confounded by the problem of interpreting data to identify a user's intention of selection. Nikolov et al [45] propose a system for construction of gaze-contingent multi-modality displays of multi-layered geographical maps. Gaze contingent multi-resolutional displays (GCMRDs) centre high-resolution information on the user's gaze position, matching the user's interest. In this system, different map information is channelled to the central and the peripheral vision giving real performance advantage. The Infrared (IR) Eye [85] was developed in order to improve the efficiency of airborne search-and-rescue operations. The camera views the scene simultaneously through two optical systems, one covering a wide area with a wide field of view of 40^{o} at low resolution for search and detection, and the other covering a smaller area with a narrow field of view of 10^{o} at high resolution for identification.

The small field of view can be steered by the operator's line-of-sight, to investigate any area in the larger field. An innovative display system is necessary to present both fields of view simultaneously and without discontinuity to the operator. Imperial College Innovation filed a patent [104] on a system of knowledge gathering for decision support in image understanding/analysis through eye-tracking. A generic image feature extraction library comprising an archive of common image features is constructed. Information extracted from the dynamics of an expert's saccadic eye movements for a given image type are used to determine the visual characteristics of the image features or attributes fixated by the domain experts such that the most significant parts of the image type can be identified. Thus, when a specific type of image, for example a scan of a particular part of the human body, is analysed by an expert, those of the common image attributes, or "feature extractors", from the archive that are most relevant to the visual assessment by the expert for that image type are determined automatically from tracking the expert's eye. These attributes are aspects such as the texture of the image at the fixated point because these are underlying features rather than the physical location or co-ordinates of a fixation point, additional information can be inferred. The dynamics of the visual search can subsequently be analysed mathematically to provide training information to novices on how and where to look for image features. The invention thus captures the encapsulating and perceptual factors that are subconsciously applied by experienced radiologists during visual assessment. The invention is enhanced by allowing the sequence of fixation points also to be analysed and applied in training decision support.

In passive mode, the eye-tracking device simply monitors eye activities for subsequent diagnostic analysis. Marketing researchers can determine what features of product advertisement attracts buyer attention. Researchers use it for experimental investigation of eye behaviour [32][48][56][57], especially in cases of disabled persons, infants and animals, as they cannot use a mouse. It also provides a comprehensive approach to studying interaction processes such as the placement of menus within web sites and to influence design guidelines more widely [40].

Duchowski presents an in-depth review of eye tracking applications and divides them into diagnostic and interactive usage [10], based on offline and real-time analysis respectively.

2.1.3. Usability Studies

Although eye tracking has not yet been implemented on mobile devices, research is underway on how the detection of regions of interest can be used to improve the quality of images presented on small screens. Nokia [78] conducted a usability evaluation on two mobile Internet sites and discovered the importance of search on mobile phones contrary to the initial hypothesis that users would not like to use search because of the effort of keying inputs. The research also showed that customers prefer any interface that produces a successful search. This

evaluation confirms that users do have a need for information retrieval for mobile usage. Simple searches such as a name-search are straightforward processing and are already implemented on mobiles. Text messaging has proved to be successful partly because the user can write out texts in quiet environments and of the low cost of sending texts. Hence there are a number of other factors that may influence image search on mobile phones apart from speed and interface, which plays an important part in the determination of the success of mobile search.

Xin Fan et al [82] propose an image viewing technique based on an adaptive attention-shifting model, which looks at the issue of browsing large images on limited and heterogeneous screen zones of mobile phones. This paper focuses on facilitating image viewing on devices with limited display sizes.

The Collage Machine [35] is an agent of web recombination. It deconstructs web sites and re-presents them in collage form. It can be taught to bring media of interest to the user on the basis of the user's interactions. The evolving model provides an extremely flexible way of presenting relevant visual information to the user on a variety of devices.

Farid [15] describes the implementation and initial experimentation of systems based on the user's eye gaze behaviour. It was concluded that the systems performed well because of minimal latency and obtrusiveness. Examples include user navigation in large images that occur in astronomy or medicine. It was noted that reducing the resolution of the visual window for eye pointing, affects the efficiency of smaller clickable icon links highlighting the jittery movement of the human eye that limits the window size for eye pointing. It has also been well documented over the years that one cannot rely on dwell time to determine link selection. However, the implementation presented allows for continual user change of mind, which increases the user exploration experience. A zooming technique is adopted with a magnified region of interest and multiple video streams.

2.1.4. Gaze Interfaces

An approach to visual search should be consistent with the known attributes of the human visual system and account should be taken of the perceptual importance of visual material. Recent research in human perception of image content [31] suggests the importance of semantic cues for efficient retrieval. Relevance feedback mechanisms [7] are often proposed as techniques for overcoming many of the problems faced by fully automatic systems by allowing the user to interact with the computer to improve retrieval performance. This reduces the burden on unskilled users to set quantitative pictorial search parameters or to select images (using a mouse) that come closest to meeting their goals.

Yamato et al [83] conducted an experiment to evaluate two adjustment techniques, in which computer users use both their eye and hand in carrying out operations in GUI environments. In the first technique the cursor moves to the closest GUI button when the user pushes a mouse

button. The second adjustment involves gross movement of cursor by the eye and the user makes final adjustments and moves the mouse onto the GUI button. The second adjustment performed better because users were able to use the eye tracking device for rough cursor movement followed by the mouse for delicate adjustment. In this case the input device is switched from the eye tracking device when the user moves the mouse in the manual adjustment, so the user has to be careful not to move the mouse until required. Ware and Mikaelian [81] evaluated the eye tracker as a device for computer input by investigating three types of selection methods (button press, fixation dwell time and screen select button) and the effect of target size. Their results showed that an eye tracker can be used as a fast selection device providing the target size is not too small. Eye gaze has also been shown to be faster than the mouse for the operation of a menu based interface [47]. Sibert and Jacob [68] performed two experiments involving circles and letters respectively. The former required little thought, while the latter required comprehension and search effort from participants. Eye gaze interaction was found to be faster than the mouse in both experiments.

The mouse has been a successful pointing device in the decision making process and has influenced new research into use of the eye as a faster source of feedback. There has been some recent work on document retrieval in which implicit relevance feedback inferred from eye movement signals, combined with collaborative filtering (a user rating profile model) has been used to refine the accuracy of relevance predictions [58]. Starker and Bolt [69] use eye tracking to monitor users' interests and make inferences about what items or collection of items shown, holds most relative interest for the user. Material identified is then zoomed in for a closer look and described in more detail via synthesized speech. Three models of user interest were implemented for determining the apparent level of user interest in a given object.

Model One: When the screen coordinate of the gaze point corresponds to an object or objects, the tally for that object is incremented by one. The interest level equals the tally.

Model Two: The elapsed time since a given object was seen is multiplied by a constant, *k2*, and subtracted from a constant, *k1* times the tally of glances for that object:

$$interestlevel = k1 * tally - k2 * elapsedtime$$

Model Three: In this model, whenever there is a fresh look at an object, the old value is decayed by the proper amount and then incremented by a constant ("fresh look constant"):

if (object was just looked at)

$$interestlevel=(interestlevel).e^{\frac{-t}{r}}+FreshLookConstant$$

else

$$interestlevel = (interestlevel) \cdot e^{\frac{-t}{r}}$$

where

FreshLookConstant = constant

t= elapsed time since object was last seen

r= time constant

Recently, research has been conducted in the use of eye tracking data for image retrieval. The Eye-Vision-Bot project was presented by Scherffig [64]. The objective of the project was to optimise image retrieval from databases and the internet with the aid of eye tracking and adaptive algorithms. The system uses an eye-tracker to measure in real-time the attention received by various images displayed on the computer screen. The search process of Eye-Vision-Bot begins by selecting and presenting a random set of images. While the images are watched, viewing times are gathered and stored, and form the basis for displaying new images. Searches based on metadata and structure are performed. In the metadata search images belonging to the same artist and the same category as those that were most watched are searched. In the latter, the Gnu Image Finding Tool (GIFT) is asked to return images that are structurally similar to those watched. GIFT is an open source application developed at the computer vision laboratory of the University of Geneve. Here two different algorithms defining the way GIFT weights the images the query is based on are used each in two separate queries. The results of both search methods then are mixed and presented again. This enables an analysis of the performance of the system in which the images compete for attention, although no experimental analysis was conducted.

In another similar work, Essig [14] introduces Visual-Based Image Retrieval (VBIR), which uses an eye tracker for relevance feedback to determine the importance of different image regions for the retrieval process. VBIR aims to improve the retrieval process by increasing the weight of the features (colour, shape and texture) in the image regions that attract the most fixations. Image regions are equal sized sub-blocks in the image. Initial results show that the average number of retrieval steps per image for VBIR was found to be lower than random retrieval and conventional CBIR (based on whole image regions rather than sub-blocks). The choice of test data was limited to 1000 flower images. Images were indexed using an optimal weight combination of colour, shape and texture values with the highest Shannon entropy (a measure of the uncertainty associated with a random variable).

Grecu [19] also proposes a similar approach that attempts to learn on-line from eye-measurement data. Offline image indexing provides a structured representation of the image repository content. The image indexing starts with an automatic detection of the virtual-fixations (using a saliency measure). Once extracted, each virtual-fixation is associated with a set of visual content descriptors, which are stored in the database. Retrieved images are

displayed sequentially to the user. The user provides a relevance feedback (relevant/non-relevant) regarding the currently displayed image(s). The eye tracking system records all the eye movements associated with the displayed stimulus, as well as the user's input (relevance tag). The relevance feedback learning phase teaches the system to discriminate between fixations that are relevant and those that are non-relevant for the current search task. The recorded eye movements are analyzed in order to extract the actual fixations of attention and a number of additional attention metrics, such as fixation duration, or scan-path length. For all actual fixations, the corresponding visual descriptors are computed with exactly the same approach employed for the virtual-fixations. A supervised classifier is trained (using actual fixations) to rate the relevance of the fixations (actual or virtual). A relevance score can thus be computed and top ranked images can be presented to the user for a further retrieval loop. The proposed system was not functional as a fully integrated system, however retrieval experiments were simulated offline and results showed that it is possible to monitor and exploit the user's attention while the user is interacting with the image retrieval system.

The eye interpretation engine [13] was created to adapt in real-time to changes in a user's natural eye-movement behaviours and intentions. It defines three behaviours (knowledgeable movement, searching and prolonged searching) and discovered two features of eye movement patterns (revisits and significant fixations) that makes easier the recognition of high-level patterns in users' natural movements.

No apparent strategies have been easily discerned for image viewing but this has not hampered research efforts in investigating the feasibility of using gaze behaviour for retrieving images.

2.1.5. Visual Attention and Perception

Humans cannot attend to all things at once, thus our attention capability is used to focus our vision on selected regions of interest. Our capacity for information processing is limited, therefore visual scene inspection is performed with particular attention to selected stimuli of interest. A good definition of visual attention was given by James [33]:

> "Every one knows what attention is. It is the taking possession by the mind, in clear and vivid form, of one out of what seem several simultaneously possible objects or trains of thought. Focalization, concentration, of consciousness are of its essence. It implies withdrawal from some things in order to deal effectively with others".

This definition implies that visual attention modelling is relevant to the objective of obtaining better image content understanding. From a historical perspective, Broadbent [5] proposed the filter theory of selective attention, where auditory experiments were performed to demonstrate the selective nature of attention. It was concluded that information enters in parallel but is then

selectively filtered to sensory channels and that it is important that a good visual attention framework must be able to discriminate selectively within an image. This led to the feature integration theory of Treisman [87], which was derived from visual search experiments. Based on this theory, Koch and Ullman's framework [36] for simulating human visual attention focuses on the idea that the control structure underlying visual attention needs to represent such locations within a topographic saliency map, especially given that the purpose of visual attention is to focus computational resources on a specific, conspicuous or salient region within a scene. Multiple image features such as colour, orientation and intensity are combined to form a saliency map that reflects areas of attention. Itti et al [30] builds on the framework for interpreting complex scenes and suggest supervised learning as a strategy to bias the relative weights of the features in order to tune the system towards specific target detection tasks. Wolfe's Guided Search Model [86] proposes that pre-attentive feature processes could direct the deployment of attention in serial attentive searches. In his model, stimuli are divided into two pre-attentive processes (a colour process and an orientation process) which are combined into an attention-guiding activation map. Reinagel and Zador [59] investigated the eye positions of human subjects while they viewed images of natural scenes. Subjects looked at image regions that had high spatial contrasts and in these regions, the intensities of nearby image points (pixels) were less correlated with each other than in images selected at random. Their important assumption is that there is a competition between top-down and bottom-up cues for the control of visual attention.

Privitera et al [57] use 10 image processing algorithms to compare human identified regions of interest with regions of interest determined by an eye tracker and defined by a fixation algorithm. The comparative approach used a similarity measurement to compare 2 aROIs (algorithmically-detected Region of Interests), 2 hROIs (human-identified Region of Interests) and an aROI plus hROI. The prediction accuracy was compared in order to identify the best matching algorithms. Different algorithms fared better under differing conditions. They concluded that aROIs cannot always be expected to be similar to hROIs in the same image because 2 hROIs produce different results in separate runs. This means that algorithms are unable in general to predict the sequential ordering of fixation points.

Jaimes, Pelz et al [32] compare eye movement across categories and link category-specific eye tracking results to automatic image classification techniques. They hypothesise that the eye movements of human observers differ for images of different semantic categories, and that this information may be effectively used in automatic content-based classifiers. The eye tracking results suggest that similar viewing patterns occur when different subjects view different images in the same semantic category. Five different categories are considered: handshakes, crowds, landscapes, main object in uncluttered background and miscellaneous images. More consistent viewing patterns were found within the handshake and main object categories. Although, it was

unclear on how it can be used to influence automatic classification techniques, they suggested that it is possible to apply the Privitera's fixation clustering approach [57] to cluster gaze points. Privitera et al [57] used a similarity index to estimate the prediction accuracy of the algorithms and presented the figures accordingly. The Visual Apprentice framework [32], which was used to illustrate how data can be used to build classifiers, relied on manual clicks from users to construct classifiers. The study does show that similar viewing patterns can be category-specific hence this factor needs to be considered in future algorithms.

Pomplun and Ritter [55] present a three-level model, which is able to explain about 98% of empirical data collected in six different experiments of comparative visual search. Pairs of almost identical items are compared requiring subjects to switch between images several times before detecting a possible mismatch. The model consists of the global scan-path strategy (upper level), shifts of attention between two visual hemifields (intermediate level) and eye movement patterns (lower level). Simulated gaze trajectories obtained from this model are compared with experimental data. Results suggest that the model data of most variables presents a remarkably good correspondence to the empirical data.

The strength of a particular feature in an area of the image does not in itself guarantee that ones attention will be drawn to that image area. However, detecting parts of an image that are most different from the rest of the scene presents a perceptually relevant approach towards detecting visual attention. Saliency of an image feature can be defined to be inversely proportional to the probability of occurrence of that image feature. That is, the higher the saliency or distinction of that feature, the lower the probability of the feature re-occurring within the image. Walker et al. [79] uses this basis to present a method for locating salient object features due to the low probability of the features being misclassified with any other feature within the image. Stentiford's visual attention model which follows the thinking of Walker et al [79] is introduced in [70] and applied to Content Based Image Retrieval in [2][103] and image compression in [71]. This model is based upon the dissimilarity between neighbourhoods in an image and uses neighbourhood differences to identify uncommon textures and other features in an image. This measure can be used to identify regions of interest in many categories of images. No *a priori* guidance is introduced into the scoring mechanism.

The pre-attentive stage of human vision is followed by a higher-level cognitive process, which describe our voluntary intent to attend to other portions of the scene based on our interests. This post-attentive stage is evident in Yarbus' work [84], which demonstrated that scan-path characteristics such as their order of progression can be task dependent. This cannot be compared with Privitera's alternative findings [70] because he did not consider task dependency. People will view a picture differently based on what they are looking for. The eye movements recorded demonstrated sequential viewing patterns over particular regions in the image. Norton and Stark's scan-path theory [88] suggested that subjects tend to fixate

identifiable regions of interest, containing informative details. Both studies suggest that a coherent picture of the visual field is built from serially viewed regions of interests. It is however not clear how our brains assemble information obtained from visual scanning to form a conceptual image or notion of the scene. A clear depiction of eye movements has been particularly helpful in ascertaining whether recognition of the scene is performed by a parallel one-step process or serial scanning strategy. Ongoing research has been limited in this respect, in comparison with reading [89].

Human eye movement is characterized by the circumstances in which they arise as depicted by Kahneman's [34] classification of eye movements into three general types of looking. Firstly, spontaneous looking occurs when the subject views a scene without any specific task in mind (such as free-viewing experiments). The eye is attracted to regions of the scene that convey the most important information for scene recognition. Secondly, task-relevant looking is performed when the subject views the scene with a particular question or goal in mind. Finally, orientation of thought looking occurs when the subject is not paying much attention to where he/she is looking but is attending to inner thought (covert attention). The latter poses a big problem for eye movement analysis as humans can voluntarily dissociate attention from ocular eye movements (foveal direction of gaze). It is difficult to spot when the user does not perceive the region fixated, hence it is impossible to obtain meaningful data during this stage.

The eye is attracted to regions of a scene that convey what is thought at the time to be the most important information for scene interpretation. Initially these regions are pre-attentive in that no recognition takes place, but moments later in the gaze the fixation points depend more upon either our own personal interests and experience or a set task. Humans perceive visual scenes differently. We are presented with visual information when we open our eyes and carry out non-stop interpretation without difficulty. Research in the extraction of information from visual scenes has been explored by Rayner [89], Yarbus [84], Mackworth and Morandi [39], and Hendersen and Hollingworth [22]. Mackworth and Morandi [39] found that fixation density was related to the measure of informativeness for different regions of a picture and that few fixations were made to regions rated as uninformative. The picture was segmented and a separate group of observers were asked to grade the informativeness. Henderson and Hollingworth [22] described semantic informativeness as the meaning of an image region and visual informativeness as the structural information. Fixation positions were more influenced by the former compared to the latter. The determination of informativeness and corresponding eye movements is influenced by task demands [84]. Underwood [91] was also able to show in a task requiring detection of a small target, that the visual saliency of non-targets did not influence fixations (viewers were able to ignore visually prominent objects). The failure of low-level saliency maps prompted a modification to take task dependency into account in Navalpakkam and Itti's new model [44]. The model determines the task relevance of an entity, biases attention

for the low-level visual features of desired targets, recognizes these targets using the same features and incrementally builds a visual map of task relevance at every scene location.

The dominance of a high saliency object in a memory experiment was also not present in another search task conducted by Underwood [90]. Four models of eye guidance were evaluated with data from two separate memory experiments by Tatler et al [73] and Underwood et al [90].

The *salience divergence* model proposes that the balance between top down and bottom up control of saccade target selection changes over time. Specifically, the bottom up component is more influential early in viewing, but becomes less so as viewing progresses [54]. This framework predicts that the difference between saliency at fixated locations and at non-fixated locations will be greatest early in viewing. Tatler et al [73] and Underwood et al [90] rejected this model, as they did not find variations in the saliency values of fixated and non-fixated locations.

In the *salience rank* model, locations in the scene are ranked according to their visual salience and the oculomotor system selects targets sequentially according to this ranking [30]. Sequential selection of targets based upon visual salience rankings would predict large differences between saliencies at saccaded to locations and those at non-saccaded to locations early in viewing, but smaller differences later on. Again, the data from Tatler et al [73] and Underwood et al [90] did not provide support, as there was no change in the discrimination between the salience at saccaded to and non-saccaded to locations.

The *random selection with distance weighting* model of target selection [41] suggests that targets are selected using a proximity-weighted random walk process. Within this model, the selection of locations for fixation is essentially random with respect to both bottom-up and top-down processes. This model predicts the variability of inspection patterns between viewers inspecting the same scene, whereas there was consistency in the locations of early fixations in the Tatler et al [73] experiment. Underwood found predictable and consistent inspection patterns in the inspection of two objects of interest in each picture.

The fourth model for saccadic targeting considered is *strategic divergence* [73], where the influence of low-level visual feature salience on saccadic targeting does not change during viewing, but cognitive influences do vary. This framework is consistent with findings from both Tatler et al [73] and Underwood et al's [90] experiments. Consistency in fixation location changes between viewers over time, but the influence of image features does not. Thus the strategic divergence account proposes that the strategies chosen by viewers have the same bottom up framework for eye movements, but over time viewers use different top-down strategies to complete the memory task imposed in these experiments.

Henderson and Hollingworth [22] review three areas of high-level scene perception research. The first concerns the role of eye movements in scene perception, focusing on the influence of ongoing cognitive processing on the position and duration of fixations in a scene. They

speculate on whether ongoing perceptual and semantic processing accounts for the variability of fixation durations, which range from less than 50ms to more than 1000ms in a skewed distribution with a mode of about 230ms. The average fixation duration during scene viewing is also said to be 330ms, with a significant variability around this mean. Their review of eye movement studies during scene viewing suggests that fixation positions are non-random, with fixations clustering on both visually and semantically informative regions. They also found that the placement of the first few fixations in a scene seems to be controlled by the visual features in the scene and the global (not local) semantic characteristics of the scene. As viewing progresses and local regions are fixated and semantically analyzed, positions of later fixations come to be controlled by both the visual and semantic characteristics of those local regions. The length of time the eyes remain in a given region is immediately affected by both characteristics. It was noted that a number of factors varied from study to study, including image size, viewing time per scene, image content and viewing tasks.

The second area concerns the nature of the scene representation that is retained across a saccade and other brief time intervals during ongoing scene perception. The literature reviewed suggests that only a limited amount of information is carried across saccades during complex, natural scene viewing and that this information is coded and stored in a relatively abstract (non-perceptual) format. The change blindness effect [60] suggests that little of the information that is latent in the retinal image during a fixation is encoded into an enduring form that can be retained across a saccade or other intervening temporal gap. Rensink et al [92] proposed that a limited-capacity attentional mechanism must select perceptual information from an iconic store during a fixation and transfer it to a more stable and longer-lasting visual short-term memory (VSTM) representation if it is to be retained. In this hypothesis, scene regions that are more likely to be attended during scene viewing should be more likely to be encoded and stored in a stable format. Rensink [92] found that change detection was better when the changing object was semantically informative. On the assumption that semantic informativeness holds attention, attention is needed to transfer information to a stable medium (e.g. VSTM) if that information is to be available to support the detection of changes.

Thirdly, Henderson et al review research on the relationship between scene and object identification, focusing particularly on whether the meaning of a scene influences the identification of constituent objects. Research in scene identification has focussed primarily on the time course of scene identification and the types of information used to identify a scene. Potter's studies [93] presented a series of photographs of scenes in rapid succession. When a verbal description of a target scene was provided prior to presentation of the series, participants were able to detect a target scene at a presentation rate of 113ms. This led to the conclusion that a scene can be identified in approximately 100ms. Note that scene descriptions did not specify the global identity of the scene but instead described individual objects in the scene. Schyns &

Oliva [94] have demonstrated that a photograph of a scene can be identified as a particular scene type from a masked presentation in as short as 45 – 135 ms. These results demonstrate that the information necessary to identify a scene can be extracted quickly. Most research has supported the idea that early scene processing is based on global scene information rather than local object information. Schyns & Oliva [94] demonstrated that scenes can be identified from low-spatial-frequency images that preserve the spatial relations between large-scale structures in the scene but which lack the visual detail needed to identify local objects. In addition, when identifying a scene from a very brief view (50ms), participants tend to base their interpretation on low-frequency information rather than on high-frequency information. Henderson et al conclude that scene context facilitates the identification of objects.

Rayner's review [89] also concluded that given the existing data, there is fairly good evidence that information is abstracted throughout the time course of viewing a scene. While the gist of the scene is obtained early in viewing, further information from the scene is obtained after the initial fixations.

2.2. Commercial Review

The management (storage, retrieval and processing) of digital visual data is becoming more important in this information age. Integration of digital devices such as digital cameras, mobile phones, PDAs and computers has contributed to the critical need for automated multimedia indexing and retrieval of relevant information. Many everyday life activities result in the accumulation of huge amounts of data containing different kinds of information (text, pictures, audio, videos, etc.). The goal of information retrieval technologies is to allow one to make an effective use of such data. Storage devices seem to be growing fast and coping with this demand but it has also meant data is sometimes stored and almost never used. Mostly, this is because users either forget possessing this data or cannot locate it when it is needed. This is applicable especially with digital visual data, where users would like to improve access mechanisms and interaction with this data.

This critical need for good interfaces is leading to exploration of natural or perceptual user interfaces that make use of facial expression, gestures, touch, speech and eye movements. Nearly all computer applications today operate by some sort of command system (by explicit command-line interfaces or direct manipulation interfaces), requiring the user to view the computer as a collection of tools that must be activated to solve a required task. As a result, information from natural interfaces such as gestures, expressions and/or eyes may be employed for issuing commands to solve tasks. The use of these natural interfaces has not been in demand because these mediums are presented as a replacement for conventional interfaces (such as the mouse and keyboard). The next generation of interactive user interfaces should be able to

determine users' interests from normal user activities. The mouse, keyboard, speech, and touch require a thought process before issuing commands. Important information is lost during this transfer which may be more effectively captured by eye tracking. It has been shown and widely accepted in prior eye tracking studies that determination of relevance and corresponding eye movements are influenced by task demands [84][88][91]. This raises the likelihood of modelling behaviour based on respective applications or set tasks, prompting an exploration of interactive eye tracking applications.

Understanding human gaze behaviour is critical in obtaining effective interfaces and has been the subject of scientific research since the 1800s. The improvement in eye tracking hardware is extending its usage beyond the laboratory. Though it is not a widely adopted technology at the moment, it is being widely recognised as the most convenient and non-invasive medium for understanding human behaviour [11]. This usage ranges from laboratory experiments for medical research [109] to the more recent customer and usability research [40]. Historically organisations have always been preoccupied with new ways of finding the right customer due to increasing competition, which has brought about the need for better advertising.

In summary, eye tracking technology can enhance access to information and in so doing improves efficiency for both individuals and organisations. This information can be in the form of where, when and how the user is looking.

2.2.1. Applications

This subsection summarises current and potential applications (refer to [10] or [11] for a detailed review of eye tracking applications).

- Eye tracking serves as a viable alternative to conventional input devices (e.g. mouse and keyboard) for certain disabled users [6]. This technology will continue to be useful for this type of users.
- Eye tracking can potentially be used as a safety device or early warning system for indications of drowsiness or lack of concentration when operating machinery such as motor vehicles, power stations and air traffic control systems [16][65].
- Eye tracking is increasingly being used by marketing companies to investigate the usability of products and effectiveness of advertisements [110]. Conventional usability techniques rely on data, which may have been obtained by leading questions that can bias the judgement of users and relies heavily on the diligence of the usability researcher. Analysing what potential customers may be looking for in an advert through objective data produced by an eye tracker, can be used to optimise the effectiveness of the adverts. Advertisements can take the form of TV commercials, and printed and website advertisements. It can also be used in

investigating catalogue browsing online or in-store product browsing and to test the effectiveness of interfaces such as websites [40].

- Eye tracking serves as a good indication of interest for improving human computer interaction. Eye tracking interfaces can aid automatic scrolling function on screens, zooming interfaces [69][80], video conferencing [111], etc. The improvement can vary from the system automatically issuing a command based on user's gaze behaviour to smart systems that can anticipate the user's need based on knowledge acquired by the system during real-time viewing. However, outstanding issues (such as accuracy and interpretation) need further research.
- Historically eye tracking has been used for neurological and psychological research to understand the human visual system and its cognitive processes [112]. Numerous findings have been useful for understanding certain neurological disorders [109] and improving human machine interaction by computer scientists [47][68].
- Eye tracking can be used for applications that require visual inspections such as search and rescue operations [85], manufacturing defects, x-rays and picture interpretation (art) [113]. Tracking eye movement of an expert's visual inspection may be used to train novice inspectors providing a gaze pattern emerges [12].

2.2.2. Market Analysis

It takes a huge effort to develop markets for new technology. The processes of making and demonstrating the possibilities of innovation, developing new standards and encouraging complementary products and services are often only available to the largest organisations. Unless smaller organisations can attract the attention of larger partners, they are often left to fit new technology into older standards, and have to wait for changes in complementary technologies, infrastructure, regulations, skills and priorities.

Probably the most obvious trend is the increase in the marketing of eye tracking devices (Table 2.1), which has led to a reduction in prices. Limited demand has certainly contributed to the high cost of purchase. A typical eye tracker comprises LED (infrared source), hot mirror (filter that reflects the infrared into a CCD camera), fibre optic bundle (communicating device), CCD camera and framegrabber (for capturing image from camera into the host computer). Software development is then required to enable the technology to be used in the application domain.

The greater emphasis in society on quick and reliable access to relevant information will drive political and organisational agendas on the need for compact, relatively cheap, non-intrusive methods of exploration and interaction. An example is the rising public demand and

government initiatives for a decrease in road accidents could influence changes in policy to accommodate eye trackers in vehicles for monitoring driver awareness.

In order to see where we are going, we need to see where we are. Eye tracking has experienced significant growth since the early laboratory studies at the beginning of the 20th century to the video-based reflection methods of the latter decades. Yet eye tracking remains at the very early stage of adoption, leaving one to wonder why such a technology has not crossed into the mass market. The advances in eye tracking technology occurred mostly as a result of advances in computing and imaging technology in the late 80s, which led to the realisation of the interactive capability of eye tracking [10]. This has given support to the speculation that eye tracking may enter the mass market (i.e. cross the chasm as shown in Figure 2.4) through interactive applications.

The Sony EyeToy™ (Sony Computer Entertainment Inc., http://www.eyetoy.com/) introduced a new full body interaction game using a camera to monitor body movements for the PlayStation 2. It shows an image of the user inside the game environment. The user is then monitored by analysing the video frames. The success of this technology highlights the possible future influence of games based on natural interaction such as the eyes.

The Canon EOS Camera Series and the UC-X1 Hi Video Camera tracks the eye to control camera focussing. Canon EOS Elan 7E is the latest in the EOS series and uses the nearest of 7 eye-selection points in the viewfinder shown through the ocular and the camera adjusts its features (e.g. focus) accordingly.

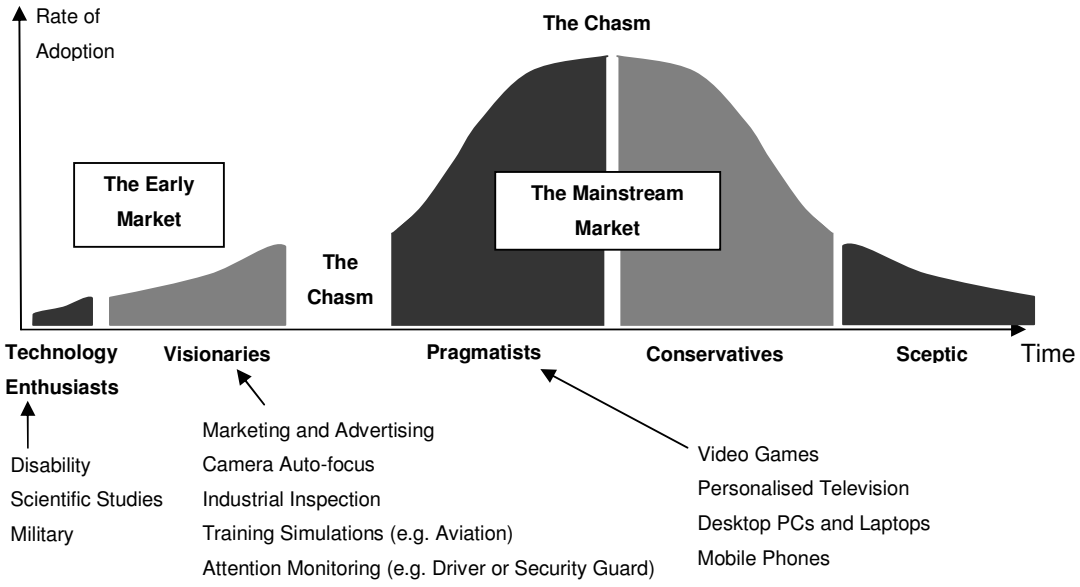

Figure 2.4: Potential evolution of the eye tracking market

Sharp recently filed a patent in November 2004 (International Application Number: PCT/US2004/039085) titled Liquid Crystal Display with Adaptive Colour. It uses a method for correcting the colour shift of the gaze location on a display based on viewing angle. The patent aims to maximise viewing clarity regardless of the viewing angle of the user (i.e. during off-centre viewing).

44 other eye tracking related patents has been filed with the World Intellectual Property Organisation [102] since 1998, which are described briefly in Appendix D. The international application numbers are provided to allow further investigation on the WIPO website [102]. The number of filed patents that utilises this technology also serves to highlight the anticipation of eye tracking technology take-up and the need to protect this possible source of future revenue.

The success of Cannon's EOS series has been largely due to this automated focus capability, which is reliant on eye tracking. Sharp's patent also serves to highlight the anticipation of software based face/eye/gaze tracking on PCs and/or laptops. Eye-toy introduced a new form of social gaming that is independent of commands. Its success is thus a good precursor for gaze-based gaming.

2.3. Technology

2.3.1. Comparison of Recent Commercial Eye Trackers

Table 2.1 lists some of the recent commercial eye trackers available on the market and highlights their characteristics. This list is by no means exhaustive and the prices are a reflection of the functionality. There has been a significant increase in sampling rates from 50Hz to 1250Hz, which means that future eye trackers will be able to track fast saccadic movements very accurately.

Table 2.1: Commercial Video-based Eye Trackers

Eye trackers	Uniqueness	Sampling Rate (Hz)†	Subject Contact	Measurement technique*	Typical Price*‡
SR Research's Eyelink II [28]	Fast and Binocular	500	Headmount	PCR	€29,950 (h,s)
SR Research's Eyelink 1000 [28]	Fast sampling	1000	Chinrest	PCR	€29,950 (h,s)
LC Technologies' Eyegaze [27]	-	60	None	PCR	$17,900 (h,s,pc,m)
LC Technologies' EyeFollower [27]	Binocular, remote and free head range	120	None	PCR	$43,400 (h,s,pc,m)
ASL H6 [25]	lightweight	360	Headmount	PCR	
ASL R6 [25]	Remote and optional fast sampling	360	None	PCR	
SMI's iView X Hi-Speed	Very fast sampling	1250	Chinrest	PCR	
SMI's iView X HED	-	50/60	Headmount	PCR	
Seeing Machine's faceLAB4	Eye and Head tracking	60	None	Software	£20,000 (-)
Tobii 1750	Binocular and integrated into monitor	50	None	PCR	£15,500 (h,m)
Tobii x50	Remote scene viewing	50	None	PCR	£16,800 (h,m)
CRS Video Eye Tracker	Low-cost	50	Chinrest	PCR	£6000 (h,s)
CRS High-Speed VET	-	250	Chinrest	PCR	£10,000 (h,s)
ERT's Erica System	Low-cost	60	None	PCR	$7,900 (-)
Smarteye Pro	Includes face tracking	60	None	PCR	€25,000 (-)
Arrington's Viewpoint Quickclamp System	Low-cost	60	Chinrest	PCR	$6,498 (h,s,m,pc)
Arrington's Remote System with precision head positioner	Low-cost	60	None	PCR	$7,998 (h,s,m,pc)
Microguide BIRO	Lightweight	100	Headmount	PCR	
Eyetech Digital's Quickglance 2SH	Low-cost	15	None	PCR	€6,000 (h,s)
ISCAN's Visiontrak Standard	-	60	Headmount	PCR	$17,100 (h,s,m,pc)
ISCAN's Visiontrak ETL-300	-	60	None	PCR	$17,400 (h,s,m,pc)

* What is included (h – main hardware; s – basic software; PCR – Pupil Corneal Reflection; pc – host system; m – monitor). ‡ Price difference can also be due to other factors such as tracking accuracy.
† Some manufacturers offer higher sampling rate as an additional option.

2.3.2. Threats and Mitigations

In the early years of eye tracking in interactive applications, the focus was on using the eye as a replacement for conventional input devices (mouse and keyboard). While this may be fine for disabled users, it was not a good enough reason to expect other types of users to forsake conventional devices. Recently research is moving towards using the eye as a continuous indication of interest and not just for selection, which could make it a radical innovation and thus a worthy competitor for the conventional input device.

Multimodal interfaces (such as gaze and speech) have been suggested for more effective interfaces.

Eye tracking may not work on a percentage of population (i.e. users wearing thick lens spectacles or certain disabled users with spinal cord injuries). The proportion of the population that are excluded is not clear but it may not be large.

Lack of interoperability, lack of standards within and across industries, concerns about the stability (permanence) of eye tracking technology, lack of widespread deployment and costs have all contributed to the slow take-up but this is expected from an emerging technology.

The reduction in intrusiveness, the improvements in cost, speed and accuracy are all expected to continue. At the Eye Tracking Research and Applications 2006 conference in San Diego, California, the I-Prize [100] was launched as a grand challenge for human computer interaction. Its aim is to encourage radical innovations in eye tracking. This type of grand challenge has been successful in stimulating and initiating commercial space flights, land speed records and fully autonomous vehicles. The aim is to revolutionize eye tracking by seeking 'factors of 10' improvements in the price ($10000 → $100), accuracy ($1^o$ → 0.1^o), speed (50/100Hz → 500Hz) and intrusiveness (remote and calibration-free).

The demand on user attention required by eye tracking is not an attractive aspect of the system. This level of attention may induce long-term stress. Lack of concentration such as user looking away or attending to inner thoughts, complicates the real-time analysis of resulting data.

The feasibility of using eye trackers in an uncontrolled environment is a serious problem. For example, the reflections caused by certain eyeglasses have been approached with adaptive threshold techniques to differentiate the pupil glint and corneal reflection from the reflection of the glass lens. More robust imaging techniques are needed to solve this problem. Most eye trackers require limited head movement which is not ideal for real-world applications. Recently LC Technologies released EyeFollower which accommodates a wider range of free head movement. Such innovations highlight the continuous progress of eye trackers.

Security and access control may be an issue. The system has to be able to identify which user's eye movement is controlling an eye tracking system.

Increased investment is needed for further investigations of adaptive algorithms to improve selection or interest prediction models for individual users.

As with most technologies that are capable of extracting and digitising intimate details about individual users, public perception will need to be improved by sufficient consumer education and maintenance of ethical standards.

A recent report [99] identifies several projects and Networks of excellence funded by the European Union Framework Programme (FP6), of which COGAIN stands out. COGAIN (Communication by Gaze Interaction) is a Network of Excellence which integrates cutting-edge expertise on interface technologies for the benefit of users with disabilities with emphasis on eye tracking. The European Union presently uses Networks of Excellence (NoE) to strengthen the scientific and technological excellence on a particular research topic. A recent report deliverable is available in [101]. The project costs 2.72 million euro and received 2.90 million euro funding from the EU research budget. The COGAIN NoE is a major step that may lead to more eye tracking projects sponsored in future EU research projects.

2.4. Discussion

Eye behaviour is a reflection of our interests. Eye tracking systems provide an approach for characterizing a computer user's ocular behaviour. Eye tracking equipments have developed substantially from the invasive methods employed before the 70's [8][61] to the current and more efficient non-invasive methods using video and/or infrared technology [24][25][26][27][28][29][37]. These advances have led to a significant price reduction and increases in sampling rates, enabling more efficient tracking of saccades. Two main shortcomings have been identified with eye tracking systems and attempts have been made with varying success to minimise their effects [42][67]. Firstly, eye tracking hardware systems must limit image processing to attain real-time performance in order to achieve maximum accuracy of the eye movement measurement [42]. Blinking has been suggested both for rapid eye localisation [3] and solving the Midas-touch problem (i.e. recognizing when the user needs to make a selection) [13]. Besides, experiments have shown that the eye is relatively faster than the mouse as a source of computer inputs in various applications [47][68][81][83]. Secondly, even though eye fixations provide some of the best measures of visual interest, they do not necessarily provide a measure of cognitive interest. Though eye tracking offers an objective view of overt human visual and attention processes, it does not provide a measure of covert attention due to the orientation of thought looking [18]. We are confronted with an overwhelming amount of visual information whenever we open our eyes. Covert attention allows us to select visual information at a cued location, without eye movements, and to grant such information priority in processing. The lack of eye tracking data during this attentional

state could affect the validity of any conclusions regarding interest however incidences of covert attention are reduced when tasks are set.

Research in eye tracking has become more focused depending on the application and this has helped in achieving highly accurate analysis. Indeed, the application ranges from interactive usage (i.e. gaze contingent displays [45], assisting disabled users [6], varying screen scrolling speed [46], activation of controls in aircrafts [65], improving efficiency of search and rescue operations [85]) to passive usage [32][48][55][57], which involves subsequent diagnostic analysis.

The increase in interactive applications has prompted research into usability requirements for effective interfaces, mostly motivated by the integration of digital devices. Dasher's text entry interface [80] employs a suggestive zooming interface that may be applicable to images, thus presenting a promising interface worthy of further investigation. Xin Fan et al [82] conducted a user feedback evaluation on their image viewing technique using the mouse to indicate interest. The validity of this approach is confounded by the fact that cognitive feedback at the time of viewing and the feedback at the time of evaluation are not necessarily similar. Hence an alternative method of conducting such evaluations using real-time systems such as eye trackers for validation is a distinct possibility. Nonetheless, Xin Fan's image viewing technique [82], the collage form of web recombination [35], and Farid's zooming technique [15] provide interface methods that may be implemented in future eye tracking interfaces. Nokia's usability evaluation [78] also provides encouraging results with regard to the viability of future implementations of image search on digital devices such as mobile phones.

Eye tracking work has also concentrated upon replacing and extending existing computer interface mechanisms rather than creating a new form of interaction. As gaze reflects our attention, intention and desire, it can be used as a natural form of interaction [4][18]. The imprecise nature of saccades and fixation points makes it difficult to yield benefits over conventional human interfaces. Fixations and saccades are used to analyze eye movements, but it is evident that the statistical approaches to interpretation (such as clustering, summation and differentiation) are insufficient for identifying salience in an image due to the differences in humans' perception of image content.

Several eye tracking experiments have been conducted on images, mostly with the aim of creating or improving algorithms and/or models that simulate the human visual system [32][54][55][56][57][70]. The recent advances in eye tracking technology have played a large part in encouraging more research into image analysis. Eye tracking experiments enable better understanding of the human visual system (HVS) from which models are derived as well as improved interactive applications. For example, the eye tracking experiments conducted by Privitera [57] and Jaimes [32] were used to provide a validation for visual attention models. Computational models of visual search have been implemented in CBIR systems such as QBIC

[95], MARS [96], PICASSO [97] and Blobworld [98]. CBIR systems normally rank the relevance between a query image and target images according to a similarity measure based on a set of features (colour, shape, edges). Research in visual attention and perception has identified the importance of cognitive influences in determining relevant materials from a picture or scene [22][73][91]. The formulation of queries that are both easy and intuitive to create whilst at the same time being effective for retrieval is a problem that is common to all CBIR systems. It has been shown that data derived from eye gaze behaviour indicates salience and therefore provides a likely source of relevance feedback for query formulation. However, there is little published research that carries this belief forward to a retrieval mechanism that makes use of this channel of information and CBIR is an application that would benefit from positive findings in this field.

2.5. Thesis Statement

Different individuals or even the same individual in different situations can perceive the same visual content differently. This is clearly a barrier to efficient CBIR that may be overcome with more effective interfaces. This adds motivation for the thesis that will be addressed in this research, which can be stated as follows:

"Eye tracking data provides more information relevant for query formulation in image retrieval that is not otherwise obtainable through existing conventional interfaces".

An eye controlled image retrieval interface will not only provide a more natural mode of retrieval but also potentially have the ability to anticipate the user's requirements of rapidly retrieving images with a minimum of thought and manual involvement. To the author's knowledge, there are only three other research groups [14][19][64] where eye tracking has been used in related work, however, they lack experimental validity in the context of CBIR.

2.5.1. Key Research Questions

To support this thesis statement, key research questions will need to be answered:

1. Is there an informative relationship between gaze behaviour and a computational model of visual search?
2. Can data from gaze behaviour be used to exceed the performance of other interface devices for visual tasks?
3. What methodology should be used to measure subjects' gaze behaviour?
4. How can fixations and saccades from eye tracking data provide extra information relevant to image retrieval?
5. Are there any limits to the speed of operation of a gaze driven retrieval interface?

6. What software and data frameworks are needed for the human eye to control an image retrieval interface?

The literature review has shown the viability of eye tracking as a way of inferring interest. Question 1 investigates the relationship between gaze behaviour and a model of visual attention in order to partly validate the model and to assess the validity of the gaze data.

Question 2 is aimed at investigating the effectiveness of an interface controlled by gaze behaviour when compared with other interfaces.

Question 3 establishes the comparative framework within which each experiment is conducted to obtain significant results.

Question 4 goes further by asking how this human visual behaviour can be exploited as visual input into a CBIR system and whether the time sequence of the eye tracking data can also provide new information relevant to image retrieval. For example, the mouse click is a mode of selection that takes place after a thought process. In this case, information from the thought process cannot be recorded. However eye tracking data provides a means of recording this information which may yield new and relevant information.

Question 5 investigates the limits of speed of operation of the eye gaze interface for controlling image retrieval.

Question 6 investigates the implementation needed to produce an eye controlled image retrieval interface. It defines the types of data and storage requirements as well as the processing resources and the timing constraints.

Chapter 3. Methodology

3.1. Proposed System

In this system it is proposed that the eye movement is used to formulate queries for CBIR processing as depicted in Figure 3.1. It is intended that this should provide a rapid and natural interface for searching visual digital data in an image database. A pre-computed network of similarities (Figure 3.13) between images in an image collection may be traversed very rapidly using eye tracking providing the users' gaze behaviours yield suitable information about their intentions. It is reasonable to believe that users will look at the objects in which they are interested during a search and this provides the machine with the necessary information to retrieve plausible candidate images for the user. Retrieved images will contain regions that possess similarity links with the previously gazed regions, and can be presented to the user in a variety of ways.

As shown in Figure 3.1, the system is composed of four main parts: the eye tracking interface, the query formulation process, the image retrieval process and the indexing process. Eye tracking systems produce gaze parameters that may be compared and significant gaze patterns extracted. Parameters that can be obtained for query formulation include:

- the duration of time that the user spends looking at an image (fixation),
- the number of fixations on an image,
- scan patterns (i.e. which images were viewed before or after other images), and
- longer term changes in pupil size (e.g. during a session).

The indexing process uses a similarity measure for the offline computation of similarity between images so that images similar to the query image can be successively presented to the user in the search process. Relevant images are retrieved using the similarity links generated.

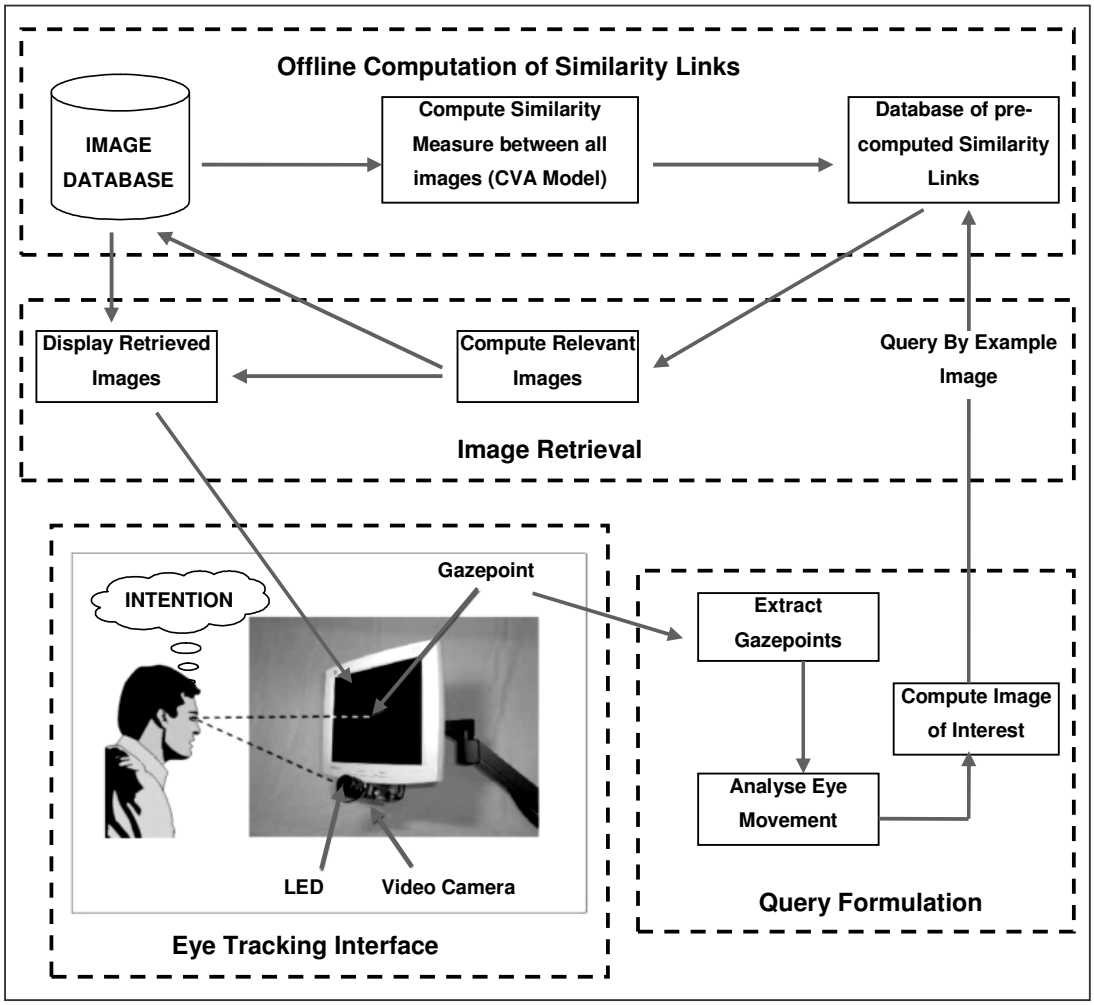

Figure 3.1: System Architecture

3.2. Eye Tracking Apparatus and Setup

The technical facility employed in the conduct of experiments is the Eyegaze eye tracker produced by LC Technologies Inc. [27].

3.2.1. Eye Tracking Equipment

The Eyegaze system is an eye tracker designed to measure where a person is looking on a computer screen. The Eyegaze System tracks the subject's gazepoint on the screen automatically and in real time. The experimental setup of the system is shown in Figure 3.2.

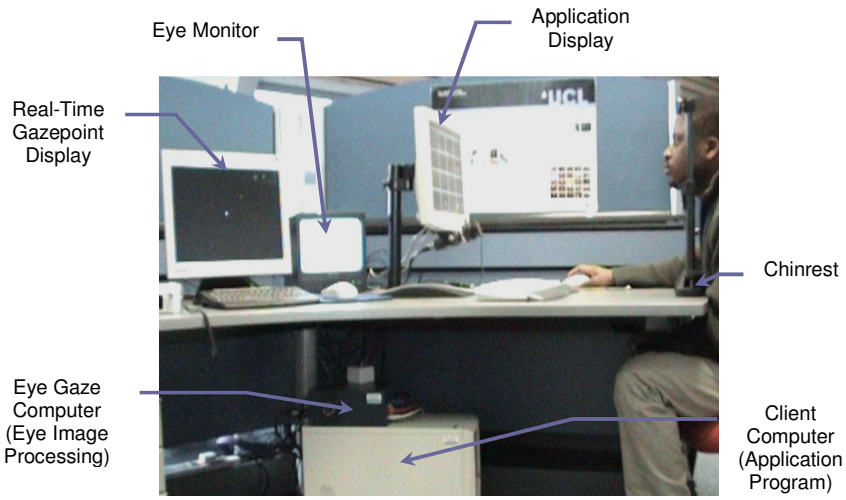

Figure 3.2: Experimental Setup

The Eyegaze System uses the Pupil-Centre/Corneal-Reflection (PCCR) method to determine the eye's gaze direction. A video camera located below the computer screen remotely and unobtrusively observes the subject's eye. No attachments to the head are required. A small low power infrared light emitting diode (LED) located at the centre of the camera lens illuminates the eye. The LED generates the corneal reflection and causes the bright pupil effect, which enhances the camera's image of the pupil (Figure 3.3).

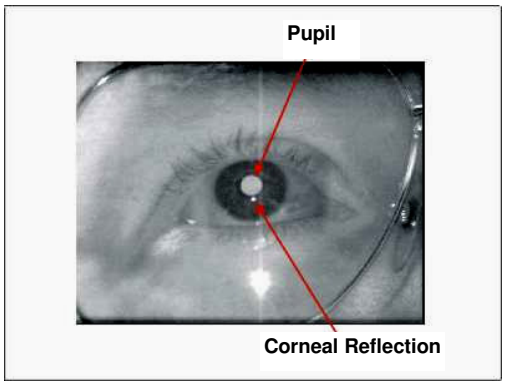

Figure 3.3: Camera image of eye, illustrating bright image pupil and corneal reflection (adapted from [37])

The accuracy of eye tracking systems depends in large measure on how precisely the image processing algorithms can locate the relative positions of pupil centre and the corneal reflection. Though it is possible to determine the boundary of the pupil in a normal picture of the eye, early

eye tracking systems used the bright-eye effect to enhance the image of the pupil, significantly increasing the accuracy of pupil location. To achieve the bright-eye effect, light is shone into the eye along the axis of the camera lens. The eye's lens focuses the light that enters the pupil onto a point on the retina. Because the typical retina is highly reflective, a significant portion of that light emerges back through the pupil, and the eye's lens serendipitously directs that light back along the camera axis right into the camera. Thus the pupil appears to the camera as a bright disk, which contrasts very clearly with the surrounding iris.

Specialized image-processing software in the Eyegaze computer identifies and locates the centres of both the pupil and corneal reflection. Trigonometric calculations project the person's gazepoint based on the positions of the pupil centre and the corneal reflection within the video image. The Eyegaze System generates raw gazepoint location data at the camera field rate of 50 Hz.

The procedure to calibrate the Eyegaze System is robust yet fast and easy to perform. The calibration procedure takes approximately 15 seconds and is fully automatic; no assistance from another person is required. The procedure does not accept full calibration until the overall gaze prediction accuracy and consistency exceed desired thresholds. To achieve high gazepoint tracking accuracy, the image processing algorithms in the Eyegaze System explicitly accommodate several common sources of gazepoint tracking error such as nonlinear gazepoint tracking equations, head range variation, pupil diameter variation and glint that straddles the pupil edge. A clamp with chin rest (Figure 3.2) provides support for chin and forehead in order to minimize the effects of head movements, although the eye tracker does accommodate head movement of up to 1.5 inches (3.8cm). It was not essential to use the chin rest, but this removed a potential source of error and eliminated any variance in head movement across subjects. A chin rest would not be acceptable in a practical CBIR system if it were used over an extended period of time. The system generates the eye found flag, gazepoint coordinates, pupil diameter, camera field count and location of the eyeball centre within the camera image.

3.2.2. Pupil Centre Corneal Reflection (PCCR) Method

The Eyegaze System uses the Pupil Centre Corneal Reflection (PCCR) method to measure the direction of the eye's gaze. The theory underlying the PCCR method states that the direction of the eye's gaze is directly related to the vector from the corneal reflection to the centre of the pupil within the camera image. This vector, often called the glint-pupil vector, is illustrated in Figure 3.4.

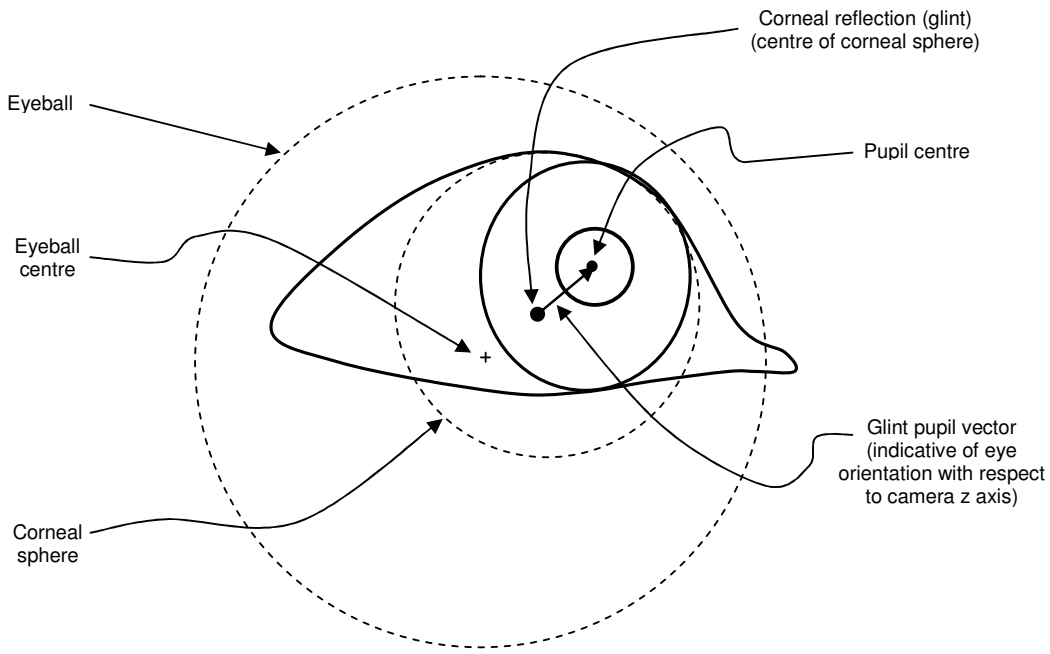

Figure 3.4: Glint-Pupil Vector and Direction of Gaze (PCCR Method) (adapted from [37])

When a person looks directly at the camera, the image of the corneal reflection appears near the centre of the pupil image. As the person rotates his gaze upwards away from the camera, the pupil centre moves upwards away from the corneal reflection and the glint-pupil vector points higher. Similarly, as the person rotates his gaze to the camera's right (which is his left), the pupil image moves to the right of the corneal reflection and the glint-pupil vector points further right. The PCCR Method applies equally whether using the bright or dark pupil effects. The PCCR theory is based on the following assumptions:

1. The eye's optic axis passes through two fixed points within the eye: the centre of the corneal sphere and the centre of the pupil.
2. The orientation of the eye can be inferred from the measurement of these two points.
3. The locations of these two points can be determined from the camera's image of the eye. The centre of the corneal sphere can be determined from the location of the corneal reflection, i.e. the reflection of the LED off the corneal surface of the eye.
4. The pupil centre can be calculated from the observable edges of the pupil image.

Figure 3.5 illustrates the geometric optics of the PCCR method. - The horizontal and vertical components of the eye's orientation angle, measured with respect to the line between the centre

of the camera lens and the centre of the corneal sphere, can thus be measured from the vector distance between the corneal reflection and the pupil centre within the camera image.

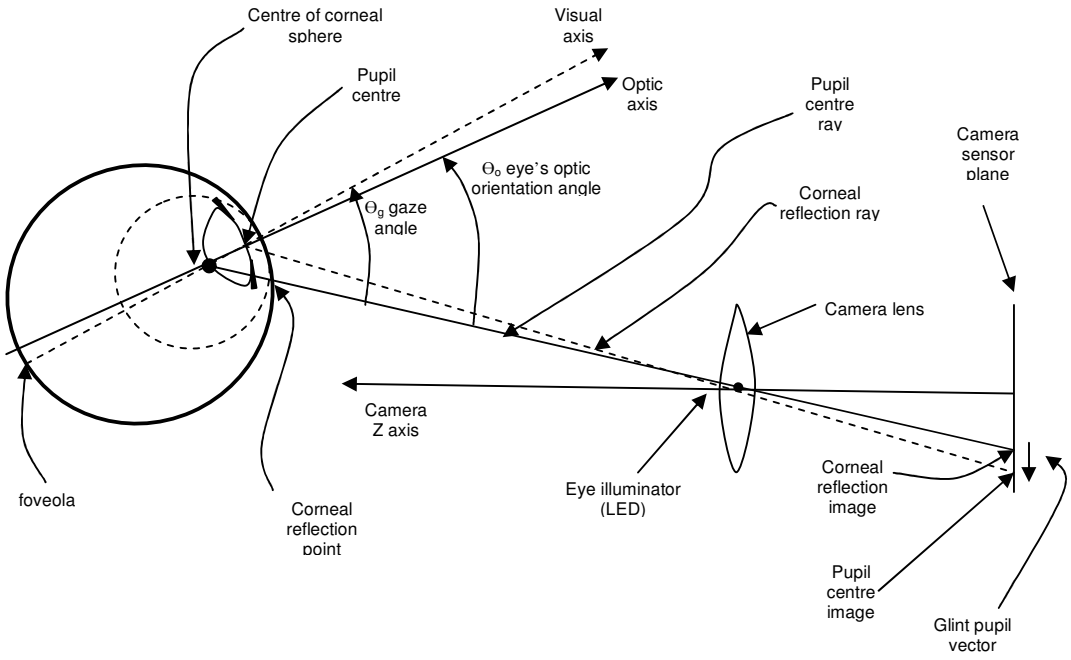

Figure 3.5: Geometric Optics of the PCCR Method (adapted from [37])

3.2.3. Computer Hardware and Software Configuration

The Eyegaze System can be used in two ways. In the Single Computer configuration, the eye tracking application program and the gazepoint calculations run directly on the Eyegaze System computer (Figure 3.6). In this case, the Eyegaze camera is mounted below the Eyegaze computer's monitor, which then performs the applications functions and drives the application display on its monitor, while also performing the Eyegaze image processing functions required to track the test subject's gazepoint. The single computer configuration is preferable for offline analysis of gaze data as it utilises limited resources. Application processing and gazepoint calculation are performed sequentially. The first experiment was performed using the Single Computer Configuration.

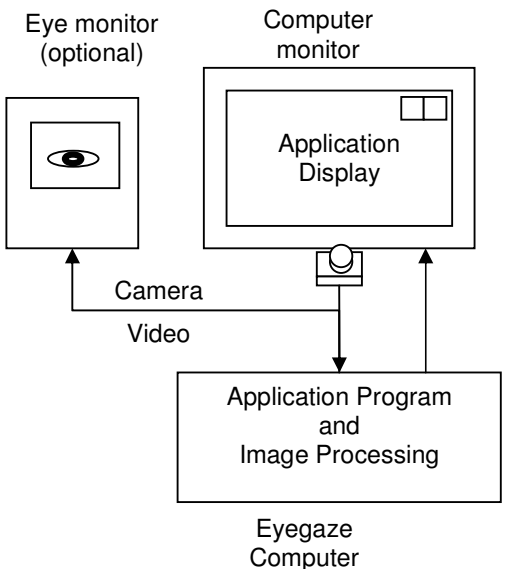

Figure 3.6: Single Computer Configuration (adapted from [37])

Subsequent experiments used the double computer configuration. In this configuration (Figure 3.7), the application program runs on another (client) computer and the Eyegaze computer acts as a peripheral eye tracking instrument, becoming a "black box" that transmits gazepoint data to the client via an Ethernet or serial communications link. The client computer performs the application functions and drives the applications display on its monitor. The Eyegaze camera is mounted below the client computer's monitor. The Eyegaze computer performs the Eyegaze image processing functions and transfers the measured gazepoint data to the client computer via either an Ethernet or a serial communications link in real time. The Eyegaze computer's monitor displays the subject's relative gazepoint in real time, allowing the application to determine the user's response online. The system can thus respond accordingly.

The double computer configuration is preferable if the application code consumes a large amount of CPU time (i.e. if there is not enough CPU time to execute both the application and Eyegaze image processing code in real time). The Eyegaze System is said to act as a peripheral device to a client computer in the Double Computer Configuration.

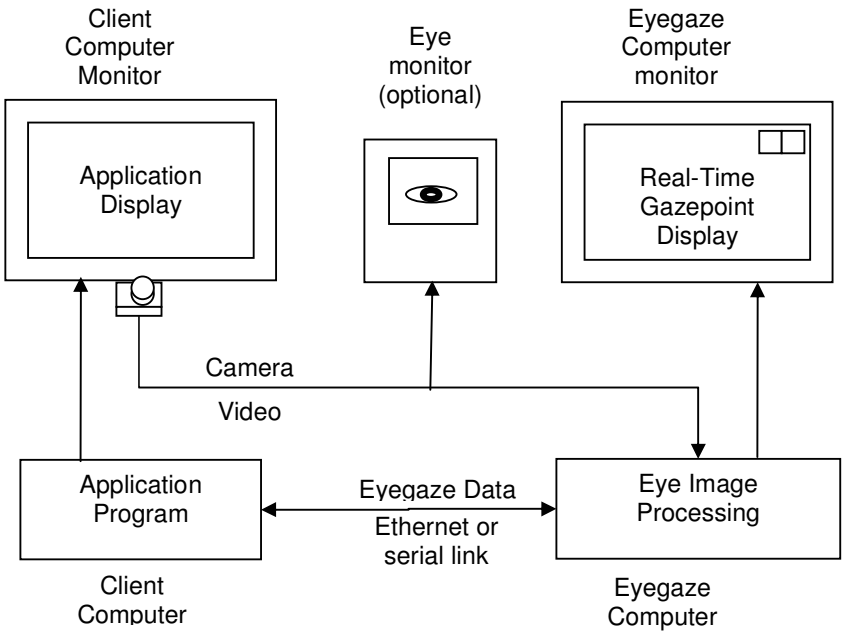

Figure 3.7: Double Computer Configuration (adapted from [37])

The Eyegaze System is used in the experiments to generate raw gazepoint location data at the camera field rate of 50 Hz (units of 20ms). There is a finite delay between the time that a subject's eye moves and the time that the Eyegaze System reports the eye movement data. The net delay is typically just less two sample intervals i.e. 35 milliseconds. Figure 3.8 illustrates the timing of these operations, highlighting the duration for Eyegaze data-collection and image processing. The Eyegaze image processing software is driven by interrupts generated from the frame grabber card. At each video field interval (20 milliseconds in the 50 Hz system), the frame grabber generates an interrupt and the frame-grabber's software drivers call back to the Eyegaze image processing software with the latest camera image (still frame) of the eye. The Eyegaze image processing software processes the camera image and sends the gaze data to the application. The Eyegaze image processing functions are given a high scheduling priority so that they can keep pace with the camera images generated in real time. The processing of information from the eye tracker is carried out on a 128MB Intel Pentium III system with a video frame grabber board.

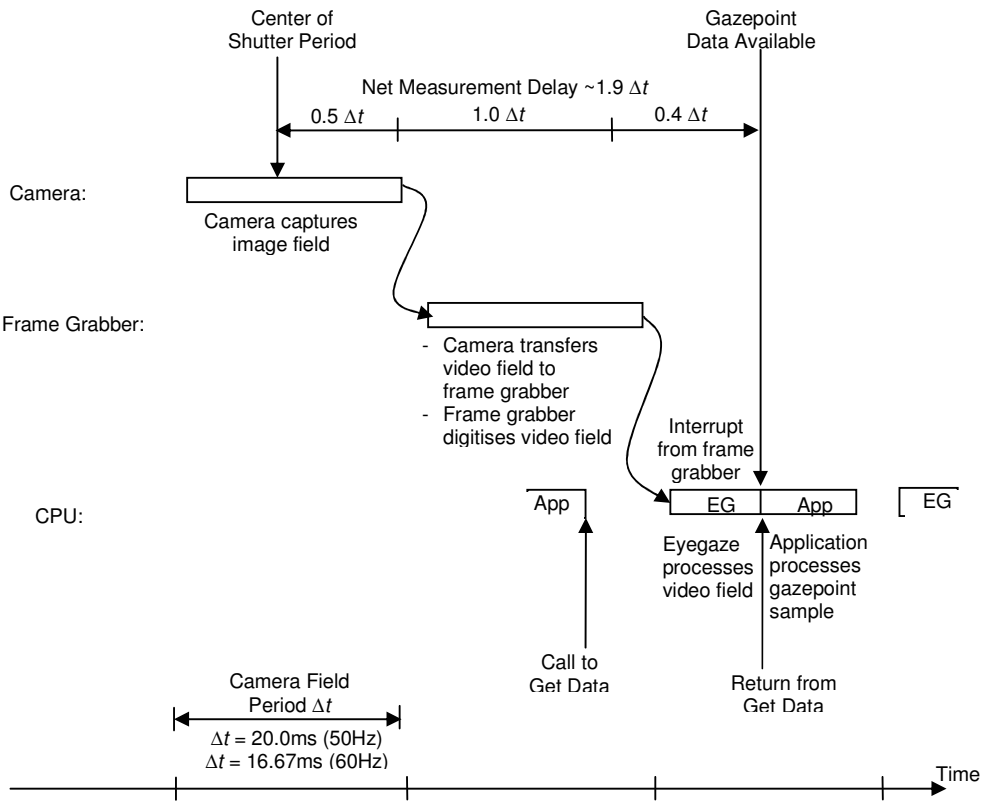

Figure 3.8: Gazepoint Measurement Delay (adapted from [37])

3.3. Eyegaze Data Collection

The eye gaze application converts a series of uniformly sampled (raw) gazepoints into a series of variable-duration saccades and fixations that can be extended based on findings from empirical data. Currently fixations are detected by looking for sequences of gazepoint measurements that remain relatively constant. If a new gazepoint lies within a circular region around the running average of an on-going fixation, the fixation is extended to include the new gazepoint. The radius of the acceptance circle on a region (Figure 3.9) is dependent on the duration of user's gazepoint on that region. The distance from average fixation to still be considered as part of that fixation (deviation threshold) was 12.7 pixels.

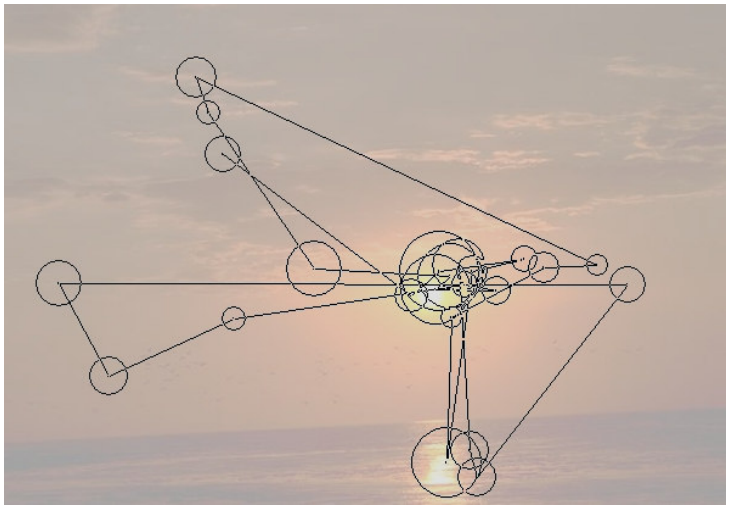

Figure 3.9: Fixations and Saccades

To accommodate noisy Eyegaze measurements, a gazepoint that exceeds the deviation threshold is included in an on-going fixation if the subsequent gazepoint returns to a position within the threshold. If a gazepoint is not found, during a blink for example, a fixation is extended if the next legitimate gazepoint measurement falls within the acceptance circle, and if there are less than the minimum fixation samples of successive missed gazepoints. Otherwise the previous fixation is considered to end at the last good gazepoint measurement. Zero or negative co-ordinates caused by blinks, excessive squinting and out of range data, could be significant and might be decipherable by careful denoising and analysis of resulting data. The Eyegaze System generates the gazepoint co-ordinates, pupil diameter, and fixation and saccade analysis.

3.4. Visual Attention and Similarity

It has been shown that attention mechanisms can be directly related to similarity measures [103] and affect the strength of those measures. During a search the human eye is attracted to salient regions and those regions probably have most impact and contribute most towards recognition and user search strategies. This work makes use of both aspects; first an attention model [103] is used to automatically identify candidate regions of interest for validation against eye tracking data where we would expect most fixations to occur; second an attention-based similarity metric is used to define visual relationships in a database of images for exploration with an eye tracking interface.

3.4.1. Overview of the Visual Attention Model

The Visual Attention (VA) model [103] employs an algorithm that assigns high attention scores to pixels where neighbouring pixel configurations do not match identical positional arrangements in other randomly selected neighbourhoods in the image. This means, for

example, that high scores will be associated with anomalous objects, or edges and boundaries, if those features do not predominate in the image. A flowchart describing this process is given in Figure 3.10.

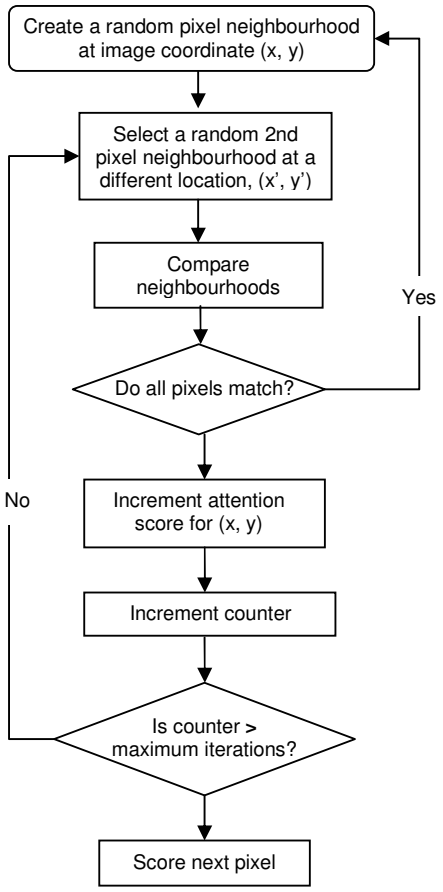

Figure 3.10: Visual Attention Model

The process of computing the attention score for a pixel *(x,y)* begins by selecting a small number of random pixels in the neighbourhood of *(x,y)*. Then another pixel *(x',y')* is selected randomly elsewhere in the image. The pixel configuration surrounding *(x,y)* is then evaluated with the same configuration around *(x',y')* and each pixel tested for a mismatch. If a mismatch is detected, the score for *(x,y)* is incremented and the process is repeated for another *(x',y')*. If the configurations match then the score is not incremented and a new random configuration around *(x,y)* is generated. The process loops for a fixed number of iterations for each *(x,y)*.

Regions obtain high scores if they possess features not present elsewhere in the image. Low scores tend to be assigned to regions that have features that are common in many other parts of the image. The VA scores for each pixel are displayed as a map using a continuous spectrum of false colours with the scores being marked with a distinctive colour as shown in Figure 3.11 .

The green colour represents the region with the highest visual attention scores while the red and black regions have lower scores.

Figure 3.11: Image with corresponding Visual Attention Map

3.4.2. Similarity Model

Studies in neurobiology and computer vision [9][31] are suggesting that human visual attention is enhanced through a process of competing interactions among neurons representing all of the stimuli present in the visual field. The competition results in the selection of a few points of attention and the suppression of irrelevant material. Such a mechanism has been explored [20] and extended to apply to the comparison of two images in which attention is drawn to those parts that are in common rather than their absence as in the case of saliency detection in a single image [1].

Image retrieval systems normally rank the relevance between a query image and target images according to a similarity measure based on a set of features. The similarity measure [103] used in this work, termed Cognitive Visual Attention (CVA model) is not dependent upon intuitively selected features, but instead upon the notion that the similarity of two patterns is determined by the number of features in common. This means that the measure can make use of a virtually unlimited universe of features rather than a tiny manually selected subset that will be unable to characterise many unseen classes of images. Moreover the features are deliberately selected from image regions that are salient according to the model and, if validated, reflect similarity as judged by a human. The CVA model relies upon the matching of large numbers of pairs of pixel groups (forks) taken from patterns A and B under comparison (Figure 3.12).

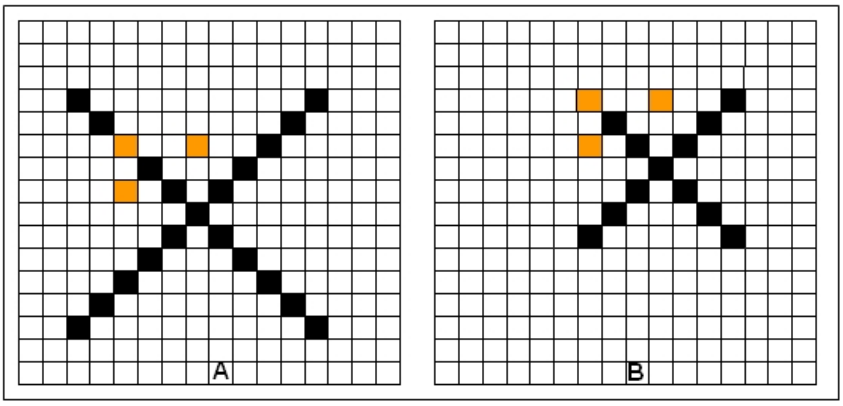

Figure 3.12: Neighbourhood at location x matching at y

Let a location $\boldsymbol{x}$ in a pattern correspond to a set of measurements $\boldsymbol{a}$

$$\boldsymbol{x} = (x_1, x_2) \text{ and } \boldsymbol{a} = (a_1, a_2, a_3)$$

Define a function $\boldsymbol{F}$ such that $\boldsymbol{a} = \boldsymbol{F}(x)$.

Select a fork of m random points S_A in Pattern A (e.g. 3 pixels shown in Figure 3.12) where

$$\boldsymbol{S_A} = \{\boldsymbol{x_1}, \boldsymbol{x_2}, \boldsymbol{x_3}, ..., \boldsymbol{x_m}\}. \quad (1)$$

Likewise select a fork of m random points S_B in Pattern B where

$$\boldsymbol{S_B} = \{\mathbf{y}_1, \boldsymbol{y_2}, \boldsymbol{y_3}, ..., \boldsymbol{y_m}\} \text{ where} \quad (2)$$

$$\boldsymbol{x_i} - \boldsymbol{y_i} = \boldsymbol{\delta} \quad (3)$$

The fork S_A matches fork S_B if

$$|\boldsymbol{F_j}(\boldsymbol{x_i}) - \boldsymbol{F_j}(\boldsymbol{y_i})| < \varepsilon_j \quad \forall i \text{ for some displacement } \boldsymbol{\delta} \quad (4)$$

In general $\boldsymbol{\varepsilon}$ is not a constant and will be dependent upon the measurements under comparison

$$\varepsilon_j = f_j(\boldsymbol{F(x)}, \boldsymbol{F(y)}) \quad (5)$$

In addition it is required that $|F_k(\boldsymbol{x}_i) - F_k(\boldsymbol{x}_j)| > \varepsilon_k$ for some k, $i \neq j$ so that some pixels in S_A mismatch each other and the similarity measure is taken over regions of high attention and not just on areas of sky, for example.

In effect up to N selections of the displacements $\boldsymbol{\delta}$ apply translations to S_A to seek a matching fork S_B.

The CVA similarity score C_{AB} is produced after generating and applying T forks S_A:

$$\boldsymbol{C_{AB}} = \sum_{i=1}^{T} \boldsymbol{w_i} \quad \text{where } w_i = 1 \text{ if } S_A \text{ matches fork } S_B \text{ or 0 otherwise.} \quad (6)$$

C_{AB} is large when a high number of forks are found to match both patterns A and B and represents features that both patterns share. In other words, the CVA similarity score is incremented each time one of the set of pixel sets matches a set in pattern B. This means that image pairs A, B which possess large numbers of matching forks will obtain high CVA scores by virtue of the number of such features they possess in common. It is important to note that if C_{AC} also has a high value it does not necessarily follow that C_{BC} is large because patterns B and C may still have no features in common. The measure is not constrained by the triangle inequality.

The CVA algorithm was applied to the 1000 images to pre-compute similarity scores for all pairs of images to obtain a similarity score matrix (Table 3.1 and Figure 3.13). The scores along the diagonal are always the largest as these are the cases where the patterns are being compared with themselves. In this example a query image 3 will produce image 8 as one of the most similar images where 241 is the highest score in the column ignoring the diagonal entry, followed by image 6 where 96 is the second highest score.

Table 3.1: Similarity Score Matrix

Images	1	2	3	4	5	6	7	8	9	10	…	1000
1	343	0	0	2	16	1	3	2	0	1	…	9
2	0	479	1	0	0	1	0	0	0	1	…	0
3	2	2	466	0	18	84	6	179	0	40	…	3
4	0	0	0	288	1	0	0	0	0	3	…	0
5	26	1	11	5	416	5	2	8	0	12	…	24
6	1	2	96	0	6	433	0	28	0	31	…	1
7	14	0	7	0	3	0	476	8	0	3	…	11
8	11	4	241	1	9	77	20	487	0	31	…	6
9	0	1	0	0	0	0	0	0	453	0	…	0
10	4	3	41	1	11	39	0	19	0	468	…	0
…	…	…	…	…	…	…	…	…	…	…	…	…
1000	22	1	9	0	37	0	18	9	0	1	11	444

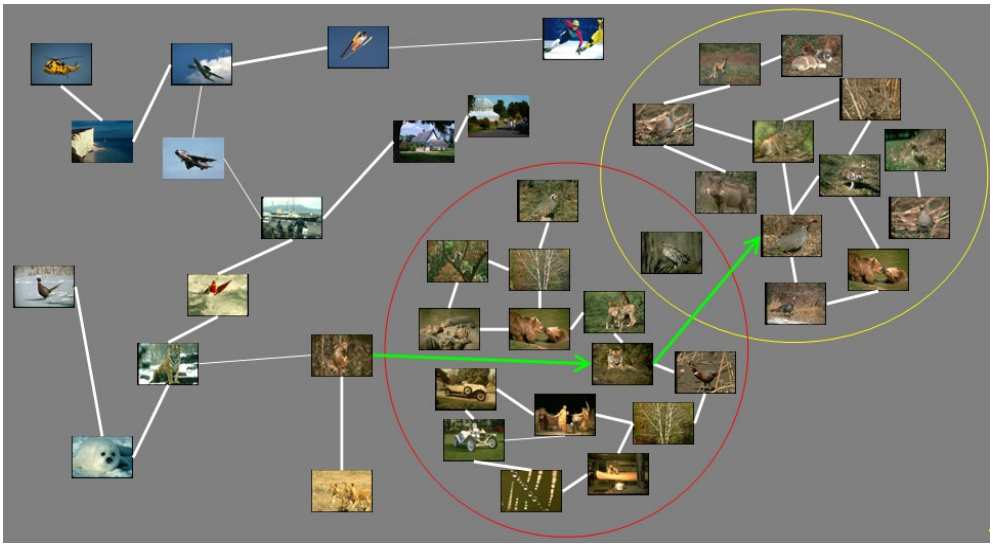

Figure 3.13: Representation of Pre-computed Similarity Links

The similarity measure is used for the offline computation of similarity between images so that images most similar to the query image can be successively presented to the user in the search process. The user is able to navigate the similarity links as illustrated by the green arrow/path in Figure 3.13.

Similarity values obtained in this way may be used to drive an image retrieval engine. However the computation requirements for the similarity matrix go up as the square of the number of images. It is envisaged that larger databases would be divided up into parts before analysis and a hierarchy of exemplars generated. Retrieval tasks would make use of such a hierarchy to identify clusters likely to contain target images rather than attempt to carry out an exhaustive search. It would be expected that as an image collection expands, new classes would be introduced and new clusters would emerge based on entirely different sets of features in common. This approach is implemented in [2], and identifies clusters within an extremely diverse set of images in the context of the identification of photo locations. It is significant that despite this diversity, the approach is able to extract visually similar clusters of images that can be classified according to location. It should be noted that the similarity metric was selected for its relationship to attention in which features are selected according to their attentiveness [103]. However, it was also selected for experimental expedience and other types of measure could have been used.

3.5. Summary

Ware and Mikaelian [81] state that the eye can be used as a fast selection device providing the target size is not too small. Eye tracking systems provide an approach for measuring a computer user's ocular behaviour, however, for query formulation in a CBIR system a

computational measure of visual similarity is required to compute relevance scores for each selected image.

The use of a clamp with chin rest is recommended to remove a potential source of error and eliminate any variance in head movement across subjects. Calibration of the Eyegaze eye tracker is necessary to measure the properties of each subject's eye before the start of each experiment and limits the application of the equipment in the field, but this should not affect the results in the laboratory.

A series of experiments are now described in the following chapters to establish the feasibility of an eye gaze driven search mechanism.

The first experiment investigates whether users look more frequently at salient regions as determined by the attention model and whether any other eye behaviour was apparent. A negative result would indicate a potential lack of information in gaze data relevant to image retrieval.

The second experiment investigates the effectiveness of an interface controlled by gaze behaviour when compared with other interfaces. In this experiment the speed of operation was compared with that of a mouse interface. Again a negative result would cast doubt on the benefits of employing eye movement in such an interface.

Finally the proposed system is implemented with the aim of investigating whether eye tracking can be used to reach target images in fewer steps than by chance. The effect of the intrinsic difficulty of finding specific images and the time allowed for the consideration of successive selections is also investigated. Further experiments are conducted to further investigate users' gaze behaviour.

The effect of processing delays in implementing the proposed system, the choice of stimuli and the variables sought are dependent on each experiment design and will be described in subsequent sections. Implementations of findings from each experiment will mean that the application will require continual development.

Chapter 4. Attentional Gaze Behaviour

4.1. Objective

The objective of this experiment is to investigate whether there is in fact an informative and useful relationship between gaze behaviour and the visual attention model introduced in section 3.4.1. Stentiford's VA model [103] uses a neighbourhood matching process that is independent of features and possesses some properties that are related to human vision. These include an assignment of importance to anomalous objects and a conformance with results obtained by Treisman [87] on human behaviour. The relationship between gaze behaviour and the attention model may be used partly to validate the model, and to establish that eye behaviour is affected by image content. A negative result at this stage would indicate a lack of information in gaze data that is related to salient regions as indicated by the VA model.

4.2. Experiment Design

The gaze behaviour of participants is compared with data obtained through a model of Visual Attention [103] as shown in Figure 4.1. Differences in behaviour arising from varying image content are detected and the relationship between gaze behaviour and the visual attention model are explored. Regions of Interest are identified both by human interaction and prior analysis and used to explore aspects of vision that would not otherwise be apparent. Images with and without obvious subjects were used in this work to accentuate any behaviour differences that might be present.

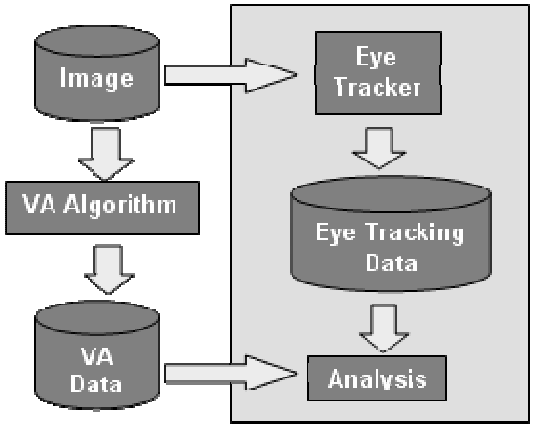

Figure 4.1: System Framework

For each image the Visual Attention Algorithm is applied to compute VA scores for each pixel. The same image is viewed by a human participant using the Eyegaze eye tracker [27].

The eye tracking data and the VA data are combined and analysed by identifying the coordinates of the gaze points on the image and obtaining the corresponding scores from the VA data.

4.2.1. Participants and Procedure

The Eyegaze system was used with the single computer configuration for this experiment. Over the course of the experiment four participants (3 males and 1 female) were presented with a series of images. The average age of the participants was 28.3 years. All participants had normal or corrected-to-normal vision and had no knowledge of the purpose of the study. All participants were encouraged to minimise head movement as no chinrest was used in this experiment. The participants were seated ~1m from the monitor. Over the course of the experiment, participants were presented a series of images for 5 seconds each separated by displays of a blank screen followed by a central black dot on a white background (Figure 4.2). Participants were asked to focus on the dot before each image was loaded.

Figure 4.2: Display Sequence

4.2.2. Data

The images were obtained from digital libraries already gathered from various royalty-free sources. All images were displayed on a 15" LCD Flat Panel Monitor at a resolution of 1024x768 pixels. Image sizes were 1017 x 723 pixels. The images were categorised according to whether they had an obvious region of interest or not. Ten images contained obvious regions of interest, and the remainder contained unclear or no regions of interests. The images with obvious regions of interest could have a single subject on the background while those without obvious regions of interest could have many competing distractors. The single-subject could be a small subject such as a distant aeroplane in the sky or large subject such as a big bird photographed closely. The selection of images was an important factor that affects the output and was an aspect of the study.

4.3. Results

Results with four participants on six images are shown in Figure 4.3 to Figure 4.8. Three images with obvious regions of interest (Figures 4.3 to 4.5), and three images with unclear or no regions of interests are presented (Figures 4.6 to 4.8). The corresponding VA maps and graphs of the

four participants are also presented. The VA score that corresponded to the pixel at each fixation point was associated with the time of the fixation and plotted as graphs for study in units of 20ms. It was observed that there was considerable variation in behaviour over the four participants, but all did not ignore the regions with the highest VA scores early in the display period, typically, in the first 2 seconds.

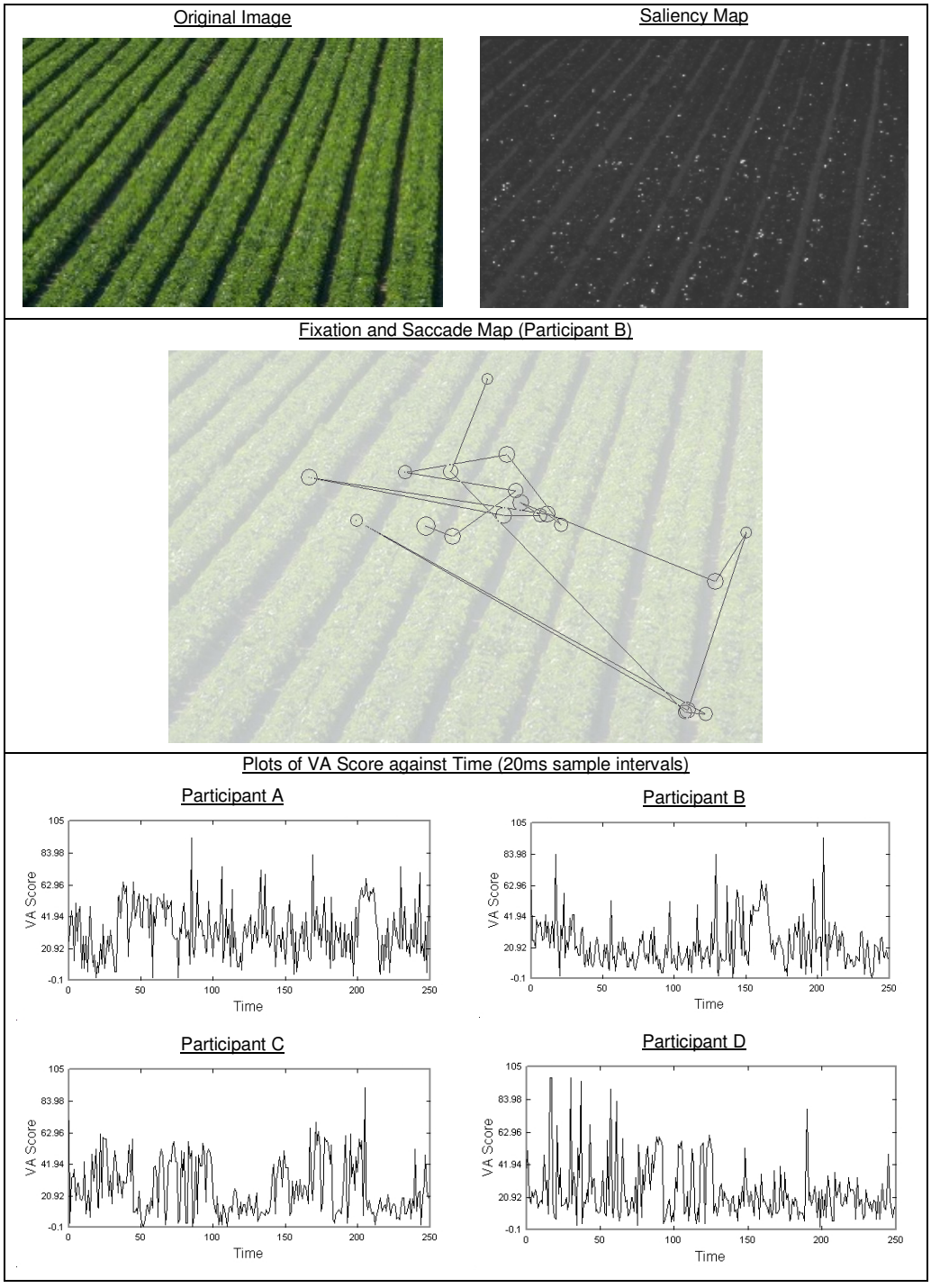

Figure 4.3: Image 1 with unclear ROI

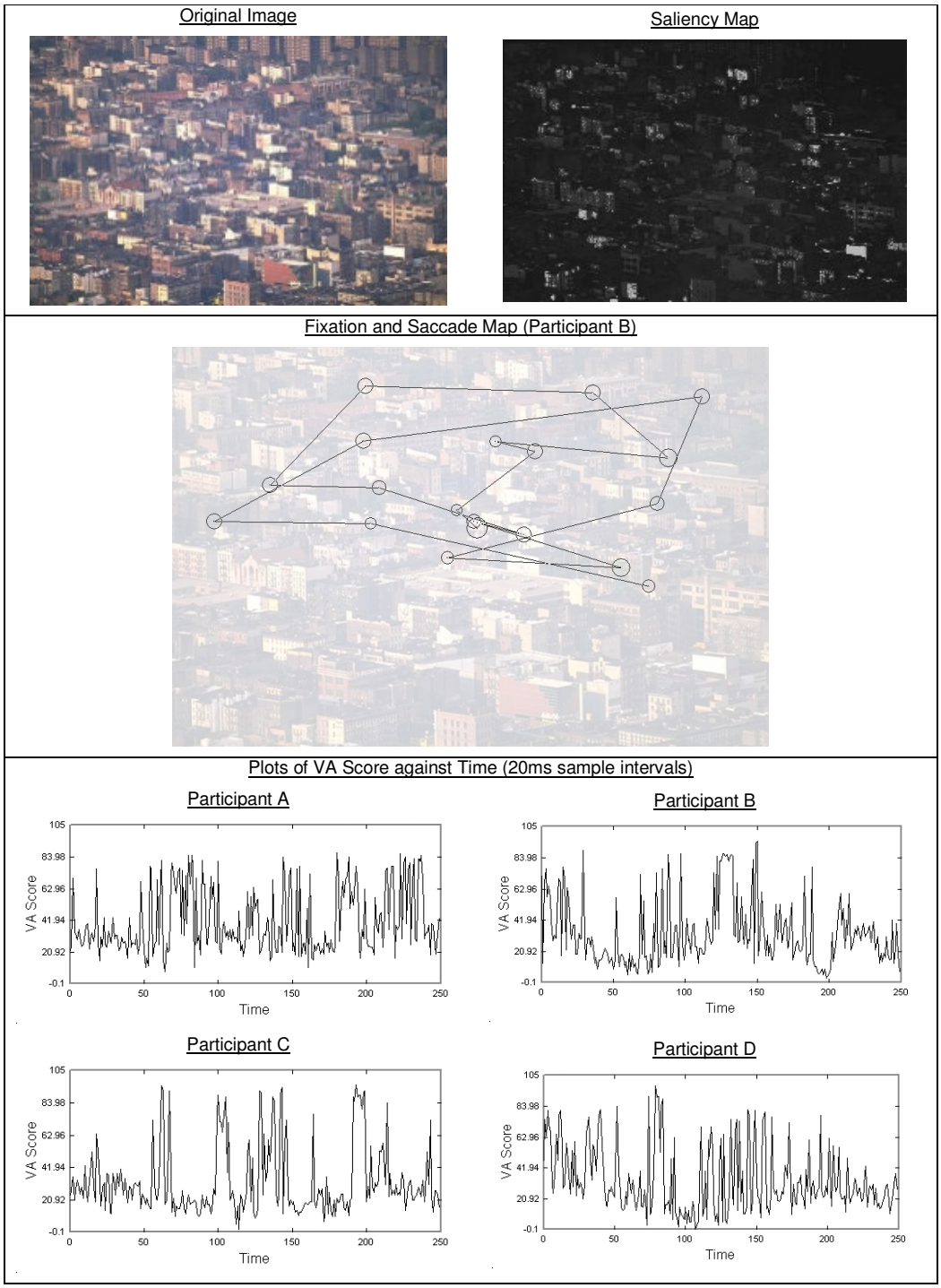

Figure 4.4: Image 2 with unclear ROI

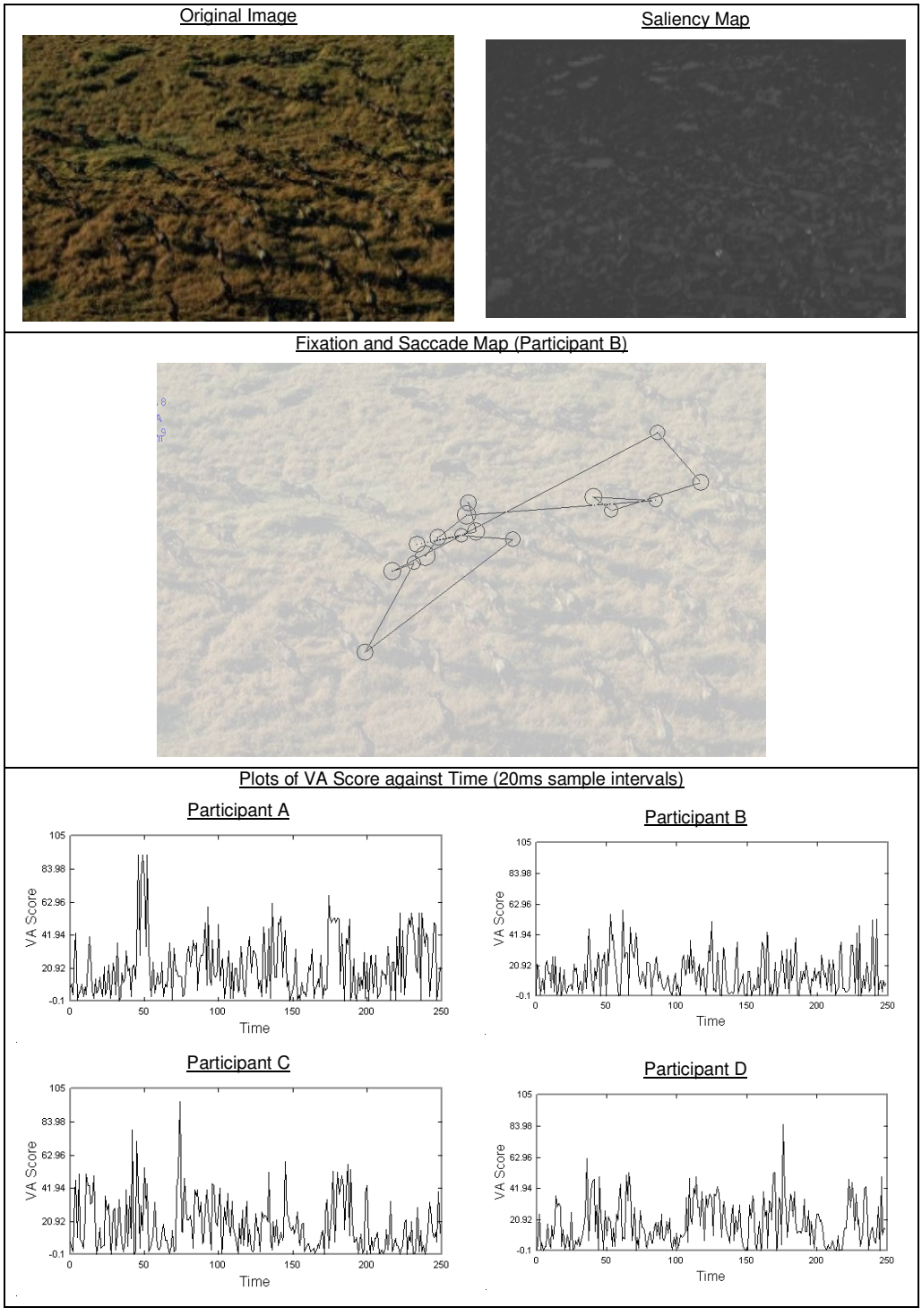

Figure 4.5: Image 3 with unclear ROI

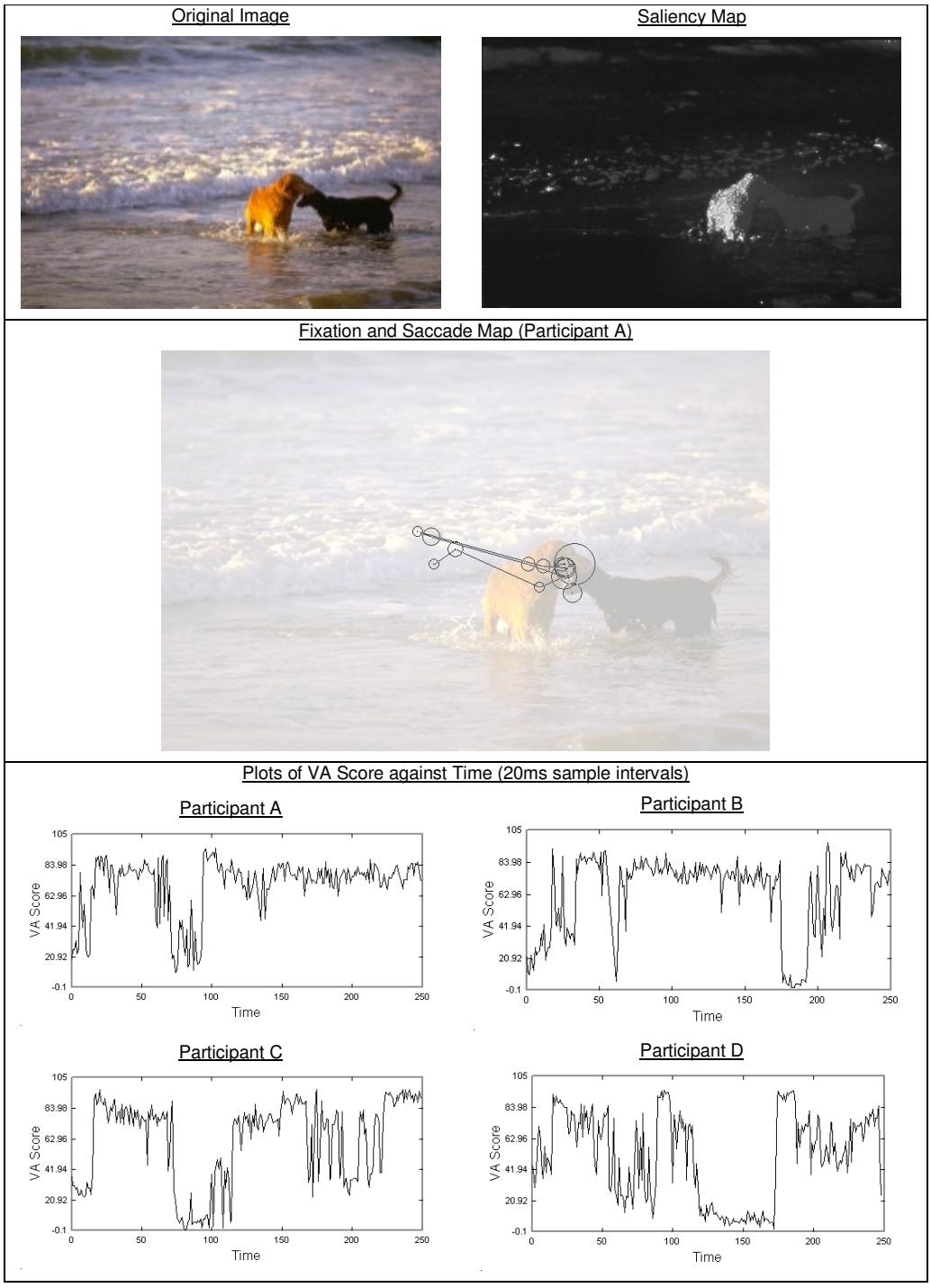

Figure 4.6: Image 4 with obvious ROI

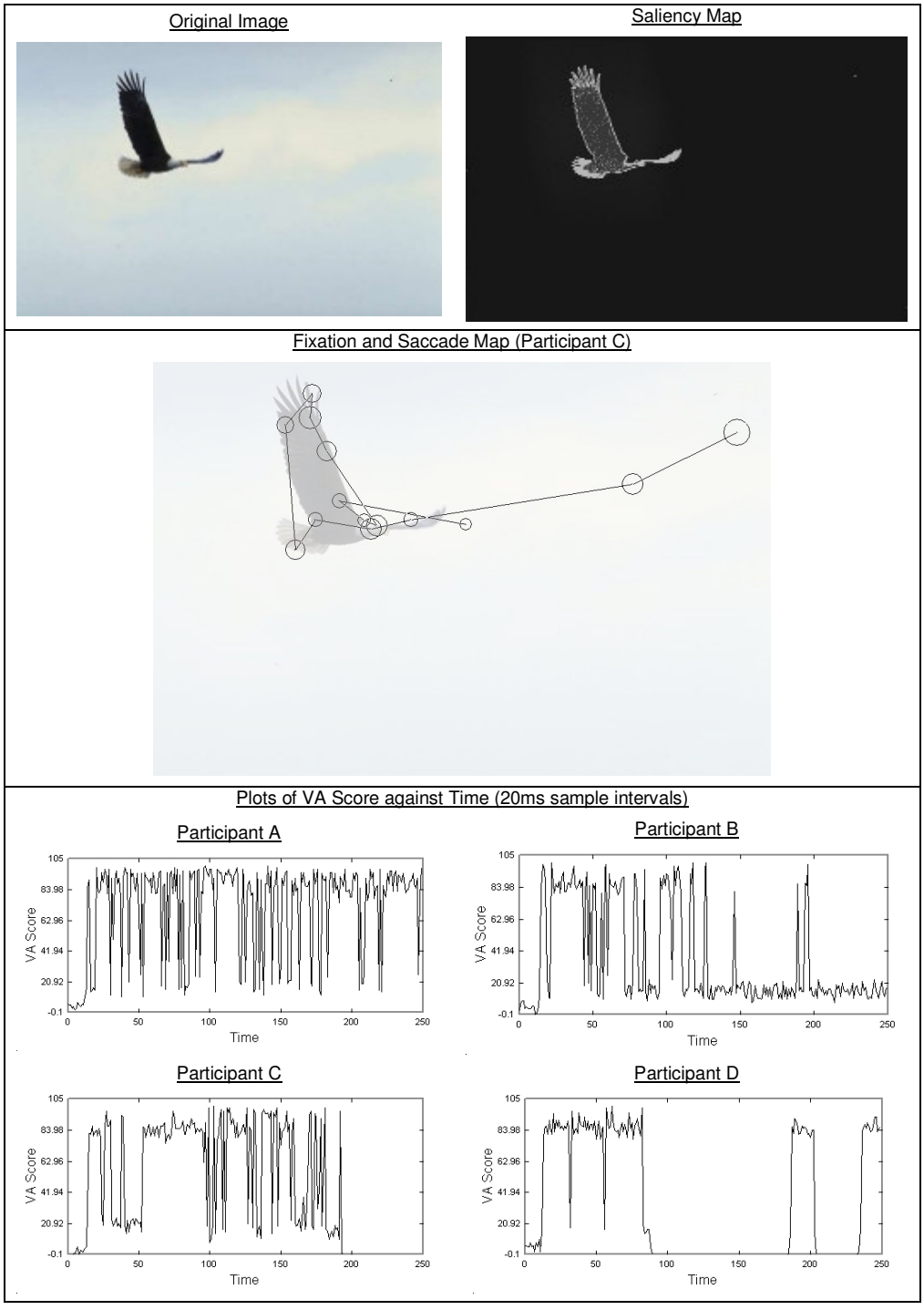

Figure 4.7: Image 5 with obvious ROI

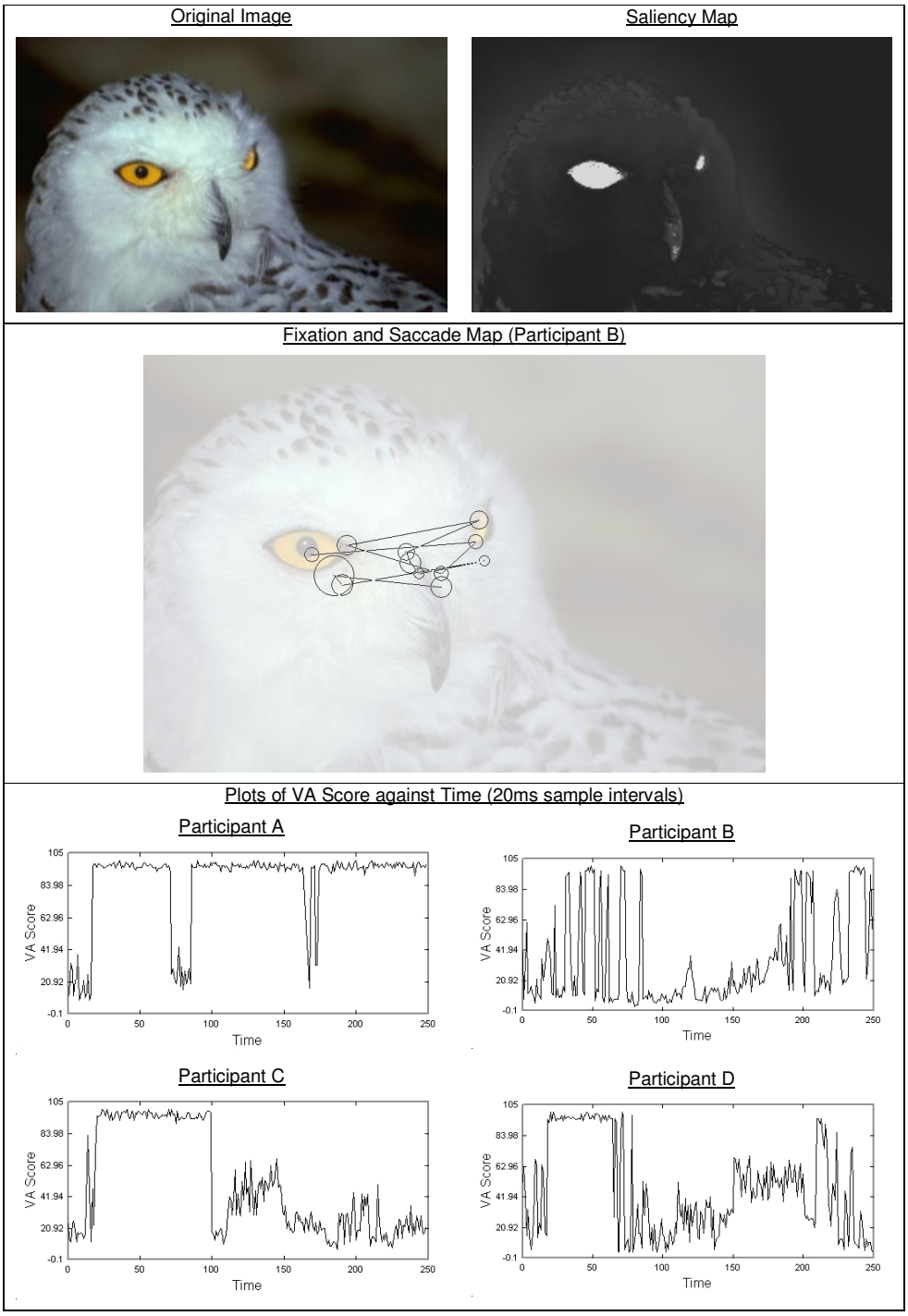

Figure 4.8: Image 6 with obvious ROI

The variability of the VA scores (x) over time is illustrated by the variance:

$$v = \frac{1}{n-1}\sum_{j=0}^{n-1}(x_j - \bar{x})^2$$

where x_j is the VA score at the $j+1$ fixation point and.

$\bar{x}$ = mean of the VA scores $x_0,...,x_{n-1}$

The variance ν measures the average spread or variability of the VA scores for the scan-path and the image. The variances of the VA scores for the first two seconds of the display period over six images for four participants and the variance of all the VA scores for each image are presented in Table 4.1 and Figure 4.9.

Table 3 shows the total length of time in ms. spent fixating on regions of high VA score for each participant on each image. This shows that in all cases a larger proportion of the 5 seconds exposure time was spent observing the salient regions than the background, if such a salient region was present in the image. Images without obvious subjects did not give such a pronounced result.

Table 4.1: Variance of the VA scores

		Image Variance	Participants			
			1	2	3	4
Unclear ROI	Image1	**298**	325	193	333	532
	Image2	**500**	479	496	328	629
	Image3	**175**	389	175	365	197
Obvious ROI	Image4	**443**	741	687	1094	857
	Image5	**246**	1432	1453	1202	1466
	Image6	**378**	1246	1226	862	1497

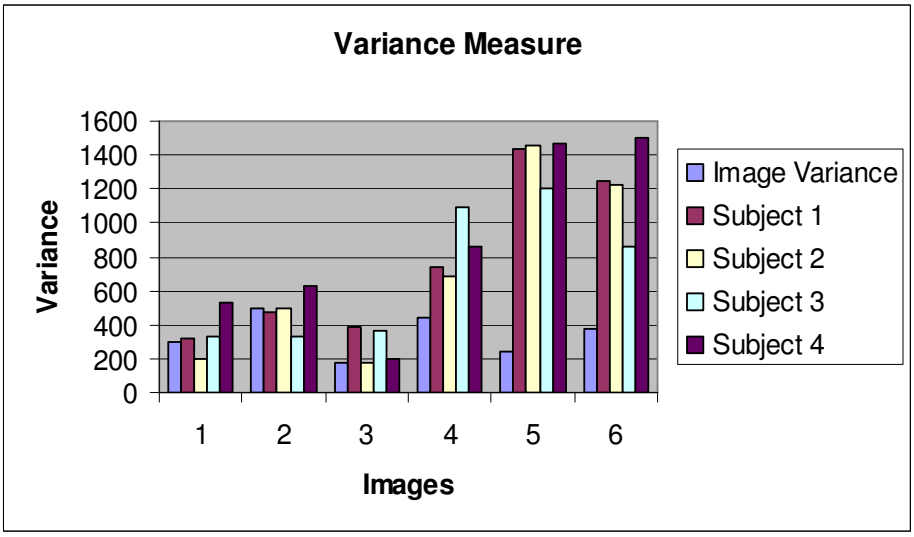

Figure 4.9: Variance histogram

Table 4.2: Times (ms.) spent fixating on regions of high VA score

Images		Participants			
		A	**B**	**C**	**D**
Unclear ROI	**1**	40	60	20	140
	2	580	420	500	400
	3	100	0	40	20
Obvious ROI	**4**	2820	2340	2420	1280
	5	3680	1480	2220	1960
	6	4240	980	1620	1240

4.4. Analysis and Discussion

The results indicate that regions with high VA scores attract eye gaze for the images studied. However, it was apparent that individual behaviours varied considerably and it was difficult to identify a pattern over such a small amount of data. Nevertheless the results did show that there was a significant tendency to spend more time looking at regions of high visual attention when these were present. Also there was a higher variance in VA score over time on images with obvious ROIs due to gaze patterns shifting between areas of high visual attention and the background. This would seem reasonable in view of a natural inclination to make rapid visual comparisons between anomalous material and a relatively predictable background. These findings do appear to support the visual attention model, which is also based on comparison of pixel regions taken from the whole image.

A substantial part of the gaze of the participants during the first two seconds of exposure is directed at areas of high visual attention as estimated by the model. The results suggest that gaze moves towards the location of salient objects where fixations take place. The eyes move from a prior foveal location, the black dot at the centre of the screen in this experiment, and quickly reposition to a salient region in the obvious ROI images which attracted attention. The fovea is now directed at the region of interest and attention is now directed at perceiving the region under inspection at high resolution if the user so desires. Many of the saccades for several participants are characterised by frequent movements to and from the areas of high visual attention, which is shown by high variances for images containing salient material. Several participants fixated on the region of interest for longer periods of time but still periodically scanned background material. This indicated the potential of an attention weighted algorithm for image search.

The *salience divergence* model by Parkhurst et al [54] proposes that the bottom up component is more influential early in viewing, but becomes less so as viewing progresses.

Their framework predicts that the difference between saliency at fixated locations and at non-fixated locations will be greatest early in viewing. Indeed our results are consistent with Parkhurst's, in that participants fixated obvious regions of interests early in the display and it became less influential, depending on individual participant, as viewing progressed. Again according to Henderson and Hollingworth [22] the visual informativeness of structural information appears to influence initial fixation placement, while the meaning of an image region influences the overall fixation density. The results in this experiment confirm that the initial fixation placement is predominantly on the visually informative region of the image if one is present.

Mackworth and Morandi [39] found that fixation density was related to the rated informativeness for different regions of a segmented picture and that few fixations were made to regions rated as uninformative. A separate group of observers were asked to grade the rate of informativeness of the segmented picture. In this thesis the visual attention model was used equivalently to score the level of informativeness in the images.

Interestingly, the results also show that the variance of VA scores for the gaze path is higher than the variance of the VA scores for every pixel in the image (Table 3.1). The participant may be gathering information by scanning between high VA regions and background material. This is especially illustrated by the high value of the variance of the VA scores for obvious-ROI images. The variance for the whole image, which is similar to the variance for unclear-ROI images, is significantly lower than the variance of the scores generated by the scan-path of participants on obvious-ROI images. This indicates that eye behaviour is attracted by salient locations, but appears to also require frequent reference to non-salient background regions.

4.5. Lessons Learnt

During the experiment some participants reported that eye blinking and blur due to continuous screen-stare were unavoidable. The eye tracking data corresponding to blinking and off-image gaze points were discarded in the analysis. The Eyegaze equipment is sensitive to excessive head movement, which disrupts calibration and so a chin rest was used in subsequent experiments.

More work is necessary to obtain statistical significance across more images and participants. The participants were not given specific tasks when viewing the images in these experiments and this may have introduced some confounding effects. Future experiments should be focused on specific retrieval tasks, which should reduce inter-subject variability.

4.6. Summary

The goal of this study was to explore the relationship between gaze behaviour and the Visual Attention model and to establish that image content is reflected in eye behaviour. Results show that obvious regions of interests are attended early in the display period and that participants discriminated within the image by periodically scanning background and foreground in the images studied. The identifiable discriminatory pattern of eye movement behaviour indicates that eye trackers may yield useful information for use in image retrieval through a suitable interface.

The next section describes experiments carried out to establish some of the benefits of using an eye tracking interface that are over and above those of conventional interfaces.

Chapter 5. Search Gaze Behaviour

This chapter investigates search behaviour on images in an eye tracking interface. Firstly, the speed efficiency of eye selection is measured. Secondly, the proposed system was implemented with the aim of investigating whether eye tracking can be used as an interface for image retrieval. The gaze behaviour is further analysed for additional sourcres of relevance from gaze behaviour.

5.1. Relative Speed of Eye and Mouse Interfaces

5.1.1. Objective

The second experiment investigates the effectiveness of an interface controlled by gaze behaviour when compared with other interfaces. In this experiment the speed of operation is compared with that of a mouse interface.

5.1.2. Equipment and Data

The Eyegaze System was used in this experiment with the double computer configuration. A clamp with chin rest provided support for chin and forehead in order to minimize the effects of head movements, although the eye tracker does accommodate head movement of up to 1.5 inches (3.8cm). Calibration was needed to measure the properties of each subject's eye before the start of the experiments. The loading of 25 images in the 5 x 5 grid display took an average of 110ms on a Pentium IV 2.4GHz PC with 512MB of RAM. Gaze data collection and measurement of variables were suspended while the system loaded the next set of images into memory. During this period the display remained unchanged and was updated instantaneously as soon as the contents of the next display had been composed.

25 images were selected from the Corel image library [105]. The initial screen including the target image is shown in Figure 5.1. These images were displayed on a 15" LCD Flat Panel Monitor at a resolution of 1024x768 pixels.

5.1.3. Experiment Design

A total of 12 participants took part in this experiment. Participants included a mix of students and university staff. All participants had normal or corrected-to-normal vision and provided no evidence of colour blindness.

Participants were asked to locate a target image from a series of 50 grid displays of 25 stimuli (24 distractors and 1 target image shown in Figure 5.1). On locating the target image, the

participants selected the target by clicking with the mouse or fixating on it for longer than 40ms with the eye. The grid was then re-displayed with the positions of the images and the target randomly re-shuffled. Participants were randomly divided into two groups (Table 5.1), the first group used the eye tracking interface first then the mouse, and the second group used the interfaces in the reverse order. This enabled any variance arising from the ordering of the input modes to be identified. Different sequences of the 50 target positions were also employed to identify any confounding effects arising from the ordering of the individual search tasks. All participants experienced same-sequence of target positions as well as different-sequences while using the two input modes. Figure 5.2 describes a typical sequence of display for the images.

A typical participant in the mouse first group performed four runs: mouse (target sequence 1), eye (target sequence 1), mouse (target sequence 2) and eye (target sequence 3). There was a 1 minute rest in between runs.

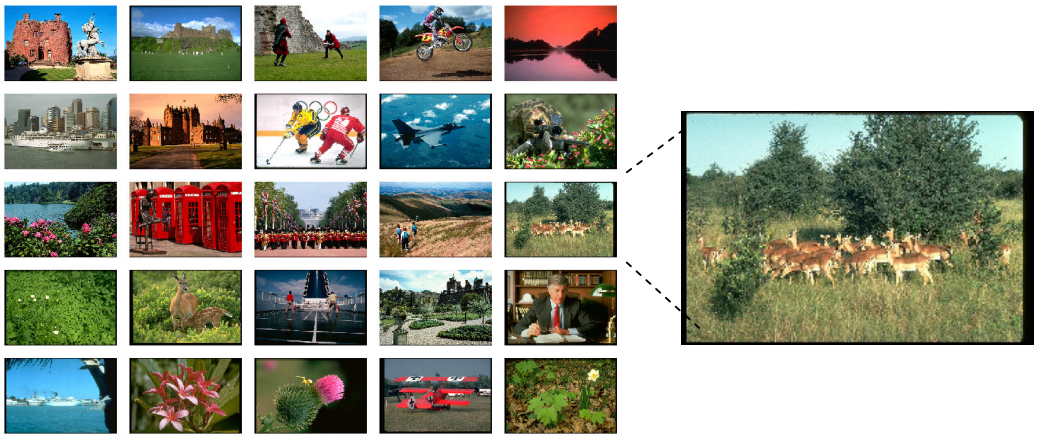

Figure 5.1: 25 images arranged in a 5x5 grid used in runs (target image expanded)

D	D	D	D	D
D	D	D	D	D
D	D	D	D	**T1**
D	D	D	D	D
D	D	D	D	D

D	D	D	D	D
D	**T2**	D	D	D
D	D	D	D	D
D	D	D	D	D
D	D	D	D	D

D	D	D	D	D
D	D	D	D	D
D	D	D	D	D
D	D	D	D	D
D	D	D	**T3**	D

D	D	D	D	D
D	D	D	D	D
D	D	D	D	D
D	D	D	D	D
T4	D	D	D	D

...

D	D	D	D	D
D	D	D	D	D
D	D	D	D	D
D	D	D	**T50**	D
D	D	D	D	D

Figure 5.2: Sequence of displays for a typical target sequence (T1=Target 1; D=Distractors)

5.1.4. Results

Order	Target Positions	Input Mode	Response Time	
			Mean	Standard Deviation
Mouse First (6 participants)	Same-sequence	Mouse	2.33	0.51
		Eye	1.79	0.35
	Different-sequence	Mouse	2.43	0.38
		Eye	1.96	0.42
Eye First (6 participants)	Same-sequence	Mouse	2.35	0.82
		Eye	2.29	0.74
	Different-sequence	Mouse	2.59	1.44
		Eye	2.27	0.73

Table 5.1: Mean response times for target image identification task

The length of time it took to find the target image from the grid display was recorded and 50 response times were obtained for each participant's run. The mean response times were calculated and presented in Table 5.1.

The 48 means were entered into a mixed design ANOVA with three factors (order of input, input mode, and target positions).

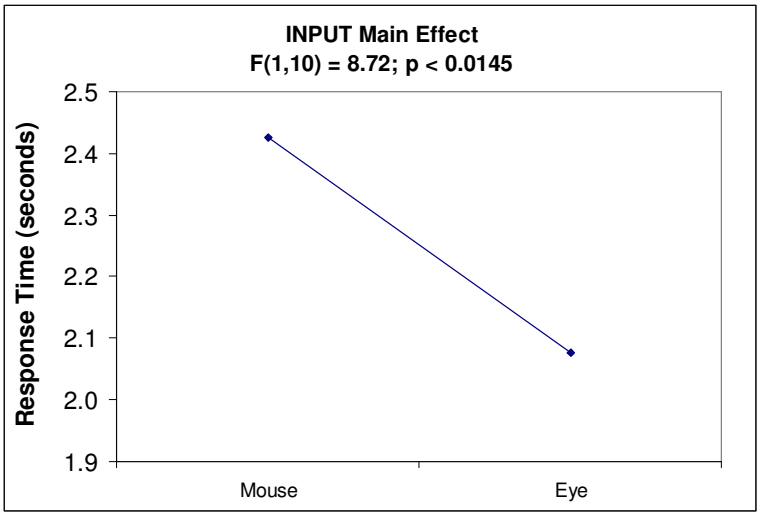

Figure 5.3: Mean response time by input

There was a significant main effect of input, F(1,10)=8.72, p=0.015 with faster response times when the eye was used as an input (2.08sec.) than when the mouse was used (2.43sec.) as shown in Figure 5.3. The main effect of the order was not significant with F(1,10)=0.43, p=0.53. The main effect of target positions was not significant, F(1,10)=0.58, p=0.47. All two-factor and three-factor interactions were not significant.

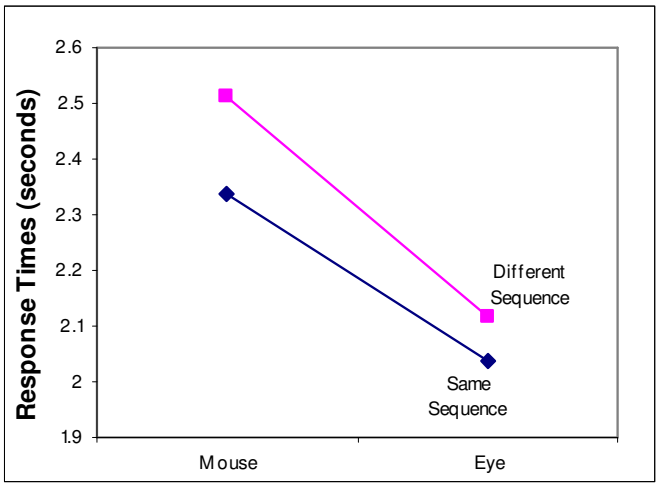

Figure 5.4: Mean response time by input and target position sequence

Further analysis of the first-order and second-order simple main effects was conducted individually on all levels of the three factors. The input modes influenced response times of subjects when they were presented with the same-sequence target positions, $F(1,10)=14.22$, $p=0.004$, with faster eye response times ($M=2.04$sec, $SD=0.61$) than the mouse ($M=2.34$sec, $SD=0.65$) as shown in Figure 5.4. The effect of the input modes on the response times was not significant when users were presented with different-sequences, $F(1,10)=3.96$, $p=0.075$, despite having a larger difference between the input modes. The eye had faster response times ($M=2.12$sec, $SD=0.59$) than the mouse ($M=2.51$sec, $SD=1.01$) as shown in Figure 5.4.

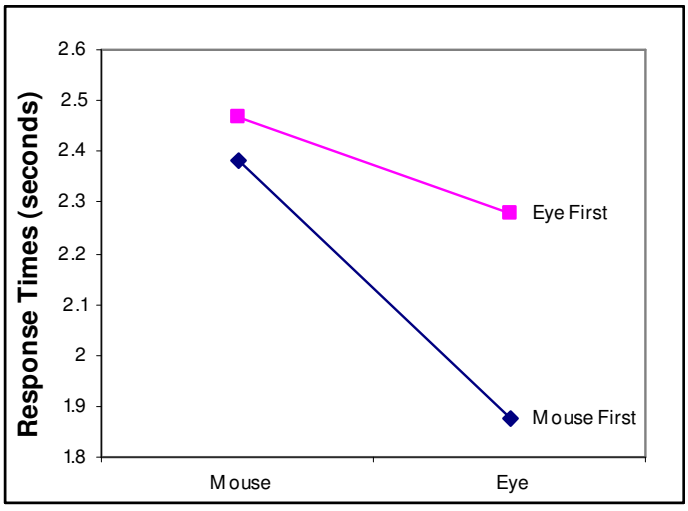

Figure 5.5: Mean response time by input and Mouse/Eye order

The input modes influenced the response times of subjects in the Mouse First group, $F(1,10)=9.09$, $p=0.013$, with faster eye response times ($M=1.878$sec, $SD=0.381$) than the mouse

(M=2.38sec, SD=0.43). The response time was faster with the eye interface than the mouse when the participants used the mouse interface first and no significant difference between the eye and mouse interfaces when the eye was used first, p=0.27 (Figure 5.5).

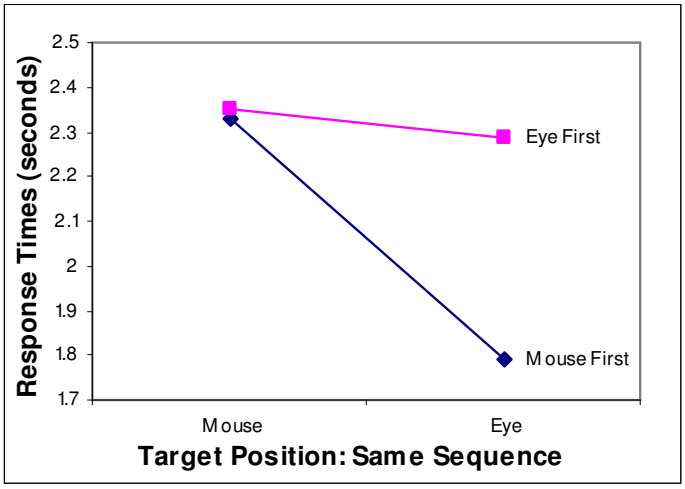

Figure 5.6: Mean response time by input, order and same-sequence target position

The input levels influenced the response times of subjects in the Mouse First group when they were presented with the same sequence target positions, F(1,10)=22.81, p=0.001, with faster eye response times (M=1.79s, SD=0.345) than the mouse (M=2.33s, SD=0.51). The response time was faster with the eye interface when the mouse was used first and participants experienced the same-sequence target positions (Figure 5.6).

There were no other significant simple main effects. A fourth factor of display was included in the mixed design ANOVA to investigate the effect of the grid display (Figure 5.1) changes. There was a significant main effect of display, F(49,490)=2.39, p<0.0001. This indicated that the displays affected the response times, as each display is affected by the contents of previous displays. It could also be argued that the effect of display changes might be present in this experiment during display changes and so the average response time is preferred in the three-factor design.

5.1.5. Analysis and Discussion

The 25 stimuli presented to each participant and the predetermined choice of image target produced a difficult task and the runs required a high cognitive load. The participant had to search for the target and then make a selection. When using the mouse the participant had to first locate the cursor and then move the mouse to the item to be selected. This can result in slower mouse responses. An eye tracking interface requires a fixation for a fixed period to make a selection. The results indicate slower mouse responses and is supported by the main effect of

input (p=0.015) and is consistent with Ware and Mikaelian's conclusions [81], who showed that fixation dwell time can be a faster selection method than button press and mouse clicks providing the target size is not too small. In addition Sibert and Jacob's experiments [68] involving circles requiring little thought, and letters that required comprehension and search effort, also found faster eye gaze interaction than the mouse in both experiments.

It could be suggested that some of the skills gained through the use of the mouse in this task are passed on and remembered during the subsequent eye gaze task thereby obtaining a large difference in response times. On the other hand any new skills acquired during the use of the eye do not make much difference to subsequent mouse performance. This may help to confirm that simple knowledge of target positions from previous tasks is not a major confounding factor in the results.

Although, there was a simple effect of the input on the same-sequence target positions, the differences in the mean response times were similar as shown in Figure 5.4. There was a significant variability around the means observed on closer scrutiny of the data. The different-sequence target positions were not affected by the input and will be the choice for future experiments. The significance of both conditions together (Mouse First and same-sequence target positions) was also tested. Given that there was a simple effect individually on the Mouse First group and same-sequence target positions, the test of significance on both conditions was not surprisingly high (p=0.001).

5.1.6. Lessons Learnt

The effects of covert attention were minimized by giving users clear and focussed instructions. Future work is aimed at devising new interfaces for content based image retrieval that are easier and more natural to use and which converge to the targets rapidly through the use of behavioural information extracted in real time from eye gaze data.

5.1.7. Summary

An image identification task involving searching for a target image from a display of 24 other distractor images yielded task completion times for two modes of interface control and two experimental conditions. Results indicated faster target identification for the eye interface than the mouse for identifying a target image on a display. There were significant simple main effects of the eye on the Mouse First group and the same-sequence target positions. This result might indicate that skill transfer was taking place when the mouse was used first but not when the eye was used first. This could suggest that the experience gained during visual tasks carried out using a mouse will benefit users if they are subsequently transferred to an eye tracking system.

Having shown that useful information is present in eye gaze data, and that selection by gaze can be faster than selection by mouse, the next section describes a task-oriented experiment using eye gaze data alone to retrieve target images. The fast selection by eye is used to infer relevance and extract and display images from the database that are likely to be closer to the target.

5.2. Image Retrieval

5.2.1. Objective

The proposed system (Figure 3.1) is implemented with the aim of investigating whether eye tracking can be used to reach target images in fewer steps than by chance selection. The effect of the intrinsic difficulty of finding specific images and the time allowed for the consideration of successive selections are also investigated.

5.2.2. Image Database

As described in methodology chapter, 1000 images were selected from the Corel image library [105] to compute similarity links. Images of 127 kilobytes and 256 x 170 pixel sizes were loaded into the database. The categories included boats, landscapes, vehicles, aircrafts, birds, animals, buildings, athletes, people and flowers. The initial screen including the target image is shown in Figure 5.7. Images were displayed as 229 x 155 pixel sizes in a 4 x 4 grid display.

5.2.3. Search Task

Images are presented in a 4 by 4 grid with the target image presented in the top left corner of the display (Figure 5.7). The user is asked to search for the target image and on the basis of the gaze behaviour the machine selects the most favoured image. The next set of 15 images is then retrieved from the database and displayed for the next selection. The loading of 16 images in the 4 x 4 grid display took an average of 100ms on the same system. Gaze data collection and measurement of variables were suspended while the system loaded the next set of images into memory. During this period the display remained unchanged and was updated instantaneously as soon as the contents of the next display had been composed.

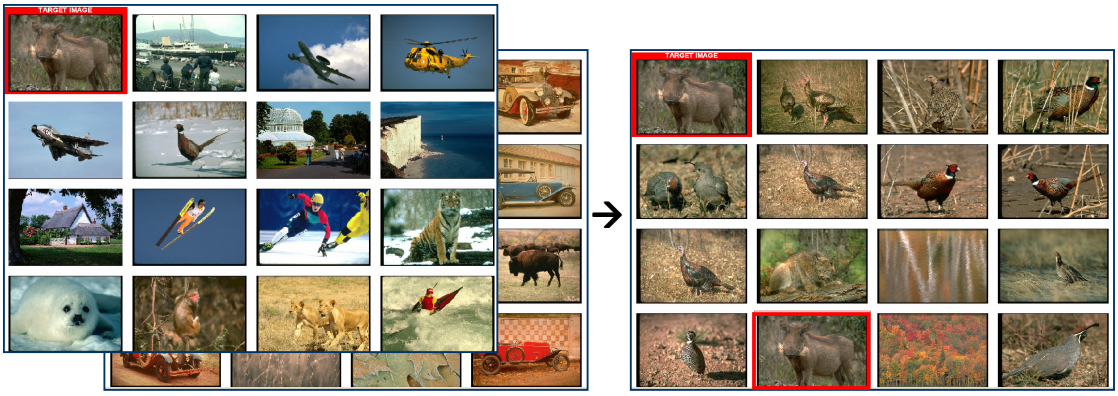

Figure 5.7: Initial screen leading to final screen with retrieved target

5.2.4. Random Selection Strategy

Searching on displays produces two main problems. Firstly if the target is not similar to any of the currently displayed set (e.g. a cluster of visually different images), then it is very difficult for the user to direct the search away from the displayed set and towards the target [77]. Secondly the user's selections from successive displays could enter a loop in which the displays lead back to each other, and no exit towards the target is possible. These two problems were explored further by using a random selection algorithm. In addition this strategy provided a performance base-line which any more intelligent approach would need to exceed.

The automatic random selection tool randomly selected an image from each successive screen holding 15 displayed images rather than by eye gaze. This enabled the following:

- initial exploration of the structure of the similarity links in the database
- guidance for the choice of the grid size
- analysis of the benefits of completely random image retrieval
- selection of target images

5.2.4.1. Similarity Measure Structure

In Table 3.1 the CVA similarity scores C_{AB} for images 3 and 8 are 179 and 241 where A=3 and B=8. The CVA algorithm is such that the number of forks found to match both images A and B will not always be the same when implemented at different occasions. The CVA similarity score is not a symmetric measure. For example, an image of one object has a higher score when compared to an image of two identical objects than the reverse, because it is easier to find features present in the single object image that are also present in the multiple object image than it is in the reverse direction. The automatic random selection tool was implemented to

investigate the likelihood of finding targets using either the asymmetric values (C_{AB}) or symmetric values computed from the average of C_{AB} and C_{BA}.

The random selection tool was repeated three times for each of the 1000 images acting as the target image. Table 5.2 shows the frequency distribution of the number of displays or steps to target. The values remained relatively similar for all three runs, reflecting a structure within the database. Interestingly the asymmetric values yielded fewer steps to target than the symmetric values and will be the choice for all subsequent experiments. This result reveals a potential benefit of an asymmetric measure and a possible disadvantage of a symmetric measure such as the Euclidean distance.

Table 5.2: Exploration of similarity matrix

Steps to target	asymmetric				symmetric			
				Mean				Mean
1-25	133	136	132	134	106	104	99	103
26-50	39	44	46	43	52	37	38	42
51-75	40	29	36	35	30	36	23	30
76-100	28	29	30	29	21	20	14	18
101-125	28	27	19	25	21	12	21	18
126-150	19	14	12	15	17	21	14	17
151-175	12	12	14	13	17	10	13	13
176-200	10	11	6	9	9	14	16	13
201-225	11	17	17	15	5	12	12	10
226-250	11	9	13	11	7	8	11	9
251-275	4	10	10	8	10	9	16	12
276-300	6	10	10	9	8	8	9	8
301-325	12	14	12	13	8	10	11	10
326-350	11	7	6	8	7	8	5	7
351-375	10	6	11	9	8	11	4	8
376-400	8	8	4	7	7	5	6	6
401-425	4	6	8	6	5	4	5	5
426-450	0	8	8	5	6	9	8	8
451-475	11	4	4	6	5	4	5	5
476-499	5	4	10	6	9	5	2	5
500 or more	598	595	592	595	642	653	668	654

5.2.4.2. Display Grid Size

A comparison of 5 x 5 and 4 x 4 grids of images was carried out using the random selection algorithm. Table 5.3 indicates that fewer steps to target were needed for the 5 x 5 grid as

compared with the 4 x 4 grid. This was mostly due to the greater fan out of 24 for the 5 x 5 grid compared with 15 for the 4 x 4 grid. A 4 x 4 grid was used in all subsequent experiments in order to obtain better discrimination between eye gaze and random selection performance over the 1000 image database. Larger grids without increasing the image database size would benefit random selection and tend to obscure the relative eye gaze performance.

Table 5.3: Exploration of display grid size

Steps to target	4 x 4 grid				5 x 5 grid			
				Mean				Mean
1-25	133	136	132	134	197	179	179	185
26-50	39	44	46	43	70	85	84	80
51-75	40	29	36	35	53	47	49	50
76-100	28	29	30	29	27	28	47	34
101-125	28	27	19	25	30	32	28	30
126-150	19	14	12	15	27	25	16	23
151-175	12	12	14	13	19	14	24	19
176-200	10	11	6	9	24	19	19	21
201-225	11	17	17	15	14	26	23	21
226-250	11	9	13	11	12	9	13	11
251-275	4	10	10	8	17	10	12	13
276-300	6	10	10	9	11	17	15	14
301-325	12	14	12	13	8	10	8	9
326-350	11	7	6	8	11	10	7	9
351-375	10	6	11	9	11	8	3	7
376-400	8	8	4	7	8	12	7	9
401-425	4	6	8	6	5	7	8	7
426-450	0	8	8	5	4	9	8	7
451-475	11	4	4	6	11	12	8	10
476-499	5	4	10	6	6	8	3	6
500 or more	598	595	592	595	435	433	439	436

5.2.4.3. Random Retrieval

The random selection tool was applied with each of the 1000 images acting as the target image and the number of steps to target recorded. This was carried out using between 0 and 15 images in the display retrieved randomly from the database rather than on the basis of the highest similarity scores. Results were consistent with a typical run displayed in Table 5.4 and Figure 5.8. The first column refers to the case where all 15 images were retrieved on the basis of similarity scores. In the second column, where one image is retrieved randomly, the likelihood of not finding targets decreased from 723 to 457. As the number of randomly retrieved images

was increased, the likelihood of finding the target image in the first 20 displays/steps to target also increased. It was felt that the effect on gaze performance of including one randomly-retrieved image in the retrieved set merited experimental investigation.

Table 5.4: Results of applying the random selection strategy to the image database (sum of each column = 1000 images)

Steps to target	Frequency Distribution															
	Number of randomly-retrieved images															
	0	1	2	3	4	5	6	7	8	9	10	11	12	13	14	15
1-20	112	142	153	164	201	189	201	221	220	237	244	257	251	229	270	225
21-40	34	76	107	111	138	168	166	190	172	159	173	171	190	198	194	215
41-60	21	75	100	88	99	87	114	119	142	146	129	142	135	134	139	139
61-80	21	39	64	91	73	79	92	92	92	101	96	112	113	104	96	111
81-100	21	47	72	61	74	66	71	70	83	79	75	82	77	84	66	77
101-120	14	43	41	60	62	59	64	50	53	44	58	52	57	69	54	63
121-140	12	45	33	46	55	67	56	49	49	43	42	50	36	55	37	37
141-160	25	20	37	37	34	45	30	38	42	39	39	25	29	35	31	32
161-180	5	30	22	42	41	28	41	34	32	31	33	24	26	21	28	20
181-200	12	26	29	26	26	22	29	25	15	20	25	18	29	14	15	23
Not found	723	457	342	274	197	190	136	112	100	101	86	67	57	57	70	58

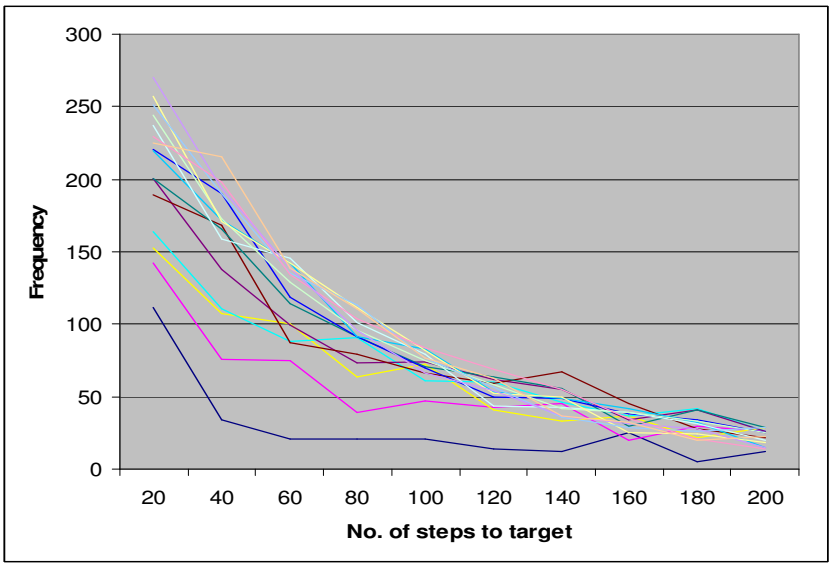

Figure 5.8: Frequency Distribution of the steps to target for random retrieval of images (15 runs)

5.2.4.4. Selection of Target Images

The automatic random selection tool was implemented to investigate the difficulty of the search task when using the same start screen (Figure 5.7). This difficulty would be largely dependent on the network of pre-computed similarity scores which needed to be evaluated to define satisfactory search tasks. Two strategies were employed to assist in the selection of target images of varying difficulty for search experiments. Firstly a plot of the frequency distribution

of steps to target for every image in the database revealed those images that were frequently found in the fewest and most number of steps.

Secondly a plot of the frequency distribution of the 15 images with the highest similarity scores with each image in the database indicated those images that were similar to most other images and were therefore most likely to be found when traversing similarity links during a search. By analysing the search performance and the retrieved image sets, the two strategies revealed the easy-to-find and hard-to-find images. Four of the easy-to-find images and four of the hard-to-find images were picked as target images for the experiment. These are shown in Figure 5.9.

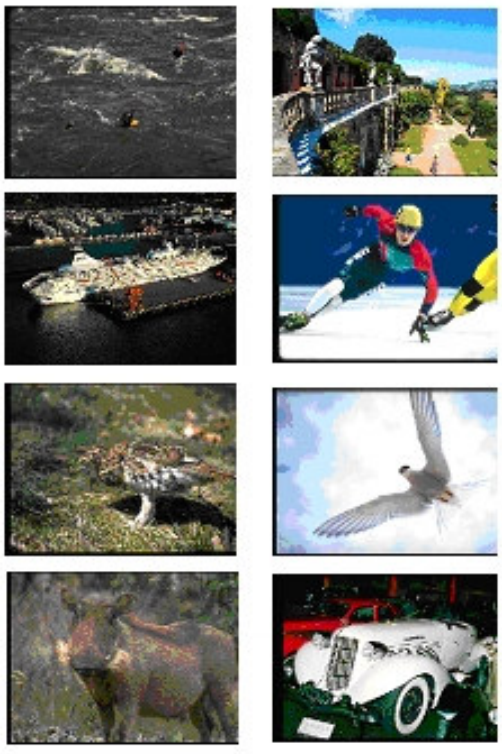

Figure 5.9: Target Images (Four easy-to-find images on the left and four hard-to-find images on the right)

5.2.5. Experiment Design

5.2.5.1. Criterion for Image Selection by Eye Gaze

The display automatically changes when the sum of the durations of all fixations of 80ms and above on a specific image exceeds a threshold. Fixations of 80ms and above were regarded as intentional fixations while all fixations less than 80ms were ignored. In this way the display changes relatively quickly if the participant concentrates on a relevant image, but takes longer if the gaze was tentative. A red rectangle is briefly flashed around an image if a fixation of 80ms

is detected. Successfully found targets are highlighted with a red border as shown on the right of Figure 5.7. Two cumulative fixation thresholds of 400ms and 800ms were employed as a factor in the experiment.

5.2.5.2. Participants

Thirteen unpaid participants took part in this experiment. Participants included a mix of students and university staff. All participants had normal or corrected-to-normal vision and provided no evidence of colour blindness.

5.2.5.3. Experimental Procedure

Four easy-to-find and four hard-to-find target images were used (Figure 5.9). Participants were given one practice run to enable a better understanding of the task and to equalise skill levels before the experiment. Participants understood that there would be a continuous change of display until they found the target but did not know what determined the display change. The display included either zero or one randomly retrieved image. Participants performed 8 runs using both easy-to-find and hard-to-find image types. Four treatment combinations of the two cumulative fixation thresholds (400ms and 800ms) and two random-retrieval levels (0 and 1) were applied to each image type. Any sequence effect was minimised by randomly allocating each participant to different sequences of target images. The first four runs were assigned to each image type. There was a 1 minute rest in between runs. The maximum number of steps to target was limited to 26 screen changes.

5.2.6. Results

Three dependent variables, the number of steps to target, the time to target (F_1), and the number of fixations (F_2) of 80ms and above were monitored and recorded during the experiment. 24 dependent variables (8 each) were recorded for each participant. The average figures are presented in Table 5.5.

Table 5.5: Analysis of Human Eye Behaviour on the Interface (rounded-off mean figures)

Image Type	Fixation Threshold	Randomly-retrieved	Target not found (frequency)	Steps to target	Time to target (seconds)	Fixation Numbers
Easy-to-find	400ms	0	38.5%	14	34.944	99
		1	53.8%	18	36.766	109
	800ms	0	38.5%	14	55.810	153
		1	15.4%	11	51.251	140
Hard-to-find	400ms	0	69.2%	23	52.686	166
		1	84.6%	23	50.029	167
	800ms	0	92.3%	24	104.999	327
		1	69.2%	19	83.535	258

104 (= 8x13) figures were entered for each dependent variable into a repeated measures ANOVA with three factors (image type, fixation threshold and randomly-retrieved).

The results of the ANOVA performed on the steps to target revealed a significant main effect of image type, $F(1,12)=23.90$, $p<0.0004$ with fewer steps to target for easy-to-find images (14 steps) than the hard-to-find images (22 steps).

The main effect of the fixation threshold was not significant with $F(1,12)=1.50$, $p<0.25$. The main effect of randomly-retrieved was also not significant, $F(1,12)=0.17$, $p<0.69$. The influence of including one randomly retrieved image in each display produced little or no difference in the steps to target, time to target and fixation numbers. This strategy appeared not to assist users to traverse the database any quicker than without the inclusion of a random image. All two-factor and three-factor interactions were not significant.

Further analysis of the first-order and second-order simple main effects was conducted individually on all levels of the three factors. The image types influenced the steps to target when participants had a set fixation threshold of 400ms $F(1,12)=15.41$, $p=0.002$, and 800ms $F(1,12)=13.39$, $p=0.003$ (Figure 5.10). The steps to target for easy-to-find images were fewer by a significant amount than the hard-to-find images, when the participants experienced a fixation threshold of 400ms (mean difference of 7 steps) and 800ms (9 steps).

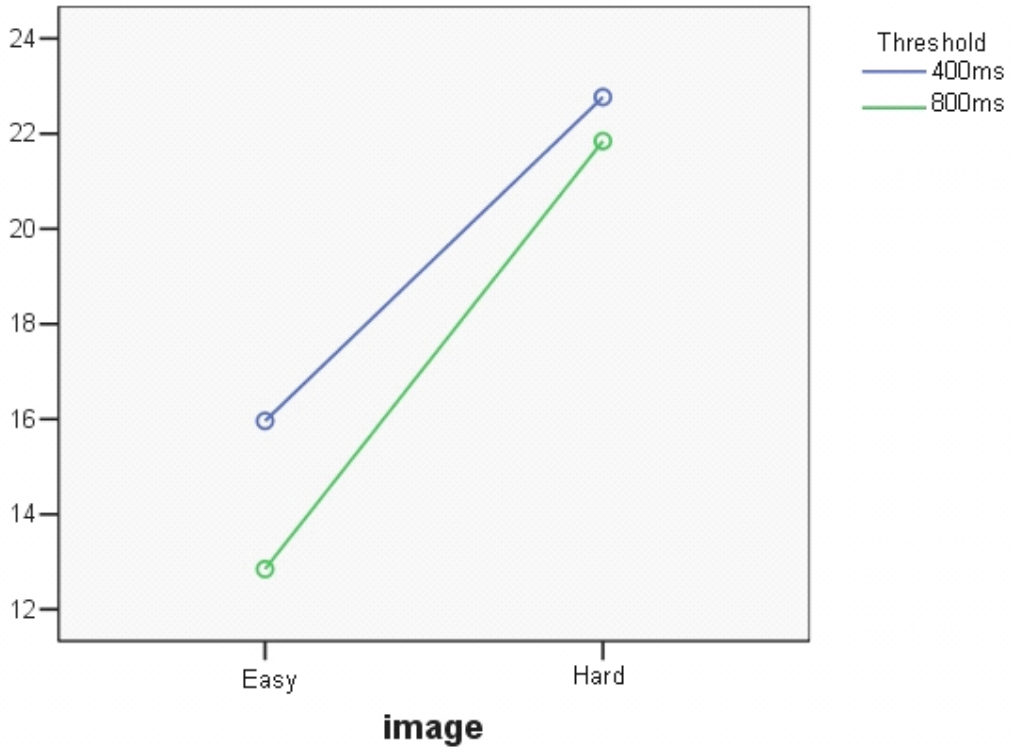

Figure 5.10: Average steps to target (Y-axis) by image type and fixation threshold

The analysis of the time to target produced similar results to the analysis of the number of fixations. There was a significant main effect of image type, $F_1(1,12)=24.11$, $p<0.0004$,

$F_2(1,12)=21.93$, $p<0.0005$, with shorter time to target and fewer fixations for easy-to-find images (40.468s and 125 fixations) than the hard-to-find images (71.331s and 229 fixations). The main effect of the fixation threshold was also similarly significant with $F_1(1,12)=18.27$, $p<0.001$ and $F_2(1,12)=16.09$, $p<0.002$. There were more fixations and more time was spent looking at hard-to-find images than the easy-to-find images.

The main effect of randomly-retrieved on the time to target and fixation numbers was not significant, $F_1(1,12)=1.49$, $p<0.25$ and $F_2(1,12)=0.76$, $p<0.40$.

Image type interacted with the fixation threshold, $F_1(1,12)=8.04$, $p<0.015$ and $F_2(1,12)=5.84$, $p<0.032$, and an analysis of simple main effects indicated a significant difference in time to target and fixation numbers for the fixation thresholds when hard-to-find images were presented, $F_1(1,12)=20.00$, $p<0.001$ and $F_2(1,12)=16.25$, $p<0.002$, but interestingly, no significant difference when easy-to-find images were presented, $F_1(1,12)=3.62$, $p<0.08$ and $F_2(1,12)=3.57$, $p<0.08$. There was no significant difference in the time to target and fixation numbers between the threshold levels for the easy-to-find images as opposed to the hard-to-find images where there was a significant difference (Figures 5.11 and 5.12).

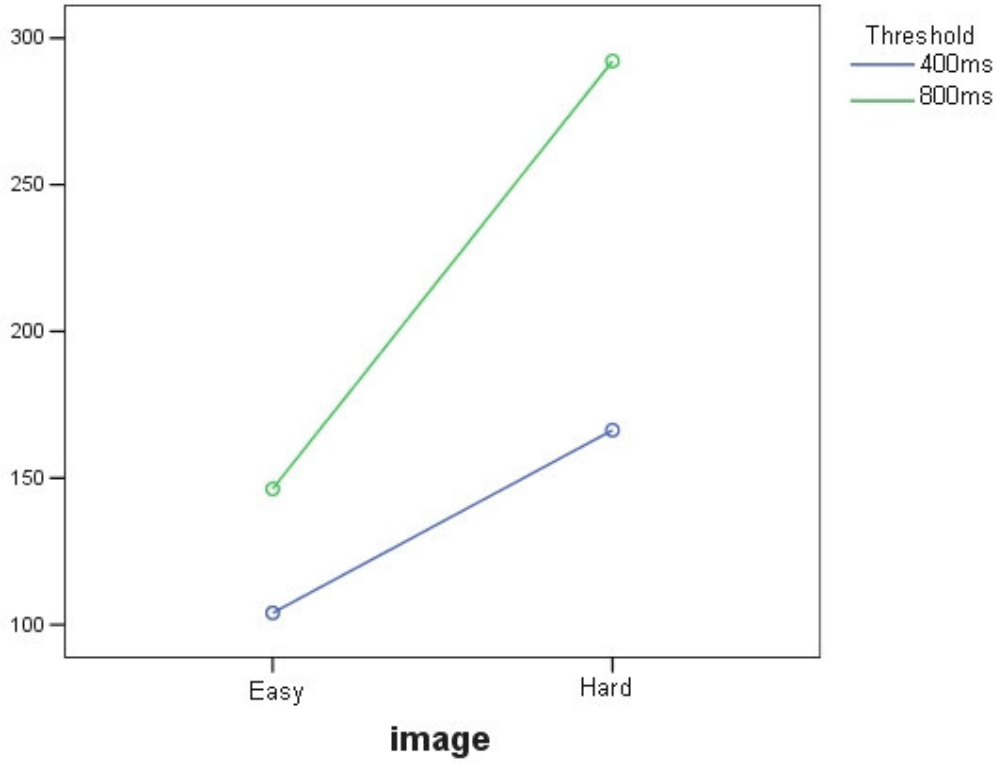

Figure 5.11: Average fixation numbers (Y-axis) by image type and fixation threshold

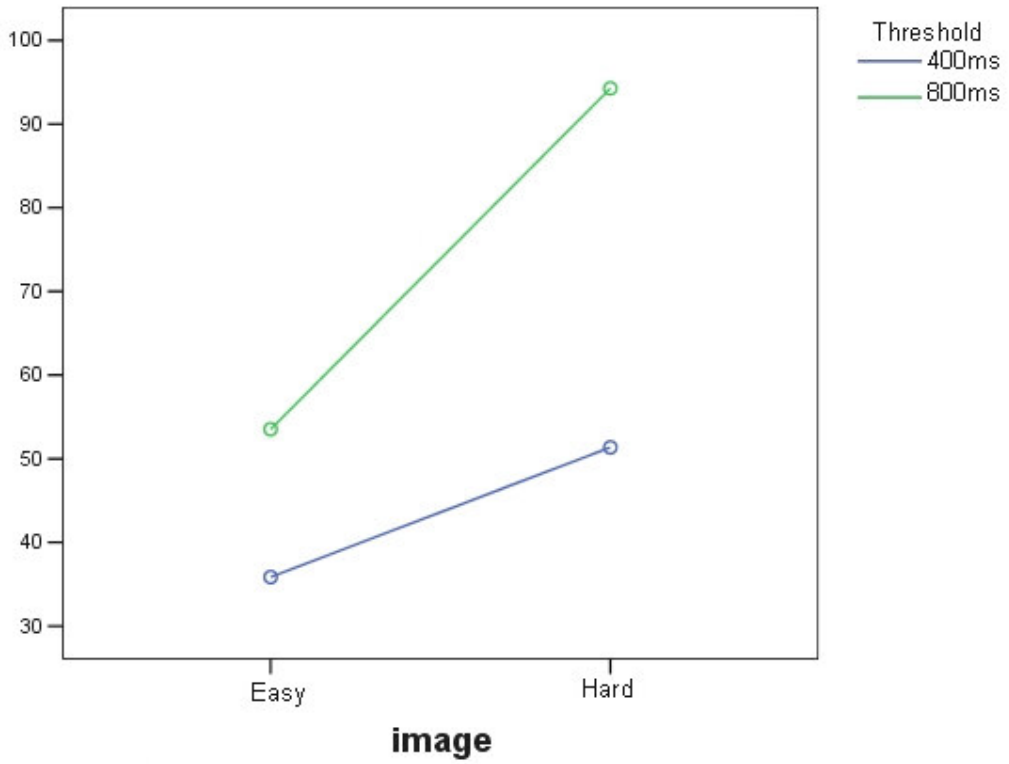

Figure 5.12: Average time to target (Y-axis) by image type and fixation threshold

The same treatment combinations experienced by all participants were applied to the random selection tool to obtain 104 dependent variables (steps to target). By combining the variables, 208 figures were entered into a mixed design multivariate ANOVA with two observations per cell and three factors (selection mode, image type and randomly-retrieved). The average figures are presented in Table 5.6.

Table 5.6: Comparison of Eye and Random Selection (rounded-off mean figures)

Selection Mode	Image Type	Randomly-retrieved	Target not found (frequency)	Steps to target
Eye gaze	Easy-to-find	0	38.5%	14
		1	34.6%	15
	Hard-to-find	0	80.8%	23
		1	76.9%	21
Random selection	Easy-to-find	0	57.7%	20
		1	38.5%	16
	Hard-to-find	0	96.2%	25
		1	92.3%	26

In summary the results of the ANOVA revealed a main effect of the selection mode, $F(2,23)=3.81$, $p<0.037$, with fewer steps to target when the eye gaze is used (18 steps) than when random selection is used (22 steps). Univariate tests on the two fixation threshold levels with corresponding random-selection values revealed significant differences between the eye

gaze and random selection for the 400ms and 800ms conditions i.e. F(1,24)=5.181, p=0.032 and F(1,24)=4.792, p=0.039 respectively (Figure 5.13).

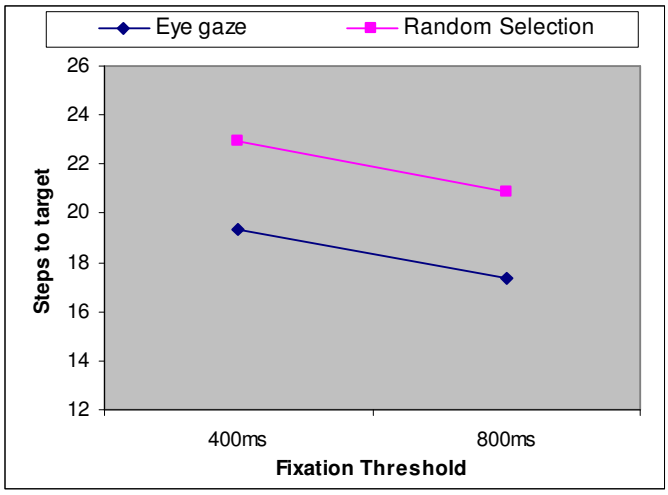

Figure 5.13: Comparison of eye gaze and random selection mode

There was also a main effect of image type, F(2,23)=28.95, p<0.00001 with fewer steps to target for easy-to-find images (16 steps) than the hard-to-find images (24 steps). Further analysis of simple main effect revealed that there was a significant difference between the modes for the hard-to-find images, F(2,23)=3.76, p<0.039 as opposed to the easy-to-find images, F(2,23)=2.02, p<0.16 (Figure 5.14). The participants using the eye tracking interface found the target in fewer steps than the automated random selection strategy and the analysis of simple effect attributed the significant difference to the hard-to-find images.

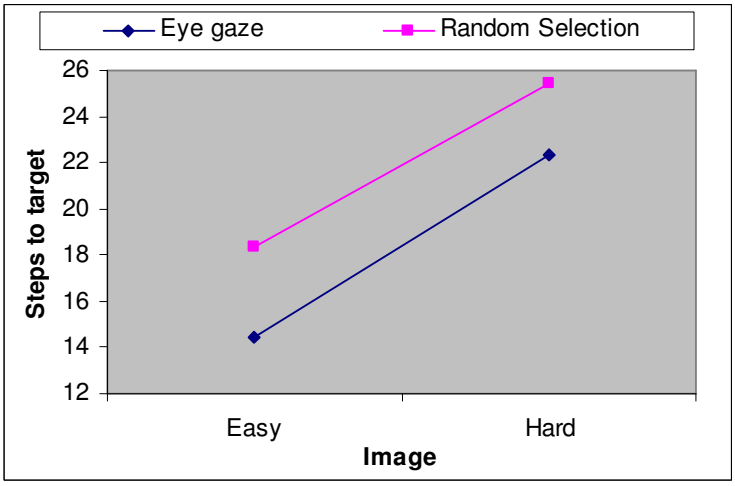

Figure 5.14: Average steps to target (Y-axis) by image type and selection mode

5.2.7. Experiment Analysis

The participants using the eye tracking interface found the target in fewer steps than the automated random selection strategy and the analysis of simple effect attributed the significant difference to the hard-to-find images. This meant that the probability of finding the hard-to-find images was significantly increased due to human cognitive abilities as opposed to the indiscriminate selection by random selection. This discriminating behaviour shows that the system is able to draw useful inference from gaze patterns.

Easy-to-find target images were found in fewer steps by participants than the hard-to-find images as predicted by the evidence obtained using the random selection tool. The random selection strategy was used for analysing the similarities within an image collection and was able to estimate the search difficulty of target images. Related work [106] describes four measures to examine retrieved documents and the documents in their vicinity and also estimate the quality of the search. The four measures comprise the following:

- *Clustering tendency* examines the hypothesis that documents relevant to a query are expected to form a group that is distinct from non-relevant documents and therefore be easier to retrieve;
- *Sensitivity to document perturbation* attempts to analyze the structure of the retrieved set by issuing a perturbed (noisy) version of the document as a pseudo-query and recording the new rank that the original document assumes with respect to the search with the modified pseudo-query;
- *Sensitivity to query perturbation* analyzes the structure of the document collection in the vicinity of the perturbed query; and
- *Change in the local intrinsic dimensionality*, where documents are considered points in a high dimensional space with coordinates corresponding to the distinct terms in the collection and the dimensionality of a subspace is occupied by a sub-collection of documents.

The search performance prediction helps to flag queries for which the system has not retrieved good search results before the results are presented to the user and may be useful in improving the chances of getting to the target. The work reflects the importance of exploring the structure of document or image collections. However, although this approach reveals much about the effectiveness or otherwise of specific queries, it does not identify specific items that are difficult or easy to retrieve whatever queries are employed.

There were more fixations and more time was spent on hard-to-find images than the easy-to-find images. This is consistent with the conclusion of Fitts et al [16] that complex information leads to longer fixation durations and higher fixation numbers.

The influence of including one randomly retrieved image in each display was investigated. Generally, there was little or no difference in the steps to target, time to target and fixation numbers. Even when compared with the random selection tool, the steps to target did not significantly differ. The selection approach used by the random selection tool produced an increase in the likelihood of finding a target image (Table 5.4), but did not affect the likelihood when used with gaze behaviour. The user probably did not pay any attention to the randomly-retrieved image in the retrieved set, as the randomly retrieved image was likely to be visually irrelevant. On the other hand attending to the randomly-retrieved image may have led the user away from a displayed cluster and decreased the likelihood of finding the target.

There was no significant difference in the time to target and fixation numbers between the threshold levels for the easy-to-find images as opposed to the hard-to-find images. In other words, setting a higher threshold did not significantly differ when either 400ms or 800ms was used for the easy-to-find images, but it did for the hard-to-find images. However, the steps to target did differ for both image types under either of the threshold conditions. A future experiment will be needed to investigate whether the thresholds can be reduced further, at least for the easy-to-find images.

Many did not reach the hard target after 26 successive displays. Future experiments could concentrate on improving the chances of getting to the target using information extracted from the scan path.

5.2.8. Gaze Parameter Analysis

There are many parameters that may be extracted from human eye movement data and potentially exploited as visual input for an image retrieval system. The hypothesis that users display similar patterns of behaviour as they move closer to the target image is tested by analysing average parameter values as the search gets closer to the target. This hypothesis, if true, would improve the interpretation of gaze behaviour for better image selection. The gaze parameters that have been extracted include:

- Number of fixations on selected images in each display
- Total number of fixations within each display
- Number of images with at least one fixation within each display
- Final duration of fixation on selection of selected image (ms)
- Saccade duration prior to selection of selected image (in units of 20ms)
- Saccadic speed prior to selection of selected image (in units of pixels per 20ms)
- Saccadic speed during scanning (in units of pixels per 20ms)
- Pupil diameter on selection of selected image

In the results below, the gaze parameters are averaged over 8 experimental runs for each participant, and in each chart the lines represent the progress of each user towards the target image. The gaze parameters are also averaged for all participants. Additionally histogram plots of each gaze parameter provide insight into gaze behaviour during the runs.

5.2.8.1. Fixations

The number of fixations on the selected image did not produce any obvious trend as the user moves towards the target within the image database. However, there were many occasions when the fixations returned twice or more to the images that were finally selected as shown in Figure 5.15.

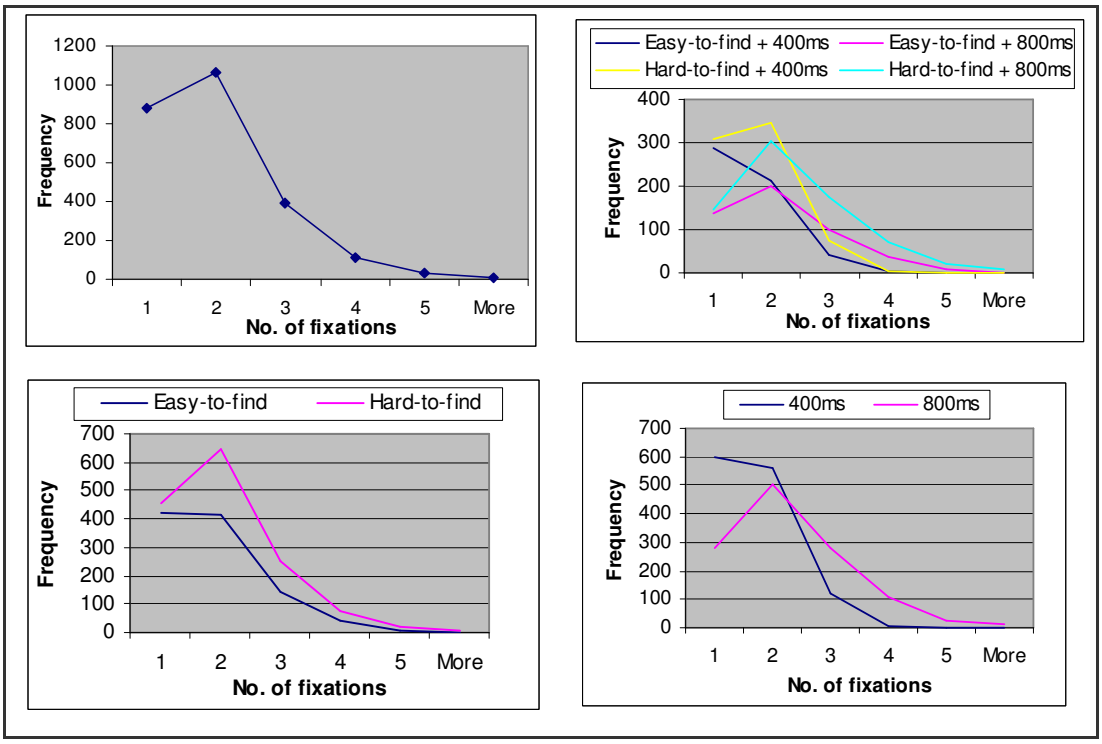

Figure 5.15: Histogram plots of the number of fixations on selected image

Table 5.7: Frequency of Revisits on selected image for each display

Treatment Levels	Selected Image		
	Revisits *	Zero revisits †	
Easy-to-find + 400ms	**260** (59.2%)	**287** (78.4%)	547
Easy-to-find + 800ms	**345** (48.1%)	**137** (62.8%)	482
Hard-to-find + 400ms	**430** (59.8%)	**310** (74.2%)	740
Hard-to-find + 800ms	**578** (45.2%)	**146** (52.1%)	724
Easy-to-find	**605** (52.9%)	**424** (73.3%)	1029
Hard-to-find	**1008** (51.4%)	**456** (67.1%)	1464
400ms	**690** (59.6%)	**597** (76.2%)	1287
800ms	**923** (46.3%)	**283** (57.2%)	1206
	1613 (52.0%)	**880** (70.1%)	2493

* The percentages in bracket represent the occasions where the first revisit occurred on the selected image
† The percentages in bracket represent the occasions where there were no revisits on any other image

Altogether in the experiment there were 2493 display changes (i.e. total steps to target) of which there were 1613 revisits on the selected images and 880 display changes with no revisits (Table 5.7). 52.0% of these revisits occurred first on the selected image within the display. The percentage of revisits that occurred first on the selected image increased from 46.3% to 59.6% when the cumulative fixation threshold was decreased from 800ms to 400ms. There was a decrease in the number of revisits from 923 to 690 and an accompanying increase in single fixations (no revisit) from 283 to 597. The users seemed to prefer the revisited image amongst the other images on the display as the gaze time was reduced.

The assumption is that users might be using more of their peripheral vision to make decisions under time constraints, since the performance still fared better than random selection. Although there were lower incidences of revisits, users still managed to revisit the selected image within a lower threshold level and also scan other images in the display. The frequency of revisits may be an indication of interest in the image. It should be noted that there were 260 display changes when the selected images were not revisited but there were revisits on other images (not selected) within the displays. In addition, 900 display changes had revisits on the selected images and other images (not selected) within the respective displays.

There was no obvious trend in either the average number of fixations within the display, or the average number of images with at least one fixation, or the average fixation duration at display change for each individual user, as the user moves towards the target image within the image database. These results highlighted the undiminishing activity in eye movement in all subjects when striving to achieve a goal (i.e. complete a search).

Two gaze parameters are averaged for all subjects and presented in Figure 5.16. The number of images with at least one fixation will be generally lower than the number of fixations within a display due to incidences of more than one visit to an image in the display.

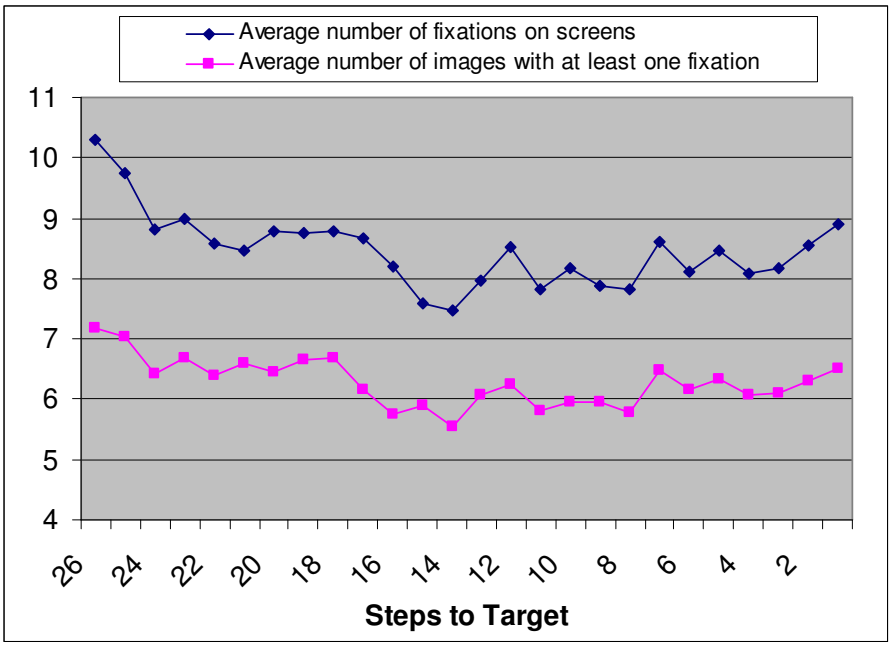

Figure 5.16: Average number of images with at least one fixation and the average number of fixations in each screen as user approaches target image

Figure 5.16 shows a correlation between the number of images with at least one fixation and the number of fixations within a display as the user moves towards the target. An increase in the number of fixations within a display is associated with a corresponding increase in the number of images being viewed. The correlation coefficient is used to determine the relationship between two data sets given by:

$$\rho_{x,y} = \frac{Cov(X,Y)}{\sigma_x.\sigma_y} \text{ where } -1 \le \rho_{xy} \le 1 \text{ and}$$

$$Cov(X,Y) = \frac{1}{n}\sum_{j=1}^{n}(x_j - \mu_x)(y_j - \mu_y)$$

A positive correlation coefficient of the two data sets confirmed that the two ranges of data move together ($\rho = 0.93$). This seems reasonable as an increase in the number of fixations is likely to be a consequence of the user looking at more images.

The computation of the image selection criteria requires the cumulation of the fixation threshold up to a limit. Therefore a 400ms limit may cause the user to utilise the first 160ms for scanning the images within a display followed by a return to the same image for a 240ms fixation and selection. Figure 5.17 shows the average fixation duration at the moment of the

selection of images. The data shows that with the 400ms threshold the final fixation duration stabilised as users moved towards the target. It is unlikely that this effect is due to any deliberate action of the users which tends always to be very diverse and user-dependent. However, it may arise as an instinctive or reflexive action in human vision which takes place preattentively.

The number of fixations varied mostly between two and eleven fixations within each display (Figure 5.18) while the number of images with at least one fixation varied between two and six fixations (Figure 5.19). These results are based on cumulative fixation thresholds of 400ms and 800ms and may yield different results with other thresholds.

The data also showed that users employed the high threshold limit of 800ms as an opportunity to conduct more revisits to selected images within a display (Table 5.7), given that the average fixation duration on selected images (at point of display change) peaked around 500ms as shown in Figure 5.17 and Figure 5.20. The highest frequency of the final fixation duration on selected images of 500ms suggests that participants comfortably made conscious decisions after around 500ms.

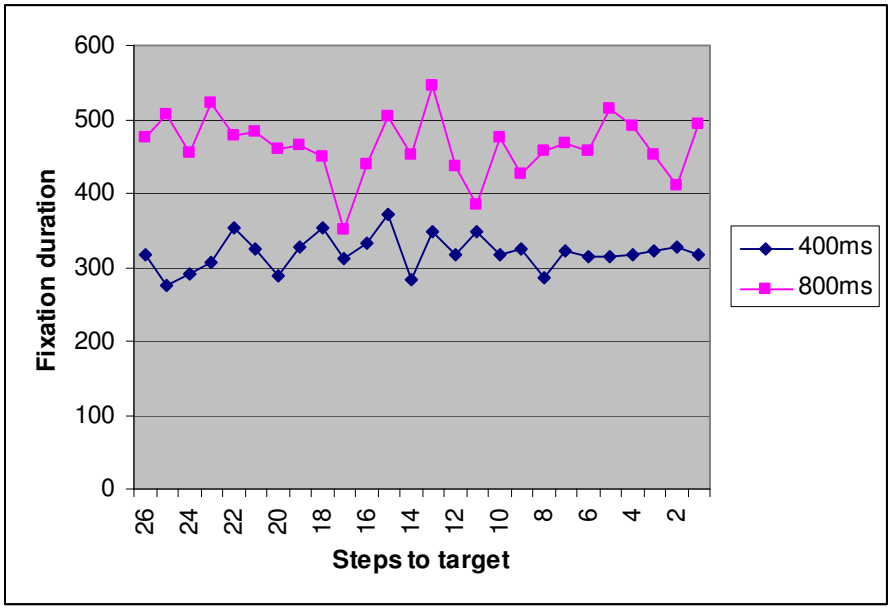

Figure 5.17: Average fixation duration on selected image at point of display change as user approaches target image

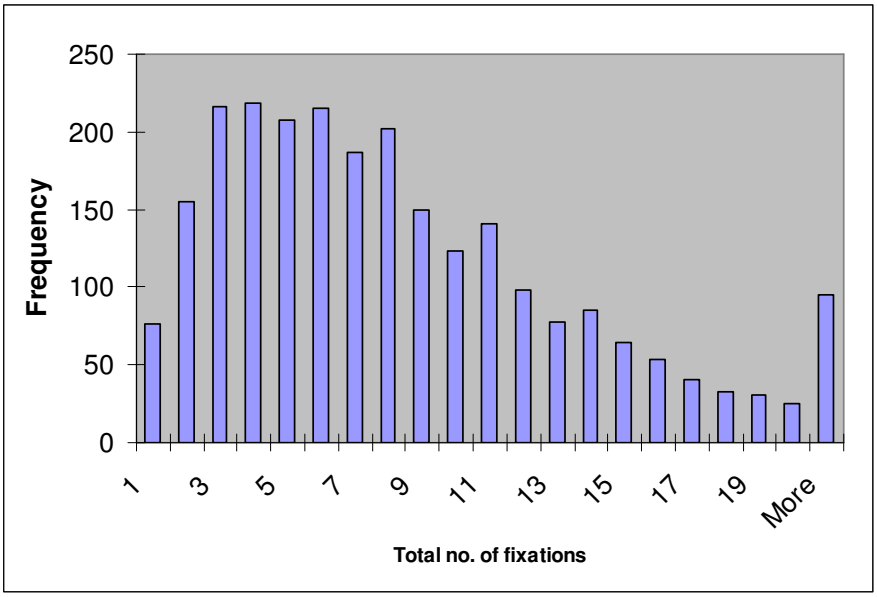

Figure 5.18: Histogram plot of the total number of fixations within each display

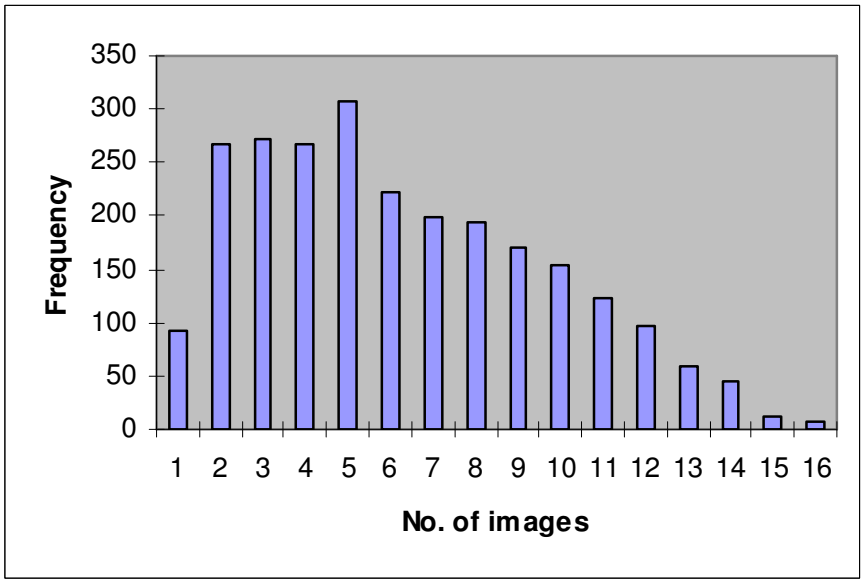

Figure 5.19: Histogram plot of the number of images with at least one fixation

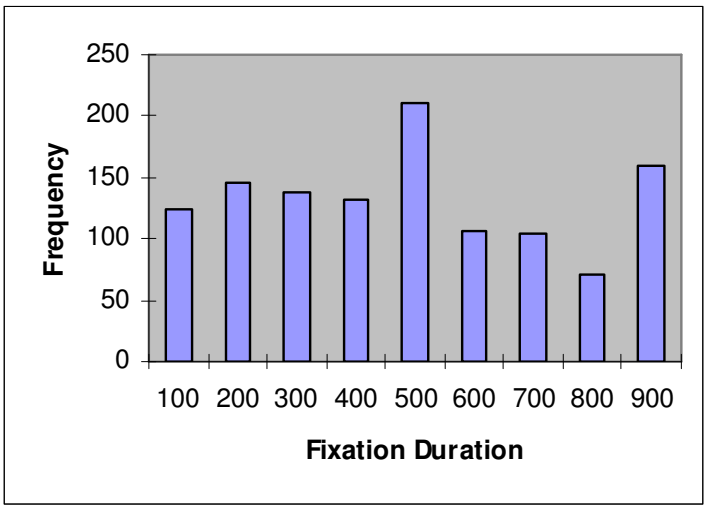

Figure 5.20: Histogram plot of the final fixation duration on selected image at point of display change (cumulative threshold of 800ms)

5.2.8.2. Saccades

Saccades are quick, simultaneous movements of both eyes in the same direction and serve as a mechanism for fixation, refixation and rapid eye movements. The dynamics of saccadic eye motion give insight into the complexity of the mechanism that controls the motion of the eye. Accordingly the duration and speed of saccade were analysed. Figure 5.21 show that the saccade duration prior to selection of the selected image did not produce any discernible trend as the user became closer to the target within the image database. This was the case for each user and when averaged across all users (Figure 5.21). Figure 5.22 indicates that users most often spent between 20ms to 60ms duration on the saccade just prior to a selection.

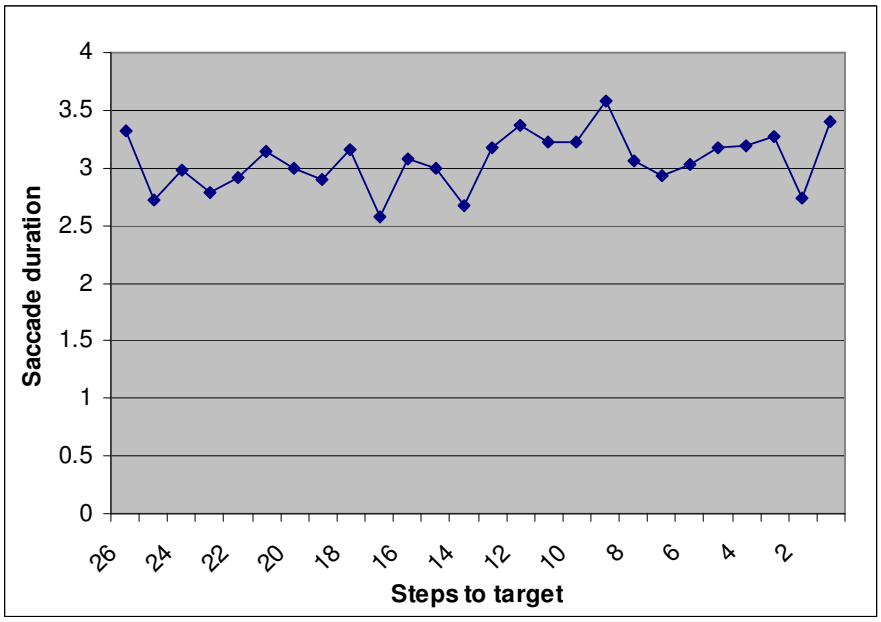

Figure 5.21: Average saccade duration across all subjects prior to selection of selected image (in units of 20ms) as user approaches target image

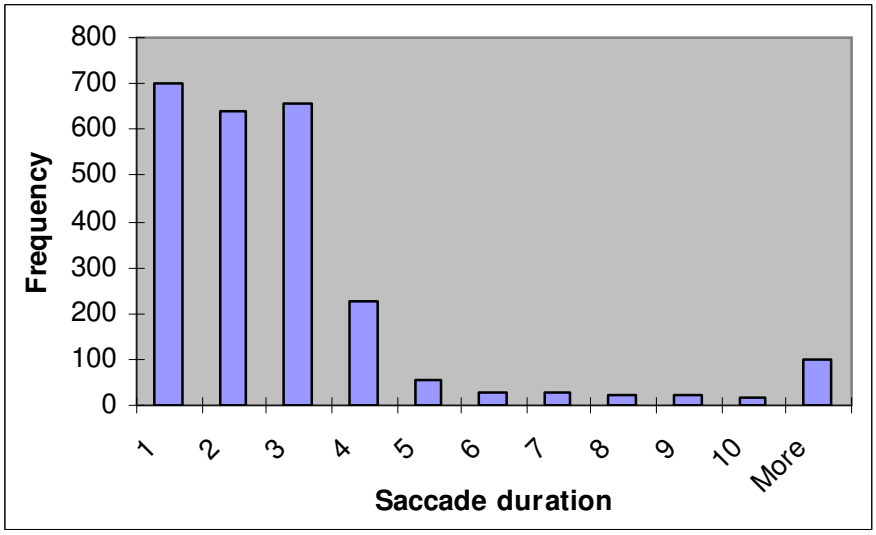

Figure 5.22: Histogram plot of the saccade duration (units of 20ms) just prior to selection of selected image

Given the display of images that participants have to search through in the experimental runs, it is also possible that there may be a variation of saccadic *speed* between two conditions:

1. Normal scanning of the display and
2. Saccadic speed just prior to selection of the selected image in the display.

The first condition refers to the average saccade speed while searching around the display and the second condition refers to the speed just before selection. There was no discernible pattern of saccadic speed across participants prior to selections and during normal scanning as they

move closer to the target. The saccadic speeds are averaged for all participants and compared in Figure 5.23. There was no correlation between the two conditions (correlation value of 0.144). This lack of correlation was explored further through a plot of the distribution of saccadic speeds under the two conditions (Figure 5.24). Interestingly this shows that saccadic speeds are frequently slower just before a selection, with a larger difference when the cumulative fixation threshold of 800ms is used (Figure 5.26) than when 400ms threshold is used (Figure 5.25). This may indicate a measure of deliberation on the part of the user who may have come to a specific decision on an image selection.

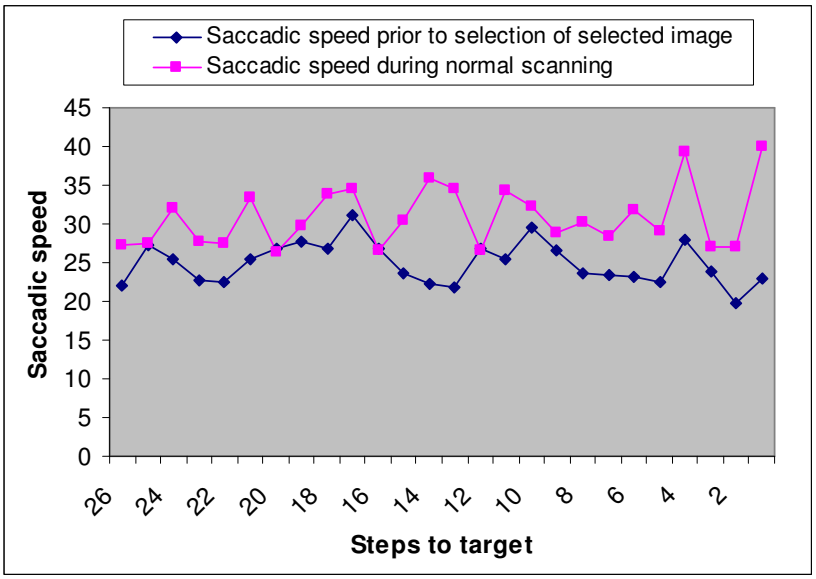

Figure 5.23: Comparison of average saccadic speeds during scanning and just prior to selection (in units of pixels per 20ms) as user approaches target image

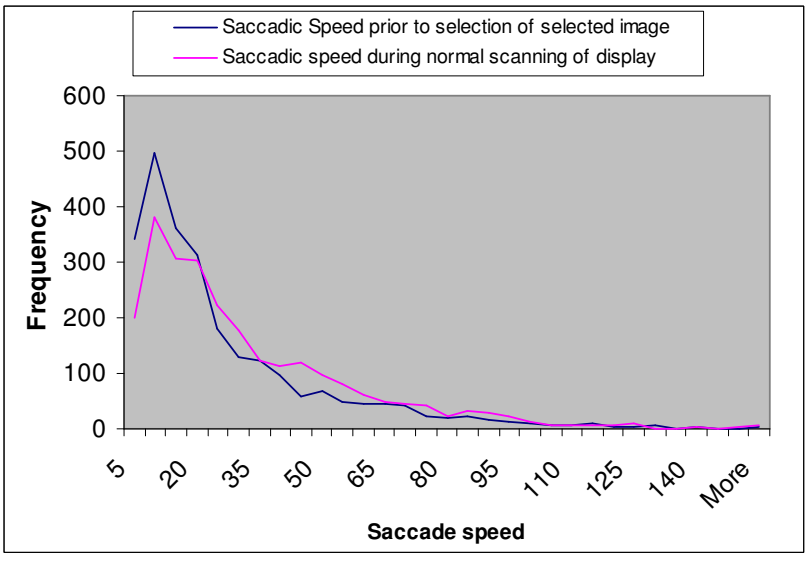

Figure 5.24: Histogram plot comparing the saccadic speed just prior to image selection with normal speeds (in units of pixels per 20ms)

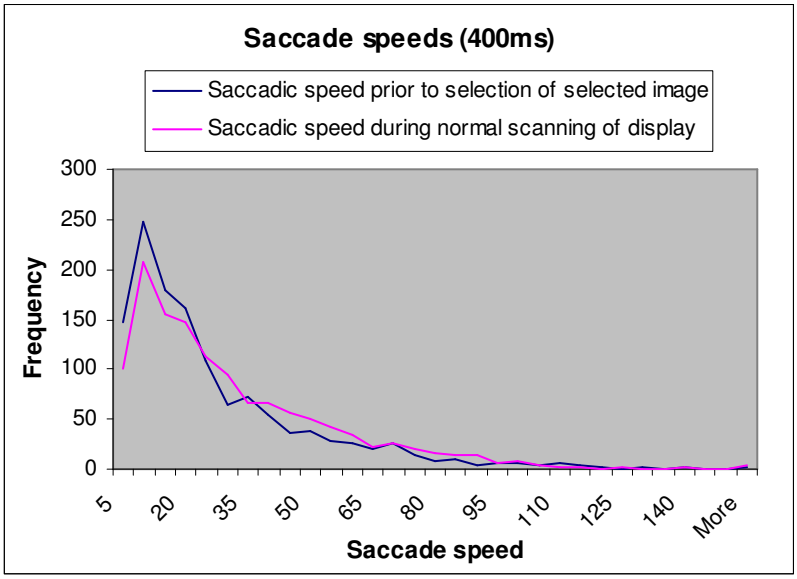

Figure 5.25: Histogram plot comparing the saccadic speeds for the 400ms cumulative threshold

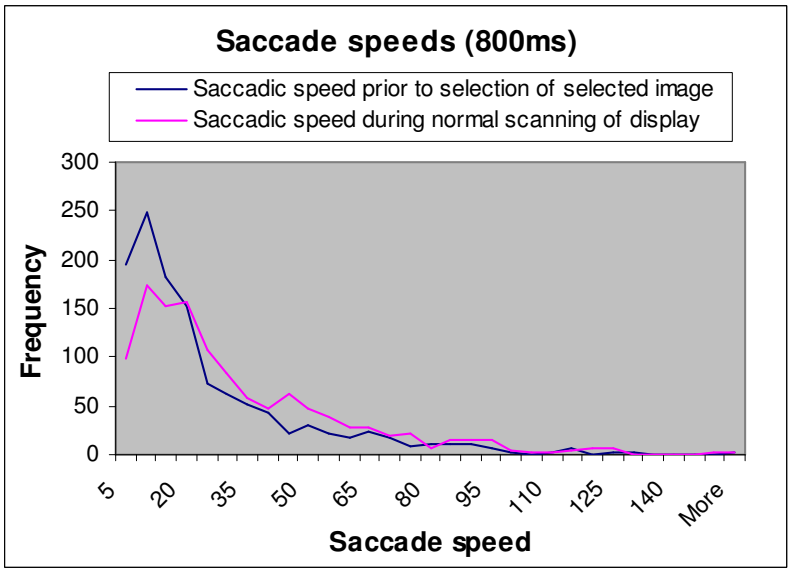

Figure 5.26: Histogram plot comparing the saccadic speeds for the 800ms cumulative threshold

5.2.8.3. Pupil Diameter

There were considerable variations in pupil diameter across users and no discernible trend as the users move towards the target (Figure 5.27). Figure 5.28 shows the frequency distribution of the pupil diameters at the moment of selection of selected image. A histogram plot of the pupil diameter for easy-to-find and hard-to-find images revealed a peaked distribution when the hard-to-find images were used. The kurtosis of a data set characterizes the relative peakness or flatness of a distribution compared with the normal distribution. Positive kurtosis indicates a

relatively peaked distribution. Negative kurtosis indicates a relatively flat distribution. Kurtosis is defined as:

$$\left\{ \frac{n(n+1)}{(n-1)(n-2)(n-3)} \sum \left(\frac{x_j - \bar{x}}{s} \right)^4 \right\} - \frac{3(n-1)^2}{(n-2)(n-3)}$$

where s is the standard deviation.

The pupil diameter on the easy-to-find target images revealed a negative kurtosis (-1.45) while the hard-to-find showed a positive kurtosis (0.27). In other words the pupil behaviour of more people becomes similar as the search task gets more difficult. Perhaps the increase in fixations associated with hard-to-find target images reduced the likelihood of diverse pupil behaviour.

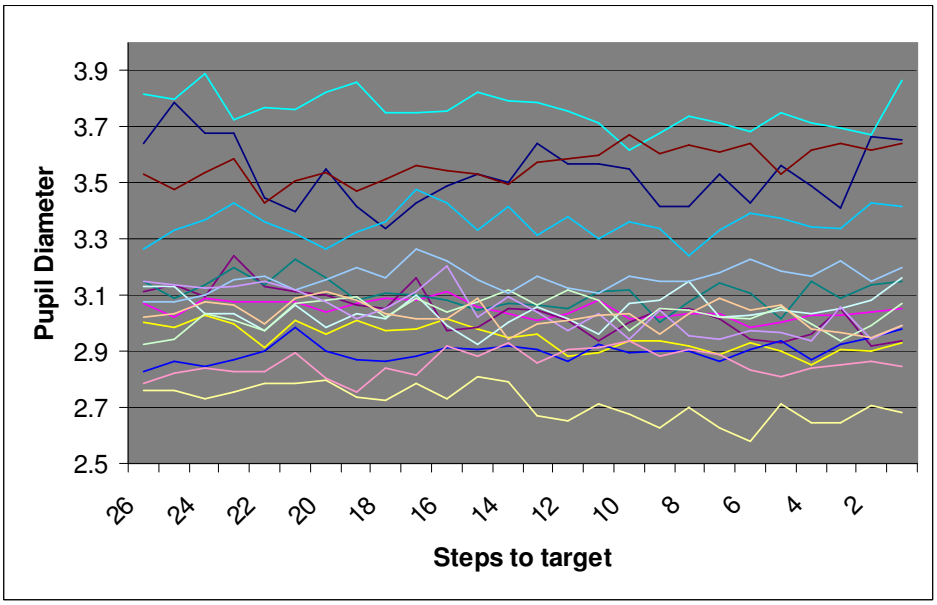

Figure 5.27: Average pupil diameter per subject on selection of selected image

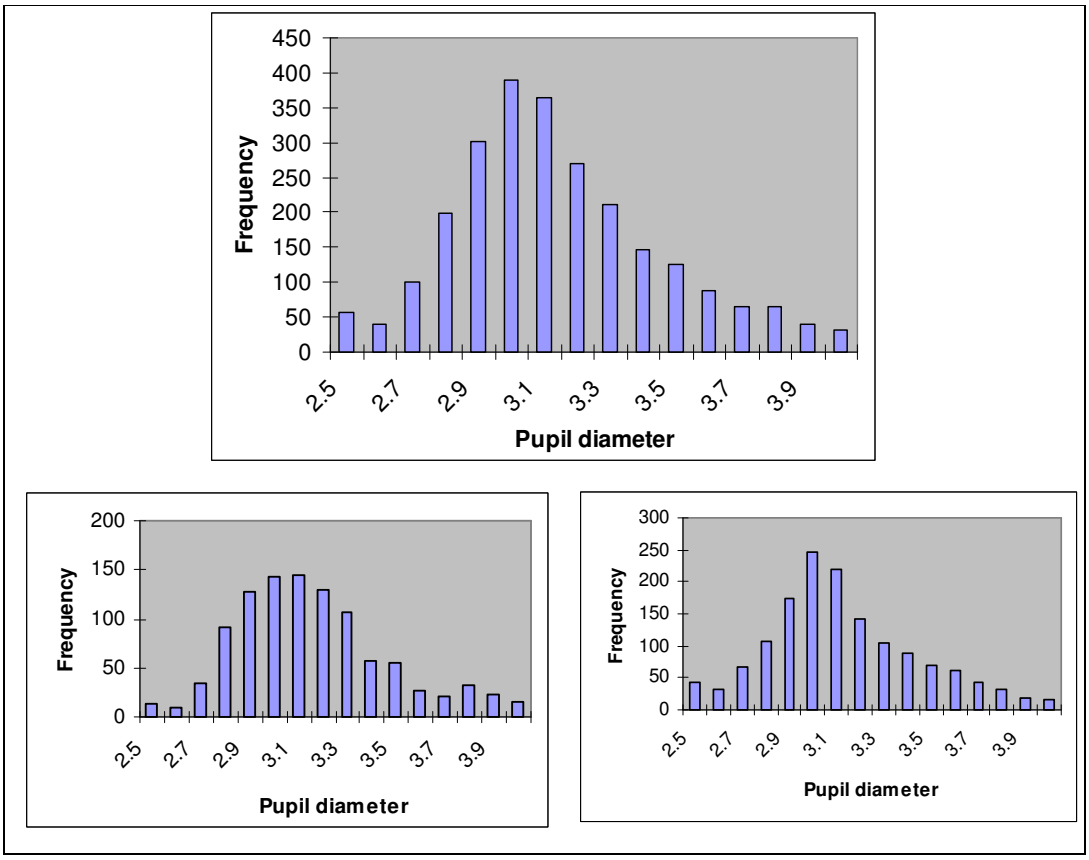

Figure 5.28: Histogram plot of the pupil diameter on selected image (bottom left chart describes the easy-to-find images while the bottom right represents the hard-to-find images).

5.2.9. Discussion

The design of this experiment was such that users' behaviour was measured by identifying the first image to exceed a designated threshold of fixation durations. Participants were able to adapt their viewing behaviour based on speed of screen changes. Images compete for attention and user fixations based on users' attraction to the most similar image in the display.

In this work, the display did remain unchanged during the period while the system loaded the next set of images into memory and was updated instantaneously as soon as the contents of the next display had been composed. However, the eye may still be fixating on a position that is no longer relevant to the current screen so the first few milliseconds of fixation on the next display should be ignored. There is no reason to believe that this has a confounding influence on the result due to the relatively higher cumulative fixation threshold values of 400ms and 800ms. In this way data from the first 120ms following screen changes will be ignored in future experiments.

In the image retrieval experiment, fixations of 80ms and above were regarded as intentional fixations while all fixations less than 80ms were ignored. Henderson and Hollingworth's review [22] indicated the variability of fixation durations range from less than 50ms to more than

1000ms in a skewed distribution with a mode of about 230ms. Schyns & Oliva [94] also demonstrated that a photograph of a scene can be identified as a particular scene type from a masked presentation in as short as 45 – 135 ms. These results demonstrate that the information necessary to identify a scene can be extracted quickly, and it was concluded that scene identification from 50ms views were based on low-level information. A fixation threshold of 80ms was therefore chosen in the experiments. Three minimum gaze samples of 20ms each were required to detect a fixation; any fewer samples would have introduced unacceptable errors. An investigation of lower thresholds with faster equipment might have yielded better results.

It may be suggested that display change artifacts might influence performance. However, Inhoff et al [108] tested the hypothesis that display changes influence the outcome of eye-contingent display change studies. The speed of a display change and the refresh rate of the display monitor were varied and no evidence was found to suggest that the results of eye-contingent change experiments were artifacts of the paradigm.

Three factors (image type, fixation threshold and randomly-retrieved) and three dependent variables (steps to target, the time to target, and the number of fixations) were investigated in this study. The results are analysed in Section 5.2.7 where the eye tracking interface was shown to perform better than the random selection strategy, demonstrating that the eye gaze interface expressed the intentions of the user and made use of the structure of the similarity data. Giving users longer viewing time did not necessarily yield significantly better results hence shorter thresholds need to be investigated in further experiments. A systematic exploration of the spatial and temporal distribution of the gaze parameters (fixation, saccade and pupil diameter) on the displays was also carried out.

The hypothesis that users display similar patterns of behaviour as they move closer to the target image was tested by analysing average parameter values as the search got closer to the target. None of the parameters investigated produced any relationship with the steps to target. This may have been a consequence of the complexity of the system and the number of factors that were investigated, though it was more likely that this result reflected the diversity of human behaviour. Indeed participants' expectations of the retrieved sets of images as computed by the similarity links would have differed and this may have caused a variation within each run.

Figure 5.17 shows that the fixation durations stabilise near the target for 400ms searches. This is probably more dependent upon involuntary vision functionality than conscious action in view of the short display times. This effect is in spite of the diverse behaviour of users. Given that the average fixation duration on selected images peaked around 500ms as shown in Figure 5.17 and Figure 5.20, this provides circumstantial evidence of unconscious pre-attentive vision as gaze time is reduced.

The frequency of refixations on images that are subsequently selected even at the faster speed of 400ms (Table 5.7) showed that refixation of an image may be an early indication of user interest. Gilchrist and Harvey [17] measured refixations in a letter search experiment and found that participants were less likely to refixate a rejected item that had been previously fixated than would be predicted by chance. Hollingworth and Henderson [23] found that relatively detailed visual information is retained in memory from previously attended objects in natural scenes. Participants successfully detected changes to a target object when the object had been previously attended but was no longer within the focus of attention when the change occurred. Change detection was said to be dependent on prior fixation of the target object. Refixation of the target object was also found to play an important role in change detection. The vast majority of detections came on refixation of the changed object, suggesting that refixation may cue the retrieval of stored information about a previously fixated and attended object. Taken together, these results lend credence to the belief that refixation may be an indication of interest in image search.

The experiment confirmed that the saccade durations in this experiment mostly ranged from 20ms to 60ms. Saccades were frequently slower just before a selection. The initiation of saccades just prior to selections might have resulted in slower saccades because selected images generally attracted revisits. Indeed it is reasonable to believe that the slower saccades before a selection were because of deliberate selection by the participant. Saccade speeds were generally higher during scanning of the display as users become aware that the system is time dependent.

Pupil diameter is regarded as a measure of the cognitive demands of a task [107]. The observed change in peakness of the pupil diameter data reflects difficulty levels of the two target image types. The peakness of the distribution of pupil diameter is high on the hard-to-find images. This pattern may be useful in determining when a user is experiencing difficulty with a task.

Combining these results may produce a more effective method of inferring intentions from users in future eye tracking interfaces.

5.2.10. Summary

Experiments have shown that an eye tracking interface together with pre-computed similarity measures yield a significantly better retrieval performance than random selection using the same similarity information. A significant effect on performance was also observed with hard-to-find images. This was not seen with easy-to-find images where with the current database size a random search might be expected to perform well.

The analysis of the fixations, saccades and pupil diameters yielded useful information that is representative of users' interests and worthy of further investigation. The next section describes

experiments designed to investigate gaze behaviour using alternative target selection criteria derived from the analysis of gaze behaviour in this section.

Chapter 6. Refixation and Pre-Attentive Vision in Image Search

6.1. Objective

The system implementation from the previous chapter confirms the feasibility of driving an image retrieval engine with an eye gaze interface. Analysis of the eye movement data during image search in the last section revealed that users frequently revisit images that are subsequently selected and do this quite happily at rapid speeds (400ms cumulative fixation threshold). The objective of this experiment is to investigate the likelihood of getting to the target image using alternative criteria for improved image selection. The effects of lower fixation thresholds and revisits are investigated.

6.2. Experiment Design

The same database of images and its pre-computed similarity links were used in this experiment. In the previous experiment, participants' search results matched the structure of the similarity links in terms of the ease or difficulty of finding the target image. Hard-to-find images were more difficult to find than Easy-to-find images. In order to increase the chance of finding target images and enable better exploration of search behaviour, eight easy-to-find target images were selected for this experiment. Screens of thumbnail images were displayed as 229 x 155 pixels in 4 x 4 arrays. The initial screen for each target is shown in Figure 6.1 to Figure 6.8, where the target image is located at the top left bordered in red. Participants begin by viewing the initial screen and looking for the target image among the other 15 images. The system computes the selected image based on gaze behaviour. The selected image determines the next 15 thumbnails to be displayed as indicated by the highest of the pre-computed similarity scores for other images in the database. The display automatically changes once the next sets of retrieved images are loaded into memory. The participant is presented with a succession of such screens (Figure 5.7) until the target image is retrieved whereupon the run halts and the successfully found target is highlighted with a red border as shown on the right of Figure 5.7.

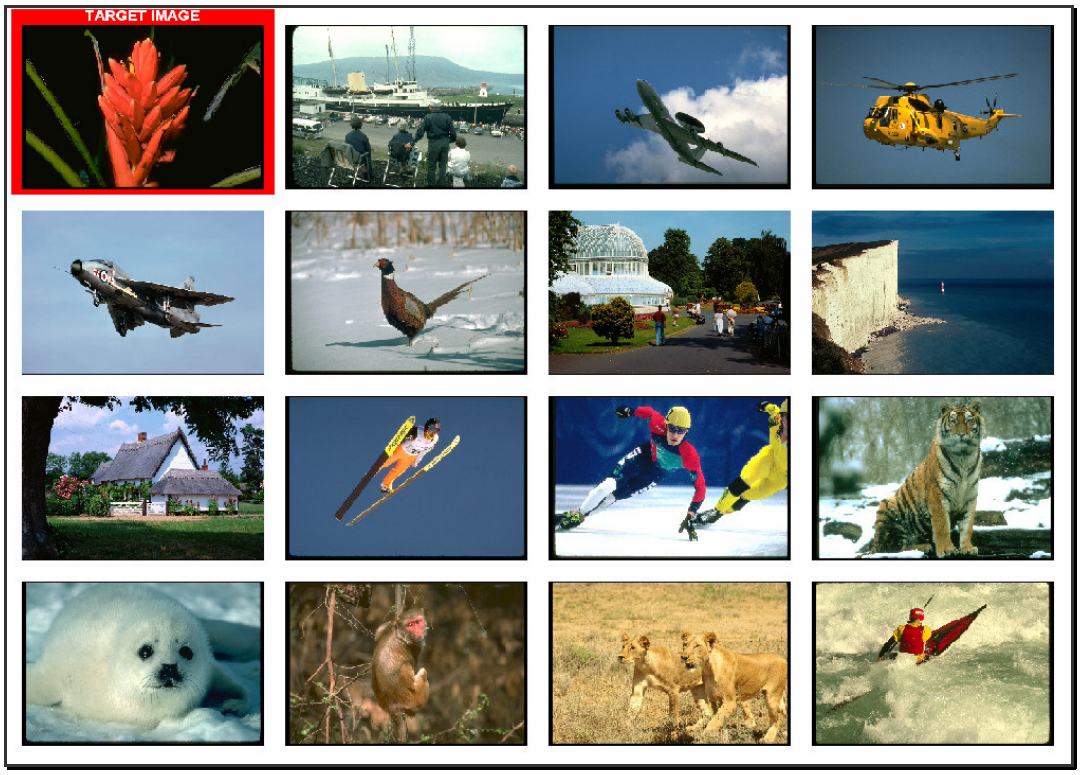

Figure 6.1: Target image 1 and its initial screen

Figure 6.2: Target image 2 and its initial screen

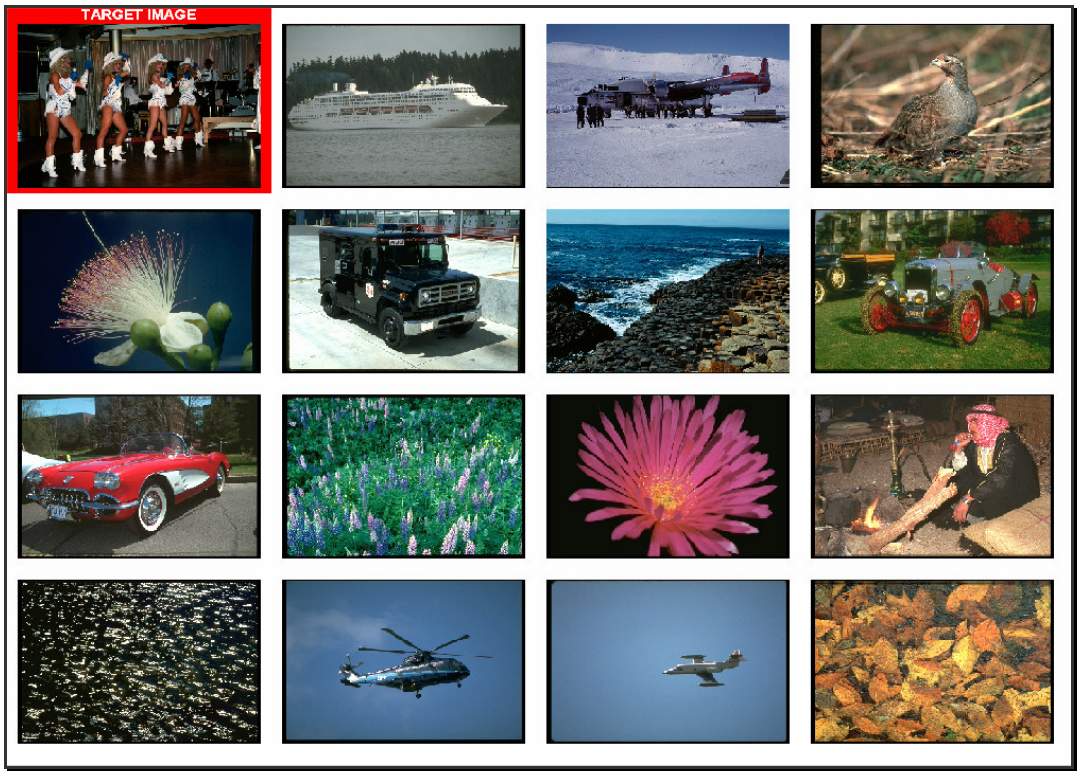

Figure 6.3: Target image 3 and its initial screen

Figure 6.4: Target image 4 and its initial screen

Figure 6.5: Target image 5 and its initial screen

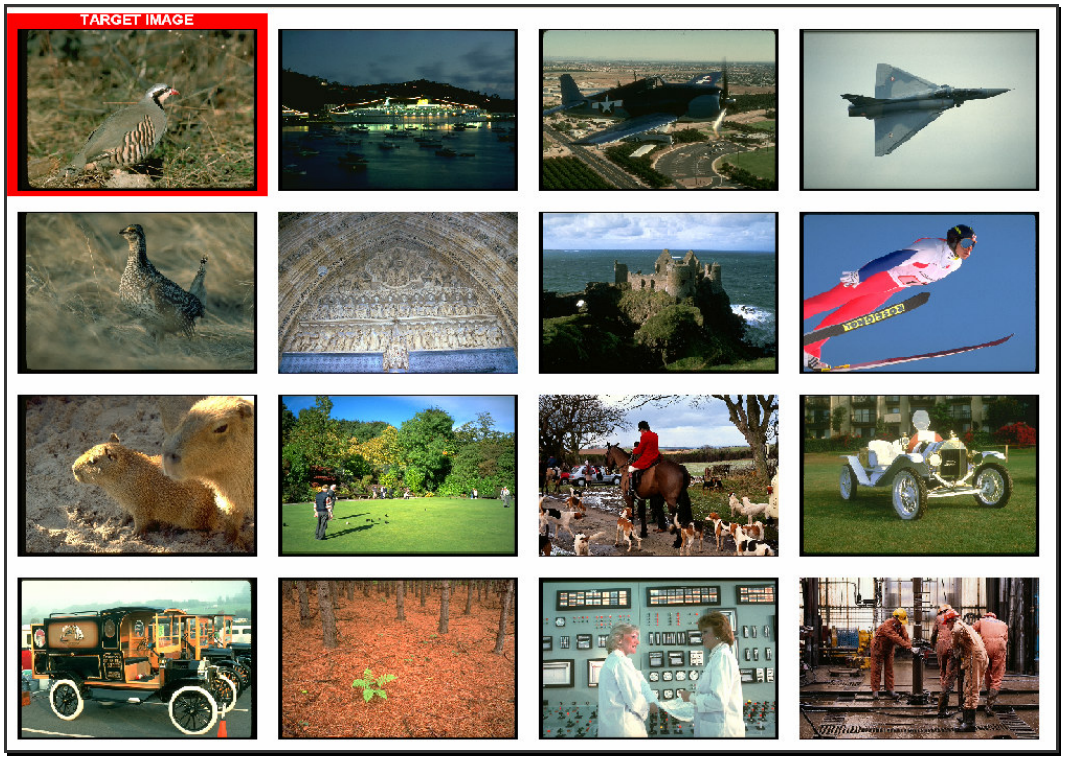

Figure 6.6: Target image 6 and its initial screen

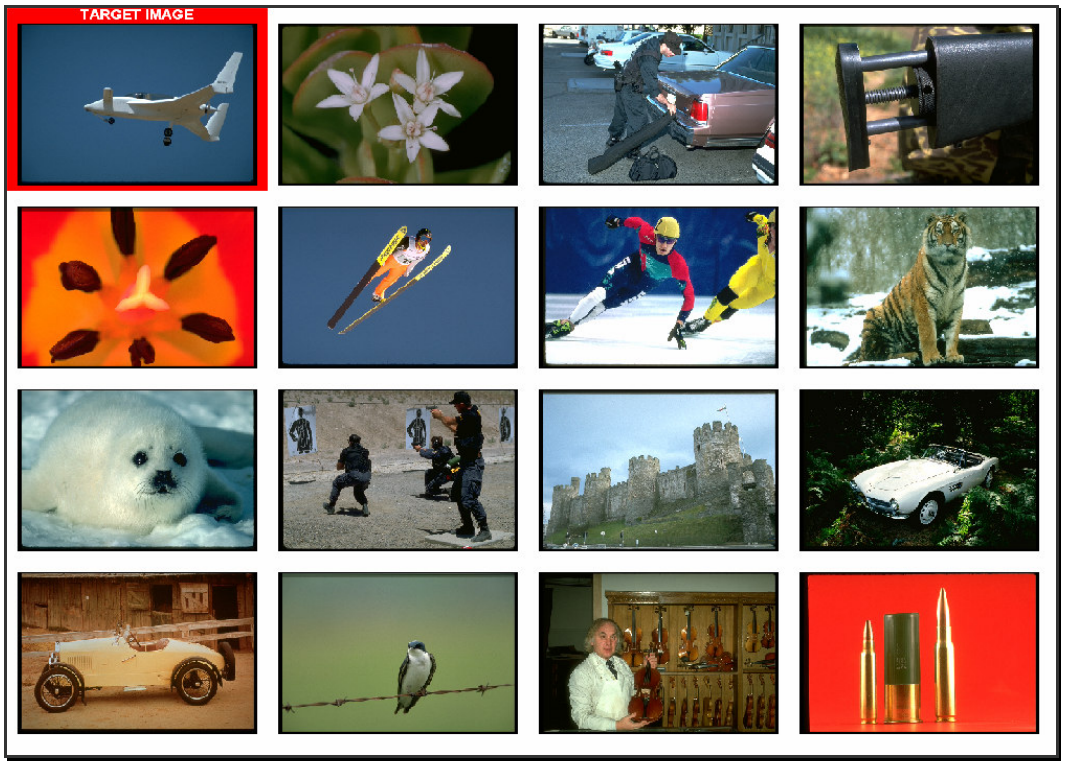

Figure 6.7: Target image 7 and its initial screen

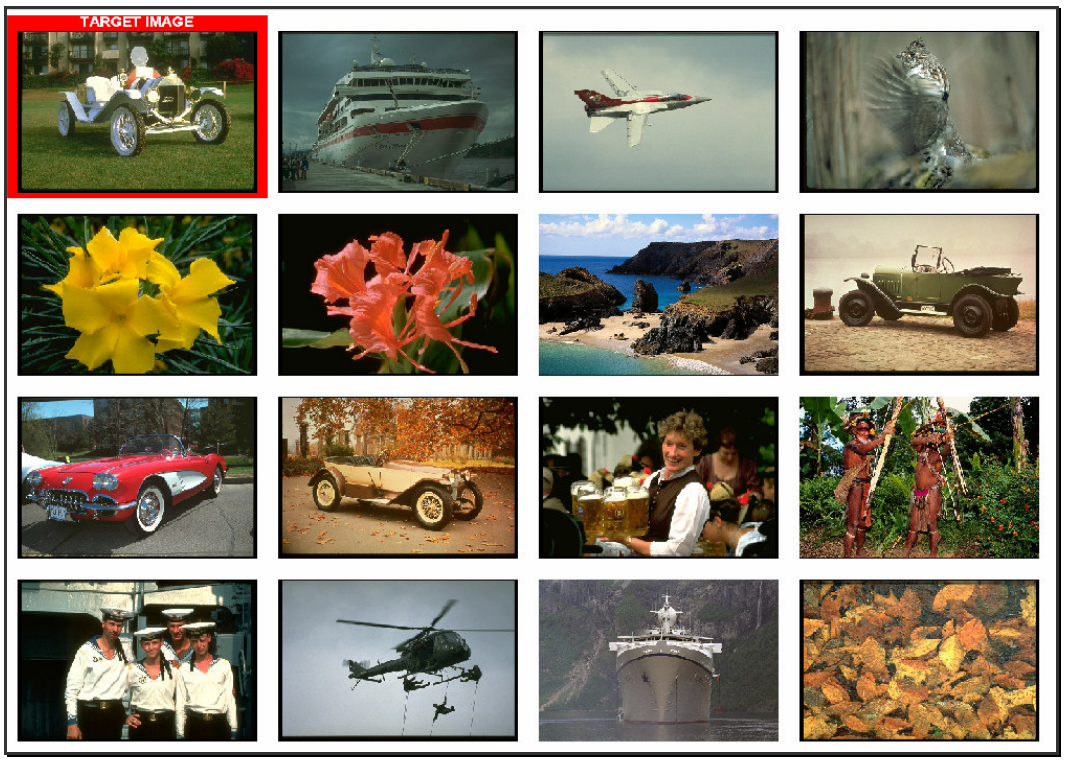

Figure 6.8: Target image 8 and its initial screen

6.2.1. Refixation and Fixation Threshold Criteria for Image Selection

The display automatically changes based on gaze behaviour. In this experiment, four treatments are used for determining best image selection:

- a cumulative fixation threshold of 400ms as before
- a shorter cumulative fixation threshold of 300ms;
- selection by revisit
- selection by revisit or cumulative fixation threshold of 400ms

As in prior experiments, the cumulative fixation threshold is determined by the accumulation of all fixations greater than 80ms on a specific image position exceeding a 300ms or 400ms threshold. A revisit is determined by the refixation of an item that has been previously fixated. In this case the first image to be visited twice is selected as the selected image. Although participants were not aware of the criteria for image selections, the Revisits condition had no time restriction. However, it was thought that participants may not refixate an image during directed search hence the fourth treatment was determined either by a revisit or the cumulative fixation threshold of 400ms whichever occurred first (i.e. the selected image is either determined by the first image revisited or the first image to exceed the cumulative threshold of 400ms).

6.2.2. Participants

Twenty-four unpaid participants (18 males and 6 females) took part in this experiment. The mean age was 28.8 years with a median of 27 and a mode of 26. Participants included a mix of students, university staff and members of the public. All participants had normal or corrected-to-normal vision and provided no evidence of colour blindness.

6.2.3. Experimental Procedure

Results in the previous section showed that the inclusion of random images in successive displays does not affect performance. In this experiment the display used either:

(a) 15 images with the highest similarity values to the selected image, or

(b) 15 images with the highest similarity values to the 15th ranked similar image to the selected image.

Theoretically condition b) should allow users to move more freely between clusters, but at the risk of moving away from the target.

Participants performed 8 runs, using easy-to-find image types. There was one practice run to enable better understanding of the task and to equalise skill levels before the experiment. Participants understood that there would be a continuous change of display until they found the target but did not know what determined the display change. Eight treatment combinations of

the four fixation thresholds (400ms, 300ms, Revisit and Revisit/400ms) and two ranking levels ((a) and (b)) were applied. Any sequence effect was minimised by randomly allocating each participant to 24 different sequences of the four fixation thresholds. There was a 1 minute rest in between runs. As before the maximum number of steps to target was limited to 26 screen changes.

6.3. Results

Three dependent variables, the number of steps to target, the time to target (F_1), and the number of fixations (F_2) of 80ms and above were monitored and recorded during the experiment. 24 dependent variables (8 each) were recorded for each participant. The average figures are presented in Table 6.1.

Table 6.1: Analysis of Human Eye Behaviour on the Interface (rounded-off mean figures)

Fixation Threshold	Target not found (frequency)	Steps to target	Time to target (seconds)	Average Time per display	Fixation Numbers	Average Fixation Numbers per display
300ms	50.0%	17	17.9	1.081	53	3
400ms	56.3%	18	28.1	1.630	86	5
Revisit	45.8%	16	37.7	2.352	99	6
Revisit/400ms	52.1%	17	24.0	1.470	72	4

192 (= 8x24) figures were entered for each dependent variable into a repeated measures ANOVA with two factors (fixation threshold and ranking). The main effect of the fixation threshold was not significant, $F(3,69) = 0.44$, $p=0.724$ with similar steps to target as shown in Table 6.1. Paired comparisons of all fixation thresholds also showed no significant difference in steps to target. The analysis of the time and fixations per display revealed that there were significant differences in the time to target and number of fixations per display for all paired comparisons. More importantly Revisit/400ms took significantly less time ($p=0.023$) and fewer fixations ($p=0.042$) than 400ms threshold for making decisions in each display. Combining revisits with a fixation threshold reduced the time spent on each display sequence without affecting the search efficiency (i.e. steps to target) compared to 400ms threshold. The time to target and fixation numbers for revisits only were significantly higher than the other conditions. This was not unexpected as users were not constrained by a cumulative fixation time threshold.

Remarkably results also reveal that users are able to locate target images at the 300ms fixation threshold level with fewer average steps to target than the 400ms threshold (Table 6.1). Although there was no significant difference between the steps to target for the 300ms and

400ms ($p<0.55$), there was a significant difference for the time to target ($p<0.0001$) and fixation numbers ($p<0.0001$) in each display.

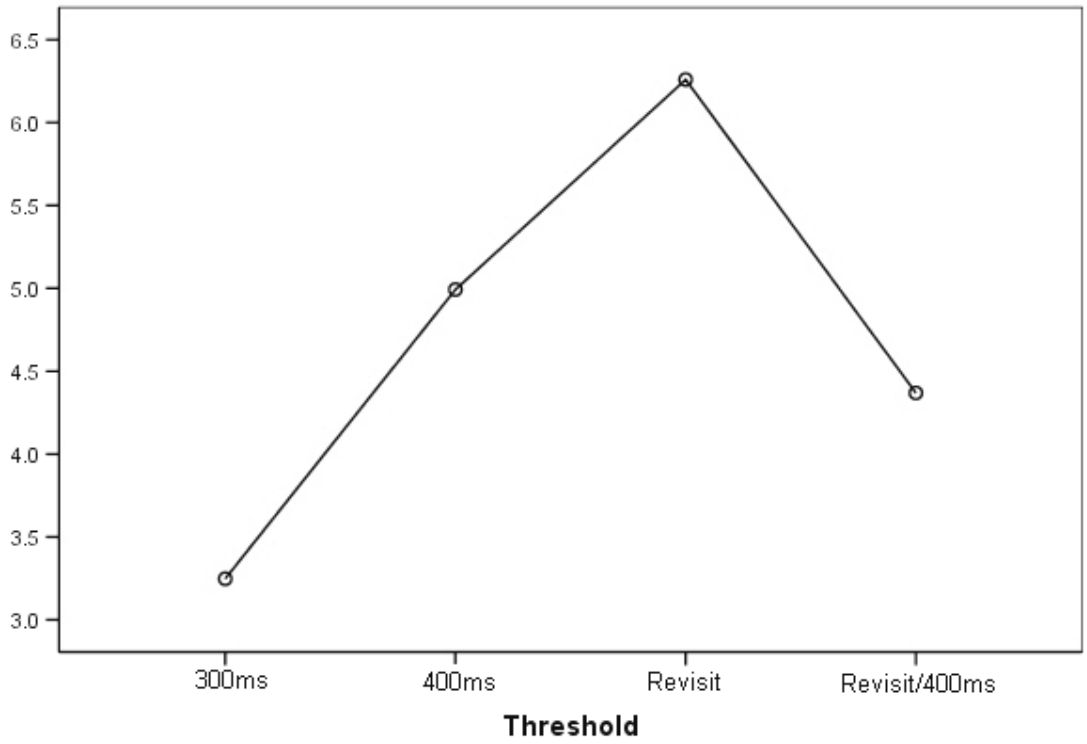

Figure 6.9: Average fixation numbers per display (Y-axis) for each fixation threshold

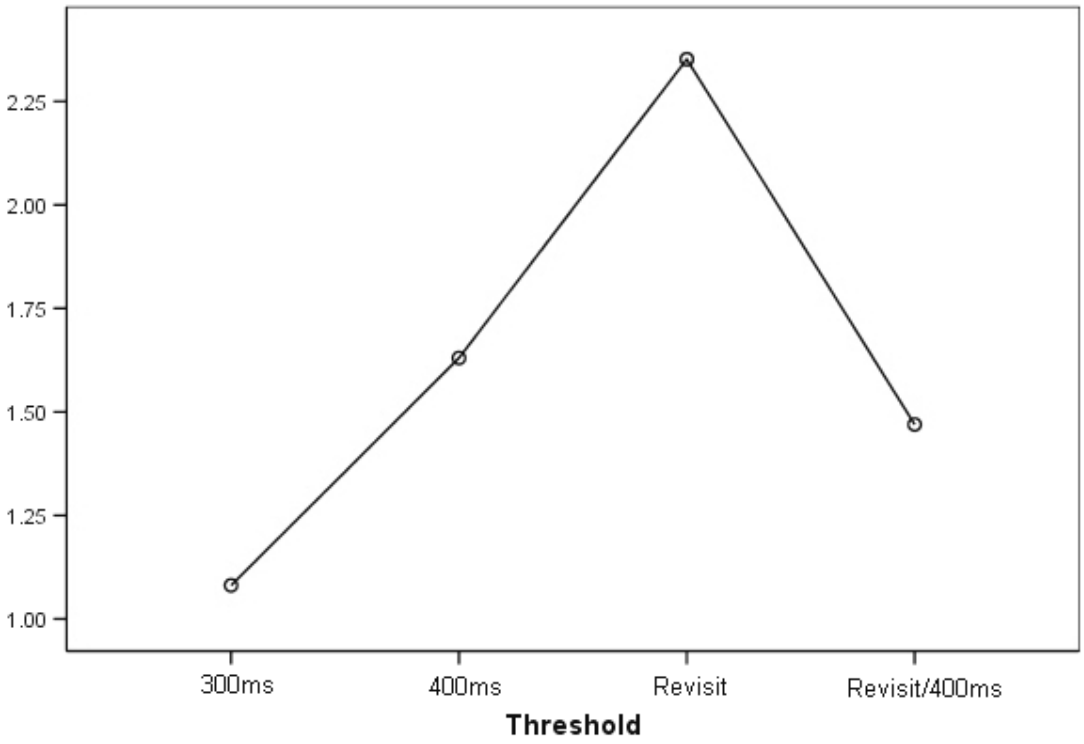

Figure 6.10: Average time to target per display (Y-axis) for each fixation threshold

There was a significant main effect of the ranking factor, $F(1,23)=4.59$, $p=0.042$. However, on closer scrutiny of the data it was found that the significance could have been a result of the variation in the target images used in this experiment. The ranking factor was not properly counterbalanced against the target images in the experiment design. In effect, 4 images were used for the (a) ranking and a different 4 images were used for the (b) ranking treatment. This affects the validity of the significance of the ranking factor, but not the threshold or mode factors which were properly counterbalanced. There was no significant interaction between the two factors.

The same treatment combinations experienced by all participants were applied to the random selection tool to obtain 192 dependent variables (steps to target). By combining the variables, 384 figures were entered into a mixed design multivariate ANOVA with four observations per cell and two factors (selection mode and ranking). The average figures are presented in Table 6.2.

Table 6.2: Comparison of Eye and Random Selection (rounded-off mean figures)

Selection Mode	Target not found (frequency)	Steps to target
Eye gaze	51.0%	17
Random selection	69.8%	21

In summary the results of the ANOVA revealed a main effect of the selection mode, $F(4,43)=5.434$, $p=0.001$, with the eye (17) taking significantly fewer steps than random selection (21). Conducting univariate tests on all four fixation threshold treatments revealed significant differences between the eye gaze and random selection for each fixation threshold treatment (Figure 6.11) as follows:

- 300ms → $F(1,46)=5.218$, $p=0.027$
- 400ms → $F(1,46)=4.152$, $p=0.047$
- Revisit → $F(1,46)=8.107$, $p=0.007$
- Revisit/400ms → $F(1,46)=5.730$, $p=0.021$

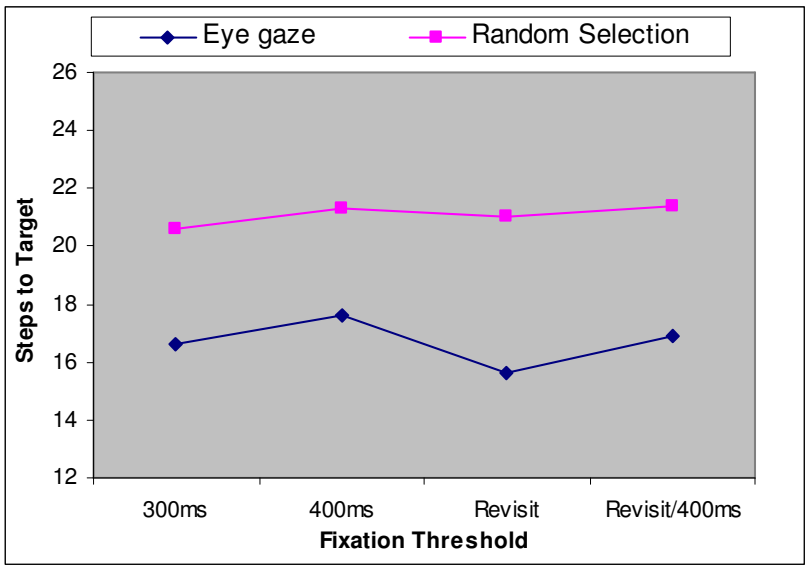

Figure 6.11: Comparison of eye gaze and random selection modes

6.4. Experiment Analysis

Two ranking strategies, (a) and (b), were compared for improvements in finding target images. Overall the target image was found 110 times for the (b) ranking, while the target image was found 108 times for the (a) ranking. However, it was found that when the (b) ranking was used whenever a selected image was repeated (391 occurrences out of 1000 tries), it led to the target image on just 7 occasions out of the 391. This means that the (b) strategy would be unlikely to effect an improvement despite the inconclusive earlier result.

An outstanding question is whether there is a limit to the speed of operation of this interface, as users appear to obtain good performance at both 300ms and 400ms fixation thresholds. Therefore the final experiment was devised to investigate three cumulative fixation threshold levels of 300ms, 200ms and 100ms.

6.5. Extended Experiment

Three of the easy-to-find target images from the previous experiment were selected for this experiment. The choice of targets was based on the target images with the least average steps to target. The initial screens for the three targets chosen are shown in Figure 6.3, Figure 6.6 and Figure 6.7 where the target image that the participant has to find is located at the top left bordered in red. The search task remained the same.

6.5.1. Criteria for Image Selection

The display automatically changes based on gaze behaviour. In this experiment, three treatments are used for determining best image selection:

- a cumulative fixation threshold of 300ms as before
- a cumulative fixation threshold of 200ms
- a cumulative fixation threshold of 100ms

As in prior experiments the cumulative fixation threshold is determined by the accumulation of all fixations greater than 80ms on a specific image position exceeding a 100ms, 200ms or 300ms threshold. The minimum period of 80ms for the gaze to remain on an image position to be considered as a fixation means that the 100ms threshold condition can emcompass only one fixation and is expected to yield random responses to displays. However, it serves as a control for comparison with the 200ms and 300ms threshold.

6.5.2. Participants

Six unpaid participants (4 males and 2 females) took part in this experiment. The average age was 36.2 years. Participants included a mix of university and company staffs. All participants had normal or corrected-to-normal vision and provided no evidence of colour blindness.

6.5.3. Experimental Procedure

Each participant performed three runs using easy-to-find image types. There was one practice run to enable better understanding of the task at hand and to equalise skill levels before the experiment. Participants understood that there would be a continuous change of display until they found the target but did not know what determined the display change.

Three treatment combinations of the three fixation thresholds (300ms, 200ms and 100ms) were applied for each participant. Any sequence effect was minimised by randomly allocating each participant to 6 different sequences of the three fixation thresholds. There was a 1 minute rest in between runs. As before, the maximum number of steps to target was limited to 26 screen changes.

6.6. Results

Three dependent variables, the number of steps to target, the time to target (F_1), and the number of fixations (F_2) of 80ms and above were monitored and recorded during the experiment. 9 dependent variables (3 each) were recorded for each participant. The average figures are presented in Table 6.3.

Table 6.3: Analysis of Human Eye Behaviour on the Interface (rounded-off mean figures)

Fixation Threshold	Steps to target	Time to target (seconds)	Average Time per Display	Fixation Numbers	Average Fixation Numbers per Display
100ms	20	8.0	0.394	20	1
200ms	12	7.0	0.634	18	2
300ms	4	5.2	1.139	17	3

18 (= 3x6) figures were entered for each dependent variable into a single factor ANOVA with three levels (300ms, 200ms and 100ms). The results of the ANOVA performed on the steps to target revealed a significant main effect of the fixation thresholds, $F(2,10)=13.098$, $p=0.018$. A paired comparison of 100ms and 300ms attributed the significant difference to a simple main effect between these two fixation thresholds ($p=0.003$). There were no significant difference between the 100ms and 200ms paired thresholds ($p=0.133$) and 200ms and 300ms paired threshold ($p=0.227$) respectively.

The same treatment combinations experienced by all participants were applied to the random selection tool to obtain 18 dependent variables (steps to target). By combining the variables, 36 figures were entered into a multivariate ANOVA with three observations per cell and one factor (selection mode). In summary the results of the ANOVA revealed a main effect of the selection mode, $F(3,8)=6.348$, $p=0.016$. The eye took significantly fewer steps to the target (=12) than the random selection (=21). Univariate tests on all three fixation threshold levels revealed significant differences between the eye gaze and random selection for the 300ms and 200ms conditions (Figure 6.12) i.e. $F(1,10)=10.390$, $p=0.009$ and $F(1,10)=9.484$, $p=0.012$ respectively. As expected, there was no significant difference between the steps to target for the eye (=20) and random selection (=19) at the cumulative threshold level of 100ms, $F(1,10)=0.056$,$p=0.817$.

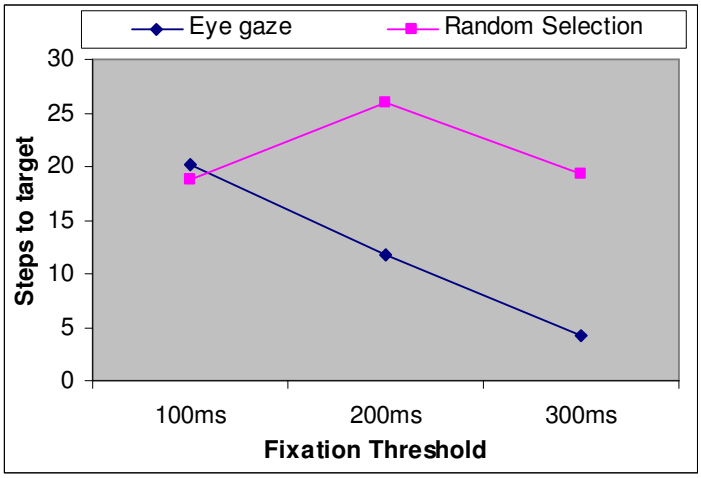

Figure 6.12: Comparison of eye gaze and random selection modes

6.7. Discussion

The notion that revisit/refixation may be an indication of interest in image search was investigated further. In addition to the cumulative fixation threshold of 400ms and 300ms, the new criterion of selection by revisit (i.e. first image to encounter a refixation) for best image selection was introduced.

Participants using the revisits only selection criterion were sometimes puzzled as to why there was no screen change during periods of search as reflected in some answers to the questionnaire. The slow and non-intuitive operation of the revisits criterion would probably prevent it from forming part of the design of any future interface. However, combining revisits with the 400ms threshold allowed users to make use of refixations and directed search as a strategy for searching the display.

Analysis of the eye movement data revealed that performance was not affected by all four selection criteria. Even when all four thresholds were paired and compared, the steps to target for each of the selection criteria did not significantly differ. It was found that combining Revisit with a 400ms threshold reduced the average time spent on searching each display without affecting search performance (i.e. steps to target). Along with previous results, it does seem reasonable to conclude that refixations can play an important role in image search and can improve search times.

It was noted that participants were still able to find target images within the cumulative fixation threshold of 300ms as well as with the 400ms threshold, although many complained that the screen changes were too fast and did not have control. An extended experiment was therefore devised to investigate the effect of reducing the cumulative fixation threshold still further. In order to increase the likelihood of finding targets, the target images with the least steps to target from the previous experiment were reused. Up to this point search performance had not been affected for 800ms, 400ms and 300ms threshold levels. The extended experiment confirmed that users were still able to locate target images at the 200ms threshold but not at the 100ms threshold. It should be noted that search behaviour at 100ms was only coarsely measured because fixations less than 80ms were not considered in these experiments. This meant that the performance measure at a 100ms was only approximate (Table 6.3).

The performance at the 300ms threshold and certainly the 200ms threshold indicated that rapid pre-attentive vision was being employed by participants to find target images within these short display times, thus confirming findings from Tatler et al [73] and Underwood et al [90] that the influence of low-level visual feature salience on saccadic targeting does not change during viewing, but cognitive influences do vary. It would also confirm Wolfe's Guided Search Model [86] which proposes that pre-attentive feature processes could direct the deployment of attention in serial attentive searches.

6.8. Summary

Additional experiments have revealed that refixations or revisits on an image during search are an indication of interest in that image. Furthermore participants were able to find target images with a 200ms fixation threshold indicating that rapid pre-attentive vision was being employed by subjects in the experiments.

The next section explores some of the possibilities for the exploitation of eye tracking technology building on the potential exposed in this research.

Chapter 7. Conclusions

A rapid and natural interface for searching visual digital data in a CBIR system is an outcome of the thesis. A pre-computed network of similarities between image regions in an image collection was traversed using users' gaze behaviours obtained from eye tracking data. Eye tracking data has been used to direct a search towards information of increasing relevance to the user.

In building this system ideas were taken from human computer interaction, visual attention and visual perception during image search and retrieval. Firstly it was shown that the eye is attracted to image regions that are predicted to be salient by an attention model and that the eye tracking system was able to gather data related to users' interests. Secondly the eye tracking interface yielded a significantly better speed performance than the mouse in a target location task. Finally in an image retrieval task users were able to successfully navigate their way to target images in a database using only eye gaze with significantly better performance than randomly generated selections. Further data analysis and experiments led to the extraction of relevant information for query formulation in image search and retrieval. In addition experiments indicated pre-attentive visual activity in rapid image search.

7.1. Significant Findings

A series of experiments was devised to establish the feasibility of an eye gaze driven search mechanism. The first experiment tested whether users looked at regions declared salient by a visual attention model. The results showed that this was the case for the images and participants involved. This results also indicated that users spent a large proportion of the five seconds exposure time observing the salient regions rather than the background and that this behaviour could be employed to drive a prototype search interface.

The second experiment went further to explore the speeds of visual processing involved in a target image identification task when compared with a conventional input device such as a mouse. Results indicated slower mouse responses, with the eye interface having significantly faster response times than the mouse interfaces. When using the mouse the participant had to spend time locating both the cursor and the item to be selected, and then use the mouse to move the cursor to the item. On the other hand the eye tracker interface was quicker because only the selected item needed to be located. However, the speed difference was not just dependent on extra mouse movement because the eye tracker required the user to fixate on the target for longer than 40ms before a screen change. The results also indicated that skills transfer was taking place when the mouse was used first but not when the eye was used first. This suggested

that experience gained during visual tasks carried out using a mouse would benefit future users if they were subsequently transferred from a mouse based system to an eye tracking system. The habituation experienced during the same-sequence target positions showed that prior knowledge of target positions can affect results. This was reduced in the image retrieval experiments by randomising positions of retrieved images in each display. Any ensuing interface design must take into account that prior knowledge of target positions will influence gaze behaviour and will affect the accurate analysis of eye tracking data.

Finally in the image retrieval experiment the participants using the eye tracking interface found the target in fewer steps than an automated random selection strategy and the analysis of the simple effect attributed the significant difference to the hard-to-find images. This meant that the probability of finding the hard-to-find images was significantly increased due to human cognitive abilities as opposed to the indiscriminate selection by the simulated random selection strategy using the same similarity information.

The random selection strategy was employed to provide a performance base-line which any more intelligent approach would need to exceed. It also enabled the initial exploration of the structure of the similarity links in the database, guidance for the choice of the grid size, analysis of the benefits of completely random image retrieval, and the choice of target images.

The asymmetric values of the pre-computed similarity score matrix provided a better chance of getting to the target image than the symmetric values. It is likely that better similarity association values would improve the retrieval performance generally.

Comparison of grid sizes revealed that larger grids for the same image database size would benefit random selection and tend to obscure the relative eye gaze performance, hence a smaller grid was used in order to obtain better discrimination between eye gaze and random selection performance. There was no effect on gaze performance of including one randomly-retrieved image in the retrieved set. The user probably did not pay any attention to the randomly-retrieved image in the retrieved set, as the randomly retrieved image may have generally been visually irrelevant.

The difficulty of the search task is largely dependent on the network of pre-computed similarity scores which needed to be evaluated to define satisfactory search tasks. Two approaches were employed (i.e. analysing the search performance and the retrieved image sets) to reveal the easy-to-find and hard-to-find images.

The eye gaze interface expressed the intentions of the user and made use of the structure of the similarity data. The additional number of fixations and time spent on hard-to-find images confirmed that complex information led to longer fixation durations and higher fixation numbers. It was also noted that giving people longer viewing time did not necessarily yield significantly better performance.

The extraction of gaze parameters that may be potentially exploited to improve performance revealed that:

- Refixation or revisit on an image may be an indication of interest in an image;
- Unconscious pre-attentive vision played a significant role in visual search;
- Saccade speeds were frequently slower just prior to the selection of images;
- Saccade durations frequently ranged from 20ms to 60ms;
- Pupil diameters peaked on the hard-to-find images.

Additional experiments have revealed that refixation or revisits on an image during a visual search of a display of images is an indication of interest in that image. Furthermore participants were able to find target images with a 200ms cumulative fixation threshold indicating that rapid pre-attentive vision is playing a significant part in visual search.

7.2. Review of Thesis Objectives

This thesis conjectured that eye tracking data provides more information relevant for query formulation in image retrieval that is not otherwise obtainable through existing conventional interfaces. Six key research questions were identified that needed to be answered to support this thesis. These questions are reviewed in turn to ascertain the extent to which they have been met by the findings identified above.

1. **Is there an informative relationship between gaze behaviour and a computational model of visual search?**

   The results from the first experiment revealed an informative relationship between the gaze data and the model that could be employed to drive a prototype search interface.

2. **Can data from gaze behaviour be used to exceed the performance of other interface devices for visual tasks?**

   The benefit of using eye movement in such a search interface was investigated in the second experiment. Indeed gaze behaviour exceeded the performance of a mouse interface device for identifying a target image on a display. More importantly experience gained during visual tasks carried out using a mouse was benefiting users when they were subsequently transferred to an eye tracking system.

3. **What methodology should be used to measure subjects' gaze behaviour?**

   The experiments followed a balanced design where all treatment combinations had the same number of observations. The Analysis of Variance (ANOVA) was used in experiments on the image retrieval system to analyse the eye gaze data. ANOVA is used to test for significant differences between means (2 or more groups) by analyzing variance. Multivariate Analysis of Variance (MANOVA) was used when there were several

correlated dependent variables, and a single overall statistical test on this set of variables was used instead of performing multiple individual tests. More importantly the experiment design allowed for a more effective analysis of gaze parameters under the different treatment combinations.

4. **How can fixations and saccades from eye tracking data provide extra information relevant to image retrieval?**

   The findings from the gaze parameter analysis identified potentially informative measures for a CBIR system from the time sequence of the eye tracking data. One of the findings (refixation) was tested in a further experiment and was shown to be beneficial in driving the image retrieval interface. Unlike dwell time, refixation is a more natural gaze behaviour that can be used to infer intentions. This thesis has shown that information from users' thought processes can be captured through gaze parameters (such as refixation, saccade speed and pupil diameter) which may yield new and relevant information that is not otherwise attainable through conventional interfaces.

5. **Are there any limits to the speed of operation of a gaze driven retrieval interface?**

   This question investigates the limits of the speed of operation of the eye gaze interface for controlling image retrieval. The finding that pre-attentive vision plays a significant part in visual search is thought to be a new discovery.

6. **What software and data frameworks are needed for the human eye to control an image retrieval interface?**

   Section 3 gives a detailed description of the methodology used in building this system. It defines the types of data and storage requirements as well as the processing resources and the timing constraints.

It is felt that the work has largely met the above objectives. The research is supported by experiments whose results were tested for significance and provide a basis for further research in visual attention, visual perception and human computer interaction.

7.3. Limitations and Recommendations

This section describes areas of further work that might be carried out to extend the functionality of the concept demonstrator and resolve outstanding questions.

7.3.1. Inferring Intentions

Eye tracking data poses the problem of interpreting a user's intention. Users occasionally look at image regions that are not necessarily of interest to them. A common way of managing this problem is by setting a threshold for the dwell time, using zooming [69] [80], or blinking [3] to

indicate a selection to the machine. The findings in this thesis may be extended to build a system that can determine behavioural patterns that would not require users to assume unnatural ways of looking. For example, refixations, saccade speeds and pupil diameter can be monitored to infer users' interests. Detection of peakness in pupil diameter data suggests that the user is experiencing difficulty and as such the system could aid the user with suggestions.

7.3.2. Similarity Measure

The similarity model that was used to determine successive displays is currently under development, but can be varied and tested. For example, the similarity network can be pre-computed using textual descriptors or any other CBIR algorithm. Retrieved image sets could be determined by a combination of conventional visual features (colour, orientation, shape, texture) and textual descriptors.

7.3.3. Usability

Experiments were conducted in this thesis with a chinrest to minimise possible errors in gaze data; this is not practical in a real-world environment. More advanced eye trackers will require less calibration and impose fewer constraints upon the user whilst still obtaining high accuracy.

7.4. Future Work

An eye controlled image retrieval interface not only provides a more natural mode of retrieval but also has the ability to anticipate the user's objectives, thereby retrieving images extremely rapidly and with a minimum of thought and manual involvement. In future interfaces eye tracking will not only be used as a rapid and continuous information gathering tool for query formulation, but also to build up a visual behavioural pattern using time series information in the data.

In this thesis attention weighting has been based on the distribution of fixations within a display. Better modelling of aspects of gaze behaviour such as refixation, saccade speed, pupil diameter and others will provide a more fruitful source of information for image retrieval.

System constraints meant that a relatively long fixation threshold of 80ms was chosen in the experiments. An investigation of lower thresholds (e.g. 60ms, 40ms, 20ms, etc) with faster equipment might have yielded better results and is worthy of further investigation.

Variations in display grid sizes (e.g. 3x3 and 4x4 display grids) may also yield different results. Dynamic and adaptable displays will make better use of screen area and should yield more intuitive and faster search interfaces.

Having confirmed that pre-attentive vision plays a significant part in visual search, new experiments are needed to determine the role of this aspect of human vision. The reduction in gaze time played a part in exposing the part played by pre-attentive vision in these experiments.

There is much research to be carried out before eye trackers can become as pervasive as keyboards and mice. The accuracy, cost and usability of equipment must improve before laboratory results can be reproduced on PCs, laptops, and even PDAs. We might expect cheap eye trackers to emerge in the games market where "look and shoot" would give faster gratification than painful button pressing or joystick pushing. Small cameras embedded in monitors and laptop lids or glasses would be obvious locations for such devices. Gaze contingent displays have great potential where additional information may be displayed dependent on eye movement. For example, larger scale maps may be offered at the focus of attention or additional details supplied related to an object being studied. Eye behaviour may also be used to drive PTZ cameras in ways that enable people to "see" their way around remote locations. Eye trackers are already a great asset to the disabled, but only as an awkward and costly replacement for existing devices, and not as a computer interface to be used just as effectively as an able-bodied person.

The results reported here indicate that eye trackers have the potential for eliciting human intentions extremely rapidly and may be applied to certain visual search tasks. It seems reasonable that reducing costs and advancing camera technology will mean that eye trackers will appear in many more applications within the next few years.

Chapter 8. Publications

1. O.K Oyekoya & F.W.M Stentiford, "Exploring the significance of visual attention by eye tracking", London Communications Symposium, pp 149 – 152, September 8-9, 2003.
2. O.K Oyekoya and F.W.M Stentiford, "Eye tracking as a new interface for image retrieval," BT Technology Journal, vol. 22, No 3, pp 161-169, July 2004.
3. O.K Oyekoya & F.W.M Stentiford, "Exploring human eye behaviour using a model of visual attention," International Conference on Pattern Recognition 2004, 23rd – 26th August, 2004.
4. O.K Oyekoya, "Managing multimedia content: a technology roadmap," Report, SIRA Innovation Ltd, April, 2005.
5. O.K Oyekoya & F.W.M Stentiford, "A performance comparison of eye tracking and mouse interfaces in a target identification task," European Workshop on the Integration of Knowledge, Semantics & Digital Media Technology, London, 30th November – 1st December, 2005.
6. O.K Oyekoya & F.W.M Stentiford, "An eye tracking interface for image search," Eye Tracking Research and Applications Symposium, San Diego, March 27-29, 2006.
7. O.K Oyekoya & F.W.M Stentiford, "Eye tracking as a new interface for image retrieval," Intelligent Spaces: the Application of Pervasive ICT, Springer-Verlag, London, pp 273-284, 2006.
8. O.K Oyekoya & F.W.M Stentiford, "Perceptual Image Retrieval Using Eye Movements," International Workshop on Intelligent Computing in Pattern Analysis/Synthesis, http://www.springerlink.com/content/y682v5072105x740/, 26-27 August, Xi'an, China, 2006.
9. O.K Oyekoya & F.W.M Stentiford, "Eye Tracking: A New Interface for Visual Exploration," BT Technology Journal, vol 24, no. 3, pp 57-66, July 2006.
10. O.K Oyekoya & F.W.M Stentiford, "Perceptual Image Retrieval Using Eye Movements," International Journal of Computer Mathematics, Special Issue on Computer Vision and Pattern Recognition, vol 84, no. 4, 2007.

Chapter 9. References and Bibliography

[1] Bamidele A. and Stentiford F.W.M. (2004). A New Enhancement to Histogram Based Approaches in Content Based Image Retrieval System, Proc. of London Communications Symposium, pp209-212.

[2] Bamidele A. and Stentiford F. W. M (2005). An Attention Based Similarity Measure Used to Identify Image Clusters, 2nd European Workshop on the Integration of Knowledge, Semantics & Digital Media Technology, London, 30th Nov - 1st Dec, 2005.

[3] Bhaskar T. N., Foo Tun Keat, Ranganath Surendra, Venkatesh Y. V. (2003). Blink Detection and Eye Tracking for Eye Localization, IEEE Tencon, India.

[4] Bolt, RA. 1982. Eyes at the interface. Proc. ACM CHI'82, 360-362.

[5] Broadbent, D. E. (1958). Perception and Communication, Oxford: Pergamon Press.

[6] Corno F., Farinetti L. and Signorile I. (2002). A cost effective solution for eye-gaze assistive technology, IEEE Int. Conf. on Multimedia and Expo, August 26-29, Lausanne.

[7] Cox I.J., Miller M. L., Minka T. P., Papathomas T. V., And Yianilos P. N. 2000. The Bayesian image retrieval system, PicHunter: theory, implementation, and Psychophysical experiments. In IEEE Trans. on Image Processing, Vol. 9, No 1.

[8] Crane, H. D., and Steele, C. S. (1978). Accurate three-dimensional eye tracker, Applied Optics, 17, 691-705.

[9] Desimone R. 1998. Visual attention mediated by biased competition in extrastriate visual cortex. In Phil. Trans. R. Soc. Lond. B, 353, 1245 – 1255.

[10] Duchowski, A. T. (2002). A Breadth-First Survey of Eye Tracking Applications, Behaviour Research Methods, Instruments, & Computers (BRMIC), 34(4), pp.455-470.

[11] Duchowski, A. T. (2003). Eye Tracking methodology: Theory and Practice, Springer Verlag

[12] Duchowski, A. T., Medlin, E., Cournia, N., Murphy, H., Gramopadhye, A., Nair, S., Vorah, J., Melloy, B. (2002). 3D Eye Movement Analysis, Behaviour Research Methods, Instruments, & Computers (BRMIC), 34(4), pp.573-591.

[13] Edwards G. (1998). A Tool for Creating Eye-aware Applications that Adapt to Changes in User Behaviours, International ACM Conference on Assistive Technologies: 67-74.

[14] Essig Kai and Ritter Helge (2005). Visual-Based Image Retrieval (VBIR) - A New Approach for Natural and Intuitive Image Retrieval. Proceedings of the 13th European Conference on Eye Movements. Bern, Switzerland., Aug / 2005

[15] Farid M., Murtagh F. and Starck J.L. (2002). Computer display control and interaction using eye-gaze, Journal of the Society for Information Display, Vol 10, No 3, pp 289-29.

[16] Fitts, P.M., Jones, R.E., and Milton, J.L. (1950). Eye Movement of Aircraft Pilots during Instrument-Landing Approaches, Aeronautical Engineering Review 9, 24-29.

[17] Gilchrist I. D. and Harvey M. (2000) Refixation frequency and memory mechanisms in visual search Curr.Biol. 10 (19):1209-1212.

[18] Glenstrup Arne John, Theo Engell-Nielsen (1995). Eye Controlled Media: Present and Future State, Thesis, Bachelor's Degree in Information Psychology at the Laboratory of Psychology, University of Copenhagen, Denmark.

[19] Grecu Horia (2006), "Content Based Image Retrieval: An Attention Monitoring Approach", PhD Thesis, Universitatea Politehnica Bucuresti.

[20] Grigorescu C., Petkov N., and Westenberg M.A. (2003). Contour detection based on nonclassical receptive field inhibition. IEEE Trans. on Image Processing, 12(7), 729-739.

[21] Hansen J.P., A.W. Anderson, and P. Roed (1995). Eye gaze control of multimedia systems, Symbiosis of Human and Artefact (Y. Anzai, K. Ogawa, and H. Mori (eds), Vol 20A, Elsevier Science, pp 37-42.

[22] Henderson John M. and Hollingworth Andrew (1999). High-Level Scene Perception, Annual Reviews Psychology 50:243-71.

[23] Hollingworth, A., & Henderson, J. M. (2002). Accurate visual memory for previously attended objects in natural scenes. Journal of Experimental Psychology: Human Perception and Performance, 28, 113-136.

[24] http://www.arringtonresearch.com/

[25] http://www.a-s-l.com/

[26] http://www.crsltd.com/

[27] http://www.eyegaze.com/

[28] http://www.eyelinkinfo.com/

[29] http://www.smarteye.se/

[30] Itti L., Koch C., Niebur E. (1998). A Model of Saliency-Based Visual Attention for Rapid Scene Analysis, IEEE Transactions on Pattern Analysis and Machine Intelligence, Vol. 20, No. 11, pp. 1254-1259.

[31] Itti, L. Automatic foveation for video compression using a neurobiological model of visual attention. IEEE Trans. on Image Processing, 13(10) (2004) 1304-1318.

[32] Jaimes A., Pelz J.B., Grabowski T., Babcock J., and Chang S.F. (2001). Using Human Observers' Eye Movements in Automatic Image Classifiers, Proceedings of SPIE Human Vision and Electronic Imaging VI, San Jose, CA.

[33] James, W. (1890). The Principles of Psychology, H. Holt and Co., New York.

[34] Kahneman, D. (1973). Attention and Effort, Prentice-Hall, Inc., Englewood Cliffs, New Jersey.

[35] Kerne, A. (2000) CollageMachine: an interactive agent of Web recombination Leonardo, Vol. 33, No. 5, pp. 347–350.

[36] Koch C. and Ullman S. (1985). Shifts in selective visual attention: towards the underlying neural circuitry, Human Neurobiology, no. 4, pp. 219—227.

[37] LC Technologies Inc. - http://www.eyegaze.com/

[38] Lee Stone, Brent Beutter, et al. Models of Tracking and Search Eye- Movement Behaviour, NASA.

[39] Mackworth, N., And Morandi, A. (1967). The gaze selects informative details within pictures, Perception and Psychophysics 2, 547–552.

[40] McCarthy, J, Sasse, M.A. & Riegelsberger, J. (2003). Could I have the menu please? An eye tracking study of design conventions, Proceedings of HCI2003, 8-12 Sep 2003, Bath, UK.

[41] Melcher D. and Kowler E. (2001). Visual scene memory and the guidance of saccadic eye movements. Vision Res. 41 (25-26):3597-3611.

[42] Mulligan J. B. and Beuttler B. R. (1995). Eye movement tracking using compressed video images, Vision Sciences and Its Applications; Optical Society Technical Digest Series, Vol.1, pp.163-166.

[43] Multimedia Understanding through Semantics, Computation and Learning, Network of Excellence. EC 6th Framework Programme. FP6-507752. http://www.muscle-noe.org/

[44] Navalpakkam Vidhya and Itti Laurent (2005). Modeling the influence of task on attention. Vision Research 45 (2005) 205–231.

[45] Nikolov S. G., Bull D. R., Gilchrist I. D. (2002). Gaze-Contingent Multi-Modality Displays of Multi-Layered Geographical Maps, Proc. of the 5th Intl. Conf. on Numerical Methods and Applications (NM&A02), Symposium on Numerical Methods for Sensor Data Processing, Borovetz, Bulgaria.

[46] Numajiri T., A. Nakamura, and Y. Kuno (2002). Speed browser controlled by eye movements, 2002 IEEE Int. Conf. on Multimedia and Expo, August 26-29, Lausanne.

[47] Ohno Takehiko (1998). Features of eye gaze interface for selection tasks, APCHI'98, Japan, 176-181

[48] Oyekoya O.K., Stentiford F.W.M. (2004). Exploring Human Eye Behaviour Using a Model of Visual Attention, International Conference on Pattern Recognition, ICPR (4) 2004: 945-948.

[49] Oyekoya O. K., Stentiford F. W. M. (2004). Eye Tracking as a New Interface for Image Retrieval, British Telecommunications Technology Journal on Intelligent Spaces (Pervasive Computing), Vol. 22, No 3, Updated in Intelligent Spaces: the Application of Pervasive ICT, Springer-Verlag, London, pp 273-284, 2006.

[50] Oyekoya O.K., Stentiford F.W.M. (2005). A Performance Comparison of Eye Tracking and Mouse Interfaces in a Target Image Identification Task, 2nd European Workshop on the Integration of Knowledge, Semantics & Digital Media Technology, London, 30th Nov - 1st Dec, 2005.

[51] Oyekoya O.K., Stentiford F.W.M. (2006). Perceptual Image Retrieval Using Eye Movements, Proceedings of International Workshop on Intelligent Computing in Pattern Analysis/Synthesis, Proc. in Advances in Machine Vision, Image Processing, and Pattern Analysis, Lecture Notes in Computer Science, DOI=10.1007/11821045_30, 281-289.

[52] O K Oyekoya, Stentiford F.W.M. (2006). An Eye Tracking Interface for Visual Exploration, British Telecommunications Technology Journal, Special Issue of the University College London, Vol 24 No 3.

[53] Oyekoya, O. and Stentiford, F. (2006). An eye tracking interface for image search. In Proceedings of the 2006 Symposium on Eye Tracking Research and Applications (San Diego, California, March 27 - 29, 2006). ETRA '06. ACM Press, New York, NY, 40-40. DOI=http://doi.acm.org/10.1145/1117309.1117324.

[54] Parkhurst, D. J., Law, K., & Niebur, E. (2002). Modeling the role of salience in the allocation of overt visual attention. Vision Research, 42(1), 107–123.

[55] Pomplun M. & H. Ritter (1999). A three-level model of comparative visual search, In M. Hahn & S. C. Stoness, (Eds.), Proceedings of the 21st Annual Conference of the Cognitive Science Society, 543-548.

[56] Pomplun, M. (1998). Analysis and Models of Eye Movements in Comparative Visual Search, Göttingen: Cuvillier (Ph.D. thesis), University of Bielefeld, May 1998.

[57] Privitera C.M., Stark L. W. (2000). Algorithms for Defining Visual Regions of Interest: Comparison with Eye Fixations, IEEE Transactions On Pattern Analysis and Machine Intelligence, Vol. 22, No 9, pp 970-982.

[58] Puolamäki K., Salojärvi J., Savia E., Simola J., Kaski S. (2005). Combining Eye Movements and Collaborative Filtering for Proactive Information Retrieval, In Proceedings of the 28th ACM Conference on Research and Development in Information Retrieval (SIGIR).

[59] Reinagel P. and Zador A. M. (1999). Natural scene statistics at the centre of gaze. Network. 10 (4):341-350.

[60] Rensink RA (2001). Change Blindness: Implications for the nature of attention. In MR Jenkin and LR Harris (eds.), Vision and Attention (pp. 169-188). New York: Springer.

[61] Robinson, D. A. (1963). A method of measuring eye movement using a scleral search coil in a magnetic field, IEEE Transactions on Biomedical Electronics, BME-10, 137-145.

[62] Salvucci D. D. (2000). An interactive model-based environment for eye-movement protocol analysis and visualization, Proceedings of the symposium on Eye Tracking Research & Applications, p.57-63, Palm Beach Gardens, Florida, United States.

[63] Salvucci, D. D., and Goldberg, J. H. (2000). Identifying fixations and saccades in eye-tracking protocols, In Proceedings of the Eye Tracking Research and Applications Symposium (pp. 71-78). New York: ACM Press.

[64] Scherffig Lasse (2005). It's in Your Eyes - Gaze Based Image Retrieval in Context. Edited by Hans H. Diebner, Institute for Basic Research, Karlsruhe.

[65] Schnell, T., Wu, T., (2000). Applying Eye Tracking As Alternative Approach for Activation of Controls and Functions in Aircraft, Proceedings of the 5th International Conference On Human Interaction with Complex Systems (HICS), April, 30 - May, 2, 2000, Urbana, Illinois, USA, pp 113.

[66] Scott D. & Findlay J. M. (1992). Visual Search, Eye Movements and Display Units, Human Factors Report. University of Durham, UK.

[67] Selker Ted, Lockerd Andrea, Martinez Jorge (2001). Eye-R, a glasses-mounted eye motion detection interface, CHI '01 extended abstracts on Human factors in computer systems, Seattle, Washington.

[68] Sibert, Linda E. and Jacob, Robert J.K. (2000). Evaluation of eye gaze interaction, In CHI 2000 Conference on Human Factors in Computing Systems, April 2000.

[69] Starker, I., & Bolt, R. A. (1990). A gaze-responsive self-disclosing display. In CHI '90 Proceedings, pp. 3–9. ACM.

[70] Stentiford F. W. M. (2001). An evolutionary programming approach to the simulation of visual attention, Congress on Evolutionary Computation, Seoul, May 27-30.

[71] Stentiford F.W.M. (2001). An estimator for visual attention through competitive novelty with application to image compression, Picture Coding Symposium, Seoul.

[72] Takehiko Ohno, Naoki Mukawa and Atsushi Yoshikawa (2002). FreeGaze: a gaze tracking system for everyday gaze interaction, Eye Tracking Research & Applications symposium, pp.125-132.

[73] Tatler Benjamin W., Baddeley Roland J., Gilchrist Iain D., Visual correlates of fixation selection: effects of scale and time, Vision Research 45 (2005) 643–659.

[74] Ter Hofstede AHM, Proper HA and van der Weide ThP. Query Formulation as an Information Retrieval Problem. The Computer Journal, 39(4):255-274, 1996.

[75] Urban J., Jose J.M., van Rijsbergen C.J. (2003). An adaptive approach towards content-based image retrieval, Proc. of the Third International Workshop on Content-Based Multimedia Indexing (CBMI'03), pp. 119-126.

[76] Venters, C.C., J.P. Eakins and R.J. Hartley (1997). The user interface and content based image retrieval systems, Proc. of the 19th BCS-IRSG Research Colloquium, Aberdeen, April.

[77] Vinay Vishwa, Cox Ingemar J., Milic-Frayling Natasa, and Wood Ken. Evaluating relevance feedback algorithms for searching on small displays. 27th European Conference on IR Research, ECIR 2005, Mar 21-23 2005. Proceedings Series: Lecture Notes in Computer Science, Losada, David E.; Fernández-Luna, Juan M. (Eds.), Springer Verlag, Heidelberg, D-69121, Germany. 3408:185-199, 2005.

[78] Virpi Roto (2003), "Search on Mobile Phones," Best Practices and Future Visions for Search User Interfaces: A Workshop, CHI 2003 Workshop.

[79] Walker, K. N., Cootes, T. F. and Taylor, C. J. (1998). Locating Salient Object Features, British Machine Vision Conference.

[80] Ward D.J. and MacKay D.J.C. (2002). Fast hands-free writing by gaze direction, Nature 418 pp 838.

[81] Ware, C. and Mikaelian, H. (1987). An evaluation of an Eye Tracker as a Device for Computer Input, Proceeding of SIGCHI+GI '87, Human Factors in Computing Systems. Also published as a special issue of the SIGCHI Bulletin. 183-88. April.

[82] Xin Fan, Xing Xie, Wei-Ying Ma, Hong-Jiang Zhang, He-Qin Zhou (2003). Visual Attention Based Image Browsing on Mobile Devices, 2003 IEEE International Conference on Multimedia and Expo., Vol I, pp 53-56, Baltimore, MD, USA.

[83] Yamato, M., Monden, A., Matsumoto, K., Inoue, K., Torii, K. (2000) Button selection for general GUIs using eye and hand together, Proc. 5th International Working Conference on Advanced Visual Interfaces (AVI2000), ACM Press, pp.270–273.

[84] Yarbus, A. (1967). Eye Movements and Vision, Plenum Press, New York.

[85] Ricard Benoit, Chevrette Paul, Pichette Mario (2003). Infrared Eye: prototype 2, Technical memorandum of the Defence Research & Development Canada, Valcartier, TM 2002-171, 2003-04-10.

[86] Wolfe, J. M. Guided Search 2.0: The Upgrade. In Proceedings of the Human Factors and Ergonomics Society, 37th Annual Meeting (Santa Monica, CA, October 1993), pp. 1295–1299.

[87] Treisman, A., and Gelade, G. A. Feature Integration Theory of Attention. Cognitive Psychology 12 (1980), 97–136

[88] Noton, D., and Stark, L. Eye Movements and Visual Perception. Scientific American 224 (1971), 34–43.

[89] Rayner K. (1998). Eye movements in reading and information processing: 20 years of research. Psychological Bulletin, 124(3), 372-422.

[90] Underwood, G., Foulsham, T., van Loon, E., Humphreys, L., & Bloyce, J. (2006). Eye movements during scene inspection: A test of the saliency map hypothesis. European Journal of Cognitive Psychology, in press.

[91] Underwood, G. and Foulsham, T., (2006). Visual saliency and semantic incongruency influence eye movements when inspecting pictures, Quarterly Journal of Experimental Psychology: in press.

[92] Rensink RA, O'Regan JK, Clark JJ. 1997. To see or not to see: the need for attention to perceive changes in scenes. Psychol. Sci. 8:368-73.

[93] Potter MC. 1976. Short-term conceptual memory for pictures. J. Exp. Psychol.: Hum. Learn. Mem. 2:509-22.

[94] Schyns PG, Oliva A. 1994. From blobs to boundary edges: evidence for time and spatial scale dependent scene recognition. Psychol. Sci. 5:195-200.

[95] Niblack W. and Flickner M. Query by image and video content: The QBIC system. IEEE Computer, pp 23-32, September 1995.

[96] Mehrotra S. and Chakrabarti K. Similarity shape retrieval in MARS. IEEE International Conference on Multimedia & Expo, New York, 2000.

[97] Del Bimbo and Pala. Visual Querying by Colour Perceptive Regions. Pattern Recognition, Vol 31, pp. 1241-1253 ,1998.

[98] Carson C., Belongie S., Greenspan H., and Malik J. Blobworld. Segmentation using Expectation-Maximisation and its Application to Querying. IEEE Trans. PAMI, Vol 24, No 8, pp 1026-1038, August 2002.

[99] Oyekoya O K, "Managing Multimedia Content: A Technology Roadmap," compiled April 2005 at SIRA Innovation Ltd.

[100] "The I-Prize, A Grand Challenge for Human Computer Interaction" http://hcvl.hci.iastate.edu/IPRIZE .

[101] Jordansen, I.K., Boedeker, S., Donegan, M., Oosthuizen, L., di Girolamo, M., and Hansen, J.P. (2005). Report on a market study and demographics of user population. Communication by Gaze Interaction (COGAIN), IST-2003-511598: Deliverable 7.2. Available at http://www.cogain.org/results/reports/COGAIN-D7.2.pdf

[102] World Intellectual Property Organisation – http://www.wipo.int/.

[103] F W M Stentiford, "Attention based similarity," Pattern Recognition, 40(3), 2007.

[104] Imperial College Innovations Ltd. Manipulation of Image Data. http://www.wipo.int/, International Patent Application No. WO 2003/024319 published on 27 March 2003.

[105] Corel Image Library, http://www.corel.com/.

[106] Vishwa Vinay, Cox I.J., Milic-Frayling N. and Wood K. (2006). On Ranking The Effectiveness of Searches, Proceedings of SIGIR 2006, August 6-11, Seattle Washington.

[107] May, J. G., Kennedy, R. S., Williams, M. C., Dunlap, W. P., & Brannan, J. R. (1990). Eye movement indices of mental workload. Acta Psychologica, 75, 75–89.

[108] Inhoff, A. W., Start, M., Liu, W., & Wang, J. (1998). Eye-movement contingent display changes are not compromised by flicker and phosphor persistence. Psychonomic Bulletin & Review, 5, 101-106.

[109] Ozyurt, J., DeSouza, P., West, P., Rutschmann, R., & Greenlee, M. W. (2001). Comparison of Cortical Activity and Oculomotor Performance in the Gap and Step Paradigms. In European Conference on Visual Perception (ECVP). Kusadasi, Turkey.

[110] Lohse, G. L. (1997). Consumer Eye Movement Patterns on Yellow Pages Advertising. Journal of Advertising, 26(1), 61-73.

[111] Vertegaal, R. (1999). The GAZE Groupware System: Mediating Joint Attention in Mutiparty Communication and Collaboration. In Human Factors in Computing Systems: CHI '99 Conference Proceedings (p. 294-301). ACM Press.

[112] Snodderly, D. M., Kagan, I., & Gur, M. (2001). Selective Activation of Visual Cortex Neurons by Fixational Eye Movements: Implications for Neural Coding. Visual Neuroscience, 18, 259-277.

[113] Schoonard, J. W., Gould, J. D., & Miller, L. A. (1973). Studies of Visual Inspection. Ergonomics, 16(4), 365-379.

Chapter 10. Appendix A: Experiment Questionnaire

Name (optional): _____

Age: _____ (number of years)

Sex: Male □ Female □

Are you: Left-handed □ Right-handed □

Do you wear glasses or prescribed contact lenses: Yes □ No □

If yes, are you: Short-sighted □ Long-sighted □ Other □

Did you wear the glasses during the experiment: Yes □ No □

Colour Vision: Normal □ Colour-blind □

Educational level (e.g. GCSE, Degree, post-graduate, etc.) _____

Motivation to participate: _____

Do you react to flashing light (e.g. epileptic fit): Yes □ No □

	Strongly Agree	Agree	Average	Disagree	Strongly Disagree
I am a computer expert	□	□	□	□	□
I work on images regularly	□	□	□	□	□
I felt under stress during the experiment	□	□	□	□	□
The experiment application software was easy to use	□	□	□	□	□
I understood the instructions clearly	□	□	□	□	□

Did you experience any problems during the experiment? If yes, state the problems:

Did you experience any frustrations during your search? If yes, describe:

Did you find that you modified your eye behaviour during the experiment? State why:

Chapter 11. Appendix B: SPSS Data

11.1. Speed Experiment

Within-Subjects Factors

Measure: MEASURE_1

position	input	Dependent Variable
1	1	Var1
	2	Var2
2	1	Var3
	2	Var4

Between-Subjects Factors

		N
Order	Eye-Mouse	6
	Mouse-Eye	6

Multivariate Tests(b)

Effect		Value	F	Hypothesis df	Error df	Sig.	Partial Eta Squared
position	Pillai's Trace	.055	.577(a)	1.000	10.000	.465	.055
	Wilks' Lambda	.945	.577(a)	1.000	10.000	.465	.055
	Hotelling's Trace	.058	.577(a)	1.000	10.000	.465	.055
	Roy's Largest Root	.058	.577(a)	1.000	10.000	.465	.055
position * Order	Pillai's Trace	.001	.007(a)	1.000	10.000	.936	.001
	Wilks' Lambda	.999	.007(a)	1.000	10.000	.936	.001
	Hotelling's Trace	.001	.007(a)	1.000	10.000	.936	.001
	Roy's Largest Root	.001	.007(a)	1.000	10.000	.936	.001
input	Pillai's Trace	.466	8.716(a)	1.000	10.000	.014	.466
	Wilks' Lambda	.534	8.716(a)	1.000	10.000	.014	.466
	Hotelling's Trace	.872	8.716(a)	1.000	10.000	.014	.466
	Roy's Largest Root	.872	8.716(a)	1.000	10.000	.014	.466
input * Order	Pillai's Trace	.147	1.721(a)	1.000	10.000	.219	.147
	Wilks' Lambda	.853	1.721(a)	1.000	10.000	.219	.147
	Hotelling's Trace	.172	1.721(a)	1.000	10.000	.219	.147
	Roy's Largest Root	.172	1.721(a)	1.000	10.000	.219	.147
position * input	Pillai's Trace	.024	.247(a)	1.000	10.000	.630	.024
	Wilks' Lambda	.976	.247(a)	1.000	10.000	.630	.024
	Hotelling's Trace	.025	.247(a)	1.000	10.000	.630	.024
	Roy's Largest Root	.025	.247(a)	1.000	10.000	.630	.024
position * input * Order	Pillai's Trace	.071	.768(a)	1.000	10.000	.401	.071
	Wilks' Lambda	.929	.768(a)	1.000	10.000	.401	.071
	Hotelling's Trace	.077	.768(a)	1.000	10.000	.401	.071
	Roy's Largest Root	.077	.768(a)	1.000	10.000	.401	.071

a Exact statistic
b Design: Intercept+Order

Within Subjects Design: position+input+position*input

Mauchly's Test of Sphericity(b)

Measure: MEASURE_1

Within Subjects Effect	Mauchly's W	Approx. Chi-Square	df	Sig.	Epsilon(a) Greenhouse-Geisser	Huynh-Feldt	Lower-bound
position	1.000	.000	0	.	1.000	1.000	1.000
input	1.000	.000	0	.	1.000	1.000	1.000
position * input	1.000	.000	0	.	1.000	1.000	1.000

Tests the null hypothesis that the error covariance matrix of the orthonormalized transformed dependent variables is proportional to an identity matrix.
a May be used to adjust the degrees of freedom for the averaged tests of significance. Corrected tests are displayed in the Tests of Within-Subjects Effects table.
b Design: Intercept+Order
Within Subjects Design: position+input+position*input

Tests of Within-Subjects Effects

Measure: MEASURE_1

Source		Type III Sum of Squares	df	Mean Square	F	Sig.	Partial Eta Squared
position	Sphericity Assumed	.185	1	.185	.577	.465	.055
	Greenhouse-Geisser	.185	1.000	.185	.577	.465	.055
	Huynh-Feldt	.185	1.000	.185	.577	.465	.055
	Lower-bound	.185	1.000	.185	.577	.465	.055
position * Order	Sphericity Assumed	.002	1	.002	.007	.936	.001
	Greenhouse-Geisser	.002	1.000	.002	.007	.936	.001
	Huynh-Feldt	.002	1.000	.002	.007	.936	.001
	Lower-bound	.002	1.000	.002	.007	.936	.001
Error(position)	Sphericity Assumed	3.207	10	.321			
	Greenhouse-Geisser	3.207	10.000	.321			
	Huynh-Feldt	3.207	10.000	.321			
	Lower-bound	3.207	10.000	.321			
input	Sphericity Assumed	1.452	1	1.452	8.716	.014	.466
	Greenhouse-Geisser	1.452	1.000	1.452	8.716	.014	.466
	Huynh-Feldt	1.452	1.000	1.452	8.716	.014	.466
	Lower-bound	1.452	1.000	1.452	8.716	.014	.466
input * Order	Sphericity Assumed	.287	1	.287	1.721	.219	.147
	Greenhouse-Geisser	.287	1.000	.287	1.721	.219	.147
	Huynh-Feldt	.287	1.000	.287	1.721	.219	.147
	Lower-bound	.287	1.000	.287	1.721	.219	.147
Error(input)	Sphericity Assumed	1.665	10	.167			
	Greenhouse-Geisser	1.665	10.000	.167			
	Huynh-Feldt	1.665	10.000	.167			
	Lower-bound	1.665	10.000	.167			
position * input	Sphericity Assumed	.027	1	.027	.247	.630	.024
	Greenhouse-Geisser	.027	1.000	.027	.247	.630	.024
	Huynh-Feldt	.027	1.000	.027	.247	.630	.024
	Lower-bound	.027	1.000	.027	.247	.630	.024
position * input * Order	Sphericity Assumed	.083	1	.083	.768	.401	.071
	Greenhouse-Geisser	.083	1.000	.083	.768	.401	.071
	Huynh-Feldt	.083	1.000	.083	.768	.401	.071

	Lower-bound	.083	1.000	.083	.768	.401	.071
Error(position*input)	Sphericity Assumed	1.081	10	.108			
	Greenhouse-Geisser	1.081	10.000	.108			
	Huynh-Feldt	1.081	10.000	.108			
	Lower-bound	1.081	10.000	.108			

Tests of Within-Subjects Contrasts

Measure: MEASURE_1

Source	position	input	Type III Sum of Squares	df	Mean Square	F	Sig.	Partial Eta Squared
position	Linear		.185	1	.185	.577	.465	.055
position * Order	Linear		.002	1	.002	.007	.936	.001
Error(position)	Linear		3.207	10	.321			
input		Linear	1.452	1	1.452	8.716	.014	.466
input * Order		Linear	.287	1	.287	1.721	.219	.147
Error(input)		Linear	1.665	10	.167			
position * input	Linear	Linear	.027	1	.027	.247	.630	.024
position * input * Order	Linear	Linear	.083	1	.083	.768	.401	.071
Error(position*input)	Linear	Linear	1.081	10	.108			

Tests of Between-Subjects Effects

Measure: MEASURE_1
Transformed Variable: Average

Source	Type III Sum of Squares	df	Mean Square	F	Sig.	Partial Eta Squared
Intercept	243.192	1	243.192	145.150	.000	.936
Order	.715	1	.715	.427	.528	.041
Error	16.755	10	1.675			

Estimated Marginal Means

Order

Estimates

Measure: MEASURE_1

Order	Mean	Std. Error	95% Confidence Interval	
			Lower Bound	Upper Bound
Eye-Mouse	2.373	.264	1.784	2.962
Mouse-Eye	2.129	.264	1.540	2.718

Pairwise Comparisons

Measure: MEASURE_1

(I) Order	(J) Order	Mean Difference (I-J)	Std. Error	Sig.(a)	95% Confidence Interval for Difference(a)	
					Lower Bound	Upper Bound
Eye-Mouse	Mouse-Eye	.244	.374	.528	-.588	1.077
Mouse-Eye	Eye-Mouse	-.244	.374	.528	-1.077	.588

Based on estimated marginal means
a Adjustment for multiple comparisons: Least Significant Difference (equivalent to no adjustments).

Univariate Tests

Measure: MEASURE_1

	Sum of Squares	df	Mean Square	F	Sig.	Partial Eta Squared

Contrast	.179	1	.179	.427	.528	.041
Error	4.189	10	.419			

The F tests the effect of Order. This test is based on the linearly independent pairwise comparisons among the estimated marginal means.

Position

Estimates

Measure: MEASURE_1

			95% Confidence Interval	
position	Mean	Std. Error	Lower Bound	Upper Bound
1	2.189	.178	1.792	2.586
2	2.313	.227	1.808	2.818

Pairwise Comparisons

Measure: MEASURE_1

					95% Confidence Interval for Difference(a)	
(I) position	(J) position	Mean Difference (I-J)	Std. Error	Sig.(a)	Lower Bound	Upper Bound
1	2	-.124	.163	.465	-.488	.240
2	1	.124	.163	.465	-.240	.488

Based on estimated marginal means
a Adjustment for multiple comparisons: Least Significant Difference (equivalent to no adjustments).

Multivariate Tests

	Value	F	Hypothesis df	Error df	Sig.	Partial Eta Squared
Pillai's trace	.055	.577(a)	1.000	10.000	.465	.055
Wilks' lambda	.945	.577(a)	1.000	10.000	.465	.055
Hotelling's trace	.058	.577(a)	1.000	10.000	.465	.055
Roy's largest root	.058	.577(a)	1.000	10.000	.465	.055

Each F tests the multivariate effect of position. These tests are based on the linearly independent pairwise comparisons among the estimated marginal means.
a Exact statistic

Input

Estimates

Measure: MEASURE_1

			95% Confidence Interval	
input	Mean	Std. Error	Lower Bound	Upper Bound
1	2.425	.227	1.919	2.931
2	2.077	.159	1.723	2.431

Pairwise Comparisons

Measure: MEASURE_1

					95% Confidence Interval for Difference(a)	
(I) input	(J) input	Mean Difference (I-J)	Std. Error	Sig.(a)	Lower Bound	Upper Bound
1	2	.348(*)	.118	.014	.085	.610
2	1	-.348(*)	.118	.014	-.610	-.085

Based on estimated marginal means

* The mean difference is significant at the .05 level.
a Adjustment for multiple comparisons: Least Significant Difference (equivalent to no adjustments).

Multivariate Tests

	Value	F	Hypothesis df	Error df	Sig.	Partial Eta Squared
Pillai's trace	.466	8.716(a)	1.000	10.000	.014	.466
Wilks' lambda	.534	8.716(a)	1.000	10.000	.014	.466
Hotelling's trace	.872	8.716(a)	1.000	10.000	.014	.466
Roy's largest root	.872	8.716(a)	1.000	10.000	.014	.466

Each F tests the multivariate effect of input. These tests are based on the linearly independent pairwise comparisons among the estimated marginal means.
a Exact statistic

Order * Input

Estimates

Measure: MEASURE_1

Order	input	Mean	Std. Error	95% Confidence Interval	
				Lower Bound	Upper Bound
Eye-Mouse	1	2.470	.321	1.754	3.185
	2	2.276	.225	1.776	2.777
Mouse-Eye	1	2.380	.321	1.665	3.095
	2	1.878	.225	1.377	2.378

Pairwise Comparisons

Measure: MEASURE_1

Order	(I) input	(J) input	Mean Difference (I-J)	Std. Error	Sig.(a)	95% Confidence Interval for Difference(a)	
						Lower Bound	Upper Bound
Eye-Mouse	1	2	.193	.167	.273	-.178	.564
	2	1	-.193	.167	.273	-.564	.178
Mouse-Eye	1	2	.502(*)	.167	.013	.131	.874
	2	1	-.502(*)	.167	.013	-.874	-.131

Based on estimated marginal means
* The mean difference is significant at the .05 level.
a Adjustment for multiple comparisons: Least Significant Difference (equivalent to no adjustments).

Multivariate Tests

Order		Value	F	Hypothesis df	Error df	Sig.	Partial Eta Squared
Eye-Mouse	Pillai's trace	.119	1.345(a)	1.000	10.000	.273	.119
	Wilks' lambda	.881	1.345(a)	1.000	10.000	.273	.119
	Hotelling's trace	.135	1.345(a)	1.000	10.000	.273	.119
	Roy's largest root	.135	1.345(a)	1.000	10.000	.273	.119
Mouse-Eye	Pillai's trace	.476	9.092(a)	1.000	10.000	.013	.476
	Wilks' lambda	.524	9.092(a)	1.000	10.000	.013	.476
	Hotelling's trace	.909	9.092(a)	1.000	10.000	.013	.476
	Roy's largest root	.909	9.092(a)	1.000	10.000	.013	.476

Each F tests the multivariate simple effects of input within each level combination of the other effects shown. These tests are based on the linearly independent pairwise comparisons among the estimated marginal means.
a Exact statistic

Position * Input

Estimates

Measure: MEASURE_1

position	input	Mean	Std. Error	95% Confidence Interval	
				Lower Bound	Upper Bound
1	1	2.339	.197	1.901	2.778
	2	2.039	.167	1.666	2.411
2	1	2.510	.304	1.832	3.189
	2	2.115	.173	1.731	2.500

Pairwise Comparisons

Measure: MEASURE_1

position	(I) input	(J) input	Mean Difference (I-J)	Std. Error	Sig.(a)	95% Confidence Interval for Difference(a)	
						Lower Bound	Upper Bound
1	1	2	.301(*)	.080	.004	.123	.478
	2	1	-.301(*)	.080	.004	-.478	-.123
2	1	2	.395	.199	.075	-.047	.837
	2	1	-.395	.199	.075	-.837	.047

Based on estimated marginal means

* The mean difference is significant at the .05 level.

a Adjustment for multiple comparisons: Least Significant Difference (equivalent to no adjustments).

Multivariate Tests

position		Value	F	Hypothesis df	Error df	Sig.	Partial Eta Squared
1	Pillai's trace	.587	14.223(a)	1.000	10.000	.004	.587
	Wilks' lambda	.413	14.223(a)	1.000	10.000	.004	.587
	Hotelling's trace	1.422	14.223(a)	1.000	10.000	.004	.587
	Roy's largest root	1.422	14.223(a)	1.000	10.000	.004	.587
2	Pillai's trace	.284	3.957(a)	1.000	10.000	.075	.284
	Wilks' lambda	.716	3.957(a)	1.000	10.000	.075	.284
	Hotelling's trace	.396	3.957(a)	1.000	10.000	.075	.284
	Roy's largest root	.396	3.957(a)	1.000	10.000	.075	.284

Each F tests the multivariate simple effects of input within each level combination of the other effects shown. These tests are based on the linearly independent pairwise comparisons among the estimated marginal means.

a Exact statistic

Order * Position * Input

Estimates

Measure: MEASURE_1

Order	position	input	Mean	Std. Error	95% Confidence Interval	
					Lower Bound	Upper Bound
Eye-Mouse	1	1	2.349	.278	1.729	2.969
		2	2.286	.237	1.759	2.813
	2	1	2.590	.431	1.631	3.549
		2	2.266	.244	1.722	2.811
Mouse-Eye	1	1	2.329	.278	1.709	2.949
		2	1.791	.237	1.264	2.318
	2	1	2.431	.431	1.472	3.390

	2	1.964	.244	1.420	2.509	

Pairwise Comparisons

Measure: MEASURE_1

Order	position	(I) input	(J) input	Mean Difference (I-J)	Std. Error	Sig.(a)	95% Confidence Interval for Difference(a)	
							Lower Bound	Upper Bound
Eye-Mouse	1	1	2	.063	.113	.589	-.188	.314
		2	1	-.063	.113	.589	-.314	.188
	2	1	2	.324	.281	.276	-.302	.949
		2	1	-.324	.281	.276	-.949	.302
Mouse-Eye	1	1	2	.538(*)	.113	.001	.287	.790
		2	1	-.538(*)	.113	.001	-.790	-.287
	2	1	2	.466	.281	.128	-.159	1.092
		2	1	-.466	.281	.128	-1.092	.159

Based on estimated marginal means

* The mean difference is significant at the .05 level.

a Adjustment for multiple comparisons: Least Significant Difference (equivalent to no adjustments).

Multivariate Tests

Order	position		Value	F	Hypothesis df	Error df	Sig.	Partial Eta Squared
Eye-Mouse	1	Pillai's trace	.030	.311(a)	1.000	10.000	.589	.030
		Wilks' lambda	.970	.311(a)	1.000	10.000	.589	.030
		Hotelling's trace	.031	.311(a)	1.000	10.000	.589	.030
		Roy's largest root	.031	.311(a)	1.000	10.000	.589	.030
	2	Pillai's trace	.117	1.328(a)	1.000	10.000	.276	.117
		Wilks' lambda	.883	1.328(a)	1.000	10.000	.276	.117
		Hotelling's trace	.133	1.328(a)	1.000	10.000	.276	.117
		Roy's largest root	.133	1.328(a)	1.000	10.000	.276	.117
Mouse-Eye	1	Pillai's trace	.695	22.809(a)	1.000	10.000	.001	.695
		Wilks' lambda	.305	22.809(a)	1.000	10.000	.001	.695
		Hotelling's trace	2.281	22.809(a)	1.000	10.000	.001	.695
		Roy's largest root	2.281	22.809(a)	1.000	10.000	.001	.695
	2	Pillai's trace	.216	2.758(a)	1.000	10.000	.128	.216
		Wilks' lambda	.784	2.758(a)	1.000	10.000	.128	.216
		Hotelling's trace	.276	2.758(a)	1.000	10.000	.128	.216
		Roy's largest root	.276	2.758(a)	1.000	10.000	.128	.216

Each F tests the multivariate simple effects of input within each level combination of the other effects shown. These tests are based on the linearly independent pairwise comparisons among the estimated marginal means.

a Exact statistic

11.2. Image Retrieval Experiment

11.2.1. Steps to Target

Within-Subjects Factors

Measure: MEASURE_1

image	Thresh (threshold)	random	Dependent Variable

1 (Easy)	1 (400ms)	1 (0)	VAR00002
		2 (1)	VAR00003
	2 (800ms)	1	VAR00004
		2	VAR00005
2 (Hard)	1	1	VAR00006
		2	VAR00007
	2	1	VAR00008
		2	VAR00009

Multivariate Tests(b)

Effect		Value	F	Hypothesis df	Error df	Sig.
image	Pillai's Trace	.666	23.897(a)	1.000	12.000	.000
	Wilks' Lambda	.334	23.897(a)	1.000	12.000	.000
	Hotelling's Trace	1.991	23.897(a)	1.000	12.000	.000
	Roy's Largest Root	1.991	23.897(a)	1.000	12.000	.000
thresh	Pillai's Trace	.111	1.496(a)	1.000	12.000	.245
	Wilks' Lambda	.889	1.496(a)	1.000	12.000	.245
	Hotelling's Trace	.125	1.496(a)	1.000	12.000	.245
	Roy's Largest Root	.125	1.496(a)	1.000	12.000	.245
random	Pillai's Trace	.014	.171(a)	1.000	12.000	.686
	Wilks' Lambda	.986	.171(a)	1.000	12.000	.686
	Hotelling's Trace	.014	.171(a)	1.000	12.000	.686
	Roy's Largest Root	.014	.171(a)	1.000	12.000	.686
image * thresh	Pillai's Trace	.050	.627(a)	1.000	12.000	.444
	Wilks' Lambda	.950	.627(a)	1.000	12.000	.444
	Hotelling's Trace	.052	.627(a)	1.000	12.000	.444
	Roy's Largest Root	.052	.627(a)	1.000	12.000	.444
image * random	Pillai's Trace	.051	.642(a)	1.000	12.000	.439
	Wilks' Lambda	.949	.642(a)	1.000	12.000	.439
	Hotelling's Trace	.053	.642(a)	1.000	12.000	.439
	Roy's Largest Root	.053	.642(a)	1.000	12.000	.439
thresh * random	Pillai's Trace	.161	2.298(a)	1.000	12.000	.155
	Wilks' Lambda	.839	2.298(a)	1.000	12.000	.155
	Hotelling's Trace	.192	2.298(a)	1.000	12.000	.155
	Roy's Largest Root	.192	2.298(a)	1.000	12.000	.155
image * thresh * random	Pillai's Trace	.001	.015(a)	1.000	12.000	.903
	Wilks' Lambda	.999	.015(a)	1.000	12.000	.903
	Hotelling's Trace	.001	.015(a)	1.000	12.000	.903
	Roy's Largest Root	.001	.015(a)	1.000	12.000	.903

a Exact statistic
b Design: Intercept
Within Subjects Design: image+thresh+random+image*thresh+image*random+thresh*random+image*thresh*random

Tests of Within-Subjects Effects

Measure: MEASURE_1

Source		Type III Sum of Squares	df	Mean Square	F	Sig.
image	Sphericity Assumed	1624.240	1	1624.240	23.897	.000
	Greenhouse-Geisser	1624.240	1.000	1624.240	23.897	.000
	Huynh-Feldt	1624.240	1.000	1624.240	23.897	.000

	Lower-bound	1624.240	1.000	1624.240	23.897	.000
Error(image)	Sphericity Assumed	815.635	12	67.970		
	Greenhouse-Geisser	815.635	12.000	67.970		
	Huynh-Feldt	815.635	12.000	67.970		
	Lower-bound	815.635	12.000	67.970		
thresh	Sphericity Assumed	106.010	1	106.010	1.496	.245
	Greenhouse-Geisser	106.010	1.000	106.010	1.496	.245
	Huynh-Feldt	106.010	1.000	106.010	1.496	.245
	Lower-bound	106.010	1.000	106.010	1.496	.245
Error(thresh)	Sphericity Assumed	850.365	12	70.864		
	Greenhouse-Geisser	850.365	12.000	70.864		
	Huynh-Feldt	850.365	12.000	70.864		
	Lower-bound	850.365	12.000	70.864		
random	Sphericity Assumed	23.087	1	23.087	.171	.686
	Greenhouse-Geisser	23.087	1.000	23.087	.171	.686
	Huynh-Feldt	23.087	1.000	23.087	.171	.686
	Lower-bound	23.087	1.000	23.087	.171	.686
Error(random)	Sphericity Assumed	1619.788	12	134.982		
	Greenhouse-Geisser	1619.788	12.000	134.982		
	Huynh-Feldt	1619.788	12.000	134.982		
	Lower-bound	1619.788	12.000	134.982		
image * thresh	Sphericity Assumed	31.240	1	31.240	.627	.444
	Greenhouse-Geisser	31.240	1.000	31.240	.627	.444
	Huynh-Feldt	31.240	1.000	31.240	.627	.444
	Lower-bound	31.240	1.000	31.240	.627	.444
Error(image*thresh)	Sphericity Assumed	597.635	12	49.803		
	Greenhouse-Geisser	597.635	12.000	49.803		
	Huynh-Feldt	597.635	12.000	49.803		
	Lower-bound	597.635	12.000	49.803		
image * random	Sphericity Assumed	43.163	1	43.163	.642	.439
	Greenhouse-Geisser	43.163	1.000	43.163	.642	.439
	Huynh-Feldt	43.163	1.000	43.163	.642	.439
	Lower-bound	43.163	1.000	43.163	.642	.439
Error(image*random)	Sphericity Assumed	807.212	12	67.268		
	Greenhouse-Geisser	807.212	12.000	67.268		
	Huynh-Feldt	807.212	12.000	67.268		
	Lower-bound	807.212	12.000	67.268		
thresh * random	Sphericity Assumed	219.240	1	219.240	2.298	.155
	Greenhouse-Geisser	219.240	1.000	219.240	2.298	.155
	Huynh-Feldt	219.240	1.000	219.240	2.298	.155
	Lower-bound	219.240	1.000	219.240	2.298	.155
Error(thresh*random)	Sphericity Assumed	1144.635	12	95.386		

	Greenhouse-Geisser	1144.635	12.000	95.386		
	Huynh-Feldt	1144.635	12.000	95.386		
	Lower-bound	1144.635	12.000	95.386		
image * thresh * random	Sphericity Assumed	1.163	1	1.163	.015	.903
	Greenhouse-Geisser	1.163	1.000	1.163	.015	.903
	Huynh-Feldt	1.163	1.000	1.163	.015	.903
	Lower-bound	1.163	1.000	1.163	.015	.903
Error(image*thresh*random)	Sphericity Assumed	905.212	12	75.434		
	Greenhouse-Geisser	905.212	12.000	75.434		
	Huynh-Feldt	905.212	12.000	75.434		
	Lower-bound	905.212	12.000	75.434		

Tests of Within-Subjects Contrasts

Measure: MEASURE_1

Source	image	thresh	random	Type III Sum of Squares	df	Mean Square	F	Sig.
image	Linear			1624.240	1	1624.240	23.897	.000
Error(image)	Linear			815.635	12	67.970		
thresh		Linear		106.010	1	106.010	1.496	.245
Error(thresh)		Linear		850.365	12	70.864		
random			Linear	23.087	1	23.087	.171	.686
Error(random)			Linear	1619.788	12	134.982		
image * thresh	Linear	Linear		31.240	1	31.240	.627	.444
Error(image*thresh)	Linear	Linear		597.635	12	49.803		
image * random	Linear		Linear	43.163	1	43.163	.642	.439
Error(image*random)	Linear		Linear	807.212	12	67.268		
thresh * random		Linear	Linear	219.240	1	219.240	2.298	.155
Error(thresh*random)		Linear	Linear	1144.635	12	95.386		
image * thresh * random	Linear	Linear	Linear	1.163	1	1.163	.015	.903
Error(image*thresh*random)	Linear	Linear	Linear	905.212	12	75.434		

Tests of Between-Subjects Effects

Measure: MEASURE_1
Transformed Variable: Average

Source	Type III Sum of Squares	df	Mean Square	F	Sig.
Intercept	35041.163	1	35041.163	280.477	.000
Error	1499.212	12	124.934		

Estimated Marginal Means

Image

Estimates

Measure: MEASURE_1

image	Mean	Std. Error	95% Confidence Interval	
			Lower Bound	Upper Bound
1	14.404	1.565	10.994	17.814
2	22.308	1.123	19.861	24.754

Pairwise Comparisons

Measure: MEASURE_1

(I) image	(J) image	Mean Difference (I-J)	Std. Error	Sig.(a)	95% Confidence Interval for Difference(a)	
					Lower Bound	Upper Bound
1	2	-7.904(*)	1.617	.000	-11.427	-4.381
2	1	7.904(*)	1.617	.000	4.381	11.427

Based on estimated marginal means
* The mean difference is significant at the .05 level.
a Adjustment for multiple comparisons: Least Significant Difference (equivalent to no adjustments).

Multivariate Tests

	Value	F	Hypothesis df	Error df	Sig.
Pillai's trace	.666	23.897(a)	1.000	12.000	.000
Wilks' lambda	.334	23.897(a)	1.000	12.000	.000
Hotelling's trace	1.991	23.897(a)	1.000	12.000	.000
Roy's largest root	1.991	23.897(a)	1.000	12.000	.000

Each F tests the multivariate effect of image. These tests are based on the linearly independent pairwise comparisons among the estimated marginal means.
a Exact statistic

Thresh

Estimates

Measure: MEASURE_1

thresh	Mean	Std. Error	95% Confidence Interval	
			Lower Bound	Upper Bound
1	19.365	1.340	16.447	22.284
2	17.346	1.404	14.287	20.405

Pairwise Comparisons

Measure: MEASURE_1

(I) thresh	(J) thresh	Mean Difference (I-J)	Std. Error	Sig.(a)	95% Confidence Interval for Difference(a)	
					Lower Bound	Upper Bound
1	2	2.019	1.651	.245	-1.578	5.616
2	1	-2.019	1.651	.245	-5.616	1.578

Based on estimated marginal means
a Adjustment for multiple comparisons: Least Significant Difference (equivalent to no adjustments).

Multivariate Tests

	Value	F	Hypothesis df	Error df	Sig.
Pillai's trace	.111	1.496(a)	1.000	12.000	.245
Wilks' lambda	.889	1.496(a)	1.000	12.000	.245
Hotelling's trace	.125	1.496(a)	1.000	12.000	.245
Roy's largest root	.125	1.496(a)	1.000	12.000	.245

Each F tests the multivariate effect of thresh. These tests are based on the linearly independent pairwise comparisons among the estimated marginal means.
a Exact statistic

Random

Estimates

Measure: MEASURE_1

random	Mean	Std. Error	95% Confidence Interval

			Lower Bound	Upper Bound
1	18.827	1.533	15.488	22.166
2	17.885	1.628	14.338	21.431

Pairwise Comparisons

Measure: MEASURE_1

					95% Confidence Interval for Difference(a)	
(I) random	(J) random	Mean Difference (I-J)	Std. Error	Sig.(a)	Lower Bound	Upper Bound
1	2	.942	2.279	.686	-4.022	5.907
2	1	-.942	2.279	.686	-5.907	4.022

Based on estimated marginal means
a Adjustment for multiple comparisons: Least Significant Difference (equivalent to no adjustments).

Multivariate Tests

	Value	F	Hypothesis df	Error df	Sig.
Pillai's trace	.014	.171(a)	1.000	12.000	.686
Wilks' lambda	.986	.171(a)	1.000	12.000	.686
Hotelling's trace	.014	.171(a)	1.000	12.000	.686
Roy's largest root	.014	.171(a)	1.000	12.000	.686

Each F tests the multivariate effect of random. These tests are based on the linearly independent pairwise comparisons among the estimated marginal means.
a Exact statistic

Image * Thresh

Estimates

Measure: MEASURE_1

				95% Confidence Interval	
image	thresh	Mean	Std. Error	Lower Bound	Upper Bound
1	1	15.962	1.830	11.975	19.948
	2	12.846	2.135	8.194	17.498
2	1	22.769	1.321	19.891	25.648
	2	21.846	1.552	18.465	25.227

Pairwise Comparisons

Measure: MEASURE_1

						95% Confidence Interval for Difference(a)	
thresh	(I) image	(J) image	Mean Difference (I-J)	Std. Error	Sig.(a)	Lower Bound	Upper Bound
1	1	2	-6.808(*)	1.734	.002	-10.587	-3.029
	2	1	6.808(*)	1.734	.002	3.029	10.587
2	1	2	-9.000(*)	2.460	.003	-14.360	-3.640
	2	1	9.000(*)	2.460	.003	3.640	14.360

Based on estimated marginal means
* The mean difference is significant at the .05 level.
a Adjustment for multiple comparisons: Least Significant Difference (equivalent to no adjustments).

Multivariate Tests

thresh		Value	F	Hypothesis df	Error df	Sig.
1	Pillai's trace	.562	15.406(a)	1.000	12.000	.002
	Wilks' lambda	.438	15.406(a)	1.000	12.000	.002

	Hotelling's trace	1.284	15.406(a)	1.000	12.000	.002
	Roy's largest root	1.284	15.406(a)	1.000	12.000	.002
2	Pillai's trace	.527	13.386(a)	1.000	12.000	.003
	Wilks' lambda	.473	13.386(a)	1.000	12.000	.003
	Hotelling's trace	1.115	13.386(a)	1.000	12.000	.003
	Roy's largest root	1.115	13.386(a)	1.000	12.000	.003

Each F tests the multivariate simple effects of image within each level combination of the other effects shown. These tests are based on the linearly independent pairwise comparisons among the estimated marginal means.
a Exact statistic

Image * Thresh

Pairwise Comparisons

Measure: MEASURE_1

image	(I) thresh	(J) thresh	Mean Difference (I-J)	Std. Error	Sig.(a)	95% Confidence Interval for Difference(a)	
						Lower Bound	Upper Bound
1	1	2	3.115	2.453	.228	-2.229	8.460
	2	1	-3.115	2.453	.228	-8.460	2.229
2	1	2	.923	1.807	.619	-3.014	4.860
	2	1	-.923	1.807	.619	-4.860	3.014

Based on estimated marginal means
a Adjustment for multiple comparisons: Least Significant Difference (equivalent to no adjustments).

Multivariate Tests

image		Value	F	Hypothesis df	Error df	Sig.
1	Pillai's trace	.119	1.613(a)	1.000	12.000	.228
	Wilks' lambda	.881	1.613(a)	1.000	12.000	.228
	Hotelling's trace	.134	1.613(a)	1.000	12.000	.228
	Roy's largest root	.134	1.613(a)	1.000	12.000	.228
2	Pillai's trace	.021	.261(a)	1.000	12.000	.619
	Wilks' lambda	.979	.261(a)	1.000	12.000	.619
	Hotelling's trace	.022	.261(a)	1.000	12.000	.619
	Roy's largest root	.022	.261(a)	1.000	12.000	.619

Each F tests the multivariate simple effects of thresh within each level combination of the other effects shown. These tests are based on the linearly independent pairwise comparisons among the estimated marginal means.
a Exact statistic

Image * Random

Estimates

Measure: MEASURE_1

image	random	Mean	Std. Error	95% Confidence Interval	
				Lower Bound	Upper Bound
1	1	14.231	2.320	9.177	19.285
	2	14.577	1.647	10.989	18.164
2	1	23.423	1.270	20.657	26.189
	2	21.192	2.344	16.085	26.300

Pairwise Comparisons

Measure: MEASURE_1

random	(I) image	(J) image	Mean Difference (I-	Std. Error	Sig.(a)	95% Confidence Interval for Difference(a)

			J)			Lower Bound	Upper Bound
1	1	2	-9.192(*)	2.142	.001	-13.859	-4.525
	2	1	9.192(*)	2.142	.001	4.525	13.859
2	1	2	-6.615(*)	2.411	.018	-11.869	-1.362
	2	1	6.615(*)	2.411	.018	1.362	11.869

Based on estimated marginal means
* The mean difference is significant at the .05 level.
a Adjustment for multiple comparisons: Least Significant Difference (equivalent to no adjustments).

Multivariate Tests

random		Value	F	Hypothesis df	Error df	Sig.
1	Pillai's trace	.605	18.416(a)	1.000	12.000	.001
	Wilks' lambda	.395	18.416(a)	1.000	12.000	.001
	Hotelling's trace	1.535	18.416(a)	1.000	12.000	.001
	Roy's largest root	1.535	18.416(a)	1.000	12.000	.001
2	Pillai's trace	.385	7.526(a)	1.000	12.000	.018
	Wilks' lambda	.615	7.526(a)	1.000	12.000	.018
	Hotelling's trace	.627	7.526(a)	1.000	12.000	.018
	Roy's largest root	.627	7.526(a)	1.000	12.000	.018

Each F tests the multivariate simple effects of image within each level combination of the other effects shown. These tests are based on the linearly independent pairwise comparisons among the estimated marginal means.
a Exact statistic

Thresh * Random

Estimates

Measure: MEASURE_1

thresh	random	Mean	Std. Error	95% Confidence Interval	
				Lower Bound	Upper Bound
1	1	18.385	1.933	14.172	22.597
	2	20.346	1.942	16.115	24.577
2	1	19.269	2.025	14.857	23.682
	2	15.423	2.187	10.659	20.187

Pairwise Comparisons

Measure: MEASURE_1

random	(I) thresh	(J) thresh	Mean Difference (I-J)	Std. Error	Sig.(a)	95% Confidence Interval for Difference(a)	
						Lower Bound	Upper Bound
1	1	2	-.885	2.507	.730	-6.346	4.577
	2	1	.885	2.507	.730	-4.577	6.346
2	1	2	4.923	2.551	.078	-.634	10.481
	2	1	-4.923	2.551	.078	-10.481	.634

Based on estimated marginal means
a Adjustment for multiple comparisons: Least Significant Difference (equivalent to no adjustments).

Multivariate Tests

random		Value	F	Hypothesis df	Error df	Sig.
1	Pillai's trace	.010	.125(a)	1.000	12.000	.730
	Wilks' lambda	.990	.125(a)	1.000	12.000	.730
	Hotelling's trace	.010	.125(a)	1.000	12.000	.730
	Roy's largest root	.010	.125(a)	1.000	12.000	.730

2	Pillai's trace	.237	3.725(a)	1.000	12.000	.078
	Wilks' lambda	.763	3.725(a)	1.000	12.000	.078
	Hotelling's trace	.310	3.725(a)	1.000	12.000	.078
	Roy's largest root	.310	3.725(a)	1.000	12.000	.078

Each F tests the multivariate simple effects of thresh within each level combination of the other effects shown. These tests are based on the linearly independent pairwise comparisons among the estimated marginal means.
a Exact statistic

Image * Thresh * Random

Estimates

Measure: MEASURE_1

image	thresh	random	Mean	Std. Error	95% Confidence Interval	
					Lower Bound	Upper Bound
1	1	1	14.231	2.799	8.132	20.330
		2	17.692	2.936	11.295	24.089
	2	1	14.231	3.132	7.407	21.055
		2	11.462	2.518	5.975	16.948
2	1	1	22.538	2.135	17.886	27.191
		2	23.000	2.038	18.559	27.441
	2	1	24.308	1.692	20.620	27.995
		2	19.385	2.939	12.982	25.787

Pairwise Comparisons

Measure: MEASURE_1

thresh	random	(I) image	(J) image	Mean Difference (I-J)	Std. Error	Sig.(a)	95% Confidence Interval for Difference(a)	
							Lower Bound	Upper Bound
1	1	1	2	-8.308(*)	3.137	.021	-15.142	-1.474
		2	1	8.308(*)	3.137	.021	1.474	15.142
	2	1	2	-5.308	3.235	.127	-12.357	1.741
		2	1	5.308	3.235	.127	-1.741	12.357
2	1	1	2	-10.077(*)	2.990	.006	-16.592	-3.562
		2	1	10.077(*)	2.990	.006	3.562	16.592
	2	1	2	-7.923(*)	3.290	.033	-15.092	-.754
		2	1	7.923(*)	3.290	.033	.754	15.092

Based on estimated marginal means
* The mean difference is significant at the .05 level.
a Adjustment for multiple comparisons: Least Significant Difference (equivalent to no adjustments).

Multivariate Tests

thresh	random		Value	F	Hypothesis df	Error df	Sig.
1	1	Pillai's trace	.369	7.015(a)	1.000	12.000	.021
		Wilks' lambda	.631	7.015(a)	1.000	12.000	.021
		Hotelling's trace	.585	7.015(a)	1.000	12.000	.021
		Roy's largest root	.585	7.015(a)	1.000	12.000	.021
	2	Pillai's trace	.183	2.692(a)	1.000	12.000	.127
		Wilks' lambda	.817	2.692(a)	1.000	12.000	.127
		Hotelling's trace	.224	2.692(a)	1.000	12.000	.127
		Roy's largest root	.224	2.692(a)	1.000	12.000	.127
2	1	Pillai's trace	.486	11.356(a)	1.000	12.000	.006
		Wilks' lambda	.514	11.356(a)	1.000	12.000	.006

		Hotelling's trace	.946	11.356(a)	1.000	12.000	.006
		Roy's largest root	.946	11.356(a)	1.000	12.000	.006
	2	Pillai's trace	.326	5.798(a)	1.000	12.000	.033
		Wilks' lambda	.674	5.798(a)	1.000	12.000	.033
		Hotelling's trace	.483	5.798(a)	1.000	12.000	.033
		Roy's largest root	.483	5.798(a)	1.000	12.000	.033

Each F tests the multivariate simple effects of image within each level combination of the other effects shown. These tests are based on the linearly independent pairwise comparisons among the estimated marginal means.
a Exact statistic

11.2.2. Time to Target

Within-Subjects Factors

Measure: MEASURE_1

image	thresh	random	Dependent Variable
1	1	1	V1
		2	V2
	2	1	V3
		2	V4
2	1	1	V5
		2	V6
	2	1	V7
		2	V8

Multivariate Tests(b)

Effect		Value	F	Hypothesis df	Error df	Sig.	Partial Eta Squared
image	Pillai's Trace	.625	24.949(a)	1.000	15.000	.000	.625
	Wilks' Lambda	.375	24.949(a)	1.000	15.000	.000	.625
	Hotelling's Trace	1.663	24.949(a)	1.000	15.000	.000	.625
	Roy's Largest Root	1.663	24.949(a)	1.000	15.000	.000	.625
thresh	Pillai's Trace	.625	25.020(a)	1.000	15.000	.000	.625
	Wilks' Lambda	.375	25.020(a)	1.000	15.000	.000	.625
	Hotelling's Trace	1.668	25.020(a)	1.000	15.000	.000	.625
	Roy's Largest Root	1.668	25.020(a)	1.000	15.000	.000	.625
random	Pillai's Trace	.093	1.537(a)	1.000	15.000	.234	.093
	Wilks' Lambda	.907	1.537(a)	1.000	15.000	.234	.093
	Hotelling's Trace	.102	1.537(a)	1.000	15.000	.234	.093
	Roy's Largest Root	.102	1.537(a)	1.000	15.000	.234	.093
image * thresh	Pillai's Trace	.326	7.266(a)	1.000	15.000	.017	.326
	Wilks' Lambda	.674	7.266(a)	1.000	15.000	.017	.326
	Hotelling's Trace	.484	7.266(a)	1.000	15.000	.017	.326
	Roy's Largest Root	.484	7.266(a)	1.000	15.000	.017	.326
image * random	Pillai's Trace	.138	2.404(a)	1.000	15.000	.142	.138
	Wilks' Lambda	.862	2.404(a)	1.000	15.000	.142	.138
	Hotelling's Trace	.160	2.404(a)	1.000	15.000	.142	.138
	Roy's Largest Root	.160	2.404(a)	1.000	15.000	.142	.138
thresh * random	Pillai's Trace	.067	1.072(a)	1.000	15.000	.317	.067
	Wilks' Lambda	.933	1.072(a)	1.000	15.000	.317	.067
	Hotelling's Trace	.071	1.072(a)	1.000	15.000	.317	.067

	Roy's Largest Root	.071	1.072(a)	1.000	15.000	.317	.067
image * thresh * random	Pillai's Trace	.022	.333(a)	1.000	15.000	.573	.022
	Wilks' Lambda	.978	.333(a)	1.000	15.000	.573	.022
	Hotelling's Trace	.022	.333(a)	1.000	15.000	.573	.022
	Roy's Largest Root	.022	.333(a)	1.000	15.000	.573	.022

a Exact statistic
b Design: Intercept
Within Subjects Design: image+thresh+random+image*thresh+image*random+thresh*random+image*thresh*random

Tests of Within-Subjects Effects

Measure: MEASURE_1

Source		Type III Sum of Squares	df	Mean Square	F	Sig.	Partial Eta Squared
image	Sphericity Assumed	25302.573	1	25302.573	24.949	.000	.625
	Greenhouse-Geisser	25302.573	1.000	25302.573	24.949	.000	.625
	Huynh-Feldt	25302.573	1.000	25302.573	24.949	.000	.625
	Lower-bound	25302.573	1.000	25302.573	24.949	.000	.625
Error(image)	Sphericity Assumed	15212.287	15	1014.152			
	Greenhouse-Geisser	15212.287	15.000	1014.152			
	Huynh-Feldt	15212.287	15.000	1014.152			
	Lower-bound	15212.287	15.000	1014.152			
thresh	Sphericity Assumed	29364.489	1	29364.489	25.020	.000	.625
	Greenhouse-Geisser	29364.489	1.000	29364.489	25.020	.000	.625
	Huynh-Feldt	29364.489	1.000	29364.489	25.020	.000	.625
	Lower-bound	29364.489	1.000	29364.489	25.020	.000	.625
Error(thresh)	Sphericity Assumed	17604.840	15	1173.656			
	Greenhouse-Geisser	17604.840	15.000	1173.656			
	Huynh-Feldt	17604.840	15.000	1173.656			
	Lower-bound	17604.840	15.000	1173.656			
random	Sphericity Assumed	1442.724	1	1442.724	1.537	.234	.093
	Greenhouse-Geisser	1442.724	1.000	1442.724	1.537	.234	.093
	Huynh-Feldt	1442.724	1.000	1442.724	1.537	.234	.093
	Lower-bound	1442.724	1.000	1442.724	1.537	.234	.093
Error(random)	Sphericity Assumed	14078.520	15	938.568			
	Greenhouse-Geisser	14078.520	15.000	938.568			
	Huynh-Feldt	14078.520	15.000	938.568			
	Lower-bound	14078.520	15.000	938.568			
image * thresh	Sphericity Assumed	5094.202	1	5094.202	7.266	.017	.326
	Greenhouse-Geisser	5094.202	1.000	5094.202	7.266	.017	.326
	Huynh-Feldt	5094.202	1.000	5094.202	7.266	.017	.326
	Lower-bound	5094.202	1.000	5094.202	7.266	.017	.326
Error(image*thresh)	Sphericity Assumed	10516.931	15	701.129			

	Greenhouse-Geisser	10516.931	15.000	701.129			
	Huynh-Feldt	10516.931	15.000	701.129			
	Lower-bound	10516.931	15.000	701.129			
image * random	Sphericity Assumed	914.631	1	914.631	2.404	.142	.138
	Greenhouse-Geisser	914.631	1.000	914.631	2.404	.142	.138
	Huynh-Feldt	914.631	1.000	914.631	2.404	.142	.138
	Lower-bound	914.631	1.000	914.631	2.404	.142	.138
Error(image*random)	Sphericity Assumed	5705.879	15	380.392			
	Greenhouse-Geisser	5705.879	15.000	380.392			
	Huynh-Feldt	5705.879	15.000	380.392			
	Lower-bound	5705.879	15.000	380.392			
thresh * random	Sphericity Assumed	1268.877	1	1268.877	1.072	.317	.067
	Greenhouse-Geisser	1268.877	1.000	1268.877	1.072	.317	.067
	Huynh-Feldt	1268.877	1.000	1268.877	1.072	.317	.067
	Lower-bound	1268.877	1.000	1268.877	1.072	.317	.067
Error(thresh*random)	Sphericity Assumed	17756.563	15	1183.771			
	Greenhouse-Geisser	17756.563	15.000	1183.771			
	Huynh-Feldt	17756.563	15.000	1183.771			
	Lower-bound	17756.563	15.000	1183.771			
image * thresh * random	Sphericity Assumed	308.802	1	308.802	.333	.573	.022
	Greenhouse-Geisser	308.802	1.000	308.802	.333	.573	.022
	Huynh-Feldt	308.802	1.000	308.802	.333	.573	.022
	Lower-bound	308.802	1.000	308.802	.333	.573	.022
Error(image*thresh*random)	Sphericity Assumed	13926.228	15	928.415			
	Greenhouse-Geisser	13926.228	15.000	928.415			
	Huynh-Feldt	13926.228	15.000	928.415			
	Lower-bound	13926.228	15.000	928.415			

Tests of Within-Subjects Contrasts

Measure: MEASURE_1

Source	image	thresh	random	Type III Sum of Squares	df	Mean Square	F	Sig.	Partial Eta Squared
image	Linear			25302.573	1	25302.573	24.949	.000	.625
Error(image)	Linear			15212.287	15	1014.152			
thresh		Linear		29364.489	1	29364.489	25.020	.000	.625
Error(thresh)		Linear		17604.840	15	1173.656			
random			Linear	1442.724	1	1442.724	1.537	.234	.093
Error(random)			Linear	14078.520	15	938.568			
image * thresh	Linear	Linear		5094.202	1	5094.202	7.266	.017	.326
Error(image*thresh)	Linear	Linear		10516.931	15	701.129			
image * random	Linear		Linear	914.631	1	914.631	2.404	.142	.138
Error(image*random)	Linear		Linear	5705.879	15	380.392			
thresh * random		Linear	Linear	1268.877	1	1268.877	1.072	.317	.067
Error(thresh*random)		Linear	Linear	17756.563	15	1183.771			
image * thresh * random	Linear	Linear	Linear	308.802	1	308.802	.333	.573	.022
Error(image*thresh*random)	Linear	Linear	Linear	13926.228	15	928.415			

Tests of Between-Subjects Effects

Measure: MEASURE_1
Transformed Variable: Average

Source	Type III Sum of Squares	df	Mean Square	F	Sig.	Partial Eta Squared
Intercept	441837.483	1	441837.483	132.202	.000	.898
Error	50131.902	15	3342.127			

Estimated Marginal Means

Image

Estimates

Measure: MEASURE_1

image	Mean	Std. Error	95% Confidence Interval	
			Lower Bound	Upper Bound
1	44.693	5.382	33.221	56.165
2	72.812	6.253	59.484	86.140

Pairwise Comparisons

Measure: MEASURE_1

(I) image	(J) image	Mean Difference (I-J)	Std. Error	Sig.(a)	95% Confidence Interval for Difference(a)	
					Lower Bound	Upper Bound
1	2	-28.119(*)	5.630	.000	-40.119	-16.120
2	1	28.119(*)	5.630	.000	16.120	40.119

Based on estimated marginal means
* The mean difference is significant at the .05 level.
a Adjustment for multiple comparisons: Least Significant Difference (equivalent to no adjustments).

Multivariate Tests

	Value	F	Hypothesis df	Error df	Sig.	Partial Eta Squared
Pillai's trace	.625	24.949(a)	1.000	15.000	.000	.625
Wilks' lambda	.375	24.949(a)	1.000	15.000	.000	.625
Hotelling's trace	1.663	24.949(a)	1.000	15.000	.000	.625
Roy's largest root	1.663	24.949(a)	1.000	15.000	.000	.625

Each F tests the multivariate effect of image. These tests are based on the linearly independent pairwise comparisons among the estimated marginal means.
a Exact statistic

Thresh

Estimates

Measure: MEASURE_1

thresh	Mean	Std. Error	95% Confidence Interval	
			Lower Bound	Upper Bound
1	43.606	3.104	36.989	50.223
2	73.899	7.805	57.262	90.535

Pairwise Comparisons

Measure: MEASURE_1

(I) thresh	(J) thresh	Mean Difference (I-J)	Std. Error	Sig.(a)	95% Confidence Interval for Difference(a)	
					Lower Bound	Upper Bound
1	2	-30.293(*)	6.056	.000	-43.201	-17.384
2	1	30.293(*)	6.056	.000	17.384	43.201

Based on estimated marginal means
* The mean difference is significant at the .05 level.
a Adjustment for multiple comparisons: Least Significant Difference (equivalent to no adjustments).

Multivariate Tests

	Value	F	Hypothesis df	Error df	Sig.	Partial Eta Squared
Pillai's trace	.625	25.020(a)	1.000	15.000	.000	.625
Wilks' lambda	.375	25.020(a)	1.000	15.000	.000	.625
Hotelling's trace	1.668	25.020(a)	1.000	15.000	.000	.625
Roy's largest root	1.668	25.020(a)	1.000	15.000	.000	.625

Each F tests the multivariate effect of thresh. These tests are based on the linearly independent pairwise comparisons among the estimated marginal means.
a Exact statistic

Random

Estimates

Measure: MEASURE_1

random	Mean	Std. Error	95% Confidence Interval	
			Lower Bound	Upper Bound
1	62.110	5.961	49.404	74.815
2	55.395	5.599	43.460	67.330

Pairwise Comparisons

Measure: MEASURE_1

(I) random	(J) random	Mean Difference (I-J)	Std. Error	Sig.(a)	95% Confidence Interval for Difference(a)	
					Lower Bound	Upper Bound
1	2	6.715	5.416	.234	-4.829	18.258
2	1	-6.715	5.416	.234	-18.258	4.829

Based on estimated marginal means
a Adjustment for multiple comparisons: Least Significant Difference (equivalent to no adjustments).

Multivariate Tests

	Value	F	Hypothesis df	Error df	Sig.	Partial Eta Squared
Pillai's trace	.093	1.537(a)	1.000	15.000	.234	.093
Wilks' lambda	.907	1.537(a)	1.000	15.000	.234	.093
Hotelling's trace	.102	1.537(a)	1.000	15.000	.234	.093
Roy's largest root	.102	1.537(a)	1.000	15.000	.234	.093

Each F tests the multivariate effect of random. These tests are based on the linearly independent pairwise comparisons among the estimated marginal means.
a Exact statistic

Image * Thresh

Estimates

Measure: MEASURE_1

image	thresh	Mean	Std. Error	95% Confidence Interval	
				Lower Bound	Upper Bound
1	1	35.855	4.122	27.069	44.641
	2	53.530	7.761	36.989	70.072
2	1	51.357	3.184	44.571	58.144
	2	94.267	10.362	72.182	116.352

Pairwise Comparisons

Measure: MEASURE_1

thresh	(I) image	(J) image	Mean Difference (I-J)	Std. Error	Sig.(a)	95% Confidence Interval for Difference(a)	
						Lower Bound	Upper Bound
1	1	2	-15.502(*)	3.963	.001	-23.950	-7.055
	2	1	15.502(*)	3.963	.001	7.055	23.950
2	1	2	-40.737(*)	9.565	.001	-61.125	-20.349
	2	1	40.737(*)	9.565	.001	20.349	61.125

Based on estimated marginal means
* The mean difference is significant at the .05 level.
a Adjustment for multiple comparisons: Least Significant Difference (equivalent to no adjustments).

Multivariate Tests

thresh		Value	F	Hypothesis df	Error df	Sig.	Partial Eta Squared
1	Pillai's trace	.505	15.299(a)	1.000	15.000	.001	.505
	Wilks' lambda	.495	15.299(a)	1.000	15.000	.001	.505
	Hotelling's trace	1.020	15.299(a)	1.000	15.000	.001	.505
	Roy's largest root	1.020	15.299(a)	1.000	15.000	.001	.505
2	Pillai's trace	.547	18.137(a)	1.000	15.000	.001	.547
	Wilks' lambda	.453	18.137(a)	1.000	15.000	.001	.547
	Hotelling's trace	1.209	18.137(a)	1.000	15.000	.001	.547
	Roy's largest root	1.209	18.137(a)	1.000	15.000	.001	.547

Each F tests the multivariate simple effects of image within each level combination of the other effects shown. These tests are based on the linearly independent pairwise comparisons among the estimated marginal means.
a Exact statistic

Image * Thresh

Pairwise Comparisons

Measure: MEASURE_1

image	(I) thresh	(J) thresh	Mean Difference (I-J)	Std. Error	Sig.(a)	95% Confidence Interval for Difference(a)	
						Lower Bound	Upper Bound
1	1	2	-17.675(*)	6.210	.012	-30.913	-4.438
	2	1	17.675(*)	6.210	.012	4.438	30.913
2	1	2	-42.910(*)	8.866	.000	-61.807	-24.013
	2	1	42.910(*)	8.866	.000	24.013	61.807

Based on estimated marginal means
* The mean difference is significant at the .05 level.
a Adjustment for multiple comparisons: Least Significant Difference (equivalent to no adjustments).

Multivariate Tests

image		Value	F	Hypothesis df	Error df	Sig.	Partial Eta Squared

1	Pillai's trace	.351	8.100(a)	1.000	15.000	.012	.351
	Wilks' lambda	.649	8.100(a)	1.000	15.000	.012	.351
	Hotelling's trace	.540	8.100(a)	1.000	15.000	.012	.351
	Roy's largest root	.540	8.100(a)	1.000	15.000	.012	.351
2	Pillai's trace	.610	23.424(a)	1.000	15.000	.000	.610
	Wilks' lambda	.390	23.424(a)	1.000	15.000	.000	.610
	Hotelling's trace	1.562	23.424(a)	1.000	15.000	.000	.610
	Roy's largest root	1.562	23.424(a)	1.000	15.000	.000	.610

Each F tests the multivariate simple effects of thresh within each level combination of the other effects shown. These tests are based on the linearly independent pairwise comparisons among the estimated marginal means.
a Exact statistic

Image * Random

Estimates

Measure: MEASURE_1

image	random	Mean	Std. Error	95% Confidence Interval	
				Lower Bound	Upper Bound
1	1	45.377	6.863	30.749	60.005
	2	44.009	4.994	33.364	54.653
2	1	78.843	5.975	66.108	91.578
	2	66.782	8.343	48.999	84.565

Pairwise Comparisons

Measure: MEASURE_1

random	(I) image	(J) image	Mean Difference (I-J)	Std. Error	Sig.(a)	95% Confidence Interval for Difference(a)	
						Lower Bound	Upper Bound
1	1	2	-33.466(*)	4.845	.000	-43.792	-23.139
	2	1	33.466(*)	4.845	.000	23.139	43.792
2	1	2	-22.773(*)	7.980	.012	-39.783	-5.763
	2	1	22.773(*)	7.980	.012	5.763	39.783

Based on estimated marginal means
* The mean difference is significant at the .05 level.
a Adjustment for multiple comparisons: Least Significant Difference (equivalent to no adjustments).

Multivariate Tests

random		Value	F	Hypothesis df	Error df	Sig.	Partial Eta Squared
1	Pillai's trace	.761	47.715(a)	1.000	15.000	.000	.761
	Wilks' lambda	.239	47.715(a)	1.000	15.000	.000	.761
	Hotelling's trace	3.181	47.715(a)	1.000	15.000	.000	.761
	Roy's largest root	3.181	47.715(a)	1.000	15.000	.000	.761
2	Pillai's trace	.352	8.143(a)	1.000	15.000	.012	.352
	Wilks' lambda	.648	8.143(a)	1.000	15.000	.012	.352
	Hotelling's trace	.543	8.143(a)	1.000	15.000	.012	.352
	Roy's largest root	.543	8.143(a)	1.000	15.000	.012	.352

Each F tests the multivariate simple effects of image within each level combination of the other effects shown. These tests are based on the linearly independent pairwise comparisons among the estimated marginal means.
a Exact statistic

Thresh * Random

Estimates

Measure: MEASURE_1

thresh	random	Mean	Std. Error	95% Confidence Interval	
				Lower Bound	Upper Bound
1	1	43.815	4.787	33.611	54.019
	2	43.397	3.053	36.890	49.904
2	1	80.405	8.921	61.391	99.418
	2	67.393	9.779	46.550	88.236

Pairwise Comparisons

Measure: MEASURE_1

random	(I) thresh	(J) thresh	Mean Difference (I-J)	Std. Error	Sig.(a)	95% Confidence Interval for Difference(a)	
						Lower Bound	Upper Bound
1	1	2	-36.590(*)	7.928	.000	-53.488	-19.691
	2	1	36.590(*)	7.928	.000	19.691	53.488
2	1	2	-23.996(*)	9.191	.020	-43.587	-4.404
	2	1	23.996(*)	9.191	.020	4.404	43.587

Based on estimated marginal means
* The mean difference is significant at the .05 level.
a Adjustment for multiple comparisons: Least Significant Difference (equivalent to no adjustments).

Multivariate Tests

random		Value	F	Hypothesis df	Error df	Sig.	Partial Eta Squared
1	Pillai's trace	.587	21.300(a)	1.000	15.000	.000	.587
	Wilks' lambda	.413	21.300(a)	1.000	15.000	.000	.587
	Hotelling's trace	1.420	21.300(a)	1.000	15.000	.000	.587
	Roy's largest root	1.420	21.300(a)	1.000	15.000	.000	.587
2	Pillai's trace	.312	6.815(a)	1.000	15.000	.020	.312
	Wilks' lambda	.688	6.815(a)	1.000	15.000	.020	.312
	Hotelling's trace	.454	6.815(a)	1.000	15.000	.020	.312
	Roy's largest root	.454	6.815(a)	1.000	15.000	.020	.312

Each F tests the multivariate simple effects of thresh within each level combination of the other effects shown. These tests are based on the linearly independent pairwise comparisons among the estimated marginal means.
a Exact statistic

Image * Thresh * Random

Estimates

Measure: MEASURE_1

image	thresh	random	Mean	Std. Error	95% Confidence Interval	
					Lower Bound	Upper Bound
1	1	1	34.944	7.103	19.804	50.084
		2	36.766	4.947	26.221	47.311
	2	1	55.810	9.790	34.943	76.677
		2	51.251	9.684	30.609	71.893
2	1	1	52.686	4.617	42.845	62.527
		2	50.029	4.810	39.776	60.282
	2	1	104.999	10.852	81.869	128.129
		2	83.535	13.308	55.169	111.901

Pairwise Comparisons

Measure: MEASURE_1

thresh	random	(I) image	(J) image	Mean Difference (I-J)	Std. Error	Sig.(a)	95% Confidence Interval for Difference(a)	
							Lower Bound	Upper Bound
1	1	1	2	-17.742(*)	7.202	.026	-33.093	-2.391
		2	1	17.742(*)	7.202	.026	2.391	33.093
	2	1	2	-13.263	7.613	.102	-29.488	2.963
		2	1	13.263	7.613	.102	-2.963	29.488
2	1	1	2	-49.189(*)	10.436	.000	-71.433	-26.945
		2	1	49.189(*)	10.436	.000	26.945	71.433
	2	1	2	-32.284(*)	12.620	.022	-59.184	-5.384
		2	1	32.284(*)	12.620	.022	5.384	59.184

Based on estimated marginal means
* The mean difference is significant at the .05 level.
a Adjustment for multiple comparisons: Least Significant Difference (equivalent to no adjustments).

Multivariate Tests

thresh	random		Value	F	Hypothesis df	Error df	Sig.	Partial Eta Squared
1	1	Pillai's trace	.288	6.068(a)	1.000	15.000	.026	.288
		Wilks' lambda	.712	6.068(a)	1.000	15.000	.026	.288
		Hotelling's trace	.405	6.068(a)	1.000	15.000	.026	.288
		Roy's largest root	.405	6.068(a)	1.000	15.000	.026	.288
	2	Pillai's trace	.168	3.035(a)	1.000	15.000	.102	.168
		Wilks' lambda	.832	3.035(a)	1.000	15.000	.102	.168
		Hotelling's trace	.202	3.035(a)	1.000	15.000	.102	.168
		Roy's largest root	.202	3.035(a)	1.000	15.000	.102	.168
2	1	Pillai's trace	.597	22.216(a)	1.000	15.000	.000	.597
		Wilks' lambda	.403	22.216(a)	1.000	15.000	.000	.597
		Hotelling's trace	1.481	22.216(a)	1.000	15.000	.000	.597
		Roy's largest root	1.481	22.216(a)	1.000	15.000	.000	.597
	2	Pillai's trace	.304	6.544(a)	1.000	15.000	.022	.304
		Wilks' lambda	.696	6.544(a)	1.000	15.000	.022	.304
		Hotelling's trace	.436	6.544(a)	1.000	15.000	.022	.304
		Roy's largest root	.436	6.544(a)	1.000	15.000	.022	.304

Each F tests the multivariate simple effects of image within each level combination of the other effects shown. These tests are based on the linearly independent pairwise comparisons among the estimated marginal means.
a Exact statistic

11.2.3. Fixation Numbers

Within-Subjects Factors

Measure: MEASURE_1

image	thresh	random	Dependent Variable
1	1	1	VAR00001
		2	VAR00002
	2	1	VAR00003
		2	VAR00004
2	1	1	VAR00005
		2	VAR00006
	2	1	VAR00007

	2	VAR00008

Multivariate Tests(b)

Effect		Value	F	Hypothesis df	Error df	Sig.	Partial Eta Squared
image	Pillai's Trace	.668	24.114(a)	1.000	12.000	.000	.668
	Wilks' Lambda	.332	24.114(a)	1.000	12.000	.000	.668
	Hotelling's Trace	2.010	24.114(a)	1.000	12.000	.000	.668
	Roy's Largest Root	2.010	24.114(a)	1.000	12.000	.000	.668
thresh	Pillai's Trace	.573	16.088(a)	1.000	12.000	.002	.573
	Wilks' Lambda	.427	16.088(a)	1.000	12.000	.002	.573
	Hotelling's Trace	1.341	16.088(a)	1.000	12.000	.002	.573
	Roy's Largest Root	1.341	16.088(a)	1.000	12.000	.002	.573
random	Pillai's Trace	.060	.765(a)	1.000	12.000	.399	.060
	Wilks' Lambda	.940	.765(a)	1.000	12.000	.399	.060
	Hotelling's Trace	.064	.765(a)	1.000	12.000	.399	.060
	Roy's Largest Root	.064	.765(a)	1.000	12.000	.399	.060
image * thresh	Pillai's Trace	.327	5.842(a)	1.000	12.000	.032	.327
	Wilks' Lambda	.673	5.842(a)	1.000	12.000	.032	.327
	Hotelling's Trace	.487	5.842(a)	1.000	12.000	.032	.327
	Roy's Largest Root	.487	5.842(a)	1.000	12.000	.032	.327
image * random	Pillai's Trace	.115	1.561(a)	1.000	12.000	.235	.115
	Wilks' Lambda	.885	1.561(a)	1.000	12.000	.235	.115
	Hotelling's Trace	.130	1.561(a)	1.000	12.000	.235	.115
	Roy's Largest Root	.130	1.561(a)	1.000	12.000	.235	.115
thresh * random	Pillai's Trace	.103	1.378(a)	1.000	12.000	.263	.103
	Wilks' Lambda	.897	1.378(a)	1.000	12.000	.263	.103
	Hotelling's Trace	.115	1.378(a)	1.000	12.000	.263	.103
	Roy's Largest Root	.115	1.378(a)	1.000	12.000	.263	.103
image * thresh * random	Pillai's Trace	.022	.274(a)	1.000	12.000	.610	.022
	Wilks' Lambda	.978	.274(a)	1.000	12.000	.610	.022
	Hotelling's Trace	.023	.274(a)	1.000	12.000	.610	.022
	Roy's Largest Root	.023	.274(a)	1.000	12.000	.610	.022

a Exact statistic
b Design: Intercept
Within Subjects Design:
image+thresh+random+image*thresh+image*random+thresh*random+image*thresh*random

Tests of Within-Subjects Effects

Measure: MEASURE_1

Source		Type III Sum of Squares	df	Mean Square	F	Sig.	Partial Eta Squared
image	Sphericity Assumed	281736.240	1	281736.240	24.114	.000	.668
	Greenhouse-Geisser	281736.240	1.000	281736.240	24.114	.000	.668
	Huynh-Feldt	281736.240	1.000	281736.240	24.114	.000	.668
	Lower-bound	281736.240	1.000	281736.240	24.114	.000	.668
Error(image)	Sphericity Assumed	140201.385	12	11683.449			
	Greenhouse-Geisser	140201.385	12.000	11683.449			
	Huynh-Feldt	140201.385	12.000	11683.449			

	Lower-bound	140201.385	12.000	11683.449			
thresh	Sphericity Assumed	183876.240	1	183876.240	16.088	.002	.573
	Greenhouse-Geisser	183876.240	1.000	183876.240	16.088	.002	.573
	Huynh-Feldt	183876.240	1.000	183876.240	16.088	.002	.573
	Lower-bound	183876.240	1.000	183876.240	16.088	.002	.573
Error(thresh)	Sphericity Assumed	137153.385	12	11429.449			
	Greenhouse-Geisser	137153.385	12.000	11429.449			
	Huynh-Feldt	137153.385	12.000	11429.449			
	Lower-bound	137153.385	12.000	11429.449			
random	Sphericity Assumed	8370.087	1	8370.087	.765	.399	.060
	Greenhouse-Geisser	8370.087	1.000	8370.087	.765	.399	.060
	Huynh-Feldt	8370.087	1.000	8370.087	.765	.399	.060
	Lower-bound	8370.087	1.000	8370.087	.765	.399	.060
Error(random)	Sphericity Assumed	131315.038	12	10942.920			
	Greenhouse-Geisser	131315.038	12.000	10942.920			
	Huynh-Feldt	131315.038	12.000	10942.920			
	Lower-bound	131315.038	12.000	10942.920			
image * thresh	Sphericity Assumed	45403.163	1	45403.163	5.842	.032	.327
	Greenhouse-Geisser	45403.163	1.000	45403.163	5.842	.032	.327
	Huynh-Feldt	45403.163	1.000	45403.163	5.842	.032	.327
	Lower-bound	45403.163	1.000	45403.163	5.842	.032	.327
Error(image*thresh)	Sphericity Assumed	93255.462	12	7771.288			
	Greenhouse-Geisser	93255.462	12.000	7771.288			
	Huynh-Feldt	93255.462	12.000	7771.288			
	Lower-bound	93255.462	12.000	7771.288			
image * random	Sphericity Assumed	7062.010	1	7062.010	1.561	.235	.115
	Greenhouse-Geisser	7062.010	1.000	7062.010	1.561	.235	.115
	Huynh-Feldt	7062.010	1.000	7062.010	1.561	.235	.115
	Lower-bound	7062.010	1.000	7062.010	1.561	.235	.115
Error(image*random)	Sphericity Assumed	54291.115	12	4524.260			
	Greenhouse-Geisser	54291.115	12.000	4524.260			
	Huynh-Feldt	54291.115	12.000	4524.260			
	Lower-bound	54291.115	12.000	4524.260			
thresh * random	Sphericity Assumed	14241.240	1	14241.240	1.378	.263	.103
	Greenhouse-Geisser	14241.240	1.000	14241.240	1.378	.263	.103
	Huynh-Feldt	14241.240	1.000	14241.240	1.378	.263	.103
	Lower-bound	14241.240	1.000	14241.240	1.378	.263	.103
Error(thresh*random)	Sphericity Assumed	124001.885	12	10333.490			
	Greenhouse-Geisser	124001.885	12.000	10333.490			

	Huynh-Feldt	124001.885	12.000	10333.490			
	Lower-bound	124001.885	12.000	10333.490			
image * thresh * random	Sphericity Assumed	3427.010	1	3427.010	.274	.610	.022
	Greenhouse-Geisser	3427.010	1.000	3427.010	.274	.610	.022
	Huynh-Feldt	3427.010	1.000	3427.010	.274	.610	.022
	Lower-bound	3427.010	1.000	3427.010	.274	.610	.022
Error(image*thresh*random)	Sphericity Assumed	150181.115	12	12515.093			
	Greenhouse-Geisser	150181.115	12.000	12515.093			
	Huynh-Feldt	150181.115	12.000	12515.093			
	Lower-bound	150181.115	12.000	12515.093			

Tests of Within-Subjects Contrasts

Measure: MEASURE_1

Source	image	thresh	random	Type III Sum of Squares	df	Mean Square	F	Sig.	Partial Eta Squared
image	Linear			281736.240	1	281736.240	24.114	.000	.668
Error(image)	Linear			140201.385	12	11683.449			
thresh		Linear		183876.240	1	183876.240	16.088	.002	.573
Error(thresh)		Linear		137153.385	12	11429.449			
random			Linear	8370.087	1	8370.087	.765	.399	.060
Error(random)			Linear	131315.038	12	10942.920			
image * thresh	Linear	Linear		45403.163	1	45403.163	5.842	.032	.327
Error(image*thresh)	Linear	Linear		93255.462	12	7771.288			
image * random	Linear		Linear	7062.010	1	7062.010	1.561	.235	.115
Error(image*random)	Linear		Linear	54291.115	12	4524.260			
thresh * random		Linear	Linear	14241.240	1	14241.240	1.378	.263	.103
Error(thresh*random)		Linear	Linear	124001.885	12	10333.490			
image * thresh * random	Linear	Linear	Linear	3427.010	1	3427.010	.274	.610	.022
Error(image*thresh*random)	Linear	Linear	Linear	150181.115	12	12515.093			

Tests of Between-Subjects Effects

Measure: MEASURE_1
Transformed Variable: Average

Source	Type III Sum of Squares	df	Mean Square	F	Sig.	Partial Eta Squared
Intercept	3265654.240	1	3265654.240	102.267	.000	.895
Error	383191.385	12	31932.615			

Estimated Marginal Means

Image

Estimates

Measure: MEASURE_1

image	Mean	Std. Error	95% Confidence Interval	
			Lower Bound	Upper Bound
1	125.154	17.764	86.449	163.859
2	229.250	22.874	179.413	279.087

Pairwise Comparisons

Measure: MEASURE_1

(I) image	(J) image	Mean Difference (I-J)	Std. Error	Sig.(a)	95% Confidence Interval for Difference(a)

					Lower Bound	Upper Bound
1	2	-104.096(*)	21.198	.000	-150.283	-57.909
2	1	104.096(*)	21.198	.000	57.909	150.283

Based on estimated marginal means
* The mean difference is significant at the .05 level.
a Adjustment for multiple comparisons: Least Significant Difference (equivalent to no adjustments).

Multivariate Tests

	Value	F	Hypothesis df	Error df	Sig.	Partial Eta Squared
Pillai's trace	.668	24.114(a)	1.000	12.000	.000	.668
Wilks' lambda	.332	24.114(a)	1.000	12.000	.000	.668
Hotelling's trace	2.010	24.114(a)	1.000	12.000	.000	.668
Roy's largest root	2.010	24.114(a)	1.000	12.000	.000	.668

Each F tests the multivariate effect of image. These tests are based on the linearly independent pairwise comparisons among the estimated marginal means.
a Exact statistic

Thresh

Estimates

Measure: MEASURE_1

			95% Confidence Interval	
thresh	Mean	Std. Error	Lower Bound	Upper Bound
1	135.154	10.838	111.540	158.768
2	219.250	26.766	160.932	277.568

Pairwise Comparisons

Measure: MEASURE_1

					95% Confidence Interval for Difference(a)	
(I) thresh	(J) thresh	Mean Difference (I-J)	Std. Error	Sig.(a)	Lower Bound	Upper Bound
1	2	-84.096(*)	20.967	.002	-129.778	-38.414
2	1	84.096(*)	20.967	.002	38.414	129.778

Based on estimated marginal means
* The mean difference is significant at the .05 level.
a Adjustment for multiple comparisons: Least Significant Difference (equivalent to no adjustments).

Multivariate Tests

	Value	F	Hypothesis df	Error df	Sig.	Partial Eta Squared
Pillai's trace	.573	16.088(a)	1.000	12.000	.002	.573
Wilks' lambda	.427	16.088(a)	1.000	12.000	.002	.573
Hotelling's trace	1.341	16.088(a)	1.000	12.000	.002	.573
Roy's largest root	1.341	16.088(a)	1.000	12.000	.002	.573

Each F tests the multivariate effect of thresh. These tests are based on the linearly independent pairwise comparisons among the estimated marginal means.
a Exact statistic

Random

Estimates

Measure: MEASURE_1

random	Mean	Std. Error	95% Confidence Interval

			Lower Bound	Upper Bound
1	186.173	20.890	140.657	231.689
2	168.231	19.701	125.306	211.155

Pairwise Comparisons

Measure: MEASURE_1

					95% Confidence Interval for Difference(a)	
(I) random	(J) random	Mean Difference (I-J)	Std. Error	Sig.(a)	Lower Bound	Upper Bound
1	2	17.942	20.515	.399	-26.757	62.642
2	1	-17.942	20.515	.399	-62.642	26.757

Based on estimated marginal means
a Adjustment for multiple comparisons: Least Significant Difference (equivalent to no adjustments).

Multivariate Tests

	Value	F	Hypothesis df	Error df	Sig.	Partial Eta Squared
Pillai's trace	.060	.765(a)	1.000	12.000	.399	.060
Wilks' lambda	.940	.765(a)	1.000	12.000	.399	.060
Hotelling's trace	.064	.765(a)	1.000	12.000	.399	.060
Roy's largest root	.064	.765(a)	1.000	12.000	.399	.060

Each F tests the multivariate effect of random. These tests are based on the linearly independent pairwise comparisons among the estimated marginal means.
a Exact statistic

Image * Thresh

Estimates

Measure: MEASURE_1

				95% Confidence Interval	
image	thresh	Mean	Std. Error	Lower Bound	Upper Bound
1	1	104.000	13.930	73.650	134.350
	2	146.308	26.228	89.162	203.453
2	1	166.308	13.284	137.364	195.251
	2	292.192	36.846	211.912	372.473

Pairwise Comparisons

Measure: MEASURE_1

						95% Confidence Interval for Difference(a)	
thresh	(I) image	(J) image	Mean Difference (I-J)	Std. Error	Sig.(a)	Lower Bound	Upper Bound
1	1	2	-62.308(*)	16.467	.003	-98.186	-26.430
	2	1	62.308(*)	16.467	.003	26.430	98.186
2	1	2	-145.885(*)	35.005	.001	-222.154	-69.615
	2	1	145.885(*)	35.005	.001	69.615	222.154

Based on estimated marginal means
* The mean difference is significant at the .05 level.
a Adjustment for multiple comparisons: Least Significant Difference (equivalent to no adjustments).

Multivariate Tests

thresh		Value	F	Hypothesis df	Error df	Sig.	Partial Eta Squared
1	Pillai's trace	.544	14.318(a)	1.000	12.000	.003	.544

	Wilks' lambda	.456	14.318(a)	1.000	12.000	.003	.544
	Hotelling's trace	1.193	14.318(a)	1.000	12.000	.003	.544
	Roy's largest root	1.193	14.318(a)	1.000	12.000	.003	.544
2	Pillai's trace	.591	17.368(a)	1.000	12.000	.001	.591
	Wilks' lambda	.409	17.368(a)	1.000	12.000	.001	.591
	Hotelling's trace	1.447	17.368(a)	1.000	12.000	.001	.591
	Roy's largest root	1.447	17.368(a)	1.000	12.000	.001	.591

Each F tests the multivariate simple effects of image within each level combination of the other effects shown. These tests are based on the linearly independent pairwise comparisons among the estimated marginal means.
a Exact statistic

Image * Thresh

Pairwise Comparisons

Measure: MEASURE_1

image	(I) thresh	(J) thresh	Mean Difference (I-J)	Std. Error	Sig.(a)	95% Confidence Interval for Difference(a)	
						Lower Bound	Upper Bound
1	1	2	-42.308	22.397	.083	-91.106	6.490
	2	1	42.308	22.397	.083	-6.490	91.106
2	1	2	-125.885(*)	31.231	.002	-193.931	-57.838
	2	1	125.885(*)	31.231	.002	57.838	193.931

Based on estimated marginal means
* The mean difference is significant at the .05 level.
a Adjustment for multiple comparisons: Least Significant Difference (equivalent to no adjustments).

Multivariate Tests

image		Value	F	Hypothesis df	Error df	Sig.	Partial Eta Squared
1	Pillai's trace	.229	3.568(a)	1.000	12.000	.083	.229
	Wilks' lambda	.771	3.568(a)	1.000	12.000	.083	.229
	Hotelling's trace	.297	3.568(a)	1.000	12.000	.083	.229
	Roy's largest root	.297	3.568(a)	1.000	12.000	.083	.229
2	Pillai's trace	.575	16.247(a)	1.000	12.000	.002	.575
	Wilks' lambda	.425	16.247(a)	1.000	12.000	.002	.575
	Hotelling's trace	1.354	16.247(a)	1.000	12.000	.002	.575
	Roy's largest root	1.354	16.247(a)	1.000	12.000	.002	.575

Each F tests the multivariate simple effects of thresh within each level combination of the other effects shown. These tests are based on the linearly independent pairwise comparisons among the estimated marginal means.
a Exact statistic

Image * Random

Estimates

Measure: MEASURE_1

image	random	Mean	Std. Error	95% Confidence Interval	
				Lower Bound	Upper Bound
1	1	125.885	24.029	73.529	178.240
	2	124.423	15.746	90.115	158.731
2	1	246.462	21.198	200.275	292.648
	2	212.038	31.587	143.217	280.860

Pairwise Comparisons

Measure: MEASURE_1

random	(I) image	(J) image	Mean Difference (I-J)	Std. Error	Sig.(a)	95% Confidence Interval for Difference(a)	
						Lower Bound	Upper Bound
1	1	2	-120.577(*)	17.548	.000	-158.811	-82.343
	2	1	120.577(*)	17.548	.000	82.343	158.811
2	1	2	-87.615(*)	30.640	.014	-154.374	-20.856
	2	1	87.615(*)	30.640	.014	20.856	154.374

Based on estimated marginal means
* The mean difference is significant at the .05 level.
a Adjustment for multiple comparisons: Least Significant Difference (equivalent to no adjustments).

Multivariate Tests

random		Value	F	Hypothesis df	Error df	Sig.	Partial Eta Squared
1	Pillai's trace	.797	47.214(a)	1.000	12.000	.000	.797
	Wilks' lambda	.203	47.214(a)	1.000	12.000	.000	.797
	Hotelling's trace	3.934	47.214(a)	1.000	12.000	.000	.797
	Roy's largest root	3.934	47.214(a)	1.000	12.000	.000	.797
2	Pillai's trace	.405	8.177(a)	1.000	12.000	.014	.405
	Wilks' lambda	.595	8.177(a)	1.000	12.000	.014	.405
	Hotelling's trace	.681	8.177(a)	1.000	12.000	.014	.405
	Roy's largest root	.681	8.177(a)	1.000	12.000	.014	.405

Each F tests the multivariate simple effects of image within each level combination of the other effects shown. These tests are based on the linearly independent pairwise comparisons among the estimated marginal means.
a Exact statistic

Thresh * Random

Estimates

Measure: MEASURE_1

thresh	random	Mean	Std. Error	95% Confidence Interval	
				Lower Bound	Upper Bound
1	1	132.423	16.198	97.131	167.715
	2	137.885	12.175	111.358	164.411
2	1	239.923	31.335	171.650	308.196
	2	198.577	33.070	126.523	270.631

Pairwise Comparisons

Measure: MEASURE_1

random	(I) thresh	(J) thresh	Mean Difference (I-J)	Std. Error	Sig.(a)	95% Confidence Interval for Difference(a)	
						Lower Bound	Upper Bound
1	1	2	-107.500(*)	27.255	.002	-166.885	-48.115
	2	1	107.500(*)	27.255	.002	48.115	166.885
2	1	2	-60.692	30.516	.070	-127.180	5.796
	2	1	60.692	30.516	.070	-5.796	127.180

Based on estimated marginal means
* The mean difference is significant at the .05 level.
a Adjustment for multiple comparisons: Least Significant Difference (equivalent to no adjustments).

Multivariate Tests

random		Value	F	Hypothesis df	Error df	Sig.	Partial Eta Squared

1	Pillai's trace	.565	15.556(a)	1.000	12.000	.002	.565
	Wilks' lambda	.435	15.556(a)	1.000	12.000	.002	.565
	Hotelling's trace	1.296	15.556(a)	1.000	12.000	.002	.565
	Roy's largest root	1.296	15.556(a)	1.000	12.000	.002	.565
2	Pillai's trace	.248	3.956(a)	1.000	12.000	.070	.248
	Wilks' lambda	.752	3.956(a)	1.000	12.000	.070	.248
	Hotelling's trace	.330	3.956(a)	1.000	12.000	.070	.248
	Roy's largest root	.330	3.956(a)	1.000	12.000	.070	.248

Each F tests the multivariate simple effects of thresh within each level combination of the other effects shown. These tests are based on the linearly independent pairwise comparisons among the estimated marginal means.
a Exact statistic

Image * Thresh * Random

Estimates

Measure: MEASURE_1

image	thresh	random	Mean	Std. Error	95% Confidence Interval	
					Lower Bound	Upper Bound
1	1	1	98.769	23.965	46.553	150.985
		2	109.231	18.002	70.008	148.453
	2	1	153.000	34.033	78.848	227.152
		2	139.615	32.497	68.811	210.420
2	1	1	166.077	18.777	125.166	206.988
		2	166.538	21.906	118.808	214.269
	2	1	326.846	38.461	243.046	410.646
		2	257.538	48.528	151.804	363.273

Pairwise Comparisons

Measure: MEASURE_1

thresh	random	(I) image	(J) image	Mean Difference (I-J)	Std. Error	Sig.(a)	95% Confidence Interval for Difference(a)	
							Lower Bound	Upper Bound
1	1	1	2	-67.308(*)	28.361	.035	-129.101	-5.514
		2	1	67.308(*)	28.361	.035	5.514	129.101
	2	1	2	-57.308	31.860	.097	-126.724	12.108
		2	1	57.308	31.860	.097	-12.108	126.724
2	1	1	2	-173.846(*)	36.709	.000	-253.829	-93.863
		2	1	173.846(*)	36.709	.000	93.863	253.829
	2	1	2	-117.923(*)	49.472	.035	-225.714	-10.132
		2	1	117.923(*)	49.472	.035	10.132	225.714

Based on estimated marginal means
* The mean difference is significant at the .05 level.
a Adjustment for multiple comparisons: Least Significant Difference (equivalent to no adjustments).

Multivariate Tests

thresh	random		Value	F	Hypothesis df	Error df	Sig.	Partial Eta Squared
1	1	Pillai's trace	.319	5.632(a)	1.000	12.000	.035	.319
		Wilks' lambda	.681	5.632(a)	1.000	12.000	.035	.319
		Hotelling's trace	.469	5.632(a)	1.000	12.000	.035	.319
		Roy's largest root	.469	5.632(a)	1.000	12.000	.035	.319
	2	Pillai's trace	.212	3.236(a)	1.000	12.000	.097	.212
		Wilks' lambda	.788	3.236(a)	1.000	12.000	.097	.212

		Hotelling's trace	.270	3.236(a)	1.000	12.000	.097	.212
		Roy's largest root	.270	3.236(a)	1.000	12.000	.097	.212
2	1	Pillai's trace	.651	22.427(a)	1.000	12.000	.000	.651
		Wilks' lambda	.349	22.427(a)	1.000	12.000	.000	.651
		Hotelling's trace	1.869	22.427(a)	1.000	12.000	.000	.651
		Roy's largest root	1.869	22.427(a)	1.000	12.000	.000	.651
	2	Pillai's trace	.321	5.682(a)	1.000	12.000	.035	.321
		Wilks' lambda	.679	5.682(a)	1.000	12.000	.035	.321
		Hotelling's trace	.473	5.682(a)	1.000	12.000	.035	.321
		Roy's largest root	.473	5.682(a)	1.000	12.000	.035	.321

Each F tests the multivariate simple effects of image within each level combination of the other effects shown. These tests are based on the linearly independent pairwise comparisons among the estimated marginal means.
a Exact statistic

Image * Thresh * Random

Pairwise Comparisons

Measure: MEASURE_1

image	random	(I) thresh	(J) thresh	Mean Difference (I-J)	Std. Error	Sig.(a)	95% Confidence Interval for Difference(a)	
							Lower Bound	Upper Bound
1	1	1	2	-54.231	33.993	.137	-128.296	19.834
		2	1	54.231	33.993	.137	-19.834	128.296
	2	1	2	-30.385	42.053	.484	-122.009	61.240
		2	1	30.385	42.053	.484	-61.240	122.009
2	1	1	2	-160.769(*)	43.200	.003	-254.894	-66.645
		2	1	160.769(*)	43.200	.003	66.645	254.894
	2	1	2	-91.000(*)	40.975	.046	-180.276	-1.724
		2	1	91.000(*)	40.975	.046	1.724	180.276

Based on estimated marginal means
* The mean difference is significant at the .05 level.
a Adjustment for multiple comparisons: Least Significant Difference (equivalent to no adjustments).

Multivariate Tests

image	random		Value	F	Hypothesis df	Error df	Sig.	Partial Eta Squared
1	1	Pillai's trace	.175	2.545(a)	1.000	12.000	.137	.175
		Wilks' lambda	.825	2.545(a)	1.000	12.000	.137	.175
		Hotelling's trace	.212	2.545(a)	1.000	12.000	.137	.175
		Roy's largest root	.212	2.545(a)	1.000	12.000	.137	.175
	2	Pillai's trace	.042	.522(a)	1.000	12.000	.484	.042
		Wilks' lambda	.958	.522(a)	1.000	12.000	.484	.042
		Hotelling's trace	.044	.522(a)	1.000	12.000	.484	.042
		Roy's largest root	.044	.522(a)	1.000	12.000	.484	.042

Each F tests the multivariate simple effects of thresh within each level combination of the other effects shown. These tests are based on the linearly independent pairwise comparisons among the estimated marginal means.
a Exact statistic

11.2.4. Eye and Random Comparison

Within-Subjects Factors

Measure	image	random	Dependent Variable
t400	1	1	VAR00011

		2	VAR00012
	2	1	VAR00013
		2	VAR00014
t800	1	1	VAR00015
		2	VAR00016
	2	1	VAR00017
		2	VAR00018

Between-Subjects Factors

		N
Mode	Eye	13
	Random	13

Multivariate Tests(b)

Effect			Value	F	Hypothesis df	Error df	Sig.	Partial Eta Squared
Between Subjects	Intercept	Pillai's Trace	.977	498.081(a)	2.000	23.000	.000	.977
		Wilks' Lambda	.023	498.081(a)	2.000	23.000	.000	.977
		Hotelling's Trace	43.311	498.081(a)	2.000	23.000	.000	.977
		Roy's Largest Root	43.311	498.081(a)	2.000	23.000	.000	.977
	Mode	Pillai's Trace	.249	3.813(a)	2.000	23.000	.037	.249
		Wilks' Lambda	.751	3.813(a)	2.000	23.000	.037	.249
		Hotelling's Trace	.332	3.813(a)	2.000	23.000	.037	.249
		Roy's Largest Root	.332	3.813(a)	2.000	23.000	.037	.249
Within Subjects	image	Pillai's Trace	.716	28.945(a)	2.000	23.000	.000	.716
		Wilks' Lambda	.284	28.945(a)	2.000	23.000	.000	.716
		Hotelling's Trace	2.517	28.945(a)	2.000	23.000	.000	.716
		Roy's Largest Root	2.517	28.945(a)	2.000	23.000	.000	.716
	image * Mode	Pillai's Trace	.007	.076(a)	2.000	23.000	.927	.007
		Wilks' Lambda	.993	.076(a)	2.000	23.000	.927	.007
		Hotelling's Trace	.007	.076(a)	2.000	23.000	.927	.007
		Roy's Largest Root	.007	.076(a)	2.000	23.000	.927	.007
	random	Pillai's Trace	.069	.847(a)	2.000	23.000	.442	.069
		Wilks' Lambda	.931	.847(a)	2.000	23.000	.442	.069
		Hotelling's Trace	.074	.847(a)	2.000	23.000	.442	.069
		Roy's Largest Root	.074	.847(a)	2.000	23.000	.442	.069
	random * Mode	Pillai's Trace	.107	1.372(a)	2.000	23.000	.274	.107
		Wilks' Lambda	.893	1.372(a)	2.000	23.000	.274	.107
		Hotelling's Trace	.119	1.372(a)	2.000	23.000	.274	.107
		Roy's Largest Root	.119	1.372(a)	2.000	23.000	.274	.107
	image * random	Pillai's Trace	.004	.044(a)	2.000	23.000	.957	.004
		Wilks' Lambda	.996	.044(a)	2.000	23.000	.957	.004
		Hotelling's Trace	.004	.044(a)	2.000	23.000	.957	.004
		Roy's Largest Root	.004	.044(a)	2.000	23.000	.957	.004
	image * random * Mode	Pillai's Trace	.080	1.004(a)	2.000	23.000	.382	.080
		Wilks' Lambda	.920	1.004(a)	2.000	23.000	.382	.080
		Hotelling's Trace	.087	1.004(a)	2.000	23.000	.382	.080
		Roy's Largest Root	.087	1.004(a)	2.000	23.000	.382	.080

a Exact statistic
b Design: Intercept+Mode
Within Subjects Design: image+random+image*random

Tests of Within-Subjects Effects

Multivariate(b,c)

Within Subjects Effect		Value	F	Hypothesis df	Error df	Sig.	Partial Eta Squared
image	Pillai's Trace	.716	28.945(a)	2.000	23.000	.000	.716
	Wilks' Lambda	.284	28.945(a)	2.000	23.000	.000	.716
	Hotelling's Trace	2.517	28.945(a)	2.000	23.000	.000	.716
	Roy's Largest Root	2.517	28.945(a)	2.000	23.000	.000	.716
image * Mode	Pillai's Trace	.007	.076(a)	2.000	23.000	.927	.007
	Wilks' Lambda	.993	.076(a)	2.000	23.000	.927	.007
	Hotelling's Trace	.007	.076(a)	2.000	23.000	.927	.007
	Roy's Largest Root	.007	.076(a)	2.000	23.000	.927	.007
random	Pillai's Trace	.069	.847(a)	2.000	23.000	.442	.069
	Wilks' Lambda	.931	.847(a)	2.000	23.000	.442	.069
	Hotelling's Trace	.074	.847(a)	2.000	23.000	.442	.069
	Roy's Largest Root	.074	.847(a)	2.000	23.000	.442	.069
random * Mode	Pillai's Trace	.107	1.372(a)	2.000	23.000	.274	.107
	Wilks' Lambda	.893	1.372(a)	2.000	23.000	.274	.107
	Hotelling's Trace	.119	1.372(a)	2.000	23.000	.274	.107
	Roy's Largest Root	.119	1.372(a)	2.000	23.000	.274	.107
image * random	Pillai's Trace	.004	.044(a)	2.000	23.000	.957	.004
	Wilks' Lambda	.996	.044(a)	2.000	23.000	.957	.004
	Hotelling's Trace	.004	.044(a)	2.000	23.000	.957	.004
	Roy's Largest Root	.004	.044(a)	2.000	23.000	.957	.004
image * random * Mode	Pillai's Trace	.080	1.004(a)	2.000	23.000	.382	.080
	Wilks' Lambda	.920	1.004(a)	2.000	23.000	.382	.080
	Hotelling's Trace	.087	1.004(a)	2.000	23.000	.382	.080
	Roy's Largest Root	.087	1.004(a)	2.000	23.000	.382	.080

a Exact statistic
b Design: Intercept+Mode
Within Subjects Design: image+random+image*random
c Tests are based on averaged variables.

Univariate Tests

Source	Measure		Type III Sum of Squares	df	Mean Square	F	Sig.	Partial Eta Squared
image	t400	Sphericity Assumed	1098.500	1	1098.500	30.744	.000	.562
		Greenhouse-Geisser	1098.500	1.000	1098.500	30.744	.000	.562
		Huynh-Feldt	1098.500	1.000	1098.500	30.744	.000	.562
		Lower-bound	1098.500	1.000	1098.500	30.744	.000	.562
	t800	Sphericity Assumed	1895.538	1	1895.538	35.419	.000	.596
		Greenhouse-Geisser	1895.538	1.000	1895.538	35.419	.000	.596
		Huynh-Feldt	1895.538	1.000	1895.538	35.419	.000	.596
		Lower-bound	1895.538	1.000	1895.538	35.419	.000	.596
image * Mode	t400	Sphericity Assumed	2.462	1	2.462	.069	.795	.003

		Greenhouse-Geisser	2.462	1.000	2.462	.069	.795	.003
		Huynh-Feldt	2.462	1.000	2.462	.069	.795	.003
		Lower-bound	2.462	1.000	2.462	.069	.795	.003
	t800	Sphericity Assumed	5.538	1	5.538	.103	.750	.004
		Greenhouse-Geisser	5.538	1.000	5.538	.103	.750	.004
		Huynh-Feldt	5.538	1.000	5.538	.103	.750	.004
		Lower-bound	5.538	1.000	5.538	.103	.750	.004
Error(image)	t400	Sphericity Assumed	857.538	24	35.731			
		Greenhouse-Geisser	857.538	24.000	35.731			
		Huynh-Feldt	857.538	24.000	35.731			
		Lower-bound	857.538	24.000	35.731			
	t800	Sphericity Assumed	1284.423	24	53.518			
		Greenhouse-Geisser	1284.423	24.000	53.518			
		Huynh-Feldt	1284.423	24.000	53.518			
		Lower-bound	1284.423	24.000	53.518			
random	t400	Sphericity Assumed	.962	1	.962	.015	.903	.001
		Greenhouse-Geisser	.962	1.000	.962	.015	.903	.001
		Huynh-Feldt	.962	1.000	.962	.015	.903	.001
		Lower-bound	.962	1.000	.962	.015	.903	.001
	t800	Sphericity Assumed	167.538	1	167.538	1.746	.199	.068
		Greenhouse-Geisser	167.538	1.000	167.538	1.746	.199	.068
		Huynh-Feldt	167.538	1.000	167.538	1.746	.199	.068
		Lower-bound	167.538	1.000	167.538	1.746	.199	.068
random * Mode	t400	Sphericity Assumed	120.615	1	120.615	1.901	.181	.073
		Greenhouse-Geisser	120.615	1.000	120.615	1.901	.181	.073
		Huynh-Feldt	120.615	1.000	120.615	1.901	.181	.073
		Lower-bound	120.615	1.000	120.615	1.901	.181	.073
	t800	Sphericity Assumed	44.462	1	44.462	.463	.503	.019
		Greenhouse-Geisser	44.462	1.000	44.462	.463	.503	.019
		Huynh-Feldt	44.462	1.000	44.462	.463	.503	.019
		Lower-bound	44.462	1.000	44.462	.463	.503	.019
Error(random)	t400	Sphericity Assumed	1522.923	24	63.455			
		Greenhouse-Geisser	1522.923	24.000	63.455			
		Huynh-Feldt	1522.923	24.000	63.455			
		Lower-bound	1522.923	24.000	63.455			
	t800	Sphericity Assumed	2303.500	24	95.979			
		Greenhouse-Geisser	2303.500	24.000	95.979			
		Huynh-Feldt	2303.500	24.000	95.979			
		Lower-bound	2303.500	24.000	95.979			

image * random	t400	Sphericity Assumed	4.654	1	4.654	.079	.781	.003
		Greenhouse-Geisser	4.654	1.000	4.654	.079	.781	.003
		Huynh-Feldt	4.654	1.000	4.654	.079	.781	.003
		Lower-bound	4.654	1.000	4.654	.079	.781	.003
	t800	Sphericity Assumed	1.385	1	1.385	.019	.891	.001
		Greenhouse-Geisser	1.385	1.000	1.385	.019	.891	.001
		Huynh-Feldt	1.385	1.000	1.385	.019	.891	.001
		Lower-bound	1.385	1.000	1.385	.019	.891	.001
image * random * Mode	t400	Sphericity Assumed	96.154	1	96.154	1.631	.214	.064
		Greenhouse-Geisser	96.154	1.000	96.154	1.631	.214	.064
		Huynh-Feldt	96.154	1.000	96.154	1.631	.214	.064
		Lower-bound	96.154	1.000	96.154	1.631	.214	.064
	t800	Sphericity Assumed	44.462	1	44.462	.620	.439	.025
		Greenhouse-Geisser	44.462	1.000	44.462	.620	.439	.025
		Huynh-Feldt	44.462	1.000	44.462	.620	.439	.025
		Lower-bound	44.462	1.000	44.462	.620	.439	.025
Error(image*random)	t400	Sphericity Assumed	1414.692	24	58.946			
		Greenhouse-Geisser	1414.692	24.000	58.946			
		Huynh-Feldt	1414.692	24.000	58.946			
		Lower-bound	1414.692	24.000	58.946			
	t800	Sphericity Assumed	1721.654	24	71.736			
		Greenhouse-Geisser	1721.654	24.000	71.736			
		Huynh-Feldt	1721.654	24.000	71.736			
		Lower-bound	1721.654	24.000	71.736			

Tests of Within-Subjects Contrasts

Source	Measure	image	random	Type III Sum of Squares	df	Mean Square	F	Sig.	Partial Eta Squared
image	t400	Linear		1098.500	1	1098.500	30.744	.000	.562
	t800	Linear		1895.538	1	1895.538	35.419	.000	.596
image * Mode	t400	Linear		2.462	1	2.462	.069	.795	.003
	t800	Linear		5.538	1	5.538	.103	.750	.004
Error(image)	t400	Linear		857.538	24	35.731			
	t800	Linear		1284.423	24	53.518			
random	t400		Linear	.962	1	.962	.015	.903	.001
	t800		Linear	167.538	1	167.538	1.746	.199	.068
random * Mode	t400		Linear	120.615	1	120.615	1.901	.181	.073
	t800		Linear	44.462	1	44.462	.463	.503	.019
Error(random)	t400		Linear	1522.923	24	63.455			
	t800		Linear	2303.500	24	95.979			
image * random	t400	Linear	Linear	4.654	1	4.654	.079	.781	.003
	t800	Linear	Linear	1.385	1	1.385	.019	.891	.001
image * random * Mode	t400	Linear	Linear	96.154	1	96.154	1.631	.214	.064
	t800	Linear	Linear	44.462	1	44.462	.620	.439	.025
Error(image*random)	t400	Linear	Linear	1414.692	24	58.946			
	t800	Linear	Linear	1721.654	24	71.736			

Tests of Between-Subjects Effects

Transformed Variable: Average

Source	Measure	Type III Sum of Squares	df	Mean Square	F	Sig.	Partial Eta Squared
Intercept	t400	46453.885	1	46453.885	739.281	.000	.969
	t800	38001.385	1	38001.385	559.332	.000	.959
Mode	t400	325.538	1	325.538	5.181	.032	.178
	t800	325.538	1	325.538	4.792	.039	.166
Error	t400	1508.077	24	62.837			
	t800	1630.577	24	67.941			

Estimated Marginal Means

Mode

Estimates

Measure	Mode	Mean	Std. Error	95% Confidence Interval	
				Lower Bound	Upper Bound
t400	Eye	19.365	1.099	17.097	21.634
	Random	22.904	1.099	20.635	25.173
t800	Eye	17.346	1.143	14.987	19.705
	Random	20.885	1.143	18.525	23.244

Pairwise Comparisons

Measure	(I) Mode	(J) Mode	Mean Difference (I-J)	Std. Error	Sig.(a)	95% Confidence Interval for Difference(a)	
						Lower Bound	Upper Bound
t400	Eye	Random	-3.538(*)	1.555	.032	-6.747	-.330
	Random	Eye	3.538(*)	1.555	.032	.330	6.747
t800	Eye	Random	-3.538(*)	1.617	.039	-6.875	-.202
	Random	Eye	3.538(*)	1.617	.039	.202	6.875

Based on estimated marginal means

* The mean difference is significant at the .05 level.

a Adjustment for multiple comparisons: Least Significant Difference (equivalent to no adjustments).

Multivariate Tests

	Value	F	Hypothesis df	Error df	Sig.	Partial Eta Squared
Pillai's trace	.249	3.813(a)	2.000	23.000	.037	.249
Wilks' lambda	.751	3.813(a)	2.000	23.000	.037	.249
Hotelling's trace	.332	3.813(a)	2.000	23.000	.037	.249
Roy's largest root	.332	3.813(a)	2.000	23.000	.037	.249

Each F tests the multivariate effect of Mode. These tests are based on the linearly independent pairwise comparisons among the estimated marginal means.

a Exact statistic

Univariate Tests

Measure		Sum of Squares	df	Mean Square	F	Sig.	Partial Eta Squared
t400	Contrast	81.385	1	81.385	5.181	.032	.178

	Error	377.019	24	15.709			
t800	Contrast	81.385	1	81.385	4.792	.039	.166
	Error	407.644	24	16.985			

The F tests the effect of Mode. This test is based on the linearly independent pairwise comparisons among the estimated marginal means.

Image

Estimates

Measure	image	Mean	Std. Error	95% Confidence Interval	
				Lower Bound	Upper Bound
t400	1	17.885	1.208	15.392	20.378
	2	24.385	.661	23.021	25.748
t800	1	14.846	1.275	12.215	17.478
	2	23.385	.843	21.645	25.124

Pairwise Comparisons

Measure	(I) image	(J) image	Mean Difference (I-J)	Std. Error	Sig.(a)	95% Confidence Interval for Difference(a)	
						Lower Bound	Upper Bound
t400	1	2	-6.500(*)	1.172	.000	-8.919	-4.081
	2	1	6.500(*)	1.172	.000	4.081	8.919
t800	1	2	-8.538(*)	1.435	.000	-11.500	-5.577
	2	1	8.538(*)	1.435	.000	5.577	11.500

Based on estimated marginal means
* The mean difference is significant at the .05 level.
a Adjustment for multiple comparisons: Least Significant Difference (equivalent to no adjustments).

Multivariate Tests

	Value	F	Hypothesis df	Error df	Sig.	Partial Eta Squared
Pillai's trace	.716	28.945(a)	2.000	23.000	.000	.716
Wilks' lambda	.284	28.945(a)	2.000	23.000	.000	.716
Hotelling's trace	2.517	28.945(a)	2.000	23.000	.000	.716
Roy's largest root	2.517	28.945(a)	2.000	23.000	.000	.716

Each F tests the multivariate effect of image. These tests are based on the linearly independent pairwise comparisons among the estimated marginal means.
a Exact statistic

Random

Estimates

Measure	random	Mean	Std. Error	95% Confidence Interval	
				Lower Bound	Upper Bound
t400	1	21.231	1.049	19.067	23.395
	2	21.038	1.153	18.659	23.418
t800	1	20.385	1.212	17.883	22.886
	2	17.846	1.297	15.169	20.524

Pairwise Comparisons

Measure	(I) random	(J) random	Mean Difference (I-	Std. Error	Sig.(a)	95% Confidence Interval for Difference(a)

			J)			Lower Bound	Upper Bound
t400	1	2	.192	1.562	.903	-3.032	3.417
	2	1	-.192	1.562	.903	-3.417	3.032
t800	1	2	2.538	1.921	.199	-1.427	6.504
	2	1	-2.538	1.921	.199	-6.504	1.427

Based on estimated marginal means
a Adjustment for multiple comparisons: Least Significant Difference (equivalent to no adjustments).

Multivariate Tests

	Value	F	Hypothesis df	Error df	Sig.	Partial Eta Squared
Pillai's trace	.069	.847(a)	2.000	23.000	.442	.069
Wilks' lambda	.931	.847(a)	2.000	23.000	.442	.069
Hotelling's trace	.074	.847(a)	2.000	23.000	.442	.069
Roy's largest root	.074	.847(a)	2.000	23.000	.442	.069

Each F tests the multivariate effect of random. These tests are based on the linearly independent pairwise comparisons among the estimated marginal means.
a Exact statistic

Mode * image

Estimates

					95% Confidence Interval	
Measure	Mode	image	Mean	Std. Error	Lower Bound	Upper Bound
t400	Eye	1	15.962	1.708	12.436	19.487
		2	22.769	.934	20.841	24.697
	Random	1	19.808	1.708	16.282	23.333
		2	26.000	.934	24.072	27.928
t800	Eye	1	12.846	1.803	9.125	16.568
		2	21.846	1.192	19.387	24.306
	Random	1	16.846	1.803	13.125	20.568
		2	24.923	1.192	22.463	27.383

Pairwise Comparisons

							95% Confidence Interval for Difference(a)	
Measure	image	(I) Mode	(J) Mode	Mean Difference (I-J)	Std. Error	Sig.(a)	Lower Bound	Upper Bound
t400	1	Eye	Random	-3.846	2.416	.124	-8.832	1.140
		Random	Eye	3.846	2.416	.124	-1.140	8.832
	2	Eye	Random	-3.231(*)	1.321	.022	-5.958	-.504
		Random	Eye	3.231(*)	1.321	.022	.504	5.958
t800	1	Eye	Random	-4.000	2.550	.130	-9.263	1.263
		Random	Eye	4.000	2.550	.130	-1.263	9.263
	2	Eye	Random	-3.077	1.685	.080	-6.555	.402
		Random	Eye	3.077	1.685	.080	-.402	6.555

Based on estimated marginal means
* The mean difference is significant at the .05 level.
a Adjustment for multiple comparisons: Least Significant Difference (equivalent to no adjustments).

Multivariate Tests

image		Value	F	Hypothesis df	Error df	Sig.	Partial Eta Squared
1	Pillai's trace	.149	2.017(a)	2.000	23.000	.156	.149
	Wilks' lambda	.851	2.017(a)	2.000	23.000	.156	.149
	Hotelling's trace	.175	2.017(a)	2.000	23.000	.156	.149
	Roy's largest root	.175	2.017(a)	2.000	23.000	.156	.149
2	Pillai's trace	.246	3.758(a)	2.000	23.000	.039	.246
	Wilks' lambda	.754	3.758(a)	2.000	23.000	.039	.246
	Hotelling's trace	.327	3.758(a)	2.000	23.000	.039	.246
	Roy's largest root	.327	3.758(a)	2.000	23.000	.039	.246

Each F tests the multivariate simple effects of Mode within each level combination of the other effects shown. These tests are based on the linearly independent pairwise comparisons among the estimated marginal means.
a Exact statistic

Univariate Tests

Measure	image		Sum of Squares	df	Mean Square	F	Sig.	Partial Eta Squared
t400	1	Contrast	96.154	1	96.154	2.535	.124	.096
		Error	910.500	24	37.938			
	2	Contrast	67.846	1	67.846	5.980	.022	.199
		Error	272.308	24	11.346			
t800	1	Contrast	104.000	1	104.000	2.461	.130	.093
		Error	1014.385	24	42.266			
	2	Contrast	61.538	1	61.538	3.333	.080	.122
		Error	443.115	24	18.463			

Each F tests the simple effects of Mode within each level combination of the other effects shown. These tests are based on the linearly independent pairwise comparisons among the estimated marginal means.

Mode * Image

Pairwise Comparisons

Measure	Mode	(I) image	(J) image	Mean Difference (I-J)	Std. Error	Sig.(a)	95% Confidence Interval for Difference(a)	
							Lower Bound	Upper Bound
t400	Eye	1	2	-6.808(*)	1.658	.000	-10.229	-3.386
		2	1	6.808(*)	1.658	.000	3.386	10.229
	Random	1	2	-6.192(*)	1.658	.001	-9.614	-2.771
		2	1	6.192(*)	1.658	.001	2.771	9.614
t800	Eye	1	2	-9.000(*)	2.029	.000	-13.188	-4.812
		2	1	9.000(*)	2.029	.000	4.812	13.188
	Random	1	2	-8.077(*)	2.029	.001	-12.265	-3.889
		2	1	8.077(*)	2.029	.001	3.889	12.265

Based on estimated marginal means
* The mean difference is significant at the .05 level.
a Adjustment for multiple comparisons: Least Significant Difference (equivalent to no adjustments).

Multivariate Tests

Mode		Value	F	Hypothesis df	Error df	Sig.	Partial Eta Squared
Eye	Pillai's trace	.582	15.985(a)	2.000	23.000	.000	.582
	Wilks' lambda	.418	15.985(a)	2.000	23.000	.000	.582
	Hotelling's trace	1.390	15.985(a)	2.000	23.000	.000	.582
	Roy's largest root	1.390	15.985(a)	2.000	23.000	.000	.582
Random	Pillai's trace	.531	13.035(a)	2.000	23.000	.000	.531

	Wilks' lambda	.469	13.035(a)	2.000	23.000	.000	.531
	Hotelling's trace	1.134	13.035(a)	2.000	23.000	.000	.531
	Roy's largest root	1.134	13.035(a)	2.000	23.000	.000	.531

Each F tests the multivariate simple effects of image within each level combination of the other effects shown. These tests are based on the linearly independent pairwise comparisons among the estimated marginal means.
a Exact statistic

Mode * Random

Estimates

Measure	Mode	random	Mean	Std. Error	95% Confidence Interval	
					Lower Bound	Upper Bound
t400	Eye	1	18.385	1.483	15.324	21.445
		2	20.346	1.631	16.981	23.711
	Random	1	24.077	1.483	21.017	27.137
		2	21.731	1.631	18.366	25.096
t800	Eye	1	19.269	1.714	15.731	22.807
		2	15.423	1.835	11.636	19.210
	Random	1	21.500	1.714	17.962	25.038
		2	20.269	1.835	16.483	24.056

Pairwise Comparisons

Measure	random	(I) Mode	(J) Mode	Mean Difference (I-J)	Std. Error	Sig.(a)	95% Confidence Interval for Difference(a)	
							Lower Bound	Upper Bound
t400	1	Eye	Random	-5.692(*)	2.097	.012	-10.020	-1.364
		Random	Eye	5.692(*)	2.097	.012	1.364	10.020
	2	Eye	Random	-1.385	2.306	.554	-6.144	3.375
		Random	Eye	1.385	2.306	.554	-3.375	6.144
t800	1	Eye	Random	-2.231	2.424	.367	-7.234	2.773
		Random	Eye	2.231	2.424	.367	-2.773	7.234
	2	Eye	Random	-4.846	2.595	.074	-10.201	.509
		Random	Eye	4.846	2.595	.074	-.509	10.201

Based on estimated marginal means
* The mean difference is significant at the .05 level.
a Adjustment for multiple comparisons: Least Significant Difference (equivalent to no adjustments).

Multivariate Tests

random		Value	F	Hypothesis df	Error df	Sig.	Partial Eta Squared
1	Pillai's trace	.241	3.642(a)	2.000	23.000	.042	.241
	Wilks' lambda	.759	3.642(a)	2.000	23.000	.042	.241
	Hotelling's trace	.317	3.642(a)	2.000	23.000	.042	.241
	Roy's largest root	.317	3.642(a)	2.000	23.000	.042	.241
2	Pillai's trace	.127	1.675(a)	2.000	23.000	.209	.127
	Wilks' lambda	.873	1.675(a)	2.000	23.000	.209	.127
	Hotelling's trace	.146	1.675(a)	2.000	23.000	.209	.127
	Roy's largest root	.146	1.675(a)	2.000	23.000	.209	.127

Each F tests the multivariate simple effects of Mode within each level combination of the other effects shown. These tests are based on the linearly independent pairwise comparisons among the estimated marginal means.
a Exact statistic

Univariate Tests

Measure	random		Sum of Squares	df	Mean Square	F	Sig.	Partial Eta Squared
t400	1	Contrast	210.615	1	210.615	7.368	.012	.235
		Error	686.000	24	28.583			
	2	Contrast	12.462	1	12.462	.361	.554	.015
		Error	829.500	24	34.563			
t800	1	Contrast	32.346	1	32.346	.847	.367	.034
		Error	916.808	24	38.200			
	2	Contrast	152.654	1	152.654	3.488	.074	.127
		Error	1050.231	24	43.760			

Each F tests the simple effects of Mode within each level combination of the other effects shown. These tests are based on the linearly independent pairwise comparisons among the estimated marginal means.

Image * Random

Estimates

Measure	image	random	Mean	Std. Error	95% Confidence Interval	
					Lower Bound	Upper Bound
t400	1	1	18.192	1.618	14.852	21.532
		2	17.577	1.924	13.606	21.548
	2	1	24.269	1.068	22.066	26.473
		2	24.500	1.019	22.397	26.603
t800	1	1	16.231	2.061	11.977	20.484
		2	13.462	1.876	9.589	17.334
	2	1	24.538	1.046	22.379	26.698
		2	22.231	1.503	19.128	25.333

Pairwise Comparisons

Measure	random	(I) image	(J) image	Mean Difference (I-J)	Std. Error	Sig.(a)	95% Confidence Interval for Difference(a)	
							Lower Bound	Upper Bound
t400	1	1	2	-6.077(*)	1.766	.002	-9.722	-2.432
		2	1	6.077(*)	1.766	.002	2.432	9.722
	2	1	2	-6.923(*)	2.040	.002	-11.134	-2.712
		2	1	6.923(*)	2.040	.002	2.712	11.134
t800	1	1	2	-8.308(*)	2.193	.001	-12.833	-3.782
		2	1	8.308(*)	2.193	.001	3.782	12.833
	2	1	2	-8.769(*)	2.197	.001	-13.304	-4.235
		2	1	8.769(*)	2.197	.001	4.235	13.304

Based on estimated marginal means

* The mean difference is significant at the .05 level.

a Adjustment for multiple comparisons: Least Significant Difference (equivalent to no adjustments).

Multivariate Tests

random		Value	F	Hypothesis df	Error df	Sig.	Partial Eta Squared
1	Pillai's trace	.550	14.060(a)	2.000	23.000	.000	.550
	Wilks' lambda	.450	14.060(a)	2.000	23.000	.000	.550
	Hotelling's trace	1.223	14.060(a)	2.000	23.000	.000	.550
	Roy's largest root	1.223	14.060(a)	2.000	23.000	.000	.550
2	Pillai's trace	.477	10.485(a)	2.000	23.000	.001	.477

	Wilks' lambda	.523	10.485(a)	2.000	23.000	.001	.477
	Hotelling's trace	.912	10.485(a)	2.000	23.000	.001	.477
	Roy's largest root	.912	10.485(a)	2.000	23.000	.001	.477

Each F tests the multivariate simple effects of image within each level combination of the other effects shown. These tests are based on the linearly independent pairwise comparisons among the estimated marginal means.
a Exact statistic

Mode * Image * Random

Estimates

Measure	Mode	image	random	Mean	Std. Error	95% Confidence Interval	
						Lower Bound	Upper Bound
t400	Eye	1	1	14.231	2.288	9.508	18.954
			2	17.692	2.721	12.076	23.308
		2	1	22.538	1.510	19.422	25.655
			2	23.000	1.441	20.026	25.974
	Random	1	1	22.154	2.288	17.431	26.877
			2	17.462	2.721	11.846	23.077
		2	1	26.000	1.510	22.884	29.116
			2	26.000	1.441	23.026	28.974
t800	Eye	1	1	14.231	2.915	8.215	20.246
			2	11.462	2.653	5.985	16.938
		2	1	24.308	1.480	21.254	27.362
			2	19.385	2.126	14.997	23.772
	Random	1	1	18.231	2.915	12.215	24.246
			2	15.462	2.653	9.985	20.938
		2	1	24.769	1.480	21.715	27.823
			2	25.077	2.126	20.689	29.464

Pairwise Comparisons

Measure	image	random	(I) Mode	(J) Mode	Mean Difference (I-J)	Std. Error	Sig.(a)	95% Confidence Interval for Difference(a)	
								Lower Bound	Upper Bound
t400	1	1	Eye	Random	-7.923(*)	3.236	.022	-14.603	-1.243
			Random	Eye	7.923(*)	3.236	.022	1.243	14.603
		2	Eye	Random	.231	3.848	.953	-7.711	8.173
			Random	Eye	-.231	3.848	.953	-8.173	7.711
	2	1	Eye	Random	-3.462	2.135	.118	-7.868	.945
			Random	Eye	3.462	2.135	.118	-.945	7.868
		2	Eye	Random	-3.000	2.038	.154	-7.206	1.206
			Random	Eye	3.000	2.038	.154	-1.206	7.206
t800	1	1	Eye	Random	-4.000	4.122	.342	-12.507	4.507
			Random	Eye	4.000	4.122	.342	-4.507	12.507
		2	Eye	Random	-4.000	3.752	.297	-11.744	3.744
			Random	Eye	4.000	3.752	.297	-3.744	11.744
	2	1	Eye	Random	-.462	2.093	.827	-4.780	3.857
			Random	Eye	.462	2.093	.827	-3.857	4.780
		2	Eye	Random	-5.692	3.006	.070	-11.897	.513
			Random	Eye	5.692	3.006	.070	-.513	11.897

Based on estimated marginal means
* The mean difference is significant at the .05 level.
a Adjustment for multiple comparisons: Least Significant Difference (equivalent to no adjustments).

Multivariate Tests

image	random		Value	F	Hypothesis df	Error df	Sig.	Partial Eta Squared
1	1	Pillai's trace	.214	3.128(a)	2.000	23.000	.063	.214
		Wilks' lambda	.786	3.128(a)	2.000	23.000	.063	.214
		Hotelling's trace	.272	3.128(a)	2.000	23.000	.063	.214
		Roy's largest root	.272	3.128(a)	2.000	23.000	.063	.214
	2	Pillai's trace	.046	.554(a)	2.000	23.000	.582	.046
		Wilks' lambda	.954	.554(a)	2.000	23.000	.582	.046
		Hotelling's trace	.048	.554(a)	2.000	23.000	.582	.046
		Roy's largest root	.048	.554(a)	2.000	23.000	.582	.046
2	1	Pillai's trace	.104	1.336(a)	2.000	23.000	.283	.104
		Wilks' lambda	.896	1.336(a)	2.000	23.000	.283	.104
		Hotelling's trace	.116	1.336(a)	2.000	23.000	.283	.104
		Roy's largest root	.116	1.336(a)	2.000	23.000	.283	.104
	2	Pillai's trace	.130	1.721(a)	2.000	23.000	.201	.130
		Wilks' lambda	.870	1.721(a)	2.000	23.000	.201	.130
		Hotelling's trace	.150	1.721(a)	2.000	23.000	.201	.130
		Roy's largest root	.150	1.721(a)	2.000	23.000	.201	.130

Each F tests the multivariate simple effects of Mode within each level combination of the other effects shown. These tests are based on the linearly independent pairwise comparisons among the estimated marginal means.
a Exact statistic

Univariate Tests

Measure	image	random		Sum of Squares	df	Mean Square	F	Sig.	Partial Eta Squared
t400	1	1	Contrast	408.038	1	408.038	5.993	.022	.200
			Error	1634.000	24	68.083			
		2	Contrast	.346	1	.346	.004	.953	.000
			Error	2310.000	24	96.250			
	2	1	Contrast	77.885	1	77.885	2.628	.118	.099
			Error	711.231	24	29.635			
		2	Contrast	58.500	1	58.500	2.167	.154	.083
			Error	648.000	24	27.000			
t800	1	1	Contrast	104.000	1	104.000	.942	.342	.038
			Error	2650.615	24	110.442			
		2	Contrast	104.000	1	104.000	1.136	.297	.045
			Error	2196.462	24	91.519			
	2	1	Contrast	1.385	1	1.385	.049	.827	.002
			Error	683.077	24	28.462			
		2	Contrast	210.615	1	210.615	3.585	.070	.130
			Error	1410.000	24	58.750			

Each F tests the simple effects of Mode within each level combination of the other effects shown. These tests are based on the linearly independent pairwise comparisons among the estimated marginal means.

Mode * Image * Random

Pairwise Comparisons

Measure	Mode	random	(I) image	(J) image	Mean Difference (I-J)	Std. Error	Sig.(a)	95% Confidence Interval for Difference(a)	
								Lower Bound	Upper Bound
t400	Eye	1	1	2	-8.308(*)	2.498	.003	-13.463	-3.153
			2	1	8.308(*)	2.498	.003	3.153	13.463

		2	1	2	-5.308	2.886	.078	-11.263	.648
			2	1	5.308	2.886	.078	-.648	11.263
	Random	1	1	2	-3.846	2.498	.137	-9.001	1.309
			2	1	3.846	2.498	.137	-1.309	9.001
		2	1	2	-8.538(*)	2.886	.007	-14.494	-2.583
			2	1	8.538(*)	2.886	.007	2.583	14.494
t800	Eye	1	1	2	-10.077(*)	3.101	.003	-16.477	-3.677
			2	1	10.077(*)	3.101	.003	3.677	16.477
		2	1	2	-7.923(*)	3.107	.018	-14.336	-1.510
			2	1	7.923(*)	3.107	.018	1.510	14.336
	Random	1	1	2	-6.538(*)	3.101	.046	-12.939	-.138
			2	1	6.538(*)	3.101	.046	.138	12.939
		2	1	2	-9.615(*)	3.107	.005	-16.028	-3.203
			2	1	9.615(*)	3.107	.005	3.203	16.028

Based on estimated marginal means
* The mean difference is significant at the .05 level.
a Adjustment for multiple comparisons: Least Significant Difference (equivalent to no adjustments).

Multivariate Tests

Mode	random		Value	F	Hypothesis df	Error df	Sig.	Partial Eta Squared
Eye	1	Pillai's trace	.502	11.611(a)	2.000	23.000	.000	.502
		Wilks' lambda	.498	11.611(a)	2.000	23.000	.000	.502
		Hotelling's trace	1.010	11.611(a)	2.000	23.000	.000	.502
		Roy's largest root	1.010	11.611(a)	2.000	23.000	.000	.502
	2	Pillai's trace	.250	3.827(a)	2.000	23.000	.037	.250
		Wilks' lambda	.750	3.827(a)	2.000	23.000	.037	.250
		Hotelling's trace	.333	3.827(a)	2.000	23.000	.037	.250
		Roy's largest root	.333	3.827(a)	2.000	23.000	.037	.250
Random	1	Pillai's trace	.241	3.644(a)	2.000	23.000	.042	.241
		Wilks' lambda	.759	3.644(a)	2.000	23.000	.042	.241
		Hotelling's trace	.317	3.644(a)	2.000	23.000	.042	.241
		Roy's largest root	.317	3.644(a)	2.000	23.000	.042	.241
	2	Pillai's trace	.378	6.975(a)	2.000	23.000	.004	.378
		Wilks' lambda	.622	6.975(a)	2.000	23.000	.004	.378
		Hotelling's trace	.606	6.975(a)	2.000	23.000	.004	.378
		Roy's largest root	.606	6.975(a)	2.000	23.000	.004	.378

Each F tests the multivariate simple effects of image within each level combination of the other effects shown. These tests are based on the linearly independent pairwise comparisons among the estimated marginal means.
a Exact statistic

11.3. Experiments on Refixation and Pre-Attentive Activity

11.3.1. Steps to Target

Within-Subjects Factors

Measure: MEASURE_1

Threshold	Ranking	Dependent Variable
1 (300ms)	1	VAR00001
	2	VAR00002
2 (400ms)	1	VAR00003
	2	VAR00004

3 (Revisit)	1	VAR00005
	2	VAR00006
4 (Revisit/400ms)	1	VAR00007
	2	VAR00008

Multivariate Tests(b)

Effect		Value	F	Hypothesis df	Error df	Sig.
Threshold	Pillai's Trace	.049	.358(a)	3.000	21.000	.784
	Wilks' Lambda	.951	.358(a)	3.000	21.000	.784
	Hotelling's Trace	.051	.358(a)	3.000	21.000	.784
	Roy's Largest Root	.051	.358(a)	3.000	21.000	.784
Ranking	Pillai's Trace	.166	4.593(a)	1.000	23.000	.043
	Wilks' Lambda	.834	4.593(a)	1.000	23.000	.043
	Hotelling's Trace	.200	4.593(a)	1.000	23.000	.043
	Roy's Largest Root	.200	4.593(a)	1.000	23.000	.043
Threshold * Ranking	Pillai's Trace	.018	.131(a)	3.000	21.000	.940
	Wilks' Lambda	.982	.131(a)	3.000	21.000	.940
	Hotelling's Trace	.019	.131(a)	3.000	21.000	.940
	Roy's Largest Root	.019	.131(a)	3.000	21.000	.940

a Exact statistic
b Design: Intercept
Within Subjects Design: Threshold+Ranking+Threshold*Ranking

Mauchly's Test of Sphericity(b)

Measure: MEASURE_1

Within Subjects Effect	Mauchly's W	Approx. Chi-Square	df	Sig.	Epsilon(a) Greenhouse-Geisser	Huynh-Feldt	Lower-bound
Threshold	.832	3.993	5	.551	.905	1.000	.333
Ranking	1.000	.000	0	.	1.000	1.000	1.000
Threshold * Ranking	.963	.823	5	.976	.977	1.000	.333

Tests the null hypothesis that the error covariance matrix of the orthonormalized transformed dependent variables is proportional to an identity matrix.
a May be used to adjust the degrees of freedom for the averaged tests of significance. Corrected tests are displayed in the Tests of Within-Subjects Effects table.
b Design: Intercept
Within Subjects Design: Threshold+Ranking+Threshold*Ranking

Tests of Within-Subjects Effects

Measure: MEASURE_1

Source		Type III Sum of Squares	df	Mean Square	F	Sig.
Threshold	Sphericity Assumed	97.224	3	32.408	.441	.724
	Greenhouse-Geisser	97.224	2.716	35.793	.441	.705
	Huynh-Feldt	97.224	3.000	32.408	.441	.724
	Lower-bound	97.224	1.000	97.224	.441	.513
Error(Threshold)	Sphericity Assumed	5070.151	69	73.480		
	Greenhouse-Geisser	5070.151	62.475	81.155		
	Huynh-Feldt	5070.151	69.000	73.480		
	Lower-bound	5070.151	23.000	220.441		
Ranking	Sphericity Assumed	453.255	1	453.255	4.593	.043
	Greenhouse-Geisser	453.255	1.000	453.255	4.593	.043
	Huynh-Feldt	453.255	1.000	453.255	4.593	.043

	Lower-bound	453.255	1.000	453.255	4.593	.043
Error(Ranking)	Sphericity Assumed	2269.870	23	98.690		
	Greenhouse-Geisser	2269.870	23.000	98.690		
	Huynh-Feldt	2269.870	23.000	98.690		
	Lower-bound	2269.870	23.000	98.690		
Threshold * Ranking	Sphericity Assumed	63.016	3	21.005	.134	.940
	Greenhouse-Geisser	63.016	2.931	21.501	.134	.937
	Huynh-Feldt	63.016	3.000	21.005	.134	.940
	Lower-bound	63.016	1.000	63.016	.134	.718
Error(Threshold*Ranking)	Sphericity Assumed	10838.359	69	157.078		
	Greenhouse-Geisser	10838.359	67.410	160.783		
	Huynh-Feldt	10838.359	69.000	157.078		
	Lower-bound	10838.359	23.000	471.233		

Tests of Within-Subjects Contrasts

Measure: MEASURE_1

Source	Threshold	Ranking	Type III Sum of Squares	df	Mean Square	F	Sig.
Threshold	Linear		2.926	1	2.926	.048	.829
	Quadratic		1.172	1	1.172	.015	.904
	Cubic		93.126	1	93.126	1.159	.293
Error(Threshold)	Linear		1407.799	23	61.209		
	Quadratic		1814.453	23	78.889		
	Cubic		1847.899	23	80.343		
Ranking		Linear	453.255	1	453.255	4.593	.043
Error(Ranking)		Linear	2269.870	23	98.690		
Threshold * Ranking	Linear	Linear	9.401	1	9.401	.054	.818
	Quadratic	Linear	.880	1	.880	.005	.942
	Cubic	Linear	52.734	1	52.734	.395	.536
Error(Threshold*Ranking)	Linear	Linear	4012.524	23	174.458		
	Quadratic	Linear	3753.745	23	163.206		
	Cubic	Linear	3072.091	23	133.569		

Tests of Between-Subjects Effects

Measure: MEASURE_1
Transformed Variable: Average

Source	Type III Sum of Squares	df	Mean Square	F	Sig.
Intercept	53500.130	1	53500.130	401.208	.000
Error	3066.995	23	133.348		

Estimated Marginal Means

Threshold

Estimates

Measure: MEASURE_1

Threshold	Mean	Std. Error	95% Confidence Interval	
			Lower Bound	Upper Bound
1	16.625	1.239	14.062	19.188
2	17.604	1.451	14.603	20.606
3	15.625	1.413	12.702	18.548
4	16.917	1.317	14.193	19.640

Pairwise Comparisons

Measure: MEASURE_1

(I) Threshold	(J) Threshold	Mean Difference (I-J)	Std. Error	Sig.(a)	95% Confidence Interval for Difference(a)	
					Lower Bound	Upper Bound
1	2	-.979	1.610	.549	-4.310	2.351
	3	1.000	1.579	.533	-2.267	4.267
	4	-.292	1.483	.846	-3.359	2.776
2	1	.979	1.610	.549	-2.351	4.310
	3	1.979	1.923	.314	-1.999	5.958
	4	.688	2.019	.737	-3.490	4.865
3	1	-1.000	1.579	.533	-4.267	2.267
	2	-1.979	1.923	.314	-5.958	1.999
	4	-1.292	1.819	.485	-5.055	2.471
4	1	.292	1.483	.846	-2.776	3.359
	2	-.688	2.019	.737	-4.865	3.490
	3	1.292	1.819	.485	-2.471	5.055

Based on estimated marginal means

a Adjustment for multiple comparisons: Least Significant Difference (equivalent to no adjustments).

Multivariate Tests

	Value	F	Hypothesis df	Error df	Sig.
Pillai's trace	.049	.358(a)	3.000	21.000	.784
Wilks' lambda	.951	.358(a)	3.000	21.000	.784
Hotelling's trace	.051	.358(a)	3.000	21.000	.784
Roy's largest root	.051	.358(a)	3.000	21.000	.784

Each F tests the multivariate effect of Threshold. These tests are based on the linearly independent pairwise comparisons among the estimated marginal means.

a Exact statistic

Ranking

Estimates

Measure: MEASURE_1

Ranking	Mean	Std. Error	95% Confidence Interval	
			Lower Bound	Upper Bound
1	18.229	1.145	15.861	20.597
2	15.156	1.052	12.980	17.333

Pairwise Comparisons

Measure: MEASURE_1

(I) Ranking	(J) Ranking	Mean Difference (I-J)	Std. Error	Sig.(a)	95% Confidence Interval for Difference(a)	
					Lower Bound	Upper Bound
1	2	3.073(*)	1.434	.043	.107	6.039
2	1	-3.073(*)	1.434	.043	-6.039	-.107

Based on estimated marginal means

* The mean difference is significant at the .05 level.

a Adjustment for multiple comparisons: Least Significant Difference (equivalent to no adjustments).

Multivariate Tests

	Value	F	Hypothesis df	Error df	Sig.
Pillai's trace	.166	4.593(a)	1.000	23.000	.043

Wilks' lambda	.834	4.593(a)	1.000	23.000	.043
Hotelling's trace	.200	4.593(a)	1.000	23.000	.043
Roy's largest root	.200	4.593(a)	1.000	23.000	.043

Each F tests the multivariate effect of Ranking. These tests are based on the linearly independent pairwise comparisons among the estimated marginal means.
a Exact statistic

11.3.2. Time to Target (Per Display)

Within-Subjects Factors

Measure: MEASURE_1

Threshold	Ranking	Dependent Variable
1	1	VAR00001
	2	VAR00002
2	1	VAR00003
	2	VAR00004
3	1	VAR00005
	2	VAR00006
4	1	VAR00007
	2	VAR00008

Multivariate Tests(b)

Effect		Value	F	Hypothesis df	Error df	Sig.
Threshold	Pillai's Trace	.934	99.477(a)	3.000	21.000	.000
	Wilks' Lambda	.066	99.477(a)	3.000	21.000	.000
	Hotelling's Trace	14.211	99.477(a)	3.000	21.000	.000
	Roy's Largest Root	14.211	99.477(a)	3.000	21.000	.000
Ranking	Pillai's Trace	.034	.804(a)	1.000	23.000	.379
	Wilks' Lambda	.966	.804(a)	1.000	23.000	.379
	Hotelling's Trace	.035	.804(a)	1.000	23.000	.379
	Roy's Largest Root	.035	.804(a)	1.000	23.000	.379
Threshold * Ranking	Pillai's Trace	.031	.221(a)	3.000	21.000	.881
	Wilks' Lambda	.969	.221(a)	3.000	21.000	.881
	Hotelling's Trace	.032	.221(a)	3.000	21.000	.881
	Roy's Largest Root	.032	.221(a)	3.000	21.000	.881

a Exact statistic
b Design: Intercept
Within Subjects Design: Threshold+Ranking+Threshold*Ranking

Mauchly's Test of Sphericity(b)

Measure: MEASURE_1

Within Subjects Effect	Mauchly's W	Approx. Chi-Square	df	Sig.	Epsilon(a)		
					Greenhouse-Geisser	Huynh-Feldt	Lower-bound
Threshold	.194	35.654	5	.000	.501	.528	.333
Ranking	1.000	.000	0	.	1.000	1.000	1.000
Threshold * Ranking	.389	20.496	5	.001	.681	.748	.333

Tests the null hypothesis that the error covariance matrix of the orthonormalized transformed dependent variables is proportional to an identity matrix.
a May be used to adjust the degrees of freedom for the averaged tests of significance. Corrected tests are displayed in the Tests of Within-Subjects Effects table.
b Design: Intercept

Within Subjects Design: Threshold+Ranking+Threshold*Ranking

Tests of Within-Subjects Effects

Measure: MEASURE_1

Source		Type III Sum of Squares	df	Mean Square	F	Sig.
Threshold	Sphericity Assumed	40.699	3	13.566	56.560	.000
	Greenhouse-Geisser	40.699	1.503	27.075	56.560	.000
	Huynh-Feldt	40.699	1.585	25.674	56.560	.000
	Lower-bound	40.699	1.000	40.699	56.560	.000
Error(Threshold)	Sphericity Assumed	16.550	69	.240		
	Greenhouse-Geisser	16.550	34.574	.479		
	Huynh-Feldt	16.550	36.460	.454		
	Lower-bound	16.550	23.000	.720		
Ranking	Sphericity Assumed	.143	1	.143	.804	.379
	Greenhouse-Geisser	.143	1.000	.143	.804	.379
	Huynh-Feldt	.143	1.000	.143	.804	.379
	Lower-bound	.143	1.000	.143	.804	.379
Error(Ranking)	Sphericity Assumed	4.086	23	.178		
	Greenhouse-Geisser	4.086	23.000	.178		
	Huynh-Feldt	4.086	23.000	.178		
	Lower-bound	4.086	23.000	.178		
Threshold * Ranking	Sphericity Assumed	.055	3	.018	.103	.958
	Greenhouse-Geisser	.055	2.043	.027	.103	.906
	Huynh-Feldt	.055	2.245	.025	.103	.921
	Lower-bound	.055	1.000	.055	.103	.751
Error(Threshold*Ranking)	Sphericity Assumed	12.277	69	.178		
	Greenhouse-Geisser	12.277	46.997	.261		
	Huynh-Feldt	12.277	51.628	.238		
	Lower-bound	12.277	23.000	.534		

Tests of Within-Subjects Contrasts

Measure: MEASURE_1

Source	Threshold	Ranking	Type III Sum of Squares	df	Mean Square	F	Sig.
Threshold	Linear		8.546	1	8.546	58.928	.000
	Quadratic		24.580	1	24.580	203.617	.000
	Cubic		7.573	1	7.573	16.687	.000
Error(Threshold)	Linear		3.335	23	.145		
	Quadratic		2.776	23	.121		
	Cubic		10.438	23	.454		
Ranking		Linear	.143	1	.143	.804	.379
Error(Ranking)		Linear	4.086	23	.178		
Threshold * Ranking	Linear	Linear	.016	1	.016	.210	.651
	Quadratic	Linear	.002	1	.002	.012	.915
	Cubic	Linear	.037	1	.037	.120	.732
Error(Threshold*Ranking)	Linear	Linear	1.775	23	.077		
	Quadratic	Linear	3.335	23	.145		
	Cubic	Linear	7.167	23	.312		

Tests of Between-Subjects Effects

Measure: MEASURE_1
Transformed Variable: Average

Source	Type III Sum of Squares	df	Mean Square	F	Sig.

Intercept	512.100	1	512.100	1673.725	.000
Error	7.037	23	.306		

Estimated Marginal Means

Threshold

Estimates

Measure: MEASURE_1

Threshold	Mean	Std. Error	95% Confidence Interval	
			Lower Bound	Upper Bound
1	1.081	.050	.977	1.185
2	1.630	.070	1.485	1.776
3	2.352	.109	2.126	2.578
4	1.470	.045	1.377	1.562

Pairwise Comparisons

Measure: MEASURE_1

(I) Threshold	(J) Threshold	Mean Difference (I-J)	Std. Error	Sig.(a)	95% Confidence Interval for Difference(a)	
					Lower Bound	Upper Bound
1	2	-.549(*)	.055	.000	-.663	-.435
	3	-1.271(*)	.119	.000	-1.517	-1.024
	4	-.388(*)	.060	.000	-.513	-.264
2	1	.549(*)	.055	.000	.435	.663
	3	-.722(*)	.146	.000	-1.024	-.420
	4	.161(*)	.066	.023	.024	.297
3	1	1.271(*)	.119	.000	1.024	1.517
	2	.722(*)	.146	.000	.420	1.024
	4	.882(*)	.116	.000	.642	1.122
4	1	.388(*)	.060	.000	.264	.513
	2	-.161(*)	.066	.023	-.297	-.024
	3	-.882(*)	.116	.000	-1.122	-.642

Based on estimated marginal means
* The mean difference is significant at the .05 level.
a Adjustment for multiple comparisons: Least Significant Difference (equivalent to no adjustments).

Multivariate Tests

	Value	F	Hypothesis df	Error df	Sig.
Pillai's trace	.934	99.477(a)	3.000	21.000	.000
Wilks' lambda	.066	99.477(a)	3.000	21.000	.000
Hotelling's trace	14.211	99.477(a)	3.000	21.000	.000
Roy's largest root	14.211	99.477(a)	3.000	21.000	.000

Each F tests the multivariate effect of Threshold. These tests are based on the linearly independent pairwise comparisons among the estimated marginal means.
a Exact statistic

Ranking

Estimates

Measure: MEASURE_1

Ranking	Mean	Std. Error	95% Confidence Interval	
			Lower Bound	Upper Bound

1	1.606	.044	1.516	1.696
2	1.660	.056	1.545	1.776

Pairwise Comparisons

Measure: MEASURE_1

(I) Ranking	(J) Ranking	Mean Difference (I-J)	Std. Error	Sig.(a)	95% Confidence Interval for Difference(a)	
					Lower Bound	Upper Bound
1	2	-.055	.061	.379	-.180	.071
2	1	.055	.061	.379	-.071	.180

Based on estimated marginal means
a Adjustment for multiple comparisons: Least Significant Difference (equivalent to no adjustments).

Multivariate Tests

	Value	F	Hypothesis df	Error df	Sig.
Pillai's trace	.034	.804(a)	1.000	23.000	.379
Wilks' lambda	.966	.804(a)	1.000	23.000	.379
Hotelling's trace	.035	.804(a)	1.000	23.000	.379
Roy's largest root	.035	.804(a)	1.000	23.000	.379

Each F tests the multivariate effect of Ranking. These tests are based on the linearly independent pairwise comparisons among the estimated marginal means.
a Exact statistic

11.3.3. Fixation Numbers (Per Display)

Within-Subjects Factors

Measure: MEASURE_1

Threshold	Ranking	Dependent Variable
1	1	VAR00001
	2	VAR00002
2	1	VAR00003
	2	VAR00004
3	1	VAR00005
	2	VAR00006
4	1	VAR00007
	2	VAR00008

Multivariate Tests(b)

Effect		Value	F	Hypothesis df	Error df	Sig.
Threshold	Pillai's Trace	.892	58.091(a)	3.000	21.000	.000
	Wilks' Lambda	.108	58.091(a)	3.000	21.000	.000
	Hotelling's Trace	8.299	58.091(a)	3.000	21.000	.000
	Roy's Largest Root	8.299	58.091(a)	3.000	21.000	.000
Ranking	Pillai's Trace	.054	1.310(a)	1.000	23.000	.264
	Wilks' Lambda	.946	1.310(a)	1.000	23.000	.264
	Hotelling's Trace	.057	1.310(a)	1.000	23.000	.264
	Roy's Largest Root	.057	1.310(a)	1.000	23.000	.264
Threshold * Ranking	Pillai's Trace	.033	.241(a)	3.000	21.000	.867
	Wilks' Lambda	.967	.241(a)	3.000	21.000	.867
	Hotelling's Trace	.034	.241(a)	3.000	21.000	.867

	Roy's Largest Root	.034	.241(a)	3.000	21.000	.867

a Exact statistic
b Design: Intercept
Within Subjects Design: Threshold+Ranking+Threshold*Ranking

Mauchly's Test of Sphericity(b)

Measure: MEASURE_1

Within Subjects Effect	Mauchly's W	Approx. Chi-Square	df	Sig.	Epsilon(a) Greenhouse-Geisser	Huynh-Feldt	Lower-bound
Threshold	.581	11.813	5	.038	.719	.796	.333
Ranking	1.000	.000	0	.	1.000	1.000	1.000
Threshold * Ranking	.767	5.750	5	.332	.865	.984	.333

Tests the null hypothesis that the error covariance matrix of the orthonormalized transformed dependent variables is proportional to an identity matrix.
a May be used to adjust the degrees of freedom for the averaged tests of significance. Corrected tests are displayed in the Tests of Within-Subjects Effects table.
b Design: Intercept
Within Subjects Design: Threshold+Ranking+Threshold*Ranking

Tests of Within-Subjects Effects

Measure: MEASURE_1

Source		Type III Sum of Squares	df	Mean Square	F	Sig.
Threshold	Sphericity Assumed	227.167	3	75.722	38.251	.000
	Greenhouse-Geisser	227.167	2.157	105.332	38.251	.000
	Huynh-Feldt	227.167	2.387	95.155	38.251	.000
	Lower-bound	227.167	1.000	227.167	38.251	.000
Error(Threshold)	Sphericity Assumed	136.594	69	1.980		
	Greenhouse-Geisser	136.594	49.604	2.754		
	Huynh-Feldt	136.594	54.909	2.488		
	Lower-bound	136.594	23.000	5.939		
Ranking	Sphericity Assumed	2.382	1	2.382	1.310	.264
	Greenhouse-Geisser	2.382	1.000	2.382	1.310	.264
	Huynh-Feldt	2.382	1.000	2.382	1.310	.264
	Lower-bound	2.382	1.000	2.382	1.310	.264
Error(Ranking)	Sphericity Assumed	41.832	23	1.819		
	Greenhouse-Geisser	41.832	23.000	1.819		
	Huynh-Feldt	41.832	23.000	1.819		
	Lower-bound	41.832	23.000	1.819		
Threshold * Ranking	Sphericity Assumed	1.467	3	.489	.271	.846
	Greenhouse-Geisser	1.467	2.594	.565	.271	.818
	Huynh-Feldt	1.467	2.953	.497	.271	.843
	Lower-bound	1.467	1.000	1.467	.271	.608
Error(Threshold*Ranking)	Sphericity Assumed	124.593	69	1.806		
	Greenhouse-Geisser	124.593	59.663	2.088		
	Huynh-Feldt	124.593	67.917	1.834		
	Lower-bound	124.593	23.000	5.417		

Tests of Within-Subjects Contrasts

Measure: MEASURE_1

Source	Threshold	Ranking	Type III Sum of Squares	df	Mean Square	F	Sig.

Threshold	Linear		51.420	1	51.420	26.662	.000
	Quadratic		158.520	1	158.520	161.718	.000
	Cubic		17.227	1	17.227	5.685	.026
Error(Threshold)	Linear		44.357	23	1.929		
	Quadratic		22.545	23	.980		
	Cubic		69.692	23	3.030		
Ranking		Linear	2.382	1	2.382	1.310	.264
Error(Ranking)		Linear	41.832	23	1.819		
Threshold * Ranking	Linear	Linear	.439	1	.439	.454	.507
	Quadratic	Linear	.057	1	.057	.027	.872
	Cubic	Linear	.971	1	.971	.418	.524
Error(Threshold*Ranking)	Linear	Linear	22.234	23	.967		
	Quadratic	Linear	48.899	23	2.126		
	Cubic	Linear	53.460	23	2.324		

Tests of Between-Subjects Effects

Measure: MEASURE_1
Transformed Variable: Average

Source	Type III Sum of Squares	df	Mean Square	F	Sig.
Intercept	4271.855	1	4271.855	849.436	.000
Error	115.668	23	5.029		

Estimated Marginal Means

Threshold

Estimates

Measure: MEASURE_1

Threshold	Mean	Std. Error	95% Confidence Interval	
			Lower Bound	Upper Bound
1	3.248	.210	2.814	3.682
2	4.992	.307	4.356	5.628
3	6.259	.230	5.783	6.735
4	4.369	.192	3.971	4.766

Pairwise Comparisons

Measure: MEASURE_1

(I) Threshold	(J) Threshold	Mean Difference (I-J)	Std. Error	Sig.(a)	95% Confidence Interval for Difference(a)	
					Lower Bound	Upper Bound
1	2	-1.744(*)	.243	.000	-2.247	-1.241
	3	-3.011(*)	.289	.000	-3.608	-2.414
	4	-1.121(*)	.239	.000	-1.615	-.627
2	1	1.744(*)	.243	.000	1.241	2.247
	3	-1.267(*)	.387	.003	-2.067	-.467
	4	.624(*)	.290	.042	.023	1.224
3	1	3.011(*)	.289	.000	2.414	3.608
	2	1.267(*)	.387	.003	.467	2.067
	4	1.890(*)	.248	.000	1.377	2.404
4	1	1.121(*)	.239	.000	.627	1.615
	2	-.624(*)	.290	.042	-1.224	-.023
	3	-1.890(*)	.248	.000	-2.404	-1.377

Based on estimated marginal means

* The mean difference is significant at the .05 level.
a Adjustment for multiple comparisons: Least Significant Difference (equivalent to no adjustments).

Multivariate Tests

	Value	F	Hypothesis df	Error df	Sig.
Pillai's trace	.892	58.091(a)	3.000	21.000	.000
Wilks' lambda	.108	58.091(a)	3.000	21.000	.000
Hotelling's trace	8.299	58.091(a)	3.000	21.000	.000
Roy's largest root	8.299	58.091(a)	3.000	21.000	.000

Each F tests the multivariate effect of Threshold. These tests are based on the linearly independent pairwise comparisons among the estimated marginal means.
a Exact statistic

Ranking

Estimates

Measure: MEASURE_1

Ranking	Mean	Std. Error	95% Confidence Interval	
			Lower Bound	Upper Bound
1	4.606	.163	4.269	4.943
2	4.828	.212	4.390	5.266

Pairwise Comparisons

Measure: MEASURE_1

(I) Ranking	(J) Ranking	Mean Difference (I-J)	Std. Error	Sig.(a)	95% Confidence Interval for Difference(a)	
					Lower Bound	Upper Bound
1	2	-.223	.195	.264	-.625	.180
2	1	.223	.195	.264	-.180	.625

Based on estimated marginal means
a Adjustment for multiple comparisons: Least Significant Difference (equivalent to no adjustments).

Multivariate Tests

	Value	F	Hypothesis df	Error df	Sig.
Pillai's trace	.054	1.310(a)	1.000	23.000	.264
Wilks' lambda	.946	1.310(a)	1.000	23.000	.264
Hotelling's trace	.057	1.310(a)	1.000	23.000	.264
Roy's largest root	.057	1.310(a)	1.000	23.000	.264

Each F tests the multivariate effect of Ranking. These tests are based on the linearly independent pairwise comparisons among the estimated marginal means.
a Exact statistic

11.3.4. Eye and Random Comparison

Within-Subjects Factors

Measure	Ranking	Dependent Variable
run1 (300ms)	1	VAR00010
	2	VAR00011
run2 (400ms)	1	VAR00012
	2	VAR00013
run3 (Revisit)	1	VAR00014
	2	VAR00015

run4 (Revisit/400ms)	1	VAR00016
	2	VAR00017

Between-Subjects Factors

		N
Mode	Eye	24
	Random	24

Multivariate Tests(b)

Effect			Value	F	Hypothesis df	Error df	Sig.	Partial Eta Squared
Between Subjects	Intercept	Pillai's Trace	.974	409.943(a)	4.000	43.000	.000	.974
		Wilks' Lambda	.026	409.943(a)	4.000	43.000	.000	.974
		Hotelling's Trace	38.134	409.943(a)	4.000	43.000	.000	.974
		Roy's Largest Root	38.134	409.943(a)	4.000	43.000	.000	.974
	Mode	Pillai's Trace	.336	5.434(a)	4.000	43.000	.001	.336
		Wilks' Lambda	.664	5.434(a)	4.000	43.000	.001	.336
		Hotelling's Trace	.505	5.434(a)	4.000	43.000	.001	.336
		Roy's Largest Root	.505	5.434(a)	4.000	43.000	.001	.336
Within Subjects	Ranking	Pillai's Trace	.248	3.547(a)	4.000	43.000	.014	.248
		Wilks' Lambda	.752	3.547(a)	4.000	43.000	.014	.248
		Hotelling's Trace	.330	3.547(a)	4.000	43.000	.014	.248
		Roy's Largest Root	.330	3.547(a)	4.000	43.000	.014	.248
	Ranking * Mode	Pillai's Trace	.014	.152(a)	4.000	43.000	.961	.014
		Wilks' Lambda	.986	.152(a)	4.000	43.000	.961	.014
		Hotelling's Trace	.014	.152(a)	4.000	43.000	.961	.014
		Roy's Largest Root	.014	.152(a)	4.000	43.000	.961	.014

a Exact statistic
b Design: Intercept+Mode
Within Subjects Design: Ranking

Tests of Within-Subjects Effects

Multivariate(b,c)

Within Subjects Effect		Value	F	Hypothesis df	Error df	Sig.	Partial Eta Squared
Ranking	Pillai's Trace	.248	3.547(a)	4.000	43.000	.014	.248
	Wilks' Lambda	.752	3.547(a)	4.000	43.000	.014	.248
	Hotelling's Trace	.330	3.547(a)	4.000	43.000	.014	.248
	Roy's Largest Root	.330	3.547(a)	4.000	43.000	.014	.248
Ranking * Mode	Pillai's Trace	.014	.152(a)	4.000	43.000	.961	.014
	Wilks' Lambda	.986	.152(a)	4.000	43.000	.961	.014
	Hotelling's Trace	.014	.152(a)	4.000	43.000	.961	.014
	Roy's Largest Root	.014	.152(a)	4.000	43.000	.961	.014

a Exact statistic
b Design: Intercept+Mode
Within Subjects Design: Ranking
c Tests are based on averaged variables.

Univariate Tests

Source	Measure		Type III Sum of	df	Mean Square	F	Sig.	Partial Eta

			Squares					Squared
Ranking	run1	Sphericity Assumed	442.042	1	442.042	3.652	.062	.074
		Greenhouse-Geisser	442.042	1.000	442.042	3.652	.062	.074
		Huynh-Feldt	442.042	1.000	442.042	3.652	.062	.074
		Lower-bound	442.042	1.000	442.042	3.652	.062	.074
	run2	Sphericity Assumed	263.344	1	263.344	2.452	.124	.051
		Greenhouse-Geisser	263.344	1.000	263.344	2.452	.124	.051
		Huynh-Feldt	263.344	1.000	263.344	2.452	.124	.051
		Lower-bound	263.344	1.000	263.344	2.452	.124	.051
	run3	Sphericity Assumed	117.042	1	117.042	1.083	.303	.023
		Greenhouse-Geisser	117.042	1.000	117.042	1.083	.303	.023
		Huynh-Feldt	117.042	1.000	117.042	1.083	.303	.023
		Lower-bound	117.042	1.000	117.042	1.083	.303	.023
	run4	Sphericity Assumed	337.500	1	337.500	3.226	.079	.066
		Greenhouse-Geisser	337.500	1.000	337.500	3.226	.079	.066
		Huynh-Feldt	337.500	1.000	337.500	3.226	.079	.066
		Lower-bound	337.500	1.000	337.500	3.226	.079	.066
Ranking * Mode	run1	Sphericity Assumed	22.042	1	22.042	.182	.672	.004
		Greenhouse-Geisser	22.042	1.000	22.042	.182	.672	.004
		Huynh-Feldt	22.042	1.000	22.042	.182	.672	.004
		Lower-bound	22.042	1.000	22.042	.182	.672	.004
	run2	Sphericity Assumed	36.260	1	36.260	.338	.564	.007
		Greenhouse-Geisser	36.260	1.000	36.260	.338	.564	.007
		Huynh-Feldt	36.260	1.000	36.260	.338	.564	.007
		Lower-bound	36.260	1.000	36.260	.338	.564	.007
	run3	Sphericity Assumed	18.375	1	18.375	.170	.682	.004
		Greenhouse-Geisser	18.375	1.000	18.375	.170	.682	.004
		Huynh-Feldt	18.375	1.000	18.375	.170	.682	.004
		Lower-bound	18.375	1.000	18.375	.170	.682	.004
	run4	Sphericity Assumed	10.667	1	10.667	.102	.751	.002
		Greenhouse-Geisser	10.667	1.000	10.667	.102	.751	.002
		Huynh-Feldt	10.667	1.000	10.667	.102	.751	.002
		Lower-bound	10.667	1.000	10.667	.102	.751	.002
Error(Ranking)	run1	Sphericity Assumed	5567.917	46	121.042			
		Greenhouse-Geisser	5567.917	46.000	121.042			
		Huynh-Feldt	5567.917	46.000	121.042			
		Lower-bound	5567.917	46.000	121.042			
	run2	Sphericity Assumed	4939.896	46	107.389			
		Greenhouse-Geisser	4939.896	46.000	107.389			
		Huynh-Feldt	4939.896	46.000	107.389			
		Lower-bound	4939.896	46.000	107.389			
	run3	Sphericity Assumed	4969.583	46	108.034			
		Greenhouse-Geisser	4969.583	46.000	108.034			
		Huynh-Feldt	4969.583	46.000	108.034			
		Lower-bound	4969.583	46.000	108.034			
	run4	Sphericity Assumed	4812.833	46	104.627			
		Greenhouse-Geisser	4812.833	46.000	104.627			
		Huynh-Feldt	4812.833	46.000	104.627			
		Lower-bound	4812.833	46.000	104.627			

Tests of Within-Subjects Contrasts

Source	Measure	Ranking	Type III Sum of Squares	df	Mean Square	F	Sig.	Partial Eta Squared
Ranking	run1	Linear	442.042	1	442.042	3.652	.062	.074
	run2	Linear	263.344	1	263.344	2.452	.124	.051
	run3	Linear	117.042	1	117.042	1.083	.303	.023
	run4	Linear	337.500	1	337.500	3.226	.079	.066
Ranking * Mode	run1	Linear	22.042	1	22.042	.182	.672	.004
	run2	Linear	36.260	1	36.260	.338	.564	.007
	run3	Linear	18.375	1	18.375	.170	.682	.004
	run4	Linear	10.667	1	10.667	.102	.751	.002
Error(Ranking)	run1	Linear	5567.917	46	121.042			
	run2	Linear	4939.896	46	107.389			
	run3	Linear	4969.583	46	108.034			
	run4	Linear	4812.833	46	104.627			

Tests of Between-Subjects Effects

Transformed Variable: Average

Source	Measure	Type III Sum of Squares	df	Mean Square	F	Sig.	Partial Eta Squared
Intercept	run1	33227.042	1	33227.042	461.081	.000	.909
	run2	36309.260	1	36309.260	461.912	.000	.909
	run3	32193.375	1	32193.375	376.411	.000	.891
	run4	35190.042	1	35190.042	422.657	.000	.902
Mode	run1	376.042	1	376.042	5.218	.027	.102
	run2	326.344	1	326.344	4.152	.047	.083
	run3	693.375	1	693.375	8.107	.007	.150
	run4	477.042	1	477.042	5.730	.021	.111
Error	run1	3314.917	46	72.063			
	run2	3615.896	46	78.606			
	run3	3934.250	46	85.527			
	run4	3829.917	46	83.259			

Estimated Marginal Means

Mode

Estimates

Measure	Mode	Mean	Std. Error	95% Confidence Interval	
				Lower Bound	Upper Bound
run1	Eye	16.625	1.225	14.159	19.091
	Random	20.583	1.225	18.117	23.050
run2	Eye	17.604	1.280	15.028	20.180
	Random	21.292	1.280	18.716	23.868
run3	Eye	15.625	1.335	12.938	18.312
	Random	21.000	1.335	18.313	23.687
run4	Eye	16.917	1.317	14.266	19.568
	Random	21.375	1.317	18.724	24.026

Pairwise Comparisons

Measure	(I) Mode	(J) Mode	Mean Difference (I-J)	Std. Error	Sig.(a)	95% Confidence Interval for Difference(a)	
						Lower Bound	Upper Bound
run1	Eye	Random	-3.958(*)	1.733	.027	-7.446	-.470
	Random	Eye	3.958(*)	1.733	.027	.470	7.446
run2	Eye	Random	-3.688(*)	1.810	.047	-7.330	-.045
	Random	Eye	3.688(*)	1.810	.047	.045	7.330
run3	Eye	Random	-5.375(*)	1.888	.007	-9.175	-1.575
	Random	Eye	5.375(*)	1.888	.007	1.575	9.175
run4	Eye	Random	-4.458(*)	1.863	.021	-8.207	-.709
	Random	Eye	4.458(*)	1.863	.021	.709	8.207

Based on estimated marginal means
* The mean difference is significant at the .05 level.
a Adjustment for multiple comparisons: Least Significant Difference (equivalent to no adjustments).

Multivariate Tests

	Value	F	Hypothesis df	Error df	Sig.	Partial Eta Squared
Pillai's trace	.336	5.434(a)	4.000	43.000	.001	.336
Wilks' lambda	.664	5.434(a)	4.000	43.000	.001	.336
Hotelling's trace	.505	5.434(a)	4.000	43.000	.001	.336
Roy's largest root	.505	5.434(a)	4.000	43.000	.001	.336

Each F tests the multivariate effect of Mode. These tests are based on the linearly independent pairwise comparisons among the estimated marginal means.
a Exact statistic

Univariate Tests

Measure		Sum of Squares	df	Mean Square	F	Sig.	Partial Eta Squared
run1	Contrast	188.021	1	188.021	5.218	.027	.102
	Error	1657.458	46	36.032			
run2	Contrast	163.172	1	163.172	4.152	.047	.083
	Error	1807.948	46	39.303			
run3	Contrast	346.688	1	346.688	8.107	.007	.150
	Error	1967.125	46	42.764			
run4	Contrast	238.521	1	238.521	5.730	.021	.111
	Error	1914.958	46	41.630			

The F tests the effect of Mode. This test is based on the linearly independent pairwise comparisons among the estimated marginal means.

Ranking

Estimates

Measure	Ranking	Mean	Std. Error	95% Confidence Interval	
				Lower Bound	Upper Bound
run1	1	20.750	1.272	18.189	23.311
	2	16.458	1.551	13.337	19.580
run2	1	21.104	1.316	18.454	23.754
	2	17.792	1.464	14.846	20.738
run3	1	19.417	1.413	16.572	22.261
	2	17.208	1.427	14.336	20.080
run4	1	21.021	1.258	18.488	23.554
	2	17.271	1.527	14.198	20.344

Pairwise Comparisons

Measure	(I) Ranking	(J) Ranking	Mean Difference (I-J)	Std. Error	Sig.(a)	95% Confidence Interval for Difference(a)	
						Lower Bound	Upper Bound
run1	1	2	4.292	2.246	.062	-.229	8.812
	2	1	-4.292	2.246	.062	-8.812	.229
run2	1	2	3.313	2.115	.124	-.945	7.570
	2	1	-3.313	2.115	.124	-7.570	.945
run3	1	2	2.208	2.122	.303	-2.062	6.479
	2	1	-2.208	2.122	.303	-6.479	2.062
run4	1	2	3.750	2.088	.079	-.453	7.953
	2	1	-3.750	2.088	.079	-7.953	.453

Based on estimated marginal means
a Adjustment for multiple comparisons: Least Significant Difference (equivalent to no adjustments).

Multivariate Tests

	Value	F	Hypothesis df	Error df	Sig.	Partial Eta Squared
Pillai's trace	.248	3.547(a)	4.000	43.000	.014	.248
Wilks' lambda	.752	3.547(a)	4.000	43.000	.014	.248
Hotelling's trace	.330	3.547(a)	4.000	43.000	.014	.248
Roy's largest root	.330	3.547(a)	4.000	43.000	.014	.248

Each F tests the multivariate effect of Ranking. These tests are based on the linearly independent pairwise comparisons among the estimated marginal means.
a Exact statistic

11.4. Extended Experiment

11.4.1. Steps to Target

Within-Subjects Factors

Measure: MEASURE_1

Threshold	Dependent Variable
1	t100
2	t200
3	t300

Multivariate Tests(b)

Effect		Value	F	Hypothesis df	Error df	Sig.	Partial Eta Squared
Threshold	Pillai's Trace	.868	13.098(a)	2.000	4.000	.018	.868
	Wilks' Lambda	.132	13.098(a)	2.000	4.000	.018	.868
	Hotelling's Trace	6.549	13.098(a)	2.000	4.000	.018	.868
	Roy's Largest Root	6.549	13.098(a)	2.000	4.000	.018	.868

a Exact statistic
b Design: Intercept
Within Subjects Design: Threshold

Mauchly's Test of Sphericity(b)

Measure: MEASURE_1

Within Subjects Effect	Mauchly's W	Approx. Chi-Square	df	Sig.	Epsilon(a)		
					Greenhouse-Geisser	Huynh-Feldt	Lower-bound
Threshold	.605	2.010	2	.366	.717	.926	.500

Tests the null hypothesis that the error covariance matrix of the orthonormalized transformed dependent variables is proportional to an identity matrix.

a May be used to adjust the degrees of freedom for the averaged tests of significance. Corrected tests are displayed in the Tests of Within-Subjects Effects table.

b Design: Intercept
Within Subjects Design: Threshold

Tests of Within-Subjects Effects

Measure: MEASURE_1

Source		Type III Sum of Squares	df	Mean Square	F	Sig.	Partial Eta Squared
Threshold	Sphericity Assumed	768.444	2	384.222	6.262	.017	.556
	Greenhouse-Geisser	768.444	1.434	535.989	6.262	.033	.556
	Huynh-Feldt	768.444	1.851	415.092	6.262	.020	.556
	Lower-bound	768.444	1.000	768.444	6.262	.054	.556
Error(Threshold)	Sphericity Assumed	613.556	10	61.356			
	Greenhouse-Geisser	613.556	7.168	85.591			
	Huynh-Feldt	613.556	9.256	66.285			
	Lower-bound	613.556	5.000	122.711			

Tests of Within-Subjects Contrasts

Measure: MEASURE_1

Source	Threshold	Type III Sum of Squares	df	Mean Square	F	Sig.	Partial Eta Squared
Threshold	Linear	768.000	1	768.000	29.091	.003	.853
	Quadratic	.444	1	.444	.005	.948	.001
Error(Threshold)	Linear	132.000	5	26.400			
	Quadratic	481.556	5	96.311			

Tests of Between-Subjects Effects

Measure: MEASURE_1
Transformed Variable: Average

Source	Type III Sum of Squares	df	Mean Square	F	Sig.	Partial Eta Squared
Intercept	2616.056	1	2616.056	31.830	.002	.864
Error	410.944	5	82.189			

Estimated Marginal Means

Grand Mean

Measure: MEASURE_1

Mean	Std. Error	95% Confidence Interval	
		Lower Bound	Upper Bound
12.056	2.137	6.563	17.548

Threshold

Estimates

Measure: MEASURE_1

Threshold	Mean	Std. Error	95% Confidence Interval	
			Lower Bound	Upper Bound
1	20.167	3.208	11.919	28.414
2	11.833	4.600	.008	23.658
3	4.167	1.641	-.053	8.386

Pairwise Comparisons

Measure: MEASURE_1

(I) Threshold	(J) Threshold	Mean Difference (I-J)	Std. Error	Sig.(a)	95% Confidence Interval for Difference(a)	
					Lower Bound	Upper Bound
1	2	8.333	4.645	.133	-3.608	20.274
	3	16.000(*)	2.966	.003	8.374	23.626
2	1	-8.333	4.645	.133	-20.274	3.608
	3	7.667	5.566	.227	-6.641	21.974
3	1	-16.000(*)	2.966	.003	-23.626	-8.374
	2	-7.667	5.566	.227	-21.974	6.641

Based on estimated marginal means
* The mean difference is significant at the .05 level.
a Adjustment for multiple comparisons: Least Significant Difference (equivalent to no adjustments).

Multivariate Tests

	Value	F	Hypothesis df	Error df	Sig.	Partial Eta Squared
Pillai's trace	.868	13.098(a)	2.000	4.000	.018	.868
Wilks' lambda	.132	13.098(a)	2.000	4.000	.018	.868
Hotelling's trace	6.549	13.098(a)	2.000	4.000	.018	.868
Roy's largest root	6.549	13.098(a)	2.000	4.000	.018	.868

Each F tests the multivariate effect of Threshold. These tests are based on the linearly independent pairwise comparisons among the estimated marginal means.
a Exact statistic

11.4.2. Time to Target (Per Display)

Within-Subjects Factors

Measure: MEASURE_1

Threshold	Dependent Variable
1	t100
2	t200
3	t300

Multivariate Tests(b)

Effect		Value	F	Hypothesis df	Error df	Sig.	Partial Eta Squared
Threshold	Pillai's Trace	.858	12.121(a)	2.000	4.000	.020	.858
	Wilks' Lambda	.142	12.121(a)	2.000	4.000	.020	.858
	Hotelling's Trace	6.060	12.121(a)	2.000	4.000	.020	.858
	Roy's Largest Root	6.060	12.121(a)	2.000	4.000	.020	.858

a Exact statistic
b Design: Intercept

Within Subjects Design: Threshold

Mauchly's Test of Sphericity(b)

Measure: MEASURE_1

Within Subjects Effect	Mauchly's W	Approx. Chi-Square	df	Sig.	Epsilon(a) Greenhouse-Geisser	Epsilon(a) Huynh-Feldt	Epsilon(a) Lower-bound
Threshold	.296	4.875	2	.087	.587	.659	.500

Tests the null hypothesis that the error covariance matrix of the orthonormalized transformed dependent variables is proportional to an identity matrix.

a May be used to adjust the degrees of freedom for the averaged tests of significance. Corrected tests are displayed in the Tests of Within-Subjects Effects table.

b Design: Intercept

Within Subjects Design: Threshold

Tests of Within-Subjects Effects

Measure: MEASURE_1

Source		Type III Sum of Squares	df	Mean Square	F	Sig.	Partial Eta Squared
Threshold	Sphericity Assumed	1.736	2	.868	22.979	.000	.821
	Greenhouse-Geisser	1.736	1.173	1.479	22.979	.003	.821
	Huynh-Feldt	1.736	1.317	1.318	22.979	.002	.821
	Lower-bound	1.736	1.000	1.736	22.979	.005	.821
Error(Threshold)	Sphericity Assumed	.378	10	.038			
	Greenhouse-Geisser	.378	5.867	.064			
	Huynh-Feldt	.378	6.586	.057			
	Lower-bound	.378	5.000	.076			

Tests of Within-Subjects Contrasts

Measure: MEASURE_1

Source	Threshold	Type III Sum of Squares	df	Mean Square	F	Sig.	Partial Eta Squared
Threshold	Linear	1.666	1	1.666	26.782	.004	.843
	Quadratic	.070	1	.070	5.252	.070	.512
Error(Threshold)	Linear	.311	5	.062			
	Quadratic	.067	5	.013			

Tests of Between-Subjects Effects

Measure: MEASURE_1
Transformed Variable: Average

Source	Type III Sum of Squares	df	Mean Square	F	Sig.	Partial Eta Squared
Intercept	9.394	1	9.394	150.236	.000	.968
Error	.313	5	.063			

Estimated Marginal Means

Grand Mean

Measure: MEASURE_1

Mean	Std. Error	95% Confidence Interval Lower Bound	95% Confidence Interval Upper Bound
.722	.059	.571	.874

Threshold

Estimates

Measure: MEASURE_1

Threshold	Mean	Std. Error	95% Confidence Interval	
			Lower Bound	Upper Bound
1	.394	.012	.363	.425
2	.634	.047	.514	.755
3	1.139	.144	.770	1.509

Pairwise Comparisons

Measure: MEASURE_1

(I) Threshold	(J) Threshold	Mean Difference (I-J)	Std. Error	Sig.(a)	95% Confidence Interval for Difference(a)	
					Lower Bound	Upper Bound
1	2	-.240(*)	.052	.006	-.373	-.107
	3	-.745(*)	.144	.004	-1.115	-.375
2	1	.240(*)	.052	.006	.107	.373
	3	-.505(*)	.120	.008	-.813	-.197
3	1	.745(*)	.144	.004	.375	1.115
	2	.505(*)	.120	.008	.197	.813

Based on estimated marginal means
* The mean difference is significant at the .05 level.
a Adjustment for multiple comparisons: Least Significant Difference (equivalent to no adjustments).

Multivariate Tests

	Value	F	Hypothesis df	Error df	Sig.	Partial Eta Squared
Pillai's trace	.858	12.121(a)	2.000	4.000	.020	.858
Wilks' lambda	.142	12.121(a)	2.000	4.000	.020	.858
Hotelling's trace	6.060	12.121(a)	2.000	4.000	.020	.858
Roy's largest root	6.060	12.121(a)	2.000	4.000	.020	.858

Each F tests the multivariate effect of Threshold. These tests are based on the linearly independent pairwise comparisons among the estimated marginal means.
a Exact statistic

11.4.3. Fixation Numbers (Per Display)

Within-Subjects Factors

Measure: MEASURE_1

Threshold	Dependent Variable
1	t100
2	t200
3	t300

Multivariate Tests(b)

Effect		Value	F	Hypothesis df	Error df	Sig.	Partial Eta Squared
Threshold	Pillai's Trace	.770	6.694(a)	2.000	4.000	.053	.770
	Wilks' Lambda	.230	6.694(a)	2.000	4.000	.053	.770
	Hotelling's Trace	3.347	6.694(a)	2.000	4.000	.053	.770

Roy's Largest Root	3.347	6.694(a)	2.000	4.000	.053	.770

a Exact statistic
b Design: Intercept
Within Subjects Design: Threshold

Mauchly's Test of Sphericity(b)

Measure: MEASURE_1

Within Subjects Effect	Mauchly's W	Approx. Chi-Square	df	Sig.	Epsilon(a) Greenhouse-Geisser	Huynh-Feldt	Lower-bound
Threshold	.550	2.388	2	.303	.690	.867	.500

Tests the null hypothesis that the error covariance matrix of the orthonormalized transformed dependent variables is proportional to an identity matrix.
a May be used to adjust the degrees of freedom for the averaged tests of significance. Corrected tests are displayed in the Tests of Within-Subjects Effects table.
b Design: Intercept
Within Subjects Design: Threshold

Tests of Within-Subjects Effects

Measure: MEASURE_1

Source		Type III Sum of Squares	df	Mean Square	F	Sig.	Partial Eta Squared
Threshold	Sphericity Assumed	19.654	2	9.827	12.196	.002	.709
	Greenhouse-Geisser	19.654	1.380	14.245	12.196	.008	.709
	Huynh-Feldt	19.654	1.734	11.332	12.196	.004	.709
	Lower-bound	19.654	1.000	19.654	12.196	.017	.709
Error(Threshold)	Sphericity Assumed	8.058	10	.806			
	Greenhouse-Geisser	8.058	6.899	1.168			
	Huynh-Feldt	8.058	8.672	.929			
	Lower-bound	8.058	5.000	1.612			

Tests of Within-Subjects Contrasts

Measure: MEASURE_1

Source	Threshold	Type III Sum of Squares	df	Mean Square	F	Sig.	Partial Eta Squared
Threshold	Linear	18.548	1	18.548	16.016	.010	.762
	Quadratic	1.106	1	1.106	2.440	.179	.328
Error(Threshold)	Linear	5.790	5	1.158			
	Quadratic	2.267	5	.453			

Tests of Between-Subjects Effects

Measure: MEASURE_1
Transformed Variable: Average

Source	Type III Sum of Squares	df	Mean Square	F	Sig.	Partial Eta Squared
Intercept	76.076	1	76.076	64.719	.000	.928
Error	5.877	5	1.175			

Estimated Marginal Means

Grand Mean

Measure: MEASURE_1

Mean	Std. Error	95% Confidence Interval Lower Bound	95% Confidence Interval Upper Bound
2.056	.256	1.399	2.713

Threshold

Estimates

Measure: MEASURE_1

Threshold	Mean	Std. Error	95% Confidence Interval	
			Lower Bound	Upper Bound
1	.988	.045	.872	1.104
2	1.705	.272	1.005	2.405
3	3.474	.623	1.873	5.076

Pairwise Comparisons

Measure: MEASURE_1

(I) Threshold	(J) Threshold	Mean Difference (I-J)	Std. Error	Sig.(a)	95% Confidence Interval for Difference(a)	
					Lower Bound	Upper Bound
1	2	-.717	.303	.064	-1.496	.061
	3	-2.486(*)	.621	.010	-4.084	-.889
2	1	.717	.303	.064	-.061	1.496
	3	-1.769(*)	.573	.027	-3.242	-.297
3	1	2.486(*)	.621	.010	.889	4.084
	2	1.769(*)	.573	.027	.297	3.242

Based on estimated marginal means
* The mean difference is significant at the .05 level.
a Adjustment for multiple comparisons: Least Significant Difference (equivalent to no adjustments).

Multivariate Tests

	Value	F	Hypothesis df	Error df	Sig.	Partial Eta Squared
Pillai's trace	.770	6.694(a)	2.000	4.000	.053	.770
Wilks' lambda	.230	6.694(a)	2.000	4.000	.053	.770
Hotelling's trace	3.347	6.694(a)	2.000	4.000	.053	.770
Roy's largest root	3.347	6.694(a)	2.000	4.000	.053	.770

Each F tests the multivariate effect of Threshold. These tests are based on the linearly independent pairwise comparisons among the estimated marginal means.
a Exact statistic

11.4.4. Eye and Random Comparison

Between-Subjects Factors

		N
Mode	Eye	6
	Random	6

Multivariate Tests(b)

Effect		Value	F	Hypothesis df	Error df	Sig.	Partial Eta Squared
Intercept	Pillai's Trace	.942	43.598(a)	3.000	8.000	.000	.942
	Wilks' Lambda	.058	43.598(a)	3.000	8.000	.000	.942
	Hotelling's Trace	16.349	43.598(a)	3.000	8.000	.000	.942
	Roy's Largest Root	16.349	43.598(a)	3.000	8.000	.000	.942
Mode	Pillai's Trace	.704	6.348(a)	3.000	8.000	.016	.704

	Wilks' Lambda	.296	6.348(a)	3.000	8.000	.016	.704
	Hotelling's Trace	2.381	6.348(a)	3.000	8.000	.016	.704
	Roy's Largest Root	2.381	6.348(a)	3.000	8.000	.016	.704

a Exact statistic
b Design: Intercept+Mode

Tests of Between-Subjects Effects

Source	Dependent Variable	Type III Sum of Squares	df	Mean Square	F	Sig.	Partial Eta Squared
Corrected Model	t100	5.333(a)	1	5.333	.056	.817	.006
	t200	602.083(b)	1	602.083	9.484	.012	.487
	t300	690.083(c)	1	690.083	10.390	.009	.510
Intercept	t100	4563.000	1	4563.000	48.048	.000	.828
	t200	4294.083	1	4294.083	67.641	.000	.871
	t300	1656.750	1	1656.750	24.945	.001	.714
Mode	t100	5.333	1	5.333	.056	.817	.006
	t200	602.083	1	602.083	9.484	.012	.487
	t300	690.083	1	690.083	10.390	.009	.510
Error	t100	949.667	10	94.967			
	t200	634.833	10	63.483			
	t300	664.167	10	66.417			
Total	t100	5518.000	12				
	t200	5531.000	12				
	t300	3011.000	12				
Corrected Total	t100	955.000	11				
	t200	1236.917	11				
	t300	1354.250	11				

a R Squared = .006 (Adjusted R Squared = -.094)
b R Squared = .487 (Adjusted R Squared = .435)
c R Squared = .510 (Adjusted R Squared = .461)

Estimated Marginal Means

Mode

Estimates

Dependent Variable	Mode	Mean	Std. Error	95% Confidence Interval	
				Lower Bound	Upper Bound
t100	Eye	20.167	3.978	11.302	29.031
	Random	18.833	3.978	9.969	27.698
t200	Eye	11.833	3.253	4.586	19.081
	Random	26.000	3.253	18.752	33.248
t300	Eye	4.167	3.327	-3.247	11.580
	Random	19.333	3.327	11.920	26.747

Pairwise Comparisons

Dependent Variable	(I) Mode	(J) Mode	Mean Difference (I-J)	Std. Error	Sig.(a)	95% Confidence Interval for Difference(a)	
						Lower Bound	Upper Bound
t100	Eye	Random	1.333	5.626	.817	-11.203	13.870
	Random	Eye	-1.333	5.626	.817	-13.870	11.203

t200	Eye	Random	-14.167(*)	4.600	.012	-24.416	-3.917
	Random	Eye	14.167(*)	4.600	.012	3.917	24.416
t300	Eye	Random	-15.167(*)	4.705	.009	-25.651	-4.683
	Random	Eye	15.167(*)	4.705	.009	4.683	25.651

Based on estimated marginal means
* The mean difference is significant at the .05 level.
a Adjustment for multiple comparisons: Least Significant Difference (equivalent to no adjustments).

Multivariate Tests

	Value	F	Hypothesis df	Error df	Sig.	Partial Eta Squared
Pillai's trace	.704	6.348(a)	3.000	8.000	.016	.704
Wilks' lambda	.296	6.348(a)	3.000	8.000	.016	.704
Hotelling's trace	2.381	6.348(a)	3.000	8.000	.016	.704
Roy's largest root	2.381	6.348(a)	3.000	8.000	.016	.704

Each F tests the multivariate effect of Mode. These tests are based on the linearly independent pairwise comparisons among the estimated marginal means.
a Exact statistic

Univariate Tests

Dependent Variable		Sum of Squares	df	Mean Square	F	Sig.	Partial Eta Squared
t100	Contrast	5.333	1	5.333	.056	.817	.006
	Error	949.667	10	94.967			
t200	Contrast	602.083	1	602.083	9.484	.012	.487
	Error	634.833	10	63.483			
t300	Contrast	690.083	1	690.083	10.390	.009	.510
	Error	664.167	10	66.417			

The F tests the effect of Mode. This test is based on the linearly independent pairwise comparisons among the estimated marginal means.

Chapter 12. Appendix C: Overview of Eye Trackers

12.1. EyeLink II (SR Research Ltd)

SR Research Ltd has the head-mounted Eyelink II and the head-supported Eyelink 1000 eye trackers. The Eyelink 1000 samples at 1 KHz.

EyeLink II® Tracking Modes

Mode	Sample Rate	Avg. Delay (Filter off/normal/ high)	Noise (RMS)	Stability
EyeLink Pupil-Only	250 Hz	6 ms / 10 ms	< 0.01°	Affected by headband slip and vibration
EyeLink II Pupil-Only	500 Hz	3 ms / 5 ms / 7ms	< 0.01°	Affected by headband slip and vibration
EyeLink II Pupil-CR	250 Hz	6 ms / 10 ms / 14 ms	< 0.022°	Good rejection of slip and vibration

Operational/Functional Specifications

Feature	EyeLink II	EyeLink
Image processing	Fully digital	Hybrid analog-digital
Pupil tracking	Hyperacuity	Hyperacuity
Corneal reflection tracking	Hyperacuity, ultra low noise	None
Sampling rate	250 or 500 Hz	250 Hz
Average data transit delay	250 Hz, filter off = 6 ms 250 Hz, filter on = 10 ms	filter off = 6 ms filter on = 10 ms

	500 Hz, filter off = 3 ms 500 Hz, filter on = 5 ms	
Resolution (Gaze)	Noise limited to <0.01° (pupil), <0.022° (pupil-CR)	Noise limited to < 0.01°
Velocity noise	< 3°/sec	<3°/sec
Gaze position accuracy	<0.5° average	<0.5° average
Pupil size: resolution and noise	0.1% of diameter (~0.004mm), Noise level < 0.01mm	0.1% of diameter (~0.004mm), Noise level < 0.01mm
Heuristic Filtering	Average velocity-matched filter	Nearest-neighbor heuristic filter
Eye tracking range	±30° horizontal, ±20° vertical in pupil only mode	±30° horizontal, ±20° vertical (pupil only)
Gaze tracking range	±20° horizontal, ±18° vertical	±20° horizontal, ±18° vertical
Head tracking range	40-140 cm (standard setup),~300 cm (special markers)	40-140 cm (standard setup),~300 cm (special markers)
Head rotation compensation range	±15° for best accuracy, ±30° conditional on gaze angle.	±15° for best accuracy, ±30° conditional on display location
Built-in calibration, validation	Calibration / validation using Pupil or Pupil-Corneal	Calibration and validation using Pupil-only
Operating environment	Tolerates significant indirect IR, CR mode can reject more slippage than pupil only mode.	Required IR-free environment, physical stability
Subject compatibility	Most eyeglasses and contact lenses in pupil only mode: less compatibility in CR mode.	Most eyeglasses and contact lenses
Data file	EDF	EDF, direct to disk
EDF file and link Data Types	Eye position, HREF position, gaze position, pupil size, buttons, messages, digital inputs.	Eye position, HREF position, gaze position, pupil size, buttons, messages
On-line eye movement analysis	Saccades, fixations, blinks, fixation updates	Saccades, fixations, blinks, fixation updates
Real-time operator feedback	Eye position cursor during calibration, validation, and recording. Camera images and tracking status.	Gaze cursor during recording and validation, eye position cursor during calibration, camera images.

Physical Specifications		
Feature	EyeLink II	EyeLink
EyeLink II Card	Half-length PCI (6.8"/176mm)	Full-length ISA (13.5"/343mm)
Headband	Headband Padded with height and size adjustments	Leather-padded, height and size adjustments

Headband weight	~420 grams, low center of gravity	~600 grams
Headband cable length	4.2meters	5 meters
Eye camera distance	40 to 80 mm	40 to 80 mm
Binocular tracking	Standard	Standard
Eye Illumination	925 nm IR (pupil) 880 nm IR (CR), IEC-825 Class 1, <1.2 mW/cm2	925 nm IR, IEC-825 Class 1, <1.2 mW/cm2
Display Markers	880 nm IR, IEC-825 Class 1	925 nm IR, IEC-825 Class 1
Ethernet Link	TCP/IP or raw, 10BASE-T, built into EyeLink II card	TCP/IP or raw, 10BASE-2 or 10BASE-T, external card with packet driver
Response box support	USB or digital	Digital
Analog output	Optional PCI card	Optional ISA or PCI card
Digital Control	Configurable	Configurable
Display Operating system API	Windows (2000, XP Professional Service Pack 1), MS-DOS, Macintosh OSX, Linux	MS-DOS, Macintosh, Windows (95 and 98)

EyeLink 1000 Tracking Modes

Mode	Sampling Rate	Sample Access Delay* Filter (Off/Normal/High)	Noise** (RMS) Filter(Off/Normal/High)
Pupil-CR	1000 Hz	< 2 ms / < 3 ms / < 4 ms	<0.02° / <0.01° / <0.01°
Pupil Only†	1000 Hz	< 2 ms / < 3 ms / < 4 ms	<0.01° / <0.01° / <0.01°

* Average End to End latency, measured from an actual physical event to availability of first data sample that registered the event on the Display / Subject PC via Ethernet or Analog output.
Actual "processing time" for each sample is < 0.5 msec.
** Measured using an artificial eye.
† With immobilized head / use of bitebar.

EyeLink 1000 Specifications

Feature	EyeLink 1000 Head Supported

Average Accuracy	down to 0.15° (0.25° to 0.5° typical) (measured with real eye fixations at multiple screen positions)
Spatial Resolution	Noise Limited, see the above EyeLink 1000 Tracking Mode table
Pupil Size Resolution	0.2% of diameter
Gaze Tracking Range	+/- 30° Horizontal, +/- 20° Vertical
Allowed Head Movement	+/- 25 mm Horizontal and Vertical, +/- 10 mm Depth
Online Event Parsing	Fixation / Saccade / Blink / Fixation Update
Realtime Operator Feedback	Eye position cursor during calibration,validation, and recording. Camera images and tracking status.
Eye Illumination	910 nm, Class 1 LED Product, <1.0 mW/cm2 in standard configuration
Headrest Dimensions	Approx. 40 cm x 75 cm x 27 cm (width x height x depth)
Digital Data Access	Ethernet
Analog Output	Optional PCI card
Response Box	7 Button USB response pad included
Host Operating System	DOS
Display Operating System	Windows, Linux, Mac OSX, Mac OS9, DOS
Approvals	FCC and CISPR Class A, 60950-1 ITE Equipment

12.2. Eyegaze (LC Technologies Inc)

LC Technologies manufactures a remote Eyegaze eye tracker and recently released the EyeFollower which is capable of free head motion within the workstation environment.

Eyegaze System Performance Specifications

Accuracy

Eyegaze Measurement	**Angular Gaze Orientation**	**Spatial Gaze Point (with head 20" (51 cm) from camera)**
Typical Average Bias Error* (over the monitor screen range)	0.45 degree	0.15 inch (0.38 cm)
Maximum Average Bias Error* (over the monitor screen range)	0.70 degree	0.25 inch (0.63 cm)
Frame-to-frame variation+	0.18 degree	0.06 inch (0.15 cm)

(1-sigma variation with eye fixed on a point)

* Bias errors result from inaccuracies in the measurement of head range, asymmetries of the pupil opening about the eye's optic axis, and astigmatism. They are constant from frame to frame and cannot be reduced by averaging or smoothing.

+ Frame-to-frame variations result from image brightness noise and pixel position quantization in the camera image and may be reduced by averaging or smoothing.

Speed

Sampling Rate: 60 Hertz camera field rate

Angular Gazetrack Range

Gaze Cone Diameter: 80 degrees, typical

Tolerance To Head Motion

Lateral Range: 1.5 inch (3.8 cm)

Vertical Range: 1.2 inch (3.0 cm)

Longitudinal Range: 1.5 inch (3.8 cm)

Computer Usage

Memory Consumption: 6 MB

CPU Time Consumption: 30-50%

Light Emitting Diode

Wave Length: 880 nanometers (near infrared)

Beam Width: 20 degrees, between half power points

Radiated Power: 20 milliwatts, radiated over the 20 degree beam width

Safety Factor: 5 -- At a range of 15 inches the LED illumination on the eye is 20% of the HEW max permissible exposure.

Totally Free Head Motion

Automatic Eye Acquisition
Binocular Eyetracking - The Eyefollower™ tracks both eyes over the full range of head motion. The gazepoint sampling rate is 120 Hz.
High Gazepoint Tracking Accuracy - The Eyegaze System achieves its highly accurate 0.45 degree gazepoint tracking accuracy throughout the operational head range.
Easy User Calibration - The user calibration employs the same, easy procedure used with the fixed-camera Eyegaze System.

Eyefollower™ Specifications:

Head Motion Volume:	Side to side	20 inches	(51 cm)
	Up and down	12 inches	(30 cm)
	Back and forth	15 inches	(38 cm)
Head Speed:		8 inches/sec	(20 cm/sec)
Head Accelerations:		20 inches/sec-sq	(50 cm/sec-sq)

12.3. ASL 6000 Series

Model H6

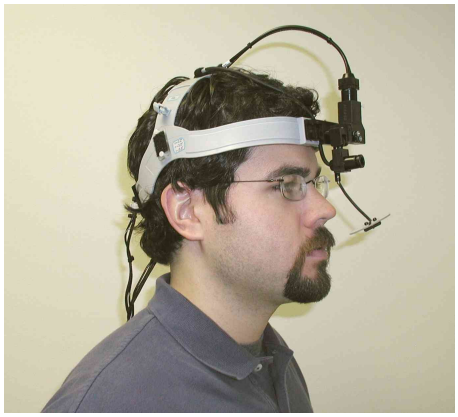

Control Unit:

Dimensions (H/W/D): 3 in/9.75 in/10.25 in

Weight: 4.25 lbs

Power: 100-240 VAC

25 watts

Display: 9 inch b&w monitors for eye and scene cameras

Head mounted optics:

Sampling and Output Rates: 50 Hz or 60 Hz 120, 240 and 360Hz (optional)

Measurement principle: pupil-corneal reflection

System accuracy: 0.5 degree visual angle

Resolution: 0.1 degree visual angle

Head movement: unlimited

Visual range: 50 degrees horizontally, 40

Model R6

Control Unit:

Dimensions (H/W/D): 3in / 9.75in / 10.25in

Weight: 4.25 lbs.

Power: 100-240 VAC; 25 watts

Display: 9 inch b&w monitors for eye and scene cameras

Remote Optics:

Sampling and Output Rates: 50 Hz or 60 Hz, 120,240, 360Hz (optional)

Measurement principle: pupil-corneal reflection

System accuracy: 0.5 degree visual angle

Resolution: 0.25 degree visual angle

Head movement: one square foot

Max. distance optics to eye: 40 in

Visual range: 50 degrees horizontally, 40 degrees vertically

degrees vertically	Dimensions (H/W/D): 4 in/5.5 in/6 in
Weight 8 oz (includes headband, optics module monocle and scene camera	Weight: 2.75 pounds
Included equipment:	**Included Equipment:**
Series 6000 Control Unit	Series 6000 Control Unit
Headband Mounted Optics	Remote Mounted Optics
Head Mounted Scene Camera (color)	Scan converter
Display Monitors (x2), black & white (or two PCI framgrabbers)	Display Monitors (x2), black & white or two PCI framegrabbers
EYEPOS operating software	EYEPOS operating software
EYENAL data analysis software	EYENAL and FIXPLOT data analysis software

12.4. SMI's iView X

The iViewX Hi-Speed 1250 eye tracker samples at up to 1250Hz.

iView X: Technical Details	**Hi-Speed (Remote)**	**HED (Head Mounted)**
Sampling Rate	240 / 350 / 500 / 1250 Hz	50/60 Hz
Tracking Resolution, Pupil/CR	< 0.01°	0.1 deg. (typ.)
Gaze Position Accuracy	down to 0.2°	0.5°-1.0 deg. (typ.)
Viewing Angle (horizontal/vertical)	± 30° / 30° (up) 45° (down)	+/- 30° horz., +/-25° vert.
Head Tracking Area	40 x 40 cm at 80 cm dist.	
Weight of head unit		450 g

12.5. FaceLAB 4

The tracking volume of faceLAB 4 is flexible and can be adjusted to meet a wide variety of scenarios. The tracking field-of-view can be configured from 45 degrees down to less than 10 degrees. Wider field-of-view (zoomed out) allows for large unconstrained head motions, whilst a narrow field-of-view (zoomed in) allows for either precision gaze, or long range tracking.

Smallest Face

• Automatic tracking initialisation when face is only 20 percent of total image width;

• 6 DOF head tracking and recovery when face is only 10 percent of total image width.

Largest Face

• Continues to track when face is so close, only half of it is visible.

Head Rotations

• Tracking and recovery up to +/- 90° around neck axis (turn head from shoulder to shoulder);

• Tracking and recovery up to +/- 45° around nod axis (look up / look down);

• Tracking up to +/- 90° and recovery up to +/- 30° around tilt axis (lean left / right).

Gaze Rotations

• Eye rotations of +/- 45°.

Recovery Time

• Tracking failure recovery times approximately 200ms for both head and eye measurements.

Obscuration

• Tracking when up to 50% of face is obscured;

• Recovery requires 80% of face to be visible.

Wide Field-Of-View Configuration

In this configuration, head-position and rotation can be automatically tracked over large volumes, without calibration.

• Camera field of view out to 45°;

• Head tracking distance range from 0.5 to 1.4m;

• Head tracking horizontal range up to 1.5m.

faceLAB Classic Configuration†

In this configuration, both head-pose and gaze tracking are possible. Gaze calibration is not required, but can be performed to remove any systematic bias. Resolution is not affected. The specifications are similar

to previous versions of faceLAB, with the exception that tracking recovery and robustness to large rotations is greatly improved.

• Camera field of view out to 30°;

• Gaze tracking distance range from 0.5 to 1.1m;

• Gaze tracking horizontal range up to 0.3m, vertical range up to 0.2m;

• Head tracking distance range from 0.5 to 1.75m;

• Head tracking horizontal range up to 1m;

• Typical static accuracy of head measurement within +/- 1mm of translational error and +/- 1° of rotational error;

• Typical static accuracy of gaze direction measurement within +/- 5° rotational error.

Precision Gaze Configuration†

In this configuration, both head-pose and gaze tracking are possible. Gaze tracking is more precise; with the trade-off that head-pose is a little more constrained. This configuration is recommended for indoor screen or simulator experiments, where accuracy is at a premium.

• Camera field of view out to 30°;

• Precision gaze tracking distance range from 0.5 to 0.8m;

• Precision gaze horizontal range up to 0.25m, vertical range up to 0.15m;

• Conventional gaze tracking distance range from 0.8 to 1.1m;

• Head tracking distance range from 0.5 to 1.4m;

• Head tracking horizontal range up to 0.5m;

• Typical static accuracy of gaze direction measurement within 1° rotational error;

• Pupil diameter (independent left/right eyes);

• Eye vergence distance (meters);

12.6. Tobii 1750 and x50 Eye-trackers

The Tobii 1750 eye-tracker is integrated into a TFT monitor. It is ideal for all studies with stimuli that can be presented on a monitor, such as slideshows, movies and text.

Accuracy	0.5 deg
Drift	< 1 deg
Frame rate	50 fps
Top head-motion speed	~10 cm/s
Time to tracking recovery	< 100 ms
Max gaze angles	+/- 40 deg
Tracking type	Binocular
Freedom of head-movement	30x15x20 cm
Head-movement compensation	< 1 deg error
Integrated monitor	17 TFT, 1280x1024 pixels

The Tobii x50 eye-tracker is a stand-alone unit designed for eyetracking studies relative to any plane, such as a monitor, a projection screen or an object set on a table.

Accuracy	0.5 degrees
Drift	< 1 degree
Tracking type	Binocular
Frame rate	50 fps
Top head-motion speed	~10 cm/s
Time to tracking recovery	< 100 ms
Max gaze angles	+/- 35 degrees
Freedom of head-movement	30x15x20 cm
Head-movement compensation	< 1 degree error
Accessories	Scene camera, calibration grid

12.7. CRS' EyeLock

Cambridge Research Systems produces a low cost, robust 50Hz video eyetracking.system for £6000 and has recently launched its newer 250Hz system.

Measurement technique	Video. Pupil and dual first Purkinje image	Video. Pupil and dual first Purkinje image
Guaranteed sampling frequency	50Hz	250Hz with no dropped frames
Resolution	0.1°	0.05°
Accuracy	0.5° - 0.25°	0.125° - 0.25°
Horizontal range	±40°	±40°
Vertical range	±20°	±20°
Allowable head movement	±10mm	±10mm
Latency	One frame (20ms)	
Measurement units	Fick, Helmholtz coordinates in degrees and screen position in mm	Fick, Helmholtz coordinates in degrees and screen position in mm

CPU utilization	10% for eye tracking with mimic and camera window (typical on a 1.8GHz Athlon processor)	25% for eye tracking with mimic and camera window (typical)
Software triggers	Implemented as Callback to user routine when subject looks into Region of Interest (ROI)	Implemented as Callback to user routine when subject looks into Region of Interest (ROI)
Number of ROIs	Over 100	Over 100
Infrared illumination wavelength	930nm	930nm
Camera type	50Hz	250Hz digital camera
Connection to PC		firewire
Image Capture	Dedicated 32 bit, 33Mhz, PCI bus-mastering frame grabber for PC	

12.8. The Erica System

ERICA'S EYE TRACKING CAMERA

THE HARDWARE OF THE ERICA SYSTEM

ERT's patented eye-tracking system, the Eye-gaze Response Interface Computer Aid (ERICA), is noninvasive and requires no attachments to be worn by the user. The system uses a camera and infrared light to create effects off the user's eye. These effects are used to compute where someone is looking. The camera and light source are compact units that can be used with any Windows based desktop or laptop or tablet PC system. It can also be mounted on a wheelchair. Furthermore, ERICA can accurately calculate the gaze position for people wearing glasses and contacts. The system can identify where someone is looking 60 times a second and has an accuracy rating of 0.5 degrees visual angle. This translates to approximately 0.5 to 1 centimeter

accuracy on a computer monitor when sitting at a normal viewing distance. ERICA's imaging system is fully integrated into the Windows™ 95, 98, ME, NT, 2000, or XP platforms.

12.9. Smart Eye Pro

Smart Eye Pro is targeted for users and applications that require high-accuracy measurements of head pose and gaze in 3 dimensions at full frame rate. Smart Eye Pro features:

- Measurements performed at frame rate (currently up to 60 Hz).
- Allows for large head motions (translation and rotation) using two or more cameras.
- Easily adaptable to various measurement situations with flexible camera mount positions.
- Handles occluded cameras using 3D head models.
- Handles high illumination variations (works in complete darkness) using active IR illumination.
- Fast intrinsic and extrinsic camera calibration through a simple checkerboard procedure.
- Pixel density approximately 15 pixels per degree. The pixel density is given by the formula pd = Pi/180 f/p_ccd, where f is the focal length [m], and p_ccd is the physical size of a pixel element [m]. Typical values for a Smart Eye system are f = 6mm and p_ccd = 7.26um which gives pd ~ 15 pixel/degree.
- Accuracy of head pose: Rotation 0,5 degrees Translation < 1 mm2.
- Accuracy of gaze-vector measurement: 1 degree3.
- Eyelid closure is measured in up to 60 discrete steps.
- Consensus and quality values for all measurement values.
- Graphical tools for definition of gaze zones and visualization of gaze tracks.
- Scene camera extension for overlay of users view.
- Statistical tools on demand for post-processing of measurement data.
- Easy to use Active-X interface to other windows applications.

12.10. Viewpoint Eyetracker

Technical Information

- Tracking Method: Infrared video, bright pupil or dark pupil or monocular.

- Software: PC or Mac.
- Measurement principle: Pupil only, corneal reflection only, or both.
- Accuracy: Approximately 0.25° - 1.0° visual arc on PC and 0.5° - 1.0° visual arc on Mac.
- Spatial resolution*: Approximately 0.15° visual arc on PC and 0.25° visual arc on Mac.
- Temporal resolution: Selectable by the user between 60 Hz & 30 Hz on PC and 30 Hz on Mac.
- Allowable head movement: Small movements allowed. Subject's pupil and corneal reflection must remain within the camera image.
- Visual range: +/- 44° of visual arc horizontally and +/- 20 ° of visual arc vertically.
- Pupil size resolution: Measures pupil height and width to better than 0.03 mm instantaneous (no averaging).
- Calibration: starts in a roughly calibrated state that is adequate for determining screen quadrants or other relative movement measurement such as objective preference-of-looking tasks. For accurate position of gaze, calibration is required only once per subject. New subject setup time between 1-5 minutes. Calibration settings can be stored and reused each time a subject returns. Easy Slip Correction feature and re-presentation of stray calibration points.
- Auto threshold: The program scans over the video image for the pupil and / or for the corneal reflection. The luminance threshold for discriminating these can be adjusted. The auto threshold feature provides good threshold levels automatically. Little or no manual adjustment required.
- Blink suppression: Automatic blink detection and suppression.
- Data recorded: Eye data includes X, Y position of gaze, pupil height and width, ocular torsion, delta time, total time, and regions of interest (ROI). Asynchronous records include state transition markers, key presses and data from other programs. Data is stored in ASCII files. Movies of the eye are recorded and analyzed.
- Real-time display: Gaze point history, gaze trace, fixation duration, pupil size and ROIs, can be graphically displayed over stimulus image. Visible to the user and / or the subject. Real-time pen plots of X and Y position of gaze, velocity, ocular torsion, pupil width and pupil aspect ratio.
- Hardware provided: IR Camera, one 940nm IR-LED for illumination, Head Positioner & Camera Mount, PCI video capture and display card for Mac, PCI video capture card for PC, universal power supply and all required cables.
- System requirements: Pentium compatible machine (except DELL Dimension or Optiplex) running Windows 98 or higher on PC and OS 8.6 - 9.x on Mac.

12.11. MicroGuide (Series 1000 Binocular Infrared Recording System (BIRO))

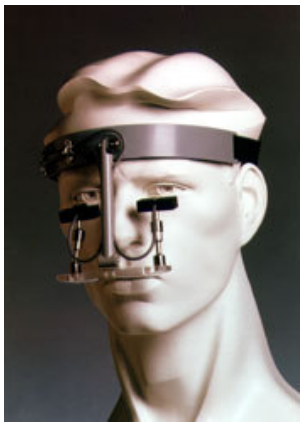

A unique method of recording eye movement based on the reflective characteristics of the front surface of the human eye. Simultaneous presentation of the infrared light (IR) and the detection of the reflected IR from the eye produce a signal corresponding to horizontal and vertical eye movement. The system is non-contact, lightweight, and easily applied to the subject. The variety and simplicity of adjustments allow fast set-up time. The mechanical stability and ease of use is due to the unique design of the headband. All paradigms and tests which involve precise recording of all classes of eye movement are accurately recorded. The system is of proven value in the clinical and research laboratory.

Features

Low Noise: Better than 0.1 degrees resolution

Low Drift: not limited by electronics of the system, excellent DC accuracy

Binocular horizontal and monocular vertical recording available simultaneously

Non-contact infrared technique does not require attachments to the eye or skin

Does not depend on the corneo-retinal potential

Calibration and adjustment in one minute

Comfortable and lightweight

Specifications

Sensitivity: At least 0.1 degree

Bandwidth: 0-100 Hz, 0-40 Hz selectable

Accuracy: Drift not limited by the electronics, excellent DC accuracy, no drift

Recording range: ± 30 degrees horizontal ± 20 degrees vertical

Linear range: within 10% up to ± 20 degrees horizontal within 10% up to ± 10 degrees vertical

Crosstalk: 10-20% minimum interference between horizontal and vertical signal from the same eye

Field of View: Unlimited horizontal, minimally restricted downward vertical

Adjustment: Three-dimensional adjustment for positioning, 40-70 mm interpupillary range

Interface: Direct to ENG MODULE or 5000 Series processor for analog output.

System Options

Available in 1-4 channel configurations

MODEL NO.	DESCRIPTION
1100	Single Channel Horizontal
1200	Dual Channel - Monocular Horizontal & Vertical or Binocular Horizontal
1300	3 Channel - Binocular Horizontal and Monocular Vertical
1400	4 Channel - Binocular Horizontal and Vertical

12.12. Quick Glance 2

Quick Glance 2 is a mouse replacement device designed for Microsoft Windows 98/XP developed by EyeTech Digital Systems. It allows the user to place the mouse pointer anywhere on the screen simply by looking at the desired location. Clicking can be done with an eye blink, a hardware switch, or by staring (dwell). Typical users are persons with disabilities: ALS, MS, CP, SCI, RSI and anyone who cannot use a standard mouse. Quick Glance 2 allows for a much greater range of head motion than Quick Glance 1, however, some head stability is still required. See the product comparison chart for details.

Product Comparison Chart

	Quick Glance 1	Quick Glance 2B	Quick Glance 2S	Quick Glance 2SH
Portability	Desktop Only	Desktop/Laptop	Desktop/Laptop	Desktop/Laptop
Connection to PC	Internal PCI card	1394 Port	1394 Port	1394 Port
Head Movement	4 by 4 cm	6 by 6 cm	6 by 6 cm	10 by 10 cm
*Motion Tolerance	2	3	4	4
*Lighting Tolerance	2	2	4	4
Speed (fps)	30	30	30	15
Camera Type	Analog	Digital	Digital with Strobe	High-Resolution Digital with Strobe

* Rated on a scale of 1 to 5: 1 = poor, 5 = perfect

Technical Specifications

- System Requirements: Pentium 800 MHz or faster, one available 1394 (FireWire) port and Windows 98/XP
- Tracking Method: Video, dark pupil, infrared illumination.
- Accuracy: 1 degree (approximate).

- Temporal Resolution: Adjustable, up to 30 samples per second for models 2B and 2S and up to 15 samples per second for model 2SH.
- Physical Configuration: For desktop computers the video camera and lights mount on the front of the computer monitor. For laptop computers the video camera is mounted on a stand which is placed on the keyboard. The IR lights are attached to the back of the laptop display and fold out toward the user. Nothing is attached to the user.
- Allowable Head Movement: The user's eye must be kept in the camera's field of view. This is about 6 by 6 cm for models 2B and 2S and about 10 x 10 cm for model 2SH. A folding chair with adjustable headrest can be purchased separately to aid in maintaining proper head position.
- Processing Hardware: The eye-tracker is hosted on a desktop or laptop PC (800 MHz or faster) running Windows 98/ XP. The PC must also have a 1394 (Firewire Port).
- Infrared Illumination: Illumination provided by LEDs with output at 880 nm. Irradiance at the user's eye under normal operating conditions is less than 0.5 mw per square cm.
- Calibration: The software displays 16 targets on the screen, which the user looks at in succession. Calibration done once and then used for subsequent sessions. Multiple users allowed with individual calibrations saved for each.

12.13. ISCAN's Visiontrak System

ISCAN, Inc. developed the standard head-mounted system and the ETL-400 Desktop system.

Features

- Remote Desktop System: The integrated pan/tilt system is used to direct the camera manually from the operator's console or to automatically follow the subject's eye. Solid state IR illuminator is imperceptible to the subject, and well below OSHA intensity limits. Camera zoom, focus and aperture controls are adjustable at the operator's console.
- Eye Imaging/Tracking: The system uses a robust dark pupil tracking methodology which automatically separates the pupil from other dark shadows or eyelashes in the eye image. The system has an effective sub-pixel resolution of 1500 x 2200 for both pupil and corneal reflection position measurements, and true, real-time 60Hz data update.
- Data Collection: The system offers operator and subject video point-of-regard overlay display outputs. Typical point of regard accuracy is better than one degree over ±20 to 25 degrees of visual angle.
- Data Calibration: The Desktop system uses simple eye angle calibration procedures with built-in fixation monitoring and blink detection subsystems. The system offers easy visual point-of regard calibration using either 5 or 9 calibration points. These selectable point-of regard calibration models may use pupil data only, pupil and corneal reflection, or a hybrid calibration allowing for both extended range and tolerance of head movement.

VisionTrak Desktop Imaging Subsystem

This system features an integrated solid state, low-level infrared illuminator and infrared sensitive eye imaging camera. The illumination is invisible to the subject. The camera and illuminator assembly is mounted on a pan/tilt platform which can automatically follow the movement of the subject's head to keep the eye in the centre of the camera's field of view. This auto-follow mode is effective within a ±6 inch horizontal by ±6 inch vertical range of the subject's head movement, as long as the subject remains facing the stimulus area. Subject-to-camera distance may be adjusted over a range of 24-40 inches.

- Eye Tracking Processor: The eye tracking processor automatically tracks the centre of a subject's pupil and a reflection from the corneal surface, and measures pupil size, all in real-time. Horizontal and vertical crosshairs automatically centre themselves over the pupil and corneal reflection to indicate proper tracking of the two targets. Calculation of the eye landmarks is accomplished in real time with a transport delay of only a single video field.
- Monitors and Cables: System includes a Pentium® III computer system, SVGA color monitor and Windows® 98. The three PCI expansion slots make it possible for all data acquisition and analysis to be done using one computer. Two nine-inch black and white monitors and all necessary cabling and connectors are also included. One video monitor displays the eye image and the other displays the scene image with superimposed point-of-regard. A VGA to NTSC converter is also supplied so that a computer generated stimuli can be used with the system.
- Auto Calibration Processor: The auto-calibration processor accurately calculates the subject's point of gaze with respect to a scene being viewed by using the raw eye position. A scene video camera, VCR output or converted computer display output provides the scene information input to the auto-calibrator. Manual cursor control allows the operator to delimit objects for quantitative gaze/object correlation, and an on-screen 24-hour clock is used for video frame-by-frame analysis of the output data.

Chapter 13. Appendix D: Filed International Patents

1. Applicant: Eastman Kodak Company
   Title: Autostereoscopic Display System (WO 2006/028708)
   Publication Date: 16 March 2006
   Description: A system for displaying images in auto-stereoscopic format, the system includes an illumination source that produces light in at least two bands in synchronization with frame sequential stereo image data; a single spatial light modulator that is driven by the frame sequential stereo image data and that receives the two bands of light from the illumination source; and a real-time eye tracking device that monitors positions of eyes of a user so that viewing is not interrupted by movement of the eyes of the user; wherein the user views the two bands of light sequentially on only the single spatial display which projects a three-dimensional image to the viewer.

2. Applicant: Tobii Technology AB
   Title: Arrangement, Method and Computer Program for Controlling a Computer Apparatus based on Eye-Tracking (WO 2005/124521)
   Publication Date: 29 December 2005
   Description: This invention relates to a computer based eye-tracking solution.

3. Applicant: SR Labs
   Title: Method to improve the Data Entry and Management of Information related to Customers Relationship Management Systems (CRM) (WO 2005/124518)
   Publication Date: 29 December 2005
   Description: The present invention concerns a method for the data entry and management of information related to customers relationship management systems (CRM). This method allows the user to use eye-tracking systems and devices for the human-computer interaction using their gaze and their voice, through speech recognition systems instead or in addition to the usual user interfaces as eye-driven keyboards, mouse, trackball, optical pens etc.

4. Applicant: Sony Electronics Inc.
   Title: Three Dimensional Acquisition and Visualization System for Personal Electronic Devices (WO 2005/091650)
   Publication Date: 29 September 2005
   Description: A three-dimensional (3D) acquisition and visualization system for personal electronic devices comprises two digital cameras which function in a variety of ways. The two digital cameras acquire 3D data which is then displayed on an auto-stereoscopic display. For clarity and ease of use, the two digital cameras also function as eye-tracking devices helping to project the proper image at

the correct angle to the user. The two digital cameras also function to aid in autofocusing at the correct depth. Each personal electronic device is also able to store, transmit and display the acquired 3D data.

5. Applicant: New York University
   Title: Method and Apparatus for an Autostereoscopic Display having a Lenticular Lenslet Array (WO 2005/079376)
   Publication Date: 01 September 2005
   Description: This invention relates to a method for producing an autostereoscopic image of a scene for an observer. The apparatus includes a lenticular lenslet array sheet through which a first portion of the scene displayed on the display passes and forms a first seamless image of the left image which is visible only to the observer's left eye, and through which a second portion of the scene displayed on the display passes through and forms a second seamless image of the right image which is visible only to the observer's right eye.

6. Applicant: Customvis Plc
   Title: Limbal-Based Eye Tracking (WO 2005/065527)
   Publication Date: 21 July 2005
   Description: A method of determining and/or tracking the position of an eye, includes utilising at least two wavelength components of a plural wavelength zone that traverses the limbus of the eye to obtain a profile of whiteness and/or redness across the zone, and identifying from the profile at least one predetermined reference position that indicates the position of the eye. Apparatus for carrying out the method is also disclosed.

7. Applicant: Alcon Refractivehorizons, Inc
   Title: Hybrid Eye Tracking System and Associated Methods (WO 2005/063154)
   Publication Date: 14 July 2005
8. Description: A system and method for tracking ocular changes during a surgical procedure include directing an eye-safe optical beam toward an undilated, unparalyzed eye. A reflected optical beam is detected, and measurements are performed based upon data contained in the reflected optical beam of at least one geometric parameter of the eye at a predetermined frequency, and from them is calculated a change in the at least one geometric parameter. The calculated change is used to dynamically adjust the directing of laser beam shots during surgery.

9. Applicant: Queen's University at Kingston
   Title: Method and Apparatus for Calibration-Free Eye Tracking (WO 2005/046465)
   Publication Date: 26 May 2005
   Description: A system and method for eye gaze tracking in human or animal subjects without calibration of cameras, specific measurements of eye geometries or the tracking of a cursor image on a screen by the subject through a known trajectory. The preferred embodiment includes one

uncalibrated camera for acquiring video images of the subject's eye(s) and optionally having an on-axis illuminator, and a surface, object, or visual scene with embedded off-axis illuminator markers.

10. Applicant: Seeing Machines Pty Ltd
    Title: Eye Tracking System and Method (WO 2004/088348)
    Publication Date: 14 October 2004
    Description: A method of tracking an expected location of a head in a computerised headtracking environment having a delayed processing requirement for locating a current head position, the method comprising the step of: utilising previously tracked positions to estimate a likely future tracked position; outputting the likely future tracked position as the expected location of the head. Kalman filtering of the previously tracked positions can be utilised in estimating the likely future tracked position.

11. Applicant: Tengshe, Vishwas, V.
    Title: Gaze Tracking System and Method (WO 2004/066097)
    Publication Date: 05 August 2004
    Description: An eye-tracking system for displaying a video screen pointer at a point of regard of a user's gaze. The system comprises a camera focused on the user's eye; a support connected to the camera for fixing the relative position of the camera to the user's pupil; a computer having a CPU, memory, video display screen, an eye-tracking interface, and computer instructions for: segmenting the digital pixel data of the image of the eye into black and white sections based upon user selectable RGB threshold settings; determining the center of the eye based upon the segmented digital data; mapping the determined center of the eye to a pair of coordinates on the video screen; and displaying a pointer on the video display screen at the point of regard.

12. Applicant: VISX Inc
    Title: Methods and Systems for Laser Calibration and Eye Tracker Camera Alignment (WO 2003/090867)
    Publication Date: 06 November 2003
    Description: The present invention provides methods, systems, and apparatus for calibrating a laser ablation system, such as an excimer laser system for selectively ablating a cornea of a patient's eye. The invention also facilitates alignment of eye tracking cameras that measure a position of the eye during laser eye surgery.

13. Applicant: Eyetools
    Title: Techniques for facilitating use of eye tracking data (WO 2003/050658)
    Publication Date: 19 June 2003
    Description: Individual eye tracking data can be used to determine whether an individual has actually looked at a particular region of a visual field. Aggregation of data corresponding to multiple individuals can provide trends and other data useful for designers of graphical representation (e.g.,

Web pages, advertisements) as well as other indicates both regions viewed and regions not viewed, can be accomplished using several different techniques. For example, percentages of the number of viewers that viewed a particular region can be represented as a particular color, or the underlying image being viewed can be blurred based on and acuity gradient and the number of individuals viewing various regions. The various regions represented as viewed can be selected based on the type of viewing activity (e.g., reading, gazing) is associated with a particular region.

14. Applicant: Imperial College Innovations Ltd
    Title: Manipulation of Image Data (WO 2003/024319)
    Publication Date: 27 March 2003
    Description: A method of analysing an image comprises carrying out eye tracking on an observer observing the image and applying factor analysis to the fixation regions to identify the underlying image attributes which the observer is seeking.

15. Applicant: Lasersight Technologies, Inc.
    Title: Eye Tracking using Edge of Corneal Flap (WO 2003/022173)
    Publication Date: 20 March 2003
    Description: A method of tracking an eye during vision correction treatment includes cutting corneal tissue to define a cut edge. At least a portion of the cut edge is tracked to track eye movements. In one embodiment, the corneal tissue is cut to define a flap-like layer such that fluid gathers near the cut edge. The fluid is illuminated prior to tracking the cut edge.

16. Applicant: Telefonaktiebolaget L M Ericsson
    Title: Method and Apparatus for Gaze Responsive Text Presentation (WO 2003/019341)
    Publication Date: 06 March 2003
    Description: Method and apparatus is provided for use with a rapid serial visual presentation (RSVP) display window in a mobile communication device to selectively adjust the presentation of text. Eye tracking sensors are used to detect when a reader's focus shifts outside the text window, indicating that the reader has become inattentive to displayed text. Thereupon, presentation of text is halted. When the eye tracking sensors detect that the focus of the reader's eyes has shifted back into the text window, text presentation is resumed. Usefully, the rate of text presentation is slowed down or speeded up, when the eye tracking sensors detect the reader's eyes to be focused on the left edge or on the right edge, respectively, of the text display window.

17. Applicant: Qinetiq Limited
    Title: Eye Tracking Systems (WO 2003/017203)
    Publication Date: 27 February 2003
    Description: An eye tracking system for monitoring the movement of a user's eye comprises an eye camera and a scene camera for supplying to interlace electronics video data indicative of an image of the user's eye and an image of the scene observed by the user.

18. Applicant: Smart Eye AB

    Title: Method for Image Analysis (WO 2003/003910)

    Publication Date: 16 January 2003

    Description: The present invention relates to a method for locating the eyes in an image of a person, for example useful in eye-tracking. The method comprises selecting a region of interest in the image, preferably including the face of the person, using information from said selection in the steps of: selecting a plurality of candidate areas ('blobs) in this region of interest, matching said candidate areas of an edge map of the image with at least one mask based on a geometric approximation of the iris, selecting the best matching pair of candidate areas, and evaluating the relative geometry of said selected candidate areas to determine if the pair of candidate areas is acceptable. The key principle of the invention is to use information from the face detection to improve the algorithm for finding the eyes.

19. Applicant: Sensomotoric Instruments GMBH

    Title: Multidimensional Eye Tracking and Position Measurement System (WO 2002/064031)

    Publication Date: 22 August 2002

    Description: The present invention relates to improved ophthalmic diagnostic measurement or treatment methods or devices, that make use of a combination of a high speed eye tracking device, measuring fast translation or saccadic motion of the eye, and an eye position measurement device, determining multiple dimensions of eye position or other components of eye, relative to an ophthalmic diagnostic or treatment instrument.

20. Applicant: Opthalmic Inventions, LLC

    Title: Topography-Guided Opthalmic Ablation and Eye-Tracking (WO 2002/056789)

    Publication Date: 25 July 2002

    Description: Systems and methods for topography-guided ophthalmic ablation and eye-tracking. A topographic map of the surface of an eye is generated. A reference pattern on the surface of the eye, such as a staining substance applied using applicator to points on the eye, is correlated with the topographic map. The eye surface pattern is continuously tracked and the correlation adjusted. Ablation of the cornea may be performed based on the correlation as it is adjusted in real time.

21. Applicant: Koninklijke Philips Electronics N.V.

    Title: System for Automatically Adjusting a Lens Power through Gaze Tracking (WO 2002/054132)

    Publication Date: 11 July 2002

    Description: The present invention relates to a device containing an automatic zoom lens, and more particularly to a zoom lens that is controlled by a processor that is linked to a gaze tracking system. As a user looks onto an object through the device, the gaze tracking system collects data relating to the position of each eye of the user. This eye position data is input into the processor where the focal

point of the user is determined. The processor then adjusts the zoom lens to zoom in or out onto the object based on either a predetermined or user input zoom factor.

22. Applicant: Ruiz, Luis, A.
    Title: Method and Apparatus for Precision Laser Surgery (WO 2002/032353)
    Publication Date: 25 April 2002
    Description: An eye laser system which includes a laser and a laser delivery system for delivering a laser beam generated by the laser to the eye and eye tracking system which monitors movement of the eye and conveys eye tracking information to the laser delivery system with the eye tracking system including a non-invasive eye tilt reference marker. The reference marker projects an energy beam that is preferably visible so as to reflect off the iris of the eye and provide microscope and surgical field illumination.

23. Applicant: Sun Microsystems, Inc.
    Title: Dynamic Depth-of-Field Emulation based on Eye-Tracking (WO 2002/029718)
    Publication Date: 11 April 2002
    Description: A graphics system comprising a rendering engine, a sample buffer and a filtering engine. This invention relates generally to the field of 3-D graphics and, more particularly, to a system and method for rendering and displaying 3-D graphical objects.

24. Applicant: Memphis Eye and Cataract Associates Ambulatory Surgery Center
    Title: Method and System for Control of High Resolution High Speed Digital Micromirror Device for Laser Refractive Eye Surgery (WO 2001/085045)
    Publication Date: 15 November 2001
    Description: A laser eye surgery system includes a laser for producing a laser beam capable of making refractive corrections, an optical system for shaping and conditioning the laser beam, a digital micromirror device (DMD) for reflecting the shaped and conditioned beam toward the eye, a computer system for controlling the mirrors of the DMD, and an eye tracking system which tracks the position of the eye and provides feedback to the computer system.

25. Applicant: Swisscom Mobile AG
    Title: Method and System for Video Conferences (WO 2001/084838)
    Publication Date: 08 November 2001
    Description: The invention relates to a method and to a system for video conference with at least three different video conferences user terminals which communicate via a telecommunications network. Multimedia data comprising at least user image data and/or user audio data are transmitted via a telecommunications network. Every user receives the user image data of the other users arranged on a display device so that they are simultaneously visible. An eye tracking system detects the line of vision of the respective user and transmits it to a communications unit. The user image data that are displayed on the display device and that are not in the current line of vision of the respective user are

transmitted via the telecommunications network to the communications device with reduced resolution and/or image transmission rate.

26. Applicant: Lai, Ming

    Title: A Hybrid Tracking System (WO 2001/074231)

    Publication Date: 11 October 2001

    Description: A hybrid tracking system is configured to combine the advantages of open loop and close loop tracking systems. The hybrid tracking system employs a position-sensing device in an open loop configuration, while the position-sensing device itself is a close loop device. A particular application of this tracking system is to track eye movement in a refractive laser surgery. The hybrid-tracking configuration enables optical and mechanical separation of the position-sensing device from the surgical laser beam. As a result, the position-sensing device can be made as a modular device, and the hybrid eye-tracking system can have a relatively large tracking range even when a curved mark such as the limbus is used as the tracking reference.

27. Applicant: Siemens Aktiengesellschaft

    Title: System and Method for Eye-Tracking Controlled Speech Processing with Generation of a Visual Feedback Signal (WO 2001/056018)

    Publication Date: 02.08.2001

    Description: The invention relates to a system and a method for the operation and monitoring of, in particular, an automation system and/or a production machine or machine tool, whereby the visual field, of a user, is recorded on at least one means of display, where the speech information, from the user, is at least intermittently determined and where a visual feedback signal is generated, in response to the processing status, with regard to recognised voice information. An improved speech interaction is thus obtained, in particular, in the field of augmented-reality applications and in complex technical plants.

28. Applicant: Nokia Corporation

    Title: Eye-Gaze Tracking (WO 2001/049167)

    Publication Date: 12 July 2001

    Description: A device and a method for tracking an eye-gaze of an observer. A deep blue or violet light source is used to emit light to eye, particularly to the retina. The deep blue light is partially reflected and partially absorbed by the retina. The absorption is most prominent around the fovea, the area of sharp vision, because of the pigment which protects the fovea from short wavelength radiation. Thus the device and method of tracking eye-gaze according to the invention comprises emitting light having a certain wavelength and transferring the light to the retina of an eye. The wavelength of the light being such as to make the fovea of the eye resolvable. The method further comprises detecting light that is reflected from the eye to form detection information including the resolvable fovea, and mapping the detection information to a predetermined surface, the surface being located at a distance from the eye, the location of the fovea on the surface forming an eye-gaze point.

29. Applicant: Visx, Inc.
Title: Two Camera Off-Axis Eye Tracker (WO 2001/024688)
Publication Date: 12 April 2001
Description: Improved laser eye surgery and/or eye tracking systems, methods, and devices make use of two image capture devices, generally with both image capture devices disposed off the optical axis of the eye and/or any laser delivery system.

30. Applicant: Memphis Eye and Cataract Associates Ambulatory Surgery Center
Title: Eye Tracking and Positioning System for a Refractive Laser System (WO 2001/010338)
Publication Date: 15 February 2001
Description: An eye tracking and positioning system for use with a refractive laser system includes a camera interface, a computer, and a system for moving the patient relative to the laser beam.

31. Applicant: Digilens Inc.
Title: Display System with Eye Tracking (WO 2001/009685)
Publication Date: 08 February 2001
Description: The present invention relates generally to display systems, and more particularly, to a head mounted display system having an eye tracking device for tracking the change in the gaze direction of a user's eye and modifying the displayed image in response to the eye movement.

32. Applicant: San Diego State University Foundation
Title: Method and Apparatus for Eye Tracking (WO 2000/054654)
Publication Date: 21 September 2000
Description: Method and apparatus for correlating pupillary response to the cognitive activity of a subject undergoing an evaluation of cognitive activity during a task which involves monitoring and recording the point of gaze and pupillary response of the subject to the task, subjecting the recorded pupillary response to wavelet analysis in order to identify any dilation reflex of the subject's pupil during the task, and assigning a pupillary response value to the result of the wavelet analysis.

33. Applicant: Sarel, Oded
Title: A System and Method for Automated Self Measurement of Alertness, Equilibrium and Coordination and for Verification of the Identity of the Person Performing Tasks (WO 2000/033155)
Publication Date: 08 June 2000
Description: This invention is an automated self-measurement device for alertness, equilibrium, and coordination testing. The device includes eye tracking, a posturograph, a computer, an electric screen board, and a magnetic card slot for identification purposes.

34. Applicant: Scientific Generics Limited
Title: Eye Tracking System (WO 2000/026713)

Publication Date: 11 May 2000

Description: The present invention relates to an apparatus and method for tracking the direction of a user's gaze. The invention has particular relevance to an eye tracking system for use with optical instruments which form a viewable image of an object, such as microscopes, cameras, telescopes etc.

35. Applicant: Synthetic Environments, Inc.
    Title: System and Method for Controlling Host System Interface with User Point-of-Interest Data (WO 2000/016185)
    Publication Date: 23 March 2000
    Description: The present invention generally relates to the field of human-computer interaction and user interface technology. More particularly, the present invention relates to a system and method that determines a user's intent or choice by comparing, for example, the user's eye motion response resulting from a computer or software generated and presented animation sequence stimulus.

36. Applicant: Leica Microsystems AG
    Title: Eye Tracking System (WO 1999/065381)
    Publication Date: 23 December 1999
    Description: An optical instrument, such as a microscope or a camera, is provided for forming a viewable image of an object. The optical instrument comprises an objective lens for forming the viewable image at an image plane, an eye sensor for sensing the direction of gaze of a user viewing the viewable image and means for controlling a controllable function of the optical instrument in dependence upon the sensed direction of gaze.

37. Applicant: University of Washington
    Title: Virtual Retinal Display with Eye Tracking (WO 1999/036826)
    Publication Date: 22 July 1999
    Description: This invention relates to retinal display devices, and more particularly to a method and apparatus for mapping and tracking a viewer's eye. A retinal display device is an optical device for generating an image upon the retina of an eye.

38. Applicant: Bullwinkel, Paul, E
    Title: Fiber Optic Eye-Tracking System (WO 1999/035961)
    Publication Date: 22 July 1999
    Description: This invention is directed to eye tracking devices and in particular to an eye tracking device suited for analyzing eye-movement of a patient undergoing diagnostic treatment within a magnetic resonance imaging apparatus. An eye tracking device for analyzing motion of an individual's eye includes an image converter subsystem, an image receiving subsystem, and processing subsystem.

39. Applicant: Dynamic Digital Depth Research Pty. Ltd.

Title: Eye Tracking Apparatus (WO 1999/027412)

Publication Date: 03 June 1999

Description: The present invention relates to a tracking system for locating the eyes of a viewer including: an illumination means; a plurality of cameras; and a processing means; wherein at least the viewer's eyes are illuminated by the illumination means to enable capture by each camera, and wherein the processing means is adapted to process images from each camera so as to detect the position of the viewer's eyes.

40. Applicant: Bid Instruments Limited

Title: Apparatus and Method for Visual Field Testing (WO 1999/022638)

Publication Date: 14 May 1999

Description: An apparatus for ocular testing is provided with means for displaying targets (T1, T2) means for tracking eye movement and means (5) for controlling the display of the targets (T1, T2) on a screen. A method comprises arranging the control means to choreograph display of the targets (T1, T2...) at different positions at the screen depending on whether the eye tracking means detects that an observer is directly looking at the target.

41. Applicant: Visx Incorporated

Title: Eye Tracking Device for Laser Eye Surgery using Corneal Margin Detection (WO 1999/018868)

Publication Date: 22 April 1999

Description: The present invention is generally concerned with ophthalmic surgery, and more particularly relates to systems, methods and apparatus for tracking the position of a human eye. The present invention is particularly useful for tracking the position of the eye during surgical procedures, such as photorefractive keratectomy (PRK), phototherapeutic keratectomy (PTK), laser in situ keratomileusis (LASIK), or the like. In an exemplary embodiment, the present invention is incorporated into a laser ablation system which is capable of modifying the spatial and temporal distribution of laser energy directed at the cornea based on the eye's position during the laser ablation procedure.

42. Applicant: Applied Science Laboratories

Title: An Eye Tracker Using an Off-Axis, Ring Illumination Source (WO 1999/005988)

Publication Date: 11 February 1999

Description: A camera assembly for use in an eye tracking apparatus, the camera assembly including a camera with a lens having an axis; and a ring shaped light source disposed around the image axis and near the periphery of the lens aperture, the light source oriented to direct light along the camera axis toward the target.

43. Applicant: Ramot-University Authority for Applied Research and Industrial Development, Ltd.

Title: Method and Apparatus for Assessing Visual Field (WO 1998/040781)

Publication Date: 17 September 1998

Description: The present invention relates to a method and apparatus for assessing the visual field of a subject which utilizes the basic human reflex of eye movement towards a target entering a subject's field of vision.

44. Applicant: Geisler, Wilson, S.

Title: Foveated Image Coding System and Method for Image Bandwidth Reduction (WO 1998/033315)

Publication Date: 30 July 1998

Description: The present invention relates generally to the field of image data compression. More specifically, it relates to a foveated imaging system which can be implemented on a general purpose computer and which greatly reduces image transmission bandwidth requirements.